THE SYNTHESIS AND CHEMISTRY OF SOME TRANSITION METAL HYDROCARBYL COMPLEXES OF MANGANESE(I), IRON(II), TUNGSTEN(II), PLATINUM(II) AND PLATINUM(IV)

XIAOLONG YIN

THE SYNTHESIS AND CHEMISTRY OF SOME TRANSITION METAL HYDROCARBYL COMPLEXES OF MANGANESE(I), IRON(II), TUNGSTEN(II), PLATINUM(II) AND PLATINUM(IV)

A thesis submitted to the

UNIVERSITY OF CAPE TOWN

in fulfillment of the requirements for the degree of

DOCTOR OF PHILOSOPHY

by

XIAOLONG YIN

(B.Sc., M.Sc.)

Department of Chemistry
University of Cape Town
Rondebosch 7701
South Africa

August 1997

ACKNOWLEDGEMENTS

My sincere thanks and appreciation are extended to:

My supervisor, Professor John R. Moss, for his interest, encouragement and support throughout this study.

Dr. Alan T. Hutton for fruitful discussion and help with the cyclic voltammetry and conductivity measurements.

Professors Klaus R. Koch and Graham Jackson for their assistance with NMR spectra.

Professor Luigi R. Nassimbini for the permission to use his autoclave.

Professor Roger Hunter for the loan of chemicals.

Dr. Bette Davidowitz for her help in promptly ordering chemicals.

Dr. Krassi Dimitrova, Ms. Margie Nair and Mr. Noel Hendricks for recording many NMR spectra.

Dr. Thinus van der Merwe (University of Stellenbosch) for recording the ES mass spectra; Dr. Phillip Boshoff (Cape Technikon), Colorado State University and the University of California, Riverside for recording the FAB mass spectra.

Mr. Piero Benincasa for the microanalysis and recording many EI mass spectra.

Riana Mohammed, Devric Dodds and Ricardo Donn for recording the DSC/TGA traces.

Drs. Jo-Ann M. Andersen and Yi-Hsien Liao for their friendship and assistance with experimental techniques.

My colleagues and friends in the Chemistry Department, especially, Meredith Hearshaw, Samantha Hughes, Reinout Meijboom and Fiona Hess for proof-reading this manuscript (or parts thereof), Earl Starr, Jacques Maré, Renqiang Zeng, Oliver Hill, Robyn George, Hadley Clayton, Paul Galatolo, Fazlin Waggie for helpful discussion.

SASOL and the Foundation for Research Development for financial support.

My wife Yali Wang for recording UV-vis spectra and proof-reading this thesis.

My family for their continuous support.

ABSTRACT

The long chain alkoxycarbonyl complexes, $[Mn(CO)_5\{C(O)OR\}]$, where R = CH_2R', and R = *n*-C_7H_{15} to *n*-$C_{10}H_{21}$, *n*-$C_{12}H_{25}$ and *n*-$C_{16}H_{33}$, have been synthesized by the reactions of the corresponding acyl complexes $[Mn(CO)_5\{C(O)R'\}]$, where R′ = *n*-C_6H_{13} to *n*-C_9H_{19}, *n*-$C_{11}H_{23}$ and *n*-$C_{15}H_{31}$, with synthesis gas in hexane. The thermal behaviour of these complexes has been investigated by differential scanning calorimetry. The reaction of the acyl complex $[Mn(CO)_5\{C(O)C_{11}H_{23}\}]$ with synthesis gas in THF gave $[Mn_2(CO)_{10}]$ and the alcohol *n*-$C_{12}H_{25}OH$ exclusively. The reaction of the alkoxycarbonyl complex $[Mn(CO)_5\{C(O)OC_{12}H_{25}\}]$ with synthesis gas in hexane at 85 °C gave the formate $HCO_2C_{12}H_{25}$, the alcohol *n*-$C_{12}H_{25}OH$ and $[Mn_2(CO)_{10}]$. The same reaction as above in THF yielded the formate $HCO_2C_{12}H_{25}$, the alcohol *n*-$C_{12}H_{25}OH$ and an ester *n*-$C_{12}H_{25}O_2C(CH_2)_3CH_3$ as well as $[Mn_2(CO)_{10}]$. These studies show that the reactions of the acyl complexes $[Mn(CO)_5\{C(O)R'\}]$ and the alkoxycarbonyl complexes $[Mn(CO)_5\{C(O)OR\}]$ with synthesis gas are both solvent and temperature dependent. The reaction of the complex $[Mn(CO)_5\{C(O)OC_{12}H_{25}\}]$ with HX (X = Cl, BF_4) gave *n*-$C_{12}H_{25}OH$ and $[Mn(CO)_6]^+$ which underwent subsequent decomposition to yield $[Mn_2(CO)_{10}]$.

The new acyl complexes $[CpFe(CO)_2\{C(O)R\}]$ (R = *n*-C_5H_{11}, *n*-C_8H_{17}, *n*-$C_{11}H_{23}$, and *n*-$C_{17}H_{35}$,), $[Cp^*Fe(CO)_2\{C(O)C_{11}H_{23}\}]$ and $[CpW(CO)_3\{C(O)C_{11}H_{23}\}]$ have been prepared by the reactions of $Na[CpFe(CO)_2]$, $Na[Cp^*Fe(CO)_2]$ and $Na[CpW(CO)_3]$ respectively with the appropriate acyl chlorides. The reactions of synthesis gas with the acyl complexes $[CpFe(CO)_2\{C(O)C_{11}H_{23}\}]$ and $[Cp^*Fe(CO)_2\{C(O)C_{11}H_{23}\}]$ yielded formates and esters in low yield, while the treatment of $[CpW(CO)_3\{C(O)C_{11}H_{23}\}]$ with synthesis gas under similar conditions resulted in no reaction. Hence the reactivity of the acyl complexes $[L_nM\{C(O)C_{11}H_{23}\}]$ [where L_nM = $Mn(CO)_5$, $CpFe(CO)_2$, $Cp^*Fe(CO)_2$ or $CpW(CO)_3$] with synthesis gas, are both metal and ligand dependent. The thermal behaviour of these acyl complexes has also been investigated by differential scanning calorimetry.

The new alkyl complexes [CpW(CO)$_3$R] (R = *n*-C_6H_{13}, *n*-C_7H_{15}, and *n*-C_8H_{17}) have been prepared by the reactions of Na[CpW(CO)$_3$] with the appropriate alkyl bromide or iodide. Information on the electrochemical and thermal behaviour of [CpW(CO)$_3$(C_7H_{15})] has been obtained from cyclic voltammetry and differential scanning calorimetry respectively. Reactions of the alkyl complexes [CpW(CO)$_3$(C_8H_{17})], [CpFe(CO)$_2$R] (R = CH_3, *n*-$C_{11}H_{23}$), [Mn(CO)$_5$(CH_3)] and [Re(CO)$_5$($C_{16}H_{33}$)] with CO_2 have been attempted but were unsuccessful under the conditions investigated. The reactions of the carbyne complexes [CpW(CO)$_2$(≡CR)] [R = C_6H_5 and C_6H_4-OMe-(4)] with CO_2 have also been investigated.

The new complexes *cis*-[PtBu$_2$(PBu$_3$)$_2$], *trans*-[PtBuCl(PBu$_3$)$_2$] and [PtMe$_2$(Me$_2$-bipy)] have been prepared and characterized. The reactions of [PtMe$_2$(Me$_2$-bipy)] with the alkyl iodides (CH_3I to *n*-$C_5H_{11}I$) led to the *trans* oxidative addition of the alkyl iodide to yield the Pt(IV) complexes [PtIMe$_2$(R)(Me$_2$-bipy)] (R = CH_3 to *n*-C_5H_{11}). The complex [Pt(NP)$_2$Cl$_2$] [NP = 1-(diphenylphosphino)-2-(2-pyridyl)ethane] was also prepared. The reactions of *cis*-[PtBu$_2$(PR$_3$)$_2$] (R = Ph, Bu) with CO_2 in NEt_3 gave the carbonate complexes [Pt(CO$_3$)(PR$_3$)$_2$]. The reactions of [PtMe$_2$(R$_2$-bipy)] (R = H, CH_3) with CO_2 in R′OH/NEt_3 gave the novel monoalkyl carbonate complexes [PtMe{OC(O)OR′}(R$_2$-bipy)] (R = H, R′ = CH_3; R = CH_3, R′ = CH_3 or C_2H_5). The complex [PtMe{OC(O)OC_2H_5}(Me$_2$-bipy)] has been fully characterized, although this and other monoalkyl carbonate complexes are unstable both in solution and in the solid state under vacuum. The reaction of the complex [PtMe{OC(O)OC_2H_5}(Me$_2$-bipy)] with ethyl iodide gave diethyl carbonate.

A new and simple method has been developed for the synthesis of the alkoxycarbonyl complexes *trans*-[Pt{C(O)OR}$_2$(PPh$_3$)$_2$] (R = Me, Et) by the reaction of *cis*-[PtCl$_2$(PPh$_3$)$_2$] with CO/ROH in NEt_3.

The new ω-bromoalkyl tungsten complexes [CpW(CO)$_3${$(CH_2)_n$Br}] (n = 5-7) and [Cp*W(CO)$_3${$(CH_2)_n$Br}] (n = 4) were easily prepared in good yields by the

reactions of $Na[CpW(CO)_3]$ or $Na[Cp^*W(CO)_3]$ with the appropriate dibromoalkanes. The iodoalkyl complexes $[CpW(CO)_3\{(CH_2)_nI\}]$ (n = 3-7) and $[Cp^*W(CO)_3\{(CH_2)_nI\}]$ (n = 3 and 4) were prepared by reacting $[CpW(CO)_3\{(CH_2)_nBr\}]$ or $[Cp^*W(CO)_3\{(CH_2)_nBr\}]$ with sodium iodide, or by reacting the $Na[CpW(CO)_3]$ with the appropriate diiodoalkanes. The properties of these complexes, including their ^{13}C NMR and mass spectra, are reported and discussed. Both similarities and differences are observed in the IR, ^1H and ^{13}C NMR and mass spectra of the respective Cp and Cp* complexes. Changes in these spectra due to the altering of the chain length and the halogens are observed for these haloalkyl complexes. Thermal properties are also affected by the change of the chain length. The reactions of $[CpW(CO)_3\{(CH_2)_3Br\}]$ with 1,1,1-tris(4'-hydroxyphenyl)ethane and 3,5-dihydroxybenzyl alcohol gave tri-nuclear and bi-nuclear complexes respectively. The ω-hydroxyalkyl tungsten complexes $[CpW(CO)_3\{(CH_2)_nOH\}]$ (n =3, 6 or 7) were synthesized by the reactions of $Na[CpW(CO)_3]$ with $Br(CH_2)_nOH$ (n = 3, 6 or 7). The reaction of $[CpW(CO)_3\{(CH_2)_7OH\}]$ with BuLi followed by *p*-anisoyl chloride gave the new complex $[CpW(CO)_3\{(CH_2)_7O_2C(C_6H_4)\text{-}OMe\text{-}(4)\}]$. The bromoalkyl rhenium complexes $[Re(CO)_5\{(CH_2)_nBr\}]$ (n =3-5) were prepared by reacting $Na[Re(CO)_5]$ with the appropriate dibromoalkanes. The new complexes $[Re(CO)_5\{(CH_2)_nBr\}]$ react with sodium iodide to yield $[Re(CO)_5\{(CH_2)_nI\}]$ (n = 3 and 4).

The reactions of the iodoalkyl complexes $[LM\{(CH_2)_nI\}]$ with $[PtMe_2(R_2\text{-bipy})]$ (R = H, CH_3) yielded the novel polymethylene bridged heterobinuclear complexes of the type $[LM(CH_2)_nPtIMe_2(R_2\text{-bipy})]$ [LM = $CpW(CO)_3$, R = H and CH_3, n = 3-5; LM = $Cp^*W(CO)_3$, R = H and CH_3, n = 3 and 4; LM = $CpFe(CO)_2$, R = H and CH_3, n = 4; LM = $CpRu(CO)_2$, R = H and CH_3, n = 4; LM = $Cp^*Fe(CO)_2$, R = H and CH_3, n = 3 and 4; and LM = $Re(CO)_5$, R = CH_3, n = 4]. This oxidative addition reaction is a new, general method for the synthesis of polymethylene bridged heterobinuclear complexes. The electrochemical behaviour of the heterobinuclear W/Pt complexes was investigated by cyclic voltammetry under

both argon and carbon dioxide atmospheres. These results were compared with those obtained for the mononuclear tungsten and platinum complexes.

The reaction of 1,5-bis(4'-methyl-2,2'-bipyridyl-4-yl)pentane with $[Pt_2Me_4(SMe_2)_2]$ gave the binuclear Pt(II) alkyl complex $[PtMe_2\{(Me\text{-}bipy)\text{-}(CH_2)_5\text{-}(Me\text{-}bipy)\}PtMe_2]$. 4-(4-bromobutyl)-4'-methyl-2,2'-bipyridine reacted with 1,1,1-tris(4'-hydroxyphenyl)ethane to give $\{Me\text{-}bipy\text{-}(CH_2)_4\text{-}OC_6H_4\}_3CCH_3$, the zero generation dendrimer. The reaction of 4-(4-bromobutyl)-4'-methyl-2,2'-bipyridine with the building block 3,5-dihydroxybenzyl alcohol gave $\{Me\text{-}bipy\text{-}(CH_2)_4\text{-}O\}_2C_6H_3\text{-}CH_2OH$ which reacted with PPh_3/CBr_4 to give the first generation dendritic benzyl bromide wedge $\{Me\text{-}bipy\text{-}(CH_2)_4\text{-}O\}_2C_6H_3\text{-}CH_2Br$. This reacted with the core molecule 1,1,1-tris(4'-hydroxyphenyl)ethane to yield the first generation dendrimer $\{[Me\text{-}bipy\text{-}(CH_2)_4\text{-}O]_2C_6H_3\text{-}CH_2O\text{-}C_6H_4\}_3CCH_3$. The zero generation Pt(II) dendrimer $[\{PtMe_2(Me\text{-}bipy)\text{-}(CH_2)_4\text{-}OC_6H_4\}_3CCH_3]$ was synthesized by the reaction of $\{Me\text{-}bipy\text{-}(CH_2)_4\text{-}OC_6H_4\}_3CCH_3$ with $[Pt_2Me_4(SMe_2)_2]$. The first generation Pt(II) dendrimer $\{[PtMe_2(Me\text{-}bipy)\text{-}(CH_2)_4\text{-}O]_2C_6H_3\text{-}CH_2O\text{-}C_6H_4\}_3CCH_3$ was similarly prepared from $\{[Me\text{-}bipy\text{-}(CH_2)_4\text{-}O]_2C_6H_3\text{-}CH_2O\text{-}C_6H_4\}_3CCH_3$ and $[Pt_2Me_4(SMe_2)_2]$. All the new compounds have been characterized and the data are discussed. The reactions of some of these compounds with CO_2 and $[CpW(CO)_3\{(CH_2)_4I\}]$ have been investigated.

ABBREVIATIONS

Å	=	angstrom
Bu	=	butyl
bipy	=	2,2′-bipyridine
compd	=	compound
COSY	=	correlated spectroscopy
Cp	=	cyclopentadienyl
Cp*	=	pentamethylcyclopentadienyl
CV	=	cyclic voltammetry
dec	=	decomposed
DSC	=	differential scanning calorimetry
EI	=	electron impact
ES-MS	=	electrospray mass spectroscopy
ether	=	diethyl ether
Et	=	ethyl
FAB	=	fast atom bombardment
Fp	=	$CpFe(CO)_2$
Fp*	=	$Cp^*Fe(CO)_2$
HETCOR	=	heteronuclear correlation
IR	=	infrared
M	=	transition metal
M^+	=	molecular ion
Me	=	methyl
Me_2-bipy	=	4,4′-dimethyl-2,2′-bipyridine
mp	=	melting point
MS	=	mass spectrometry
m/z	=	mass to charge ratio
NMR	=	nuclear magnetic resonance
Ph	=	phenyl
Pr	=	propyl
R	=	alkyl

Rp	=	$CpRu(CO)_2$
THF	=	tetrahydrofuran
TGA	=	thermal gravimetry analysis
TMS	=	tetramethylsilane
UV-vis	=	ultraviolet-visible
Wp	=	$CpW(CO)_3$
Wp*	=	$Cp^*W(CO)_3$

NOTE: COMPOUND NUMBERS AND REFERENCES ARE VALID WITH EACH INDIVIDUAL CHAPTER ONLY

TABLE OF CONTENTS

Chapter 1

Recent Developments In The Activation Of Carbon Dioxide By Metal Complexes

1.1 Introduction

Global warming, caused by the increasing emissions of greenhouse gases such as carbon dioxide, methane and others, has been recognized as a serious environmental problem [1-7]. An obvious solution has been to reduce the emissions of CO_2 [1-7] and other options are available [3-6]. These include reducing the use of energy derived from fossil fuels. Another option is the recovery of CO_2 from energy conversion processes, which is then stored in the ocean. An alternative approach is using CO_2 as a renewable resource, *i.e.* reuse of the existing CO_2 as a source of carbon for producing chemicals. The latter option has received much attention lately [7-29]. This is because the utilization of CO_2 as an alternative source of carbon has several advantages:

(1) Alleviating global climate change caused in part by the increasing CO_2 emissions.

(2) Extending the present limited carbon resources (coal, petroleum and natural gas) into an environmentally friendly and easily obtainable carbon source, *viz.* CO_2.

(3) Simulating photosynthesis and enzyme catalyzed reactions in the laboratory would be helpful in understanding the photosynthetic process in Nature and in utilizing enzyme-analogous reactions for chemical syntheses.

In spite of these advantages, the chemistry of CO_2 activation is still underdeveloped. This is due to the fact that CO_2 is highly thermodynamically stable and kinetically inert. The problem of CO_2 activation is a permanent challenge to the art of the chemist to 'force' this molecule into selective reactions under mild conditions.

CO_2 has been used in the synthesis of urea, cyclic carbonates, salicylic acid and methanol. Increased use of CO_2 would only be possible if the relatively inert CO_2 molecule could be activated. Numerous ways for CO_2 activation are currently under investigation [7-29]. These include bioconversion [7], photochemical reduction [7,8,10], electrochemical reduction [7,8,10,18], thermal heterogeneous and homogeneous reductions [5,7,11-16], and coordination to transition metals [7,8,10,17-29], as well as some combinations of two or more methods described above [7,8]. All these methods have one feature in common, which is the activation of CO_2 by the coordination of CO_2 to a transition metal centre. This coordination lowers the activation energy required in further reactions involving the CO_2 molecule thus increasing the rates of these reactions. This makes it possible to convert CO_2 with suitable reactants into useful products.

The conversion of CO_2 and a substrate RX (RX might be alkyl halides, alkenes, alkynes *etc.*) to the product RCO_2X at a transition metal centre is illustrated schematically in Scheme 1.1.

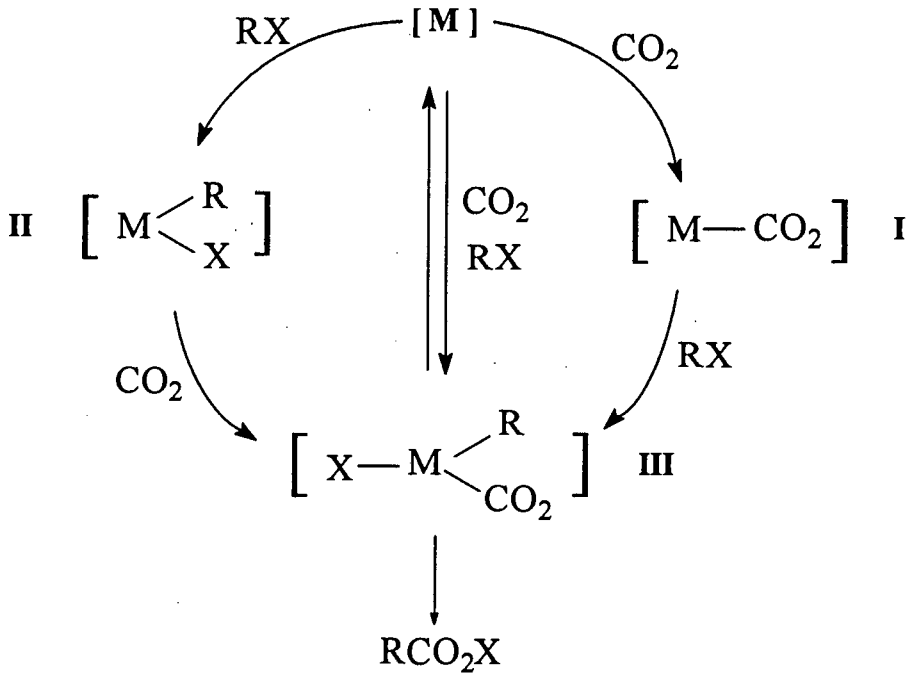

Scheme 1.1

There are three possible routes (see Scheme 1.1) for the combination of CO_2 and a substrate RX at a transition metal centre to give the product RCO_2X.

(1) Coordination of CO_2 to the metal, providing a metal-CO_2 complex [**I**], followed by the reaction of the metal-CO_2 complex [**I**] with the substrate RX to give [**III**]. Subsequent elimination would provide the product RCO_2X and reform the starting complex [M].

(2) Simultaneously coordinate both CO_2 and the substrate at the metal centre to afford [**III**], followed by reductive elimination to give the product RCO_2X and to reform the starting complex [M].

(3) Coordinate the substrate to the metal first, forming the substrate-metal complex [**II**] which could then react with CO_2. Subsequent elimination would provide the desired product RCO_2X.

Binding the CO_2 molecule and the substrate at the same transtion metal centre (structure [**III**]) would be a crucial step in both the stoichiometric and catalytic reactions of CO_2. The conversion of CO_2 by the above-mentioned three routes will be discussed in detail in sections 1.2 - 1.4.

1.2 Activation of carbon dioxide by formation of metal CO_2 complexes

The formation of a transition metal CO_2 complex *via* direct coordination is one of the most powerful and universal ways to induce the inert CO_2 molecule to undergo chemical reactions [26]. The synthesis and chemistry of transition metal CO_2 complexes have been of continuous interest and a number of reviews on this subject have appeared [7,8,10,17-29]. The latest review by Gibson, published in 1996, has covered the most recent developments of the organometallic chemistry of metal CO_2 complexes [27]. Thus, although metal CO_2 complexes are central to CO_2 activation, it will not be discussed here in detail, other than to mention some particularly relevent aspects of CO_2 activation, and to comment on the most recent work.

1.2.1 Bonding of CO_2 at a transition metal centre

The CO_2 molecule is a linear triatomic molecule. The carbon atom possesses *sp* hybridization and the C-O distance of 1.16Å is shorter than a normal C=O double bond involving an sp^2 carbon atom. The different electronegativities of oxygen and carbon lead to a negative polarization on the oxygen atoms and a partial positive charge on the carbon atom. In its ground state, CO_2 also has two sets of π molecular orbitals which are orthogonal. Thus, the CO_2 molecule exhibits several distinct positions that could interact with a metal centre in different ways as shown below:

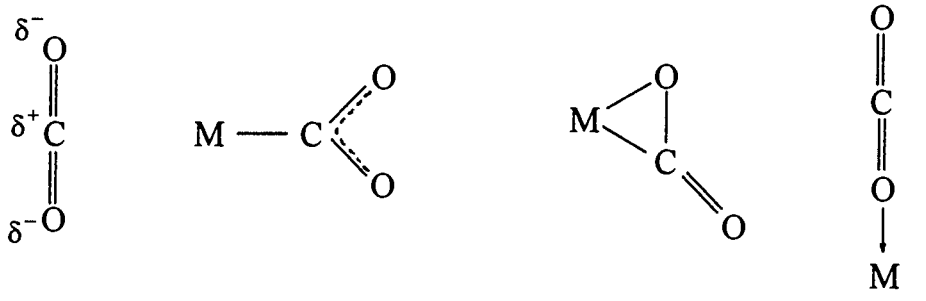

Figure 1.1. CO_2 and its possible coordination modes at a transition metal centre.

The η^1(C) and η^2(C,O) side-on coordination modes have been confirmed by X-ray crystal structure determinations of known metal CO_2 complexes [30-32], e.g. $[Rh(diars)_2(Cl)(\eta^1\text{-}CO_2)]$ [30], $[Ni(\eta^2\text{-}CO_2)(PCy_3)_2]$ [31] and $[Cp'_2Nb(\eta^2\text{-}CO_2)(CH_2SiMe_3)]$ [32]. No X-ray crystal structural data of the η^1(O) coordination mode in transition metal complexes are currently available.

Theoretical studies on the bonding of a CO_2 molecule to a metal centre have been reported [29, 33-40]. The η^1(C) *vs.* η^2(C,O) side-on coordination mode dichotomy is under both orbital and electrostatic control [40], as shown in Figure 1.2.

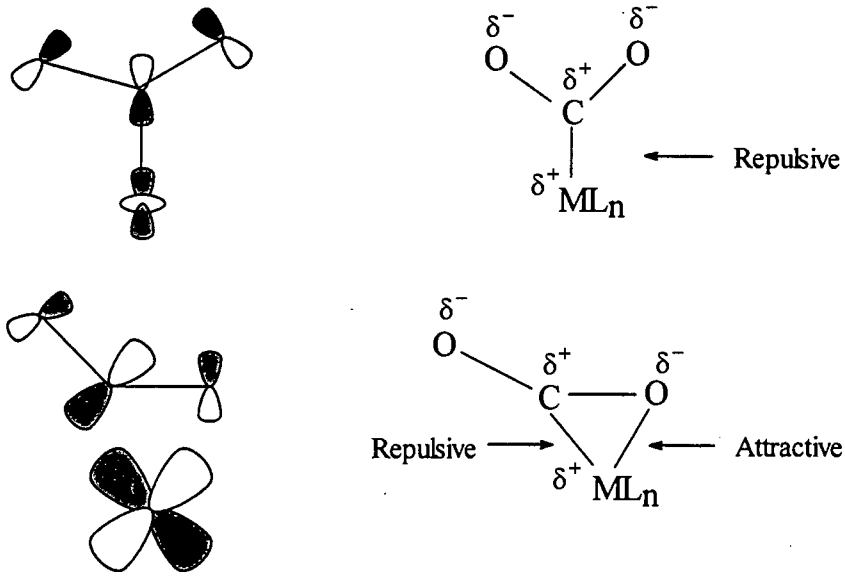

Figure 1.2. Orbital overlapping and electrostatic interaction of the η^1(C) and η^2(C,O) side-on coordination modes of CO_2.

In the η^1(C) bonding mode there is a strong, two electron stabilizing and charge transfer interaction between a d_z^2 type orbital (which is doubly occupied) and the π^* orbital of CO_2 (which is empty). In the η^2(C,O) side-on coordination mode the orbital interaction pattern is reversed. The $d\pi$ orbital interacts in a two electron stabilizing interaction with the π^* orbital of CO_2. The η^1(C) bonding mode is most favoured when the transition metal fragment ML_n has a doubly occupied $d\sigma$ type orbital that is relatively high in energy. This high energy will be best achieved if the metal is in a relatively low oxidation state which also reduces the repulsive electrostatic interaction. Examples of CO_2 complexes containing the η^1(C) bonding are [Co(salen)(η^1-CO_2)] [41] and [Rh(diars)$_2$(Cl)(η^1-CO_2)] [30].

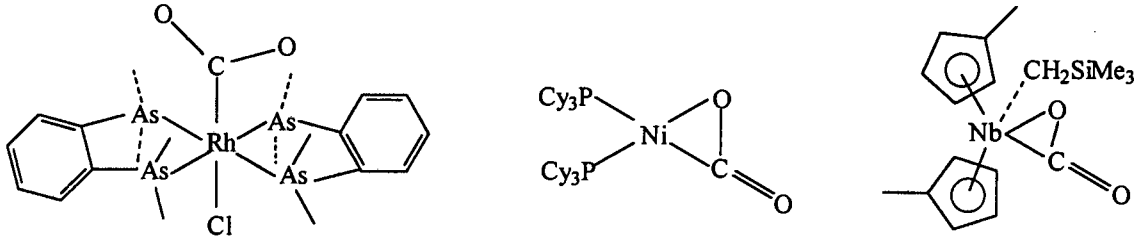

Figure 1.3. Some representative examples of complexes with η^1(C) and η^2(C,O) side-on coordination modes.

The η^2(C,O) side-on coordination mode is favoured by a high energy dπ-type orbital. A stronger stabilization of the η^2(C,O) mode will be achieved if the dσ orbital that points towards the CO_2 ligand is empty. Many complexes with the η^2(C,O) mode have been reported in the literature, such as $[Ni(PR_3)_2(\eta^2\text{-}CO_2)]$ (R = Cy, Ph, Bu, Et) [31,42], $[Fe(PMe_3)_4(\eta^2\text{-}CO_2)]$ [43], $[Cp'_2Nb(CH_2SiMe_3)(\eta^2\text{-}CO_2)]$ [32], *trans*-$[Mo(PMe_3)_4(\eta^2\text{-}CO_2)_2]$ [44], $[Cp_2Mo(\eta^2\text{-}CO_2)]$ [45].

Very recently Fujita and co-workers [46] have found evidence for charge transfer in some cobalt-CO_2 complexes by X-ray absorption near-edge spectroscopy (XANES). The XANES study of the CO_2 adducts of [Co(HMD)] (HMD = 5,6,6,12,14,14-hexamethyl-1,4,8,11-tetraazacyclotetradeca-4,11-diene) clearly indicates significant charge transfer from Co to the bound CO_2 in both five coordinate $[Co(III)(HMD)(CO_2^{2-})]^+$ and six coordinate $[Co(III)(HMD)(CO_2^{2-})(CH_3CN)]^+$ species. Binding of CO_2 to the cobalt through the electrophilic carbon, with the oxygens bending back in an η^1(C) bonding configuration is the best model to account for the observed charge transfer [46].

1.2.2 Binding of CO_2 at two or more metal centres

CO_2 can be bound by two or more metal centres *via* the coordination of the carbon atom to one metal and either one or both of the oxygen atoms of the CO_2 to other metal(s). Thus numerous complexes with bridging CO_2 ligands can be formed. The complexes with bridging CO_2 ligands can be classified according to their bonding modes [27,28], as shown in Figure 1.4.

Since the synthesis and structural characterization of CO_2 bridging complexes have been comprehensively reviewed by Gibson very recently [27], this will not be repeated here. However, it is noteworthy that the activation of CO_2 by early-late transition metal complexes is of particular interest since this bifunctional activation of CO_2 by a combination of an early, oxophilic and a late, electron rich transition metal might have great potential in successful activation of CO_2.

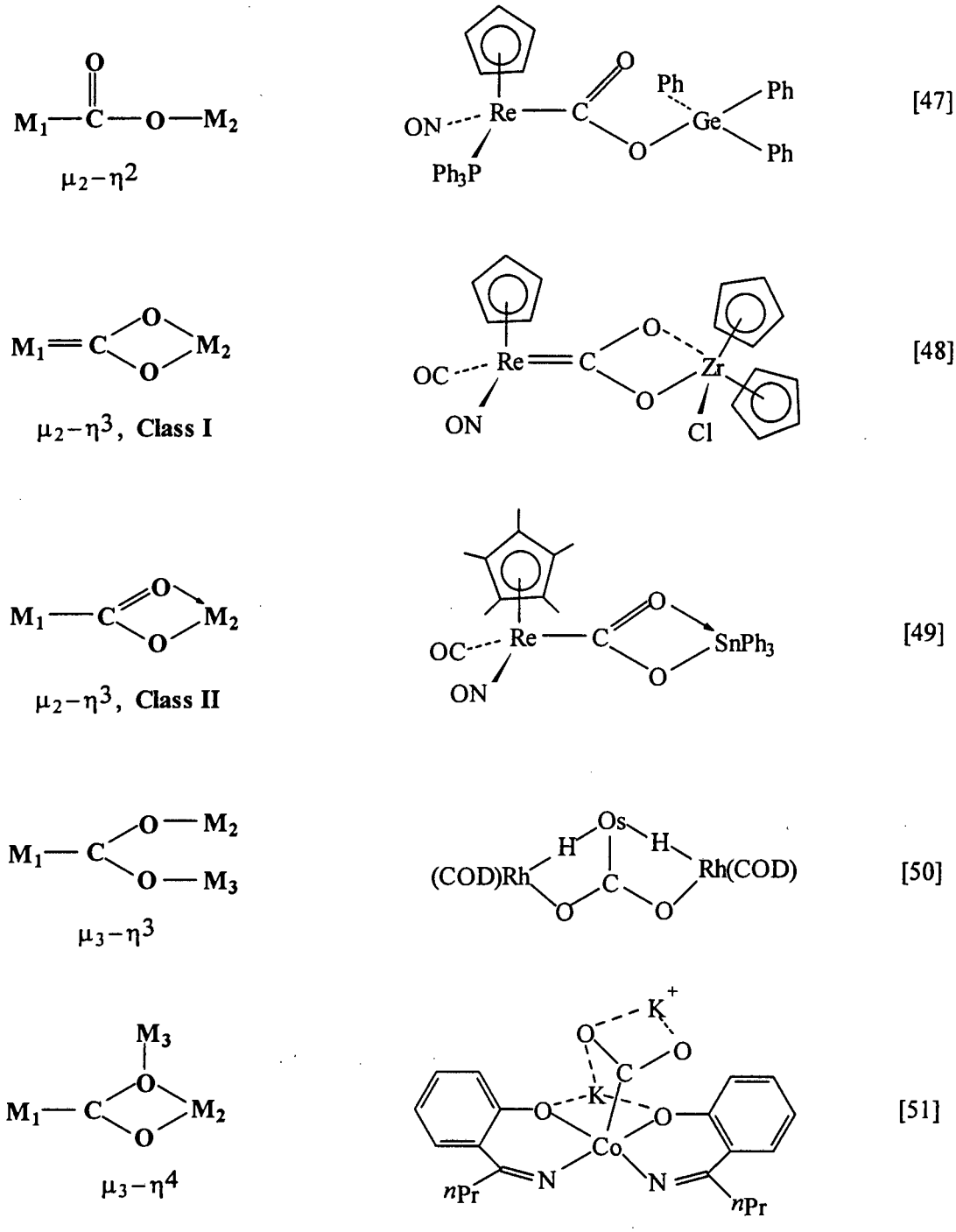

Figure 1.4. Structural types and examples of CO_2 bridging complexes.

1.2.3 The reactivity of the coordinated CO_2 ligand

Although numerous metal CO_2 complexes have been synthesized, the conversion of the CO_2 ligands in these complexes with suitable substrates to give organic products are much less well studied [27]. Recently, the reaction of the

coordinated CO_2 ligand of the complex $[Ni(PCy_3)_2(CO_2)]$ with $(CH_3)_3P{=}CH_2$, leading to a nickel ketene complex, has been reported [52]. The reaction of the ketene complex with HCl provides $[Ni(PCy_3)_2Cl_2]$ and the organic product, acetaldehyde, as shown below.

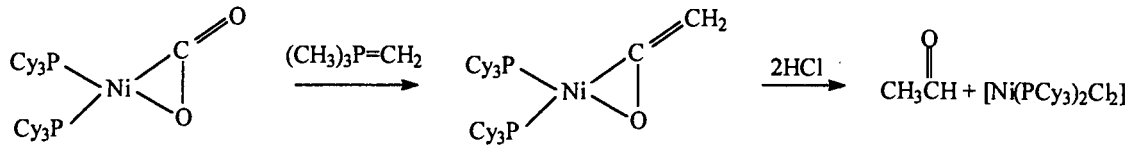

Scheme 1.2

The newly reported rhodium CO_2 complex (see Scheme 1.3) [53], prepared from the rhodium dinitrogen or ethylene complexes, can react with H_2 to form the hydrido formate complex. The hydrido formate complex can also be obtained by the reaction of the dihydrogen complex with CO_2.

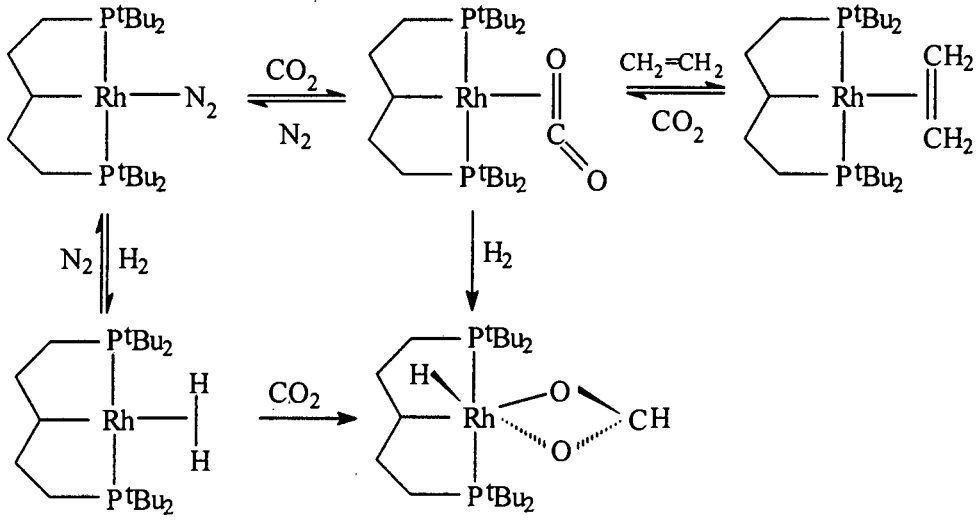

Scheme 1.3

1.3 Oxidative coupling of CO_2 with unsaturated substrates

The second route for the conversion of CO_2 into organic products is the simultaneous oxidative coupling of CO_2 and an unsaturated compound at a transition metal centre. Several reviews discussing the oxidative coupling reactions of CO_2 with unsaturated substrates have been published [11,12,22,23,54]. Due to the importance of this reaction in the conversion of CO_2

into useful organic products, a brief summary of these results and comments on recent progress is presented.

CO_2 undergoes oxidative coupling reactions with an unsaturated substrate X=Y at a metal centre [L_nM] to form the metallacycle as shown below.

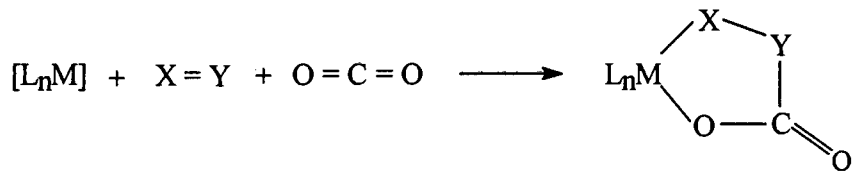

Scheme 1.4

The unsaturated compound X=Y can be a hydrocarbon (alkynes [55-57], alkenes [57-66], dienes and conjugated dienes [67-72], and cumulenes [73]), imines [22,74] or aldehydes [75]. The predominant transition metal complexes which mediate the coupling of CO_2 with unsaturated substrates are electron rich Ni(0) complexes, but some other transition metals such as Ti [11,12], Mo [11,12,23], Fe [69], Pd [11,12,23] and Pt [74] are also reactive.

The formation of nickellacycles from CO_2 and alkenes has become the basis of an extensive organonickel-based chemistry for the carboxylation of alkenes, as shown in Schemes 1.5 - 1.8.

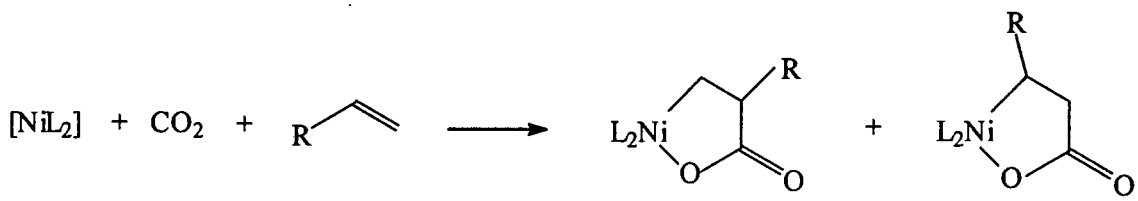

Scheme 1.5

From the coupling reaction of ethylene and CO_2 with [$Ni(COD)_2$] in the presence of 1,8-diazabicyclo[5,4,0]undec-7-ene (dbu), the complex [$(dbu)_2Ni\{\eta^2$-$CH_2CH_2C(O)O\}$] has been isolated and structurally characterized by Hoberg and co-workers [58]. This complex undergoes further ethylene insertion to give a

seven-membered ring complex, which by subsequent β-H elimination and acid hydrolysis gives pentenoic acid as shown below.

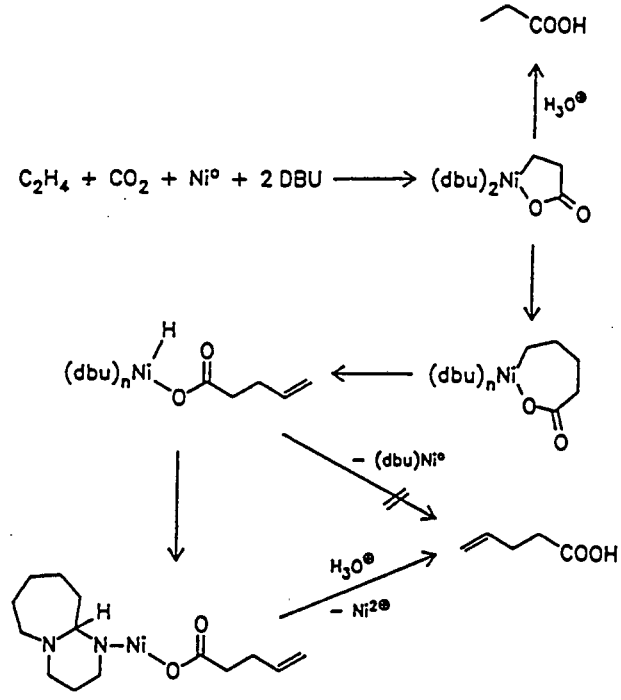

Scheme 1.6

These authors [58] have also shown that the Ni—C bond in the bis-dbu complex is available for insertion reactions with compounds containing carbon-carbon double bonds, hence various acid products could be obtained depending on the compounds and workup conditions (see Scheme 1.7).

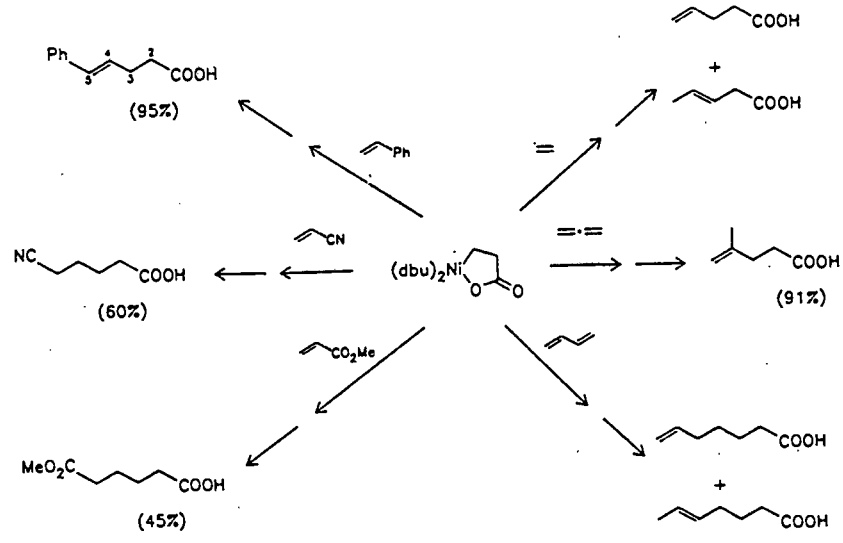

Scheme 1.7

The starting nickel(0) complexes which have been used for the coupling reaction can also be [Ni(cdt)], [Ni(COD)(bipy)] or [Ni(TMEDA)(COD)]. The ligands used

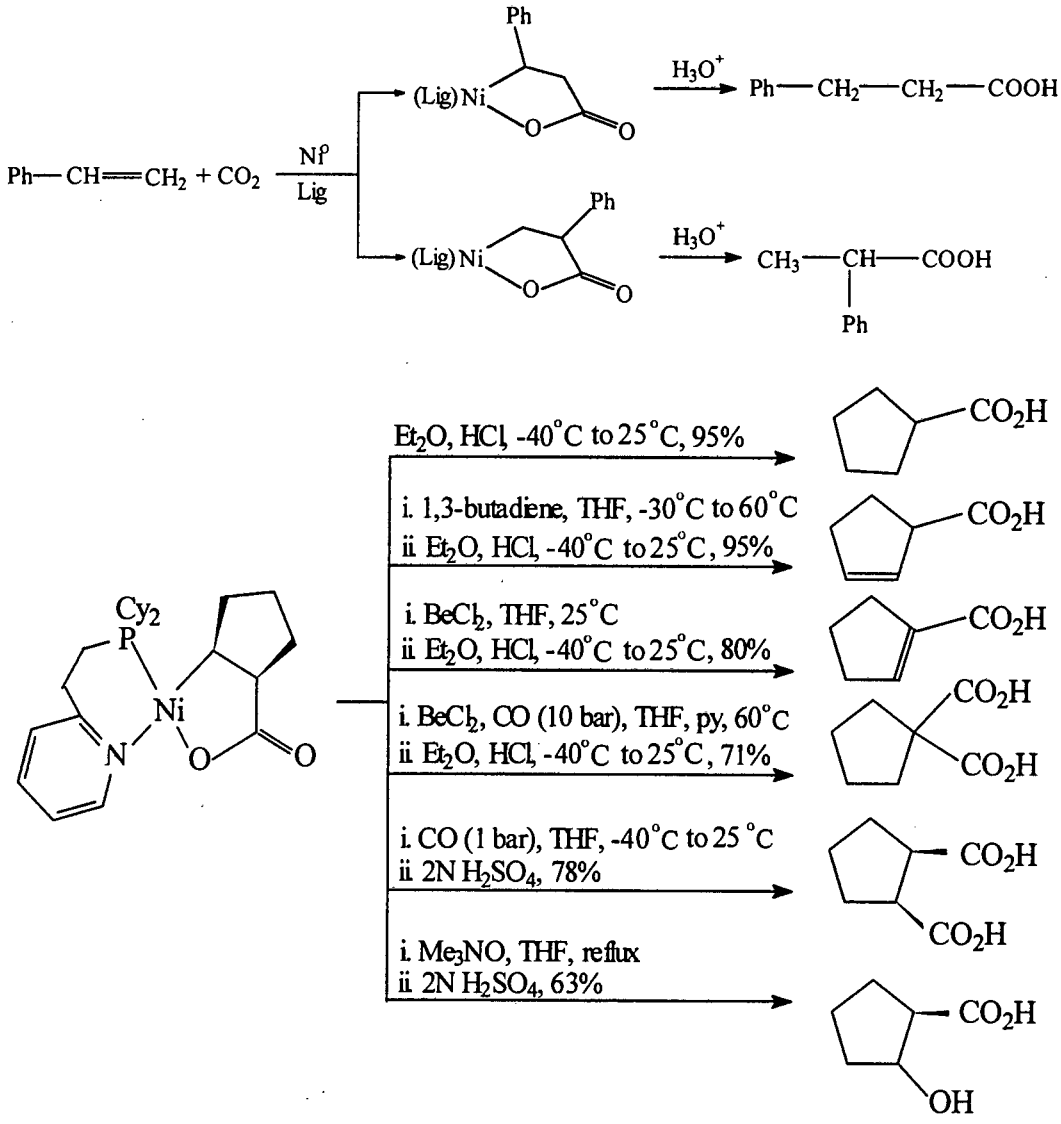

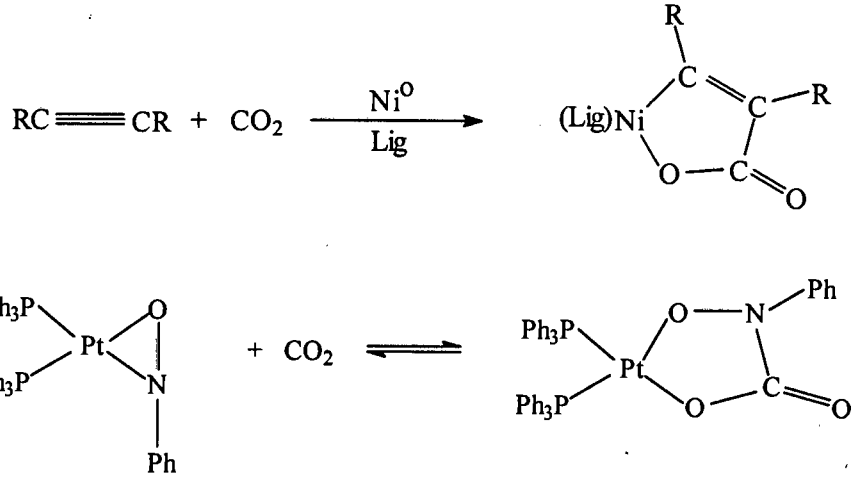

Scheme 1.8

for stablizing the Ni(0) species can be bipy, TMEDA, dcpe, dbu or dicyclohexyphosphinoethyl-2-pyridyl (dcpp). Depending on the starting organic substrates and workup conditions, an extensive range of functionalized products can be obtained (see Scheme 1.8 for some examples [57,61,62,74]).

Recent studies of the reaction of hex-3-yne with CO_2 in the presence of [Ni(TMEDA)] have revealed that a competing reaction in the catalytic cyclooligomerization of hex-3-yne and CO_2 is the formation of carbon monoxide and [Ni(TMEDA)(CO_3)] [76]. These authors have suggested that the reduction of CO_2 to CO probably proceeds *via* an intermediate in which two molecules of CO_2 are coupled head-to-tail to form a metallacycle as shown in Scheme 1.9.

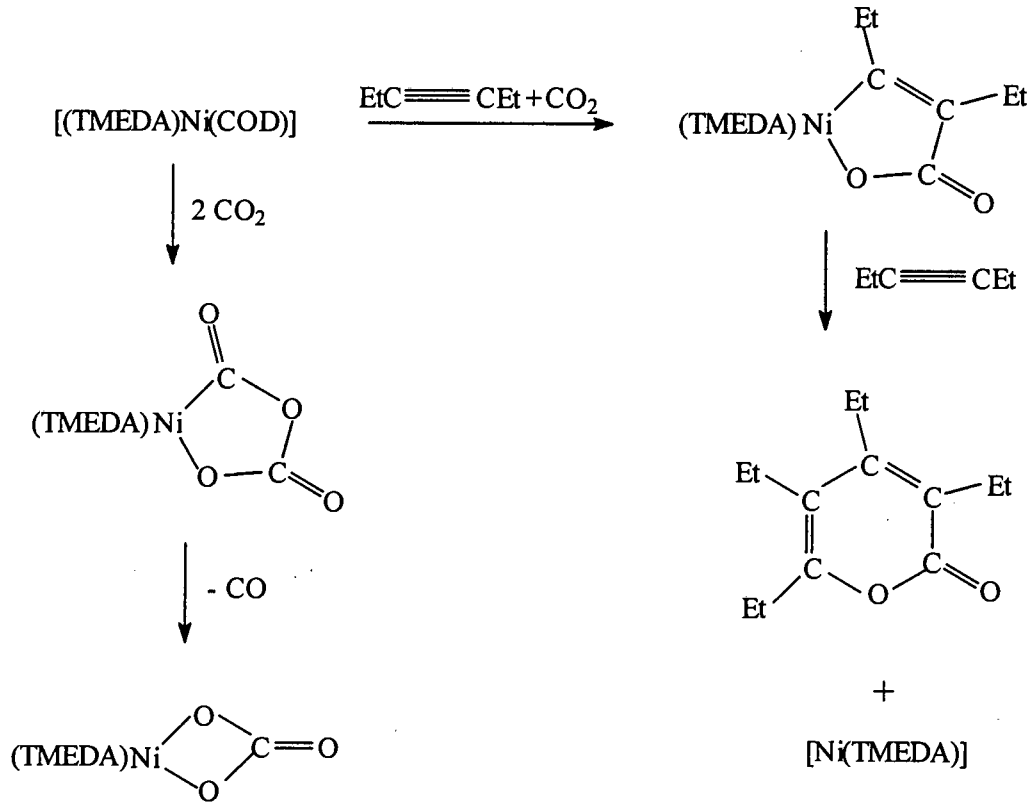

Scheme 1.9

The head-to-tail coupling of two molecules of CO_2 has been observed for an iridium complex as shown in Scheme 1.10 [77].

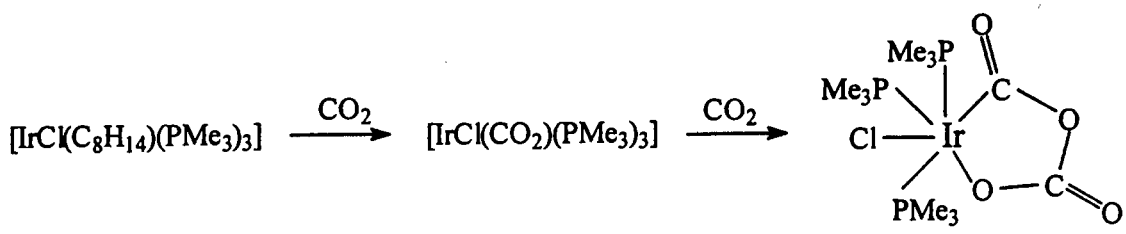

Scheme 1.10

More recently Walther and co-workers have reported that the coupling of CO_2 with 1-azadiene-type ligands (see Scheme 1.11) of the complexes [Ni(1-azadiene)$_n$]$_2$ forms nickellacyclic carbamate complexes. In these carbamate complexes, CO_2 is activated and is able to carboxylate acetophenone to yield benzoylic acid upon protolysis [78].

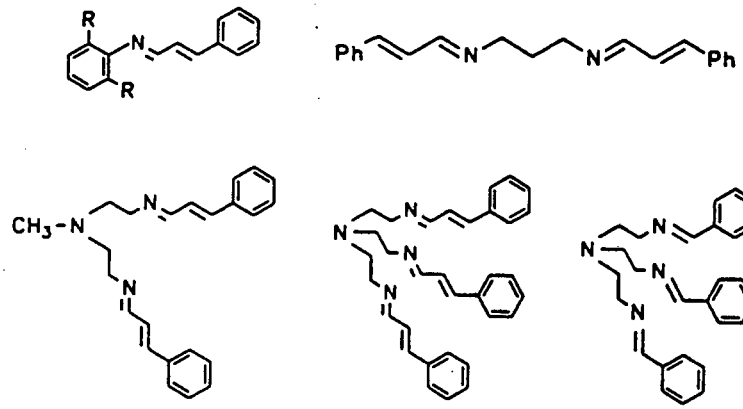

Scheme 1.11

The oxidative coupling of CO_2 with the metal carbon triple (M≡C) bond in some carbyne complexes has also been reported [79,80]. Either the carbon or one oxygen atom of a CO_2 molecule could bind to the metal depending on the nature of the metal of the carbyne complex. Fischer and co-workers [79] have reported the reaction of the anionic carbyne complexes with CO_2 to afford the oxygen-bound metallacycle as shown in Scheme 1.12.

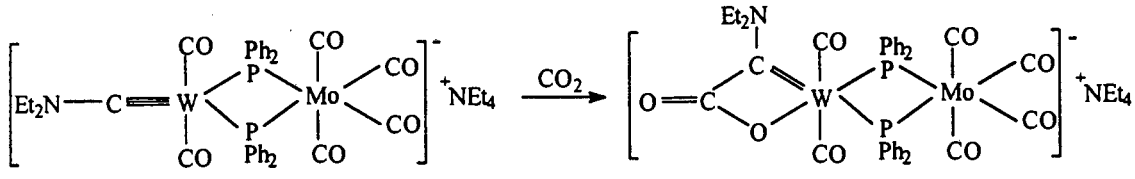

Scheme 1.12

The reaction of CO_2 with a ruthenium carbyne complex however affords the carbon-bound metallacycle as shown below [80].

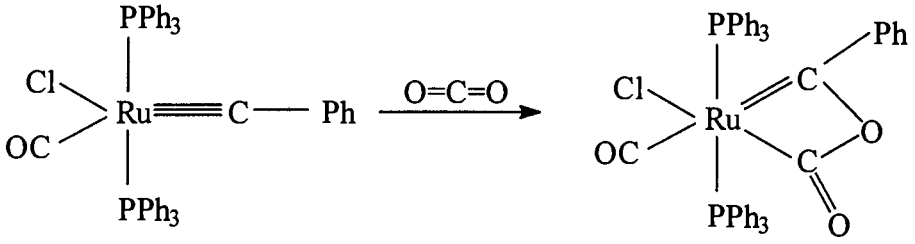

Scheme 1.13

The above-mentioned coupling reactions serve as unique examples for the oxidative coupling of CO_2 at a transition metal centre.

1.4 Insertion reactions of CO_2

The insertion of CO_2 into a pre-formed metal-element (M—E) bond is of great industrial importance. There are mainly seven types of CO_2 insertion reactions reported so far, *i.e.* the insertion of CO_2 into the M—E bond (where E = C, H, N, O, P, Si or other metal). Two possible products could be obtained from the insertion of CO_2 into the M—E bond, as shown below.

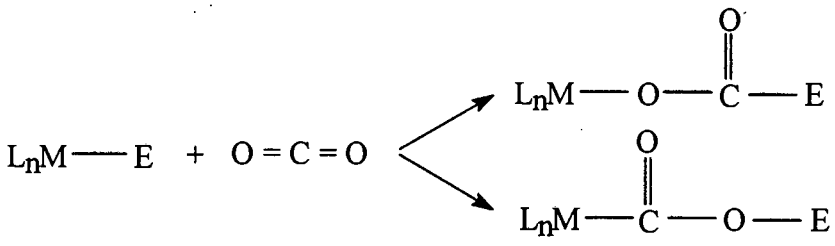

Scheme 1.14

There are several reviews on the insertion of CO_2 into the M—E bond in the literature [17,22-26], which have covered the results in this area up to 1994. Only the more recent developments in this area will be summarized. If there is no current example of a particular type of reaction, examples of earlier studies may be provided. This is to show the wide applications of the insertion reactions in

activation of CO_2. Only the successfully demonstrated examples of CO_2 insertion reactions will be included and attempted, but unsuccessful results will be excluded except in cases where a comparison between the reactivity of related complexes is made.

1.4.1 Insertion of CO_2 into the M—H bond

The insertion of CO_2 into the M—H bond can lead either to a formate complex or a metallocarboxylic acid complex as shown below.

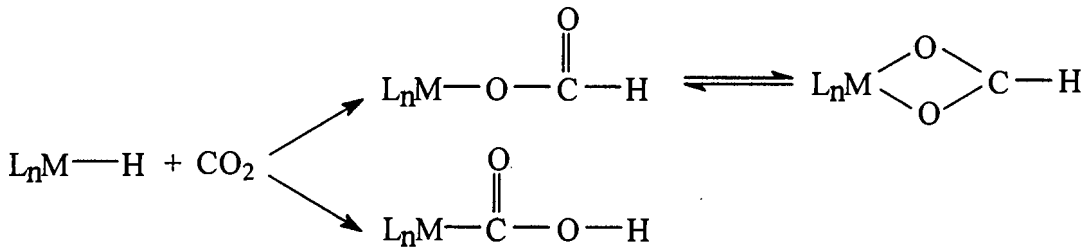

Scheme 1.15

The first step in the reaction is the nucleophilic attack of the $L_nM^{\delta+}—H^{\delta-}$ at the electrophilic carbon of CO_2 to form the polar transition states **IV** and **V**. This process requires a rather polar $M^{\delta+}—H^{\delta-}$ bond.

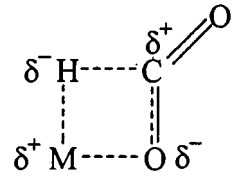

IV

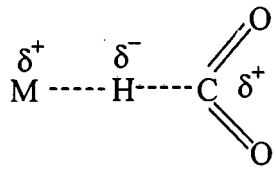

V

Rearrangement of the intermediates **IV** and **V** generally affords the formate complex, while the metallocarboxylic acid complex is a much less common product. Earlier studies have shown that the rates of insertion of CO_2 into the M—H bond of the anionic complexes $[MH(CO)_4L]^-$ (M = Cr, Mo, W; L = CO, PR_3) are dependent on the nucleophilicity of these species, which is affected by the donating ability of the ligand L [82].

The reaction of $[\{CpTi(\mu\text{-}H)\}_2(\mu\text{-}\eta^5\text{:}\eta^5\text{-}C_{10}H_8)]$ with CO_2 in toluene leads to the formation of the bis(formato) complex $[\{CpTi(\mu\text{-}\eta^1\text{-}OC(O)H)\}_2(C_{10}H_8)]$, which has been characterized by X-ray structural analysis to contain two monodendate bridging formates [83].

The heterobinuclear complex $[Cp_2Zr(H)(\mu\text{-}H)(\mu\text{-}N^tBu)IrCp^*]$ reacts rapidly with CO_2, leading to the formation of two diastereomeric heterobimetallic formate complexes as shown in Scheme 1.16 [84]. It has also been found that CO_2 inserts selectively into the terminal Zr—H bond to afford the terminal formate complex, with no evidence of insertion into the bridging hydride. The reaction of the formate complex with PhLi leads to lithium formate in 30% yield and regenerates $[Cp_2Zr(\mu\text{-}N^tBu)IrCp^*]$.

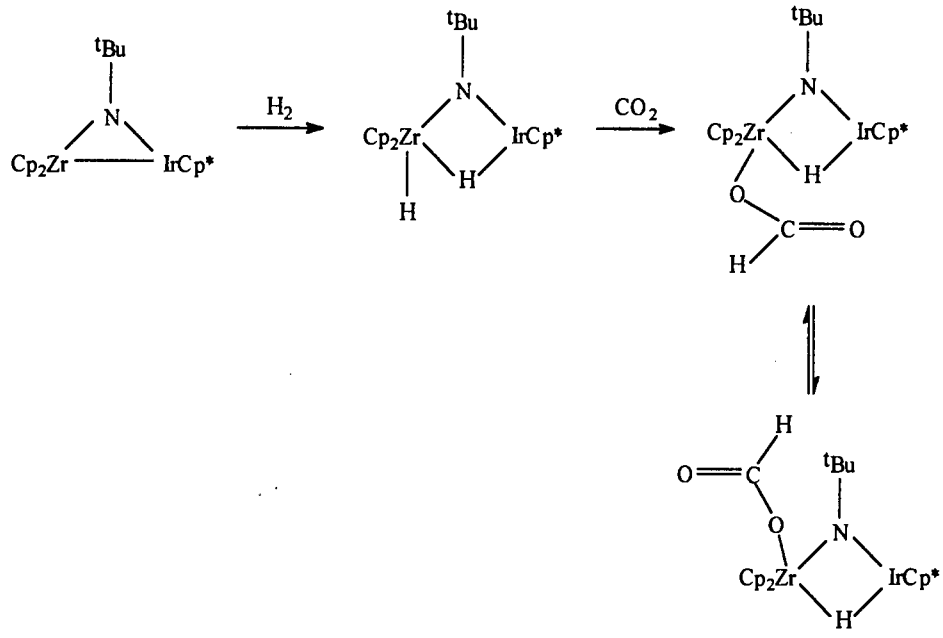

Scheme 1.16

The complex $[Nb(\eta^5\text{-}C_5H_4SiMe_3)_2H_3]$ reacts with CO_2 at 60 °C in THF to give the formate complex $[Nb(\eta^5\text{-}C_5H_4SiMe_3)_2(\eta^2\text{-}OC(O)H]$ in 95% yield [85]. The reaction of the η^2-(O,O′) formate complex with different π-acids or heterocumulene molecules results in opening of the bidendate formate ligand, giving rise to the monodentate formate-containing complexes $[Nb(\eta^5\text{-}C_5H_4SiMe_3)_2\{\eta^1\text{-}OC(O)H\}L]$ (L = CS_2, CO or 2,6-$Me_2C_6H_3NC$) as a consequence of the coordination of the incoming ligand (Scheme 1.17).

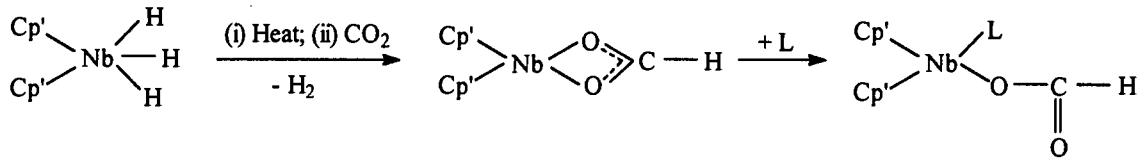

Cp' = η^5-$C_5H_4SiMe_3$

Scheme 1.17

The complex $[(\eta^5\text{-}C_5Me_5)Ta(PMe_3)(H)_2(\eta^2\text{-}CHPMe_2)]$ has been reported to undergo insertion of two equivalents of CO_2 in petroleum ether at room temperature to afford the bis(formato) complex $[(\eta^5\text{-}C_5Me_5)Ta(\eta^1\text{-}OC(O)H)(\eta^2\text{-}(O,O')OC(O)H)(\eta^2\text{-}CHPMe_2)]$ as shown in Scheme 1.18 [86].

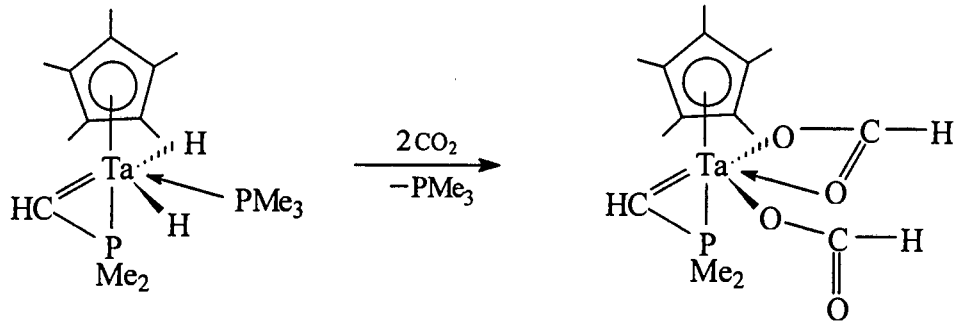

Scheme 1.18

The insertion of CO_2 into the Mn—H bond of the complexes $[Mn(NO)_2(L)_2H]$ (L = PMe_3, PEt_3) in toluene at room temperature gives the η^1-formate complexes $[Mn(NO)_2(L)_2\{OC(O)H\}]$ (L = PMe_3, PEt_3) in high yields (94-98%) [87]. The complexes $[Mn(CO)_3(L)_2H]$ (L = PMe_3, PEt_3) do not react with CO_2 even under more vigorous reaction conditions. This is attributed to the nucleophilicity of the nitrosyl-substituted complexes for the reaction with CO_2, while the carbonyl derivatives have not attained sufficient nucleophilicity for the same reaction [87].

The reactions of the complexes $[ReH(CO)_{5-n}(PMe_3)_n]$ (n = 2,3,4) with CO_2 have also been reported. The complex with n = 2 does not react with CO_2 even at elevated temperatures. The complexes with n = 3 and 4 react with CO_2 (1 bar) in toluene at room temperature, yielding the η^1-formate complexes $[Re\{OC(O)H\}(CO)(L)_n(PMe_3)_3]$ (L = CO, PMe_3) in high yield (98%). This is

proposed to be due to the increased nucleophilicity of the complexes with n = 3 and 4 compared to the complex with n = 2 [88].

The η^1-formate complex *fac*-[Re(bipy)$(CO)_3${OC(O)H}] has been prepared by irradiation of the complex *fac*-[Re(bipy)$(CO)_3(PPh_3)]^+$ in the presence of triethanolamine and CO_2. The formate complex *fac*-[Re(bipy)$(CO)_3${OC(O)H}] serves as the 'real' photocatalyst for the reduction of CO_2 to CO [89].

The reaction of *cis*-[Ru$(dmpe)_2H_2$] with CO_2 has been investigated [90]. Addition of CO_2 at 20°C results in the formation of two formate complexes: the major product is the *trans* formate hydride, *trans*-[Ru$(dmpe)_2$H{OC(O)H}], while the minor species is the bis(formate) complex *cis*-[Ru$(dmpe)_2${OC(O)H}$_2$]. When the addition of CO_2 is performed at -78 °C, both the bis(formate) and the *cis*-formate hydride, *cis*-[Ru$(dmpe)_2$H{OC(O)H}] are observed (see Scheme 1.19). The crystal structure of the complex *trans*-[Ru$(dmpe)_2$H{OC(O)H}] has been determined [90].

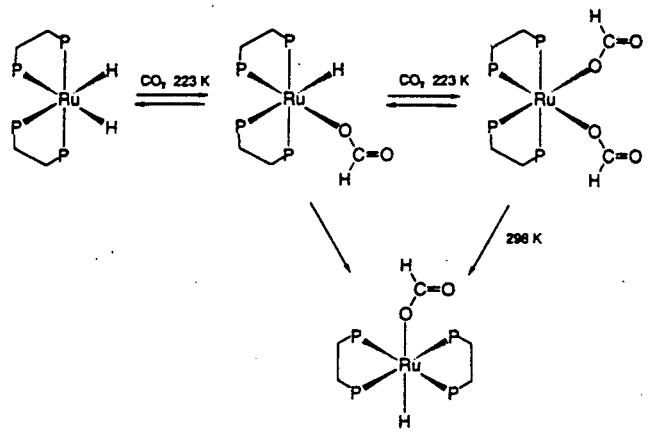

Scheme 1.19

The reaction of [Ru{MeSi$(CH_2PMe_2)_3$}(PMe_3)H(Ar)] with CO_2 does not yield a formate complex but the carbonate complex [Ru{MeSi$(CH_2PMe_2)_3$}$(PMe_3)(CO_3)$] instead [91].

It is noteworthy to highlight the recent developments in the hydrogenation of CO_2 [13,15,16] by Ru [92-94] and Rh [95-99] catalysts. The ruthenium complexes $[RuH_2(PMe_3)_4]$ and $[RuCl_2(PMe_3)_4]$ have been found to be very reactive catalysts for the hydrogenation of CO_2 in a supercritical mixture of CO_2 and H_2, for the formation of formic acid, formate esters and DMF, in the presence of NEt_3, alcohols or $HNMe_2$ [13,92,93]. A total yield of 370000 moles of DMF per mole of catalyst has been reported by Jessop and co-workers for the reaction of H_2, CO_2 and $HNMe_2$ catalyzed by $[RuCl_2(PMe_3)_4]$ [93].

Recently, Baiker and co-workers [94] have prepared a hybrid immobilized ruthenium complex catalyst using the sol-gel process. The catalyst shows high activity in the synthesis of DMF from H_2, CO_2 and $HNMe_2$ under supercritical conditions. The turnover numbers obtained with the Ru catalyst markedly exceeded previous reported values for heterogeneous catalysts but was lower than that of the homogeneous catalyst $[RuCl_2(PMe_3)_4]$ [93].

The effects of ligands on the catalytic hydrogenation of CO_2 to formic acid using *in situ* catalysts formed from $[Rh(COD)(\mu\text{-}Cl)]_2$ and monodentate and bidentate phosphorus ligands have been studied [95,96]. The mechanism of the Rh-catalyzed hydrogenation of CO_2 to formic acid has recently been investigated by kinetic and theoretical studies [97,98].

1.4.2 Insertion of CO_2 into the M—O bond

A variety of transition metal complexes with M—OR groups undergo insertion reactions with CO_2. If R is an organic moiety, alkyl or aryl carbonate complexes are formed; if R is hydrogen, hydrogen carbonate species are obtained [17,22-26].

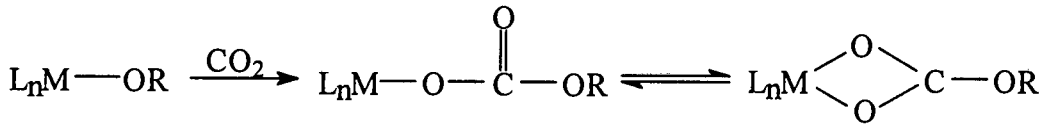

Scheme 1.20

The reaction of the methoxide tungsten complex [**VI**] (see Scheme 1.21) with an atmosphere of CO_2 in CH_2Cl_2 at 40 °C for *ca.* 72 hours results in the formation of the η^1-carbonate complex [**VII**], isolated as an air-stable yellow solid in 24% yield. Regeneration of [**VI**] when either a THF solution or a solid sample of [**VII**] is placed under vacuum demonstrates the reversible nature of this CO_2 insertion [100].

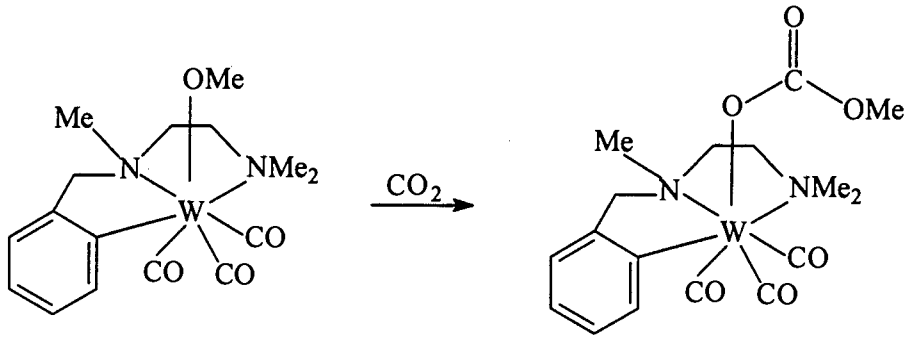

VI **VII**

Scheme 1.21

Although the insertion of CO_2 into the W—O bond of [Et_4N][$W(CO)_5OPh$] goes fast at ambient temperature and atmospheric pressure to afford the corresponding phenyl carbonate complex [Et_4N][$W(CO)_5\{O_2COPh\}$] [101], the complex [Et_4N][$W(CO)_4(PPh_2Me)OPh$] reacts slowly with CO_2, compared to [Et_4N][$W(CO)_5OPh$] [102]. The aryloxide complex [Et_4N][$W(CO)_5\{O\text{-}2,6\text{-}Ph_2\text{-}C_6H_3\}$] is found to be unreactive to CO_2 even under more vigorous conditions [102]. This lack of CO_2 reactivity is proposed to be due to the steric interference of the bulky ligand. The heterobinuclear complex [Et_4N][$W(CO)_5OPh\{Cr(CO)_3\}$] is also unreactive to CO_2 [103].

The Mn(I) and Re(I) alkoxide complexes *fac*-[$M(CO)_3$(P-P)(OR)] (M = Mn or Re; P-P = dppe or dppp; R = CH_3, C_2H_5 or CF_3CH_2) react readily at room temperature with CO_2 by insertion of CO_2 into the M—O bond, giving rise to the corresponding carbonate complexes *fac*-[$M(CO)_3$(P-P)$\{O_2COR\}$] [104]. Benzene solutions of the alkoxide complexes can even absorb CO_2 from the atmosphere. It is also found that the insertion and deinsertion of CO_2 from these complexes are

reversible under mild conditions. The crystal structure of the carbonate complex *fac*-[M(CO)$_3$(dppe){O_2COCH_3}] has been determined [104].

The fixation of CO_2 by hydroxo metal complexes to afford the metal bicarbonate or carbonate species is relevant to the fixation of CO_2 by some metalloenzymes. The enzyme, whose function is apparently related directly to the fixation of CO_2 by hydroxo metal complexes, is carbonic anhydrase [105]. The proposed mechanism for CO_2 hydration by the carbonic anhydrase is shown in Scheme 1.22 [105].

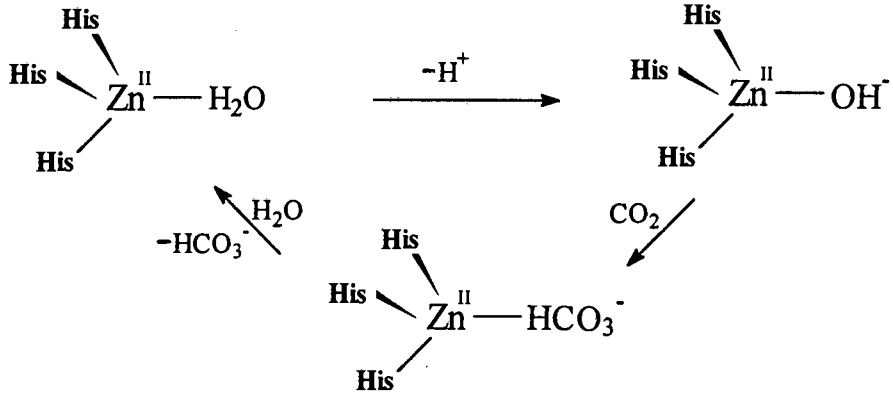

Scheme 1.22

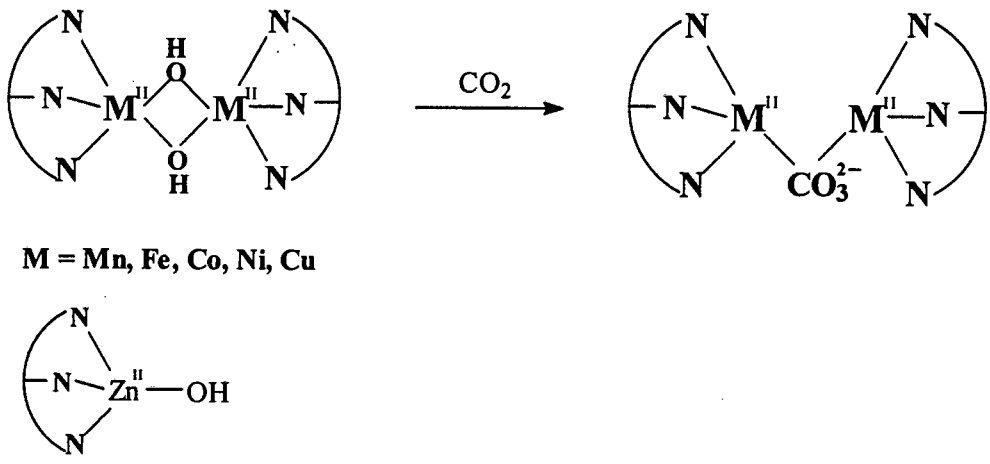

Scheme 1.23

A variety of zinc-containing carbonic anhydrase model systems have been described [106]. A series of hydroxo complexes of the first-row divalent metal ions (Mn, Fe, Co, Ni, Cu, Zn), containing the ligand $HB(3,5\text{-}^{i}Pr_2pz)_3$ (hydrotris(3,5-diisopropyl-1-pyrazolyl)-borate) as shown in Scheme 1.23, are found to react with CO_2 to afford μ-carbonato-dinuclear complexes, of which the molecular structures have been determined [106].

Solutions containing the Cu(II) and Zn(II) complexes with the macrocyclic ligand L (L = $[15]aneN_3O_2$) rapidly absorb atmospheric CO_2 to give the carbonate bridged trinuclear $[\{ZnL\}_3(\mu_3\text{-}CO_3)][(ClO_4)_4]$ and $[\{CuL\}_3(\mu_3\text{-}CO_3)][(ClO_4)_4]$ complexes [107]. The crystal structures of both complexes have been reported. The process of CO_2 fixation is believed to be due to the presence of the hydroxo species $[M(II)L(OH)]^+$ (M = Zn, Cu) [107].

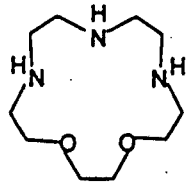

$[15]aneN_3O_2$

1.4.3 Insertion of CO_2 into the M—N bond

The insertion of CO_2 into the M—N bond has been investigated not only for transition metals [17, 22-26] but also for the group 14 elements, Ge and Sn [108].

The complexes $[Cp^*Ti(NR_2)_3]$ (R = Me or Et) react with CO_2 rapidly in toluene to give the corresponding insertion products $[Cp^*Ti(\eta^2\text{-}O_2CNR_2)_3]$ (R = Me or Et) [109]. Hydrolysis takes place if the solutions of these complexes are exposed to wet air, which leads to the formation of the complexes $[\{Cp^*Ti(\eta^2\text{-}O_2CNR_2)\}_2(\mu\text{-}O)_2]$ (R = Me or Et). The structure of the complex where R = ethyl has been determined [109].

A comparative study for the insertion of CO_2 into W—C, W—N, and W—O bonds has been carried out for three related complexes

$[Cp^*W(NO)(NHCMe_3)(CH_2CMe_3)]$, $[Cp^*W(NO)(NHCMe_3)(OCMe_3)]$ and $[Cp^*W(NO)(OCMe_3)(CH_2CMe_3)]$ [110]. The only compound which reacts with CO_2 to give the CO_2-inserted product $[Cp^*W(NO)(\eta^2\text{-}O_2CNHCMe_3)(CH_2CMe_3)]$ is the W—N bond containing complex $[Cp^*W(NO)(NHCMe_3)(CH_2CMe_3)]$. This study shows that the more nucleophilic amidonitrogen is the preferential site of CO_2 insertion.

The reaction of the complexes $[Ti(\eta^5\text{:}\eta^1\text{-}C_5H_4SiMe_2NR)Cl_2]$ (R = ^{t}Bu or CHMePh) with CO_2 leads to their conversion into the oxo derivative $[Ti(\mu\text{-}\eta^5\text{-}C_5H_4SiMe_2O)Cl_2]_2$ with elimination of the alkyl isocyanates O=C=NR (R = ^{t}Bu or CHMePh) as organic products (see Scheme 1.24). This is believed to be due to a metathesis process between CO_2 and the M—N bond (which is of partial double bond character) [111].

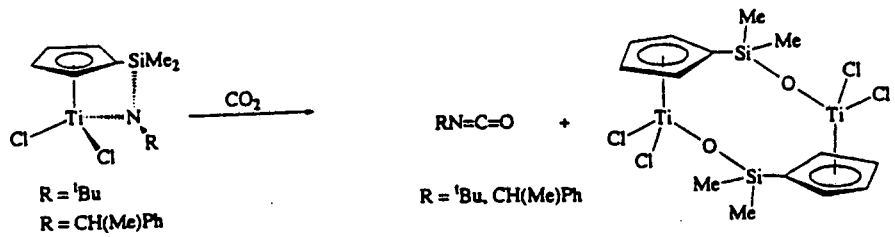

Scheme 1.24

Other examples of the metathesis between CO_2 and the M—N bond are the reactions of $[M\{N(SiMe_3)_2\}_2]$ (M = Ge and Sn) with CO_2 to give $[M\{OSiMe_3)_2\}_2]$, $Me_3SiN{=}C{=}O$ and $Me_3SiN{=}C{=}NSiMe_3$ [108]. The mechanism by which the metathesis process occurs is proposed as the insertion of CO_2 into the corresponding M—NR_2 bonds, as shown in Scheme 1.25.

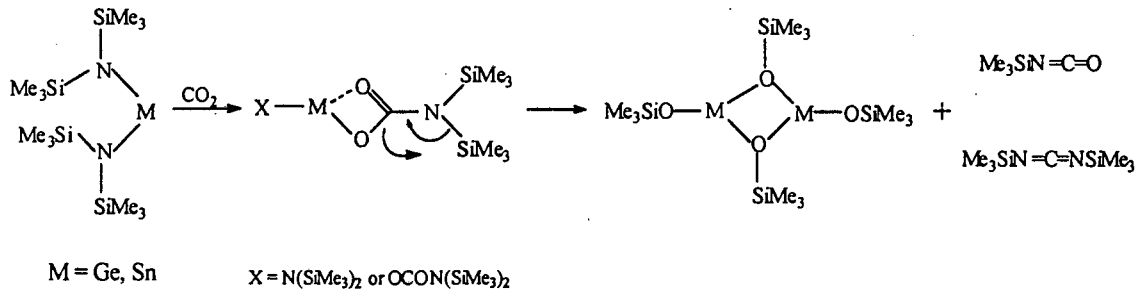

Scheme 1.25.

The insertion of CO_2 into the Pd—N bond of *trans*-[PdPh(PMe$_3$)$_2$(NHPh)] gives *trans*-[PdPh(PMe$_3$)$_2$(O$_2$CNHPh)] [112].

The dialkyl carbamato complexes [M(O$_2$CNR$_2$)$_n$] (M = Nb or Ta, R = Et, n = 5; M = Nb, R = Et or ^{i}Pr, n = 4) have been prepared from the corresponding metal chlorides with CO_2 and HNR$_2$ in toluene [113]. The reaction of [Pd(η^3-allyl)Me(PPh$_3$)] with diethylamine under an atomsphere of CO_2 has been reported to give a dinuclear complex [{Pd(PPh$_3$)}$_2$(μ-η^3-C$_3$H$_5$)(μ-O$_2$CNEt$_2$)] in 63% yield [114]. The dimethyl complexes [PdMe$_2$L$_2$] (L = tertiary phosphine) react with CO_2 and dialkylamines HNRR′ (R, R′ = H, alkyl and phenyl) to give the corresponding carbamate complexes [PdMe(O$_2$CNRR′)L$_2$] [115]. These reactions may be better regarded as ligand substitutions rather than CO_2 insertions because the formation of the carbamate complexes may go *via* the routes shown in Scheme 1.26 [23].

$$R_2NH + CO_2 \rightleftharpoons R_2NCOOH \xrightarrow[-\,HNR_2]{[L_nM\text{-}NR_2]} [L_nM\text{-}O_2CNR_2]$$

Scheme 1.26

1.4.4 Insertion of CO_2 into the M—P bond

Only two examples for the insertion of CO_2 into an M—P bond are available [116,117]. The insertion of CO_2 into both the M—N and the M—P bonds of the complexes [1,2-M$_2$(NMe$_2$)$_4$(P^{t}Bu$_2$)$_2$] (M = Mo and W) yields initially [1,2-M$_2$(O$_2$CNMe$_2$)$_2$(O$_2$CP^{t}Bu$_2$)$_2$(NMe$_2$)$_2$] (M = Mo and W) [116,117]. The molybdenum compound is labile to ligand exchange reactions in solution to yield [Mo$_2$(O$_2$CP^{t}Bu$_2$)$_4$]•2C$_6$H$_6$, a compound having a Mo-Mo quadruple bond supported by a paddle-wheel arrangement of four phosphinocarboxylate ligands that support the Mo-Mo bond [116,117].

$$[1,2\text{-}M_2(NMe_2)_4(PR_2)_2] + CO_2 \longrightarrow [M_2(O_2CNMe_2)_2(O_2CPR_2)_2(NMe_2)_2]$$

M = Mo, W; R = ^{t}Bu

Scheme 1.27

1.4.5 Insertion of CO_2 into the M—Si bond

The insertion of CO_2 into the Zr—Si bond of $[Cp_2Zr(\eta^2\text{-}SiMe_2{=}N^tBu)(PMe_3]$ has been observed at low temperature (using $^{13}CO_2$) leading to the formation of *cyclo*-$[Cp_2Zr\{OC(=O)SiMe_2N^tBu\}]$, which decomposes at 25 °C to give CO and the dimerization product as shown in Scheme 1.28 [118].

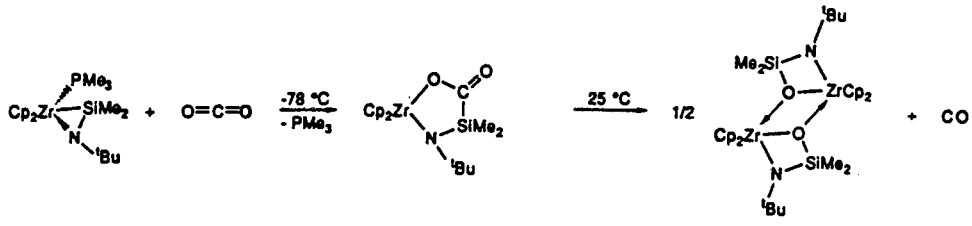

Scheme 1.28

The insertion of CO_2 into the Sc—Si bond of $[Cp_2Sc(SiR_3)(THF)]$ [R = $(SiMe_3)_3$ and $^tBuPh_2$] occurs readily to form the dimeric silanecarboxylate complexes $[Cp_2Sc(\mu\text{-}O_2CSiR_3)]_2$. The crystal strucuture of the complex where R = $SiMe_3$ has been reported [119].

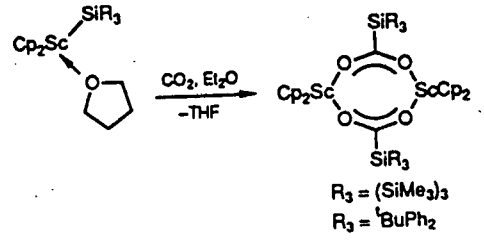

Scheme 1.29

1.4.6 Insertion of CO_2 into the metal-metal (M—M′) bond

Activation of CO_2 by simultaneous interaction with electron rich and electron deficient metal centres is of continuous interest. The concept of bifunctional CO_2 activation was first pioneered by Floriani and Fachinetti in 1974 [120]. Recently Cutler and co-workers have showed the first examples of direct insertion of CO_2 into the early—late-transition-metal bond [121]. The insertion of CO_2 into the M—Zr bond (M = Fe, Ru) of $[Cp(CO)_2M\text{-}Zr(Cl)Cp_2]$, forming the μ-

$\eta^1(C):\eta^2(O,O')$ compounds $[Cp(CO)_2M\text{-}CO_2\text{-}Zr(Cl)Cp_2]$, may involve a bifunctional CO_2 activation step as shown below [121].

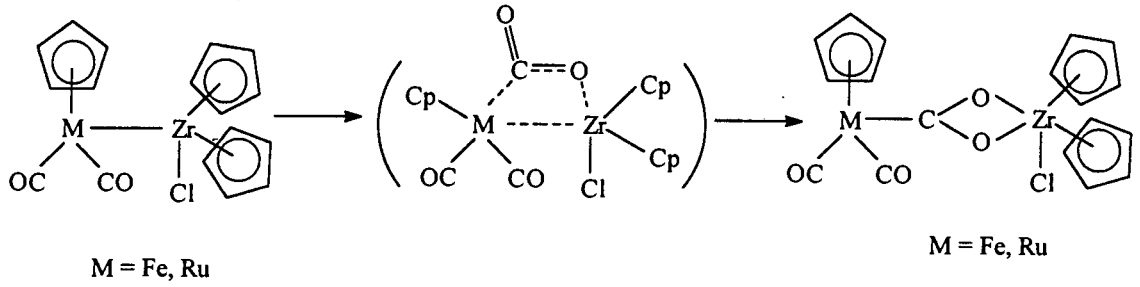

Scheme 1.30

A series of CO_2-bridged heterobimetallic complexes of the type $[LM\text{-}CO_2\text{-}L'M']$ are known, though most of them have been prepared by other routes [23,27,122]. Recently, Bergman and co-workers [84] have reported another direct insertion of CO_2 into an M—M′ bond, namely the Ir—Zr bond of the complex $[Cp_2Zr(\mu\text{-}N^tBu)IrCp^*]$, to give the unique heterobimetallic complex $[Cp_2Zr(\mu\text{-}N^tBu)(\mu\text{-}OC(O)IrCp^*]$ as shown in Scheme 1.31. The crystal structure of the complex $[Cp_2Zr(\mu\text{-}N^tBu)(\mu\text{-}OC(O)IrCp^*]$ has been determined [84].

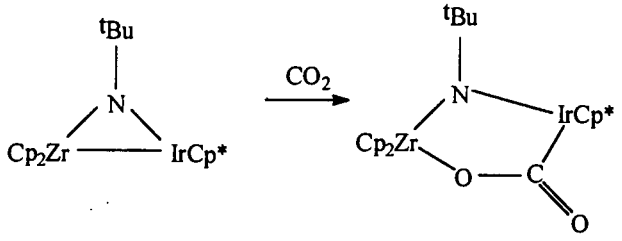

Scheme 1.31

1.4.7 Insertion of CO_2 into the M—C bond

This insertion reaction is of paramount importance in the utilization of CO_2 as a source of carbon [5,11,12,22-26]. There are two possible modes of CO_2 insertion into the M—C bond of a complex; the normal insertion leads to the formation of a carboxylate complex and the inverse insertion (or abnormal insertion) to the formation of a 1-metalated formate ester (or alkoxycarbonyl complex), as shown in Scheme 1.32.

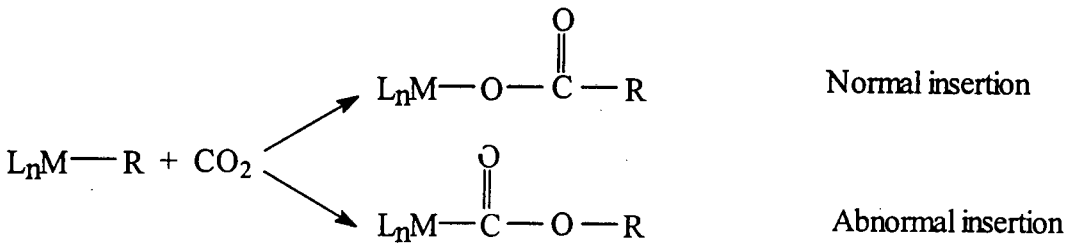

Scheme 1.32

Recent reviews of the results on CO_2 insertion into the M—C bond have covered the work up to 1993 [22-26]. Therefore, only the most recent results will be presented.

The reaction of CO_2 with [$Cp_2Ti(\eta^3$-allyl)] complexes (isolated or prepared *in situ*) takes place in a highly regioselective manner to give the β,γ-unsaturated carboxylic acid as the sole regioisomer (see Scheme 1.33) [123].

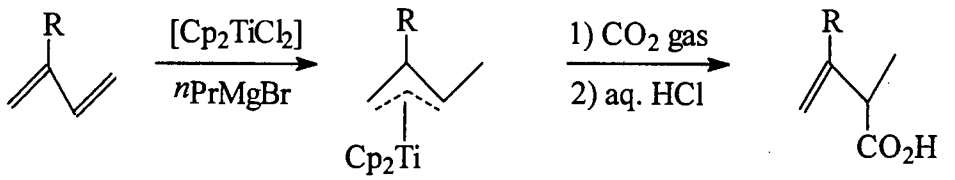

Scheme 1.33

Cyclopentadiene can also be used to prepare 2-cyclopentene-1-carboxylic acid *via* the same process. Replacement of the achiral Cp ligands of [Cp_2TiCl_2] with chiral ligands neomenthyl-η^5-cyclopentadienyl (NMCp) results in asymmetric CO_2 fixation to produce chiral β,γ-unsaturated carboxylic acids [123].

The insertion of CO_2 into the Ti—C bond of the acetylene complexes [$Cp_2Ti(PMe_3)(C_2H_2)$] and [$Cp_2Ti(C_2Me_2)$] gives the five-membered metallacycles as shown in Scheme 1.34 [124,125].

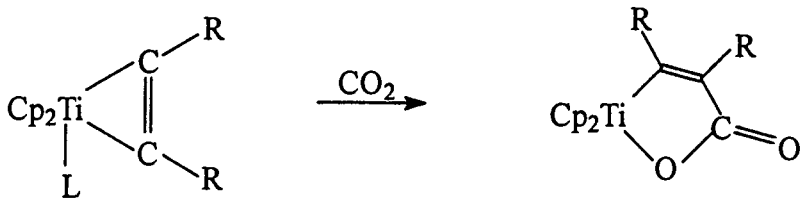

R = H, L = PMe_3
R = Me, L = None

R = H or Me

Scheme 1.34

In the interaction of the tolane complex [CpCp*Ti(PhC_2Ph)] with CO_2, the insertion of a CO_2 molecule into the Ti—C bond of the titanacyclopropene ring takes place with the formation of the titanafuranone metallacycle as shown in Scheme 1.35 [126].

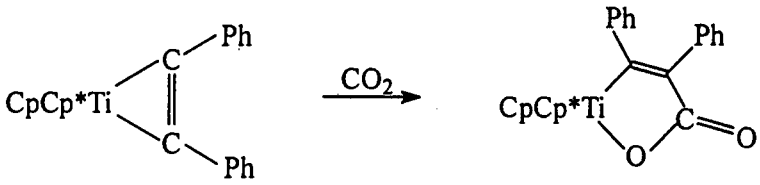

Scheme 1.35

The reaction of CO_2 with tolane, bis(trimethylsilyl)acetylene and phenyl(trimethylsilyl)acetylene complexes of titanocene [$Cp_2Ti(R^1C_2R^2)$ ($R^1 = R^2$ = Ph; $R^1 = R^2 = SiMe_3$; R^1= Ph, $R^2 = SiMe_3$) results in the displacement of *ca.* 0.5 mole of free acetylene with the formation of the unusual binuclear alkenylcarboxylate complexes of trivalent titanium [$Cp_2TiC(R^1)=C(R^2)$-$C(O)OTiCp_2$] as shown in Scheme 1.36 [127,128].

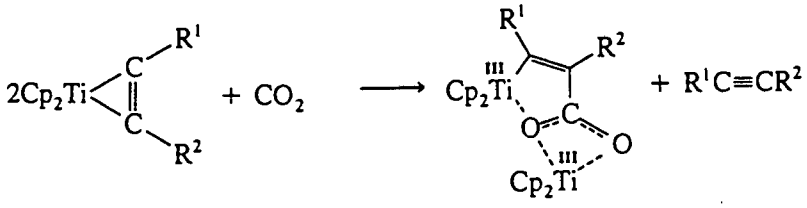

Scheme 1.36

In the interaction of CO_2 with the bis(trimethylsilyl)acetylene complex $[Cp^*_2Ti(Me_3SiC_2SiMe_3)]$, full displacement of bis(trimethylsilyl)acetylene from the titanium coordination sphere takes place and CO_2 undergoes disproportionation to form $[Cp^*_2Ti(CO)_2]$ and the binuclear carbonate complex $[\{Cp^*_2Ti\}_2CO_3]$ [128,129] (see Scheme 1.37). The structure of $[\{Cp^*_2Ti\}_2CO_3]$ has been established by an X-ray diffraction study [128]. These studies of the reactivity of the titanium complexes with CO_2 have demonstrated [124-129] that the ligands play a significant role in directing the reaction pathways of these complexes.

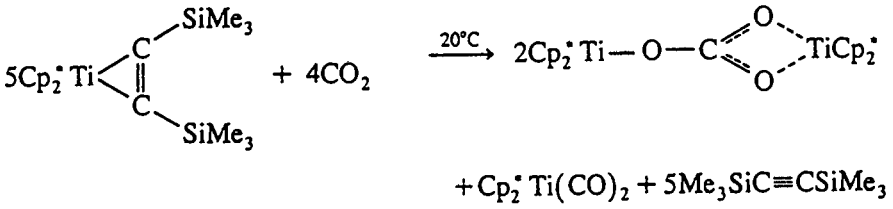

Scheme 1.37

The zirconium bis(trimethylsilyl)acetylene complex $[Cp_2Zr(THF)(Me_3SiC_2SiMe_3]$ readily reacts with CO_2 at room temperature to form the dimeric zirconafuranone metallacycle [130] (see Scheme 1.38).

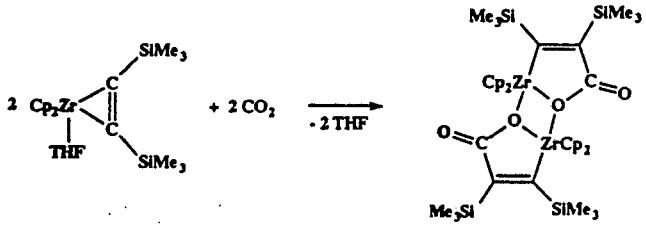

Scheme 1.38

The insertion of CO_2 into the Zr—C bond of the complex **[VIII]** gives the product **[IX]** in low yield [131].

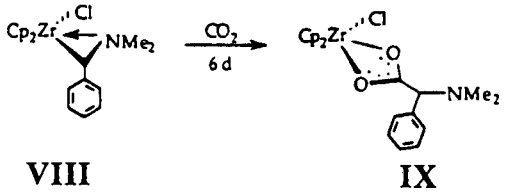

VIII **IX**

Scheme 1.39

Treatment of the zirconium porphyrin dimethyl complex [Zr(OEP)Me_2] (OEP = dianion of octaethylporphyrin) with CO_2 generates the acetate complex [Zr(OEP)$(OAc)_2$] [132]. The reaction proceeds rapidly in the dark. Controlled experiments with radical traps indicate that no radicals are involved in this reaction. Recently, the insertion of CO_2 into the Zr—C bond of the heterobimetallic complex [$Cp(PMe_3)_2RuCH{=}CHZr(Cl)Cp_2$] has been reported [133] to produce the carboxylate complex [$Cp(PMe_3)_2RuCH{=}CHCO_2Zr(Cl)Cp_2$].

The insertion of CO_2 into the V—C bonds of [$V(Mes)_3(THF)$] (Mes = 2,4,6-$Me_3C_6H_2$) gives the tris(carboxylate) derivative $[V(O_2CMes)_3]_n$ [134]. The reaction of the tris(iminoacyl) complex [$V\{\eta^2$-$C(Mes){=}N^tBu\}_3$] with CO_2 leads to the double insertion of CO_2 into the V—C bonds with the formation of the complex [**X**] [135]. The complex [**X**] has been characterized by X-ray crystallography.

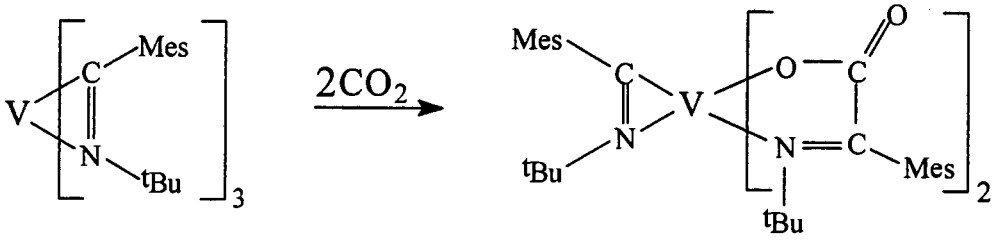

X

Scheme 1.40

A series of interesting compounds containing coordinated alkyl groups and CO_2 [$Cp'_2Nb(\eta^2$-$CO_2)R$] (R = CH_3, CH_2Ph, CH_2CMe_3, CH_2SiMe_3), have been reported [136]. These complexes may serve as model complexes for the intermediates of the CO_2 insertion into M—C bonds. The complexes [$Cp'_2Nb(\eta^2$-$CO_2)R$] can be prepared by sodium amalgam reduction of the corresponding alkyl chloride derivatives [$Cp'_2Nb\ Cl_2\ R$] in the presence of CO_2 [136]. Alternatively, these complexes can be made by aerobic oxidation of the corresponding metal carbonyl complexes [137]. The η^2-CO_2 coordination mode in the complex [$Cp'Nb(\eta^2$-$CO_2)(CH_2Ph)$] has been confirmed by X-ray crystallography [136].

The thermal and photochemical decarbonylation rather than insertion was observed for the complex $[Cp'_2Nb(\eta^2\text{-}CO_2)CH_3]$ [136, 138,139]. Recent studies of the reactivity of the complexes $[Cp'_2Nb(\eta^2\text{-}CO_2)R]$ (R = CH_3, CH_2Ph, CH_2CMe_3, CH_2SiMe_3) reveal that the reaction courses significantly depend on the nature of the alkyl group [136]. Although there is no report of the successful insertion of the ligand CO_2 into the Nb—R bond so far, a model complex $[Cp'_2Nb\{(\eta^2\text{-}(O,O')O_2CMe\}]$ (for the formal insertion of CO_2 into the Nb-R bond) has been reported [85].

The insertion of CO_2 into the M—C bond (M = Cr, Mo, W) of some neutral and anionic compounds has been summarized in earlier reviews [22-26]. Recent studies have shown that the 16-valence electron diaryl complex $[Cp^*W(NO)Ph_2]$ undergoes CO_2 insertion to give the η^2-carboxylate complex $[Cp^*W(NO)(\eta^2\text{-}O_2CPh)Ph]$ [140].

The rhodium ethylene complex $[Rh(bipy)(C_2H_4)Cl]$ reacts slowly with CO_2 at room temperature in THF to give a brown solid, which has been postulated as the metallacycle shown below [141].

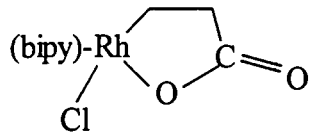

The reaction of the Ni(0) naphthalyne complex $[Ni(\eta^2\text{-}C_{10}H_6)L_2]$ (L_2 = dcpe) with CO_2 gives the CO_2 inserted product as shown in Scheme 1.41 [142]. The analogous cyclohexyne complex $[Ni(\eta^2\text{-}C_6H_8)L_2]$ (L_2 = dcpe) alsc undergoes CO_2 insertion to give the five-membered metallacycle complex. Dimethylacetylenedicarboxylate inserts into the Ni—C σ bond of the metallacycle complex to give the seven-membered metallacycle as shown in Scheme 1.42 [143].

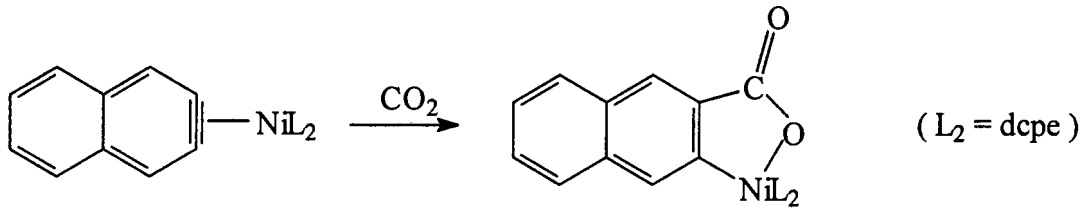

Scheme 1.41

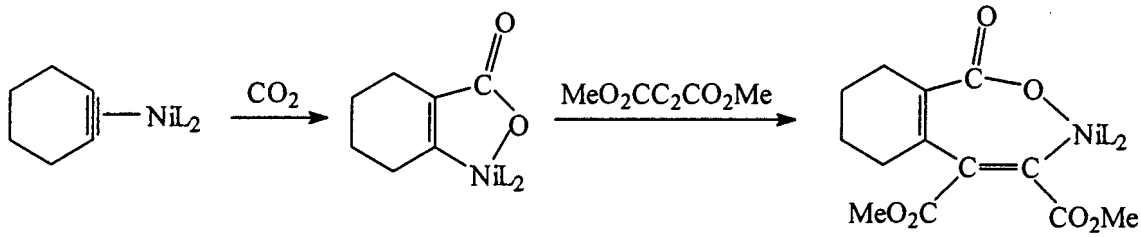

(L_2 = dcpe)

Scheme 1.42

The carboxylation of the phenyl ligand of [NiBrPh(bipy)] with CO_2 in DMF gives a mixture of benzoic acid and biphenyl after acid hydrolysis. This reaction is proposed to involve the insertion of CO_2 into the Ni—aryl bond [144].

1.5 Conclusion

The knowledge of CO_2 binding and activation has considerably increased since the first stable CO_2 complex $[Ni(CO_2)(PCy_3)_2]$ was structurally characterized more than two decades ago. Different binding modes of CO_2 in mononuclear and polynuclear metal complexes have been characterized and spectroscopic methods are available to distinguish between them. Binding of CO_2 to a metal centre leads to a net electron transfer from the metal to the LUMO of CO_2 and thus leads to its activation. Accordingly, coordinated CO_2 undergoes reactions that are impossible for free CO_2.

Many stoichiometric and most catalytic reactions involving CO_2 activation proceed *via* formal insertion of CO_2 into highly reactive M—E bonds with the

formation of new C—E bonds. These reactions do not necessarily require coordination of CO_2 as in stable complexes, but are generally initiated by nucleophilic attack of E at the Lewis acidic carbon atom of CO_2. Weak interaction between the metal and the lone pairs of one oxygen atom of CO_2 may play a role in supporting the insertion process.

It may be necessary to emphasise that only if we understand the underlying principles of CO_2 activation, the goal to use CO_2 as an environmentally friendly and economically feasible source of carbon may be achieved. Although we are more knowledgable about CO_2 activation, the effective activation of CO_2 by transition metal complexes is still a goal that is hard to reach and remains an exciting research area in organometallic chemistry.

1.6 Objectives, scope and approach of this thesis

The objectives of this thesis are to synthesize a wide range of new organometallic complexes and to investigate their reactivity towards CO_2, in attempts to convert CO_2 into useful products. Another aspect of this thesis is the synthesis of model complexes which could be derived from CO_2 insertion into a metal—carbon bond, and the investigation of the chemistry of these model complexes. This could provide us with useful information on the chemistry of CO_2-containing complexes and provide guidance on the selection of possible candidates for CO_2 activation.

Our approach includes (1) the synthesis and isolation of mononuclear, homo- and hetero-binuclear, and poly-nuclear complexes containing metal—carbon bond(s); (2) the characterization of these complexes with multi-nuclear magnetic resonance spectroscopy (including ^{1}H, ^{13}C, ^{31}P and ^{195}Pt NMR), infrared and ultraviolet-visible spectroscopy, mass spectroscopy, differential scanning calorimetry and thermal gravimetric analysis, cyclic voltammetry, and elemental analysis; and (3) the reactivity of these complexes with CO_2. Some other reactions of the new complexes are also discussed.

In Chapter 1 of the thesis, recent developments in the activation of carbon dioxide by metal complexes are discussed. Since this field is being very actively pursued many of the references are from the literature of the last few years.

Chapter 2 describes the synthesis and reactivity of new manganese alkoxycarbonyl complexes $[Mn(CO)_5\{C(O)OR\}]$. which are formal products of insertion into the Mn-C bond of $[Mn(CO)_5R]$. Chapter 3 describes related alkyl and acyl complexes as well as the reactivity of a tungsten carbyne complex with CO_2.

The theme throughout the thesis is an investigation of the interaction of CO_2 with a range of metal complexes containing metal-carbon bonds, which can be either single, double or triple bonds. Mononuclear, binuclear and polynuclear complexes are all prepared and their reactions with CO_2 are investigated.

In Chapter 4, this theme is continued with the synthesis of Pt(II) and Pt(IV) alkyl compounds and a study of their reactivity with CO_2.

Chapter 5 describes the reactivity of haloalkyl and hydroxyalkyl complexes of rhenium and tungsten, which are used to prepare some polynuclear complexes, and dendrimers described in Chapter 6. These syntheses were carried out to investigate their reactivity with CO_2. This was done because CO_2 may interact with polynuclear complexes in ways not possible for mononuclear complexes.

References

1. B. Hileman, Chem. Eng. News., November 27, 1995, p18.
2. P.S. Zurer, Chem. Eng. News., March 13, 1995, p27.
3. K.A. Magrini and D. Boron, Chemistry and Industry, 1994, 997.
4. J.C.M. Farla, C.A. Hendriks and K. Blok, Climatic Change, 1995, **29**, 436.
5. X. Yin, J. of Environmental Sciences, 1995, **7**, 129.
6. J.H. Edwards, Catalysis Today, 1995, **23**, 59.
7. M.M. Halmann, *Chemical Fixation Of Carbon Dioxide - Methods For Recycling CO_2 Into Useful Products*, CRC Press: Boa Raton, FL. 1993.
8. B.P. Sullivan, K. Krist and H.E. Guard, Eds., *Electrochemical And Electrocatalytic Reactions Of Carbon Dioxide*, Elsevier: Amsterdam, 1993.
9. (a) S. Inoue and N. Yamazaki, Eds., *Organic And Bioorganic Chemistry Of Carbon Dioxide*, Wiley and Sons: New York, 1982.
   (b) M. Aresta and J.V. Schloss, Eds., *Enzymatic And Model Carboxylation And Reduction Reactions For Carbon Dioxide Utilization*, NATO ASI Series C314, Kluwer Academic: Dordrecht, 1990.
10. J. Costamagna, G. Ferraudi, J. Canales and J. Vargas, Coord. Chem. Rev., 1996, **148**, 221.
11. P. Braunstein, D. Matt and D. Nobel, Chem. Rev., 1988, **88**, 747.
12. D. Walther, Coord. Chem. Rev., 1987, **79**, 135.
13. P. G. Jessop, T. Ikariya and R. Noyori, Chem. Rev., 1995, **95**, 259.
14. D.J. Darensbourg, M.W. Holtcamp, Coord. Chem. Rev., 1996, **153**, 155.
15. W. Leitner, Angew. Chem. Int. Ed. Engl., 1995, **34**, 2207.
16. X. Yin and C.Y. Wang, Shiyou Huagong, 1993, **22**, 557.
17. W. Leitner, Coord. Chem. Rev., 1996, **153**, 257.
18. R.J. Haines, S. Afr. J. Chem., 1994, **47**, 112.
19. J.P. Collman, L.S. Hegedus, J.R. Norton and R.G. Finke, *Principles And Applications Of Transition Metal Chemistry*, 2nd. edn., University Science Books: Mill Valley, CA, 1987, Chapter 3.
20. D.A. Palmer and R. van Eldik, Chem. Rev., 1983, **83**, 651.

21. P.A. Vigato, S. Tamburini and D.E. Fenton, Coord. Chem. Rev., 1990, **106**, 25.
22. K.K. Pandey, Coord. Chem. Rev., 1995, **140**, 37.
23. A. Behr, Angew. Chem. Int. Ed. Engl., 1988, **27**, 661.
24. R.P.A. Sneeden, in *Comprehensive Organometallic Chemistry,* Eds., G. Wilkinson, F.G.A. Stone and E.W. Abel, Pergamon: New York, 1982, vol. 8, chapter 50.4, p225.
25. A Behr, in *Catalysis in C_1 Chemistry*, Ed. W. Keim, D. Reidel Publ. Co.: Dordrecht, 1983, p 169.
26. M. E. Vol'pin and I.S. Kolomnikov, Pure Appl. Chem., 1973, **33**, 567.
27. D. H. Gibson, Chem. Rev., 1996, **96**, 2063.
28. X. Yin, C. Wang, L. Yin and Y. Ji, Tianranqi Huagong, 1992, **17**, 16.
29. A. Dedieu, C. Bo and F. Ingold, in *Metal-Ligand Interactions: From Atoms, To Clusters, To Surfaces*, Eds., D. R. Salahub and N. Russo, Kluwer Academic: Dordrecht, 1992, p 175.
30. J.C. Calabrese, T. Herskovitz and J.B. Kinney, J. Am. Chem. Soc., 1983, **105**, 5914.
31. M. Aresta and C.F. Nobile, J. Chem. Soc. Chem. Commun., 1975, 636.
32. G.S. Bristow, P.B. Hitchcock and M.F. Lappert, J. Chem. Soc. Chem. Commun., 1981, 1145.
33. S. Sakaki, K. Mine, D. Taguchi and T. Arai, Bull. Chem. Soc. Jpn., 1993, **66**, 3289.
34. H. Masuda, N. Fukushima and H. Einaga, Bull. Chem. Soc. Jpn., 1993, **66**, 3643.
35. S. Sakaki, Organometallic News, 1992, 70.
36. S. Sakaki and Y. Musashi, Inorg. Chem., 1995, **34**, 1914.
37. S. Sakaki and K. Ohkubo, Inorg. Chem., 1988, **27**, 2020.
38. M. Rosi, A. Sgamellotti, F. Tarantelli and C. Floriani, J. Organomet. Chem., 1987, **332**, 153.
39. C. Mealli, R. Hoffmann and A. Stockis, Inorg. Chem., 1984, **23**, 56.
40. S. Sakaki and A. Dedieu, Inorg. Chem., 1987, **26**, 3278.

228, C21.

(b) H. Hoberg and D. Schaefer, J. Organomet. Chem., 1982, **238**, 383.

57. H. Hoberg, D. Schaefer, G. Burkhart, C. Krüger and M.J. Romão, J. Organomet. Chem., 1984, **266**, 203.

58. H. Hoberg, Y. Peres, C. Krüger and Y-H. Tsay, Angew. Chem. Int. Ed. Engl., 1987, **26**, 771.

59. H. Hoberg and A. Ballesteros, J. Organomet. Chem., 1991, **411**, C11.

60. H. Hoberg, A. Ballesteros and A. Sigan, J. Organomet. Chem., 1991, **403**, C19.

61. H. Hoberg, Y. Peres and A. Milchereit, J. Organomet. Chem., 1986, **307**, C38.

62. H. Hoberg, A. Ballesteros, A. Sigan, C. Jegat and A. Milchereit, Synthesis, 1991, 395.

63. H. Hoberg, A. Ballesteros, A. Sigan, C. Jégat, D. Bärhausen and A. Milchereit, J. Organomet. Chem., 1991, **407**, C23.

64. H. Hoberg and D. Schaefer, J. Organomet. Chem., 1982, **236**, C28.

65. H. Hoberg, Y. Peres and A. Milchereit, J. Organomet. Chem., 1986, **307**, C41.

66. H. Hoberg and D. Schaefer, J. Organomet. Chem., 1983, **251**, C51.

67. D. Walther, E. Dinjus, J. Sieler, L. Andersen and O. Lindqvist, J. Organomet. Chem., 1984, **276**, 99.

68. H. Hoberg and D. Schaefer, J. Organomet. Chem., 1983, **255**, C15.

69. H. Hoberg, K. Jenni, C. Krüger and E. Raabe, Angew. Chem. Int. Ed. Engl., 1986, **25**, 810.

70. A. Behr and U. Kanne, J. Organomet. Chem., 1986, **317**, C41.

71. A. Behr, R. He, K.-D. Juszak, C. Krüger and Y.-H. Tsay, Chem. Ber., 1986, **119**, 991.

72. H. Hoberg and B. Apotecher, J. Organomet. Chem., 1984, **270**, C15.

73. H. Hoberg and B.W. Oster, J. Organomet. Chem., 1984, **266**, 321.

74. S. Cenini, F. Porta, M. Pizzotti and C. Crotti, J. Chem. Soc. Dalton Trans., 1985, 163.

75. J. Kaiser, J. Sieler, U. Braun, L. Golic, E. Dinjus and D. Walther, J. Organomet. Chem., 1982, **224**, 81.

76. R. Kempe, J. Sieler, D. Walther, J. Reinhold and K. Rommel, Z. anorg. allg. Chem., 1993, **619**, 1105.

77. T. Herskovitz and L.J. Guggenberger, J. Am. Chem. Soc., 1976, **98**, 1615.

78. D. Walther, S. Geβner, U. Ritter, A. Schmidt, K. Hamza, W. Imhof, H. Görls and J. Sieler, Chem. Ber., 1995, **128**, 281.

79. E.O. Fisher, A.C. Filippou, H.G. Alt and Thewalt, Angew. Chem. Int. Ed. Engl., 1985, **24**, 203.

80. R.B. Bedford, A.F. Hill, A.J.P. White and D.J. Williams, Angew. Chem. Int. Ed. Engl., 1996, **35**, 95.

81. B. P. Sullivan and T.J. Meyer, Organometallics, 1986, **5**, 1500.

82. M.Y. Darensbourg and C. E. Ash, Adv. Organomet. Chem., 1987, **27**, 1.

83. J. Ni, Y. Qiu, T.M. Cox, C.A. Jones, C. Berry , L. Melon and S. Bott, Organometallics, 1996, **15**, 4669.

84. T.A. Hanna, A.M. Baranger and R.G. Bergman, J. Am. Chem. Soc., 1995, **117**, 11363.

85. A. Antiñolo, M. Fajardo, S. García-Yuste, I. del Hierro, A. Otero, S. Elkrami, Y. Mourad and Y. Mugnier, J. Chem. Soc. Dalton Trans., 1995, 3409.

86. V.C. Gibson and T.P. Kee, J. Organomet. Chem., 1994, **471**, 105.

87. D. Nietlispach, H.W. Bosch and H. Berke, Chem. Ber., 1994, **127**, 2403.

88. D. Nietlispach, D. Veghini and H. Berke, Helv. Chim. Acta, 1994, **77**, 2197.

89. H. Hori, F.P.A. Johnson, K. Koike, K. Takeuchi, T. Ibusuki and O. Ishitani, J. Chem. Soc. Dalton Trans., 1997, 1019.

90. M.K. Whittlesey, R.N. Perutz and M.H. Moore, Organometallics, 1996, **15**, 5166.

91. C. Becker, L. Dahlenburg and S. Kerstan, Zeitschrift f'ur Naturforschung: Section B. A Journal of Chemical Sciences, 1993, **48B**, 577.

92. P.G. Jessop, Y. Hsiao, T. Ikariya and R. Noyori, J. Chem. Soc. Chem. Commun., 1995, 707.

93. P.G. Jessop, Y. Hsiao, T. Ikariya and R. Noyori, J. Am. Chem. Soc., 1994, **116**, 8851.

94. O. Kröcher, R.A. Köppel and A. Baiker, J. Chem. Soc. Chem. Commun., 1996, 1497.

95. E. Graf and W. Leitner, Chem. Ber., 1996, **129**, 91.

96. W, Leitner, E. Dinjus and F. Gaβner, J. Organomet. Chem., 1994, **475**, 257.

97. F. Hutschka, A. Dedieu, M. Eichberger, R. Fornika and W. Leitner, J. Am. Chem. Soc., 1997, **119**, 4432.

98. T. Burgemeister, F. Kastner and W. Leitner, Angew. Chem. Int. Ed. Engl., 1993, **32**, 739.

99. F. Gassner and W. Leitner, J. Chem. Soc. Chem. Commun., 1993, 1465.

100. B.P. Buffin, A.M. Arif and T.G. Richmond, J. Chem. Soc. Chem. Commun., 1993, 1432.

101. D.J. Darensbourg, K.M. Sanchez, J. H. Reibenspies and A.L Rheingold, J. Am. Chem. Soc., 1989, **111**, 7094.

102. D.J. Darensbourg, B.L. Mueller, C.J. Bischoff, S.S. Chojnacki and J.H. Reibenspies, Inorg. Chem., 1991, **30**, 2418.

103. D.J. Darensbourg, B.L. Mueller and J.H. Reibenspies, J. Organomet. Chem., 1993, **451**, 83.

104. S.K. Mandal, D.M. Ho and M. Orchin, Organometallics, 1993, **12**, 1714.

105. S.J. Lippard and J.H. Berg, *Principles of Bioinorganic Chemistry*, University Science Books: Mill Valley, CA., 1994, p270.

106. N. Kitajima, S. Hikichi, M. Tanaka and Y. Moro-oka, J. Am. Chem. Soc., 1993, **115**, 5496.

107. C. Bazzicalupi, A. Bencini, A. Bianchi, F. Corana, V. Fusi, C. Giorgi, P. Paoli, P. Paoletti, B. Valtancoli and C. Zanchini, Inorg. Chem., 1996, **35**, 5540.

108. L.R. Sita, J.R. Babcock and R. Xi, J. Am. Chem. Soc., 1996, **118**, 10912.

109. P. Gómez-Sal, A.M. Irigoyen, A.Martín, M. Mena, M. Monge and C. Yélamos, J. Organomet. Chem., 1995, **494**, C19.

110. P. Legzdins, S.J. Rettig and K.J. Ross, Organometallics, 1994, **13**, 569.

111. S. Ciruelos, T. Cuenca, R. Gómez, P. Gómez-Sal, A. Manzanero and P. Royo, Organometallics, 1996, **15**, 5577.

112. J.M. Boncella and L.A. Villanueva, J. Organomet. Chem., 1994, **465**, 297.

113. P.B. Arimondo, F. Calderazzo, U. Englert, C. Maichle-Mössmer, G. Pampaloni and J. Strähle, J. Chem. Soc. Dalton Trans., 1996, 311.

114. T-I. Son, Y-J. Kim, and C-H. Kim, Kongop Hwahak, 1995, **6**, 747; Chem. Abstr. 1996, **124**: 87308.

115. R.S. Srivastava, G. Singh, M. Nakano, K. Osakada, F. Ozawa and A. Yamamoto, J. Organomet. Chem., 1993, **451**, 221.

116. W.E. Buhro, M.H. Chisholm, K. Folting and J.C. Huffman, Inorg. Chem., 1987, **26**, 3087.

117. W.E. Buhro, M.H. Chisholm, J.D. Martin, J.C. Huffman, K. Folting and W.E. Streib, J. Am. Chem. Soc., 1989, **111**, 8149.

118. L.J. Procopio, P.J. Carroll and D.H. Berry, Organometallics, 1993, **12**, 3087.

119. B.K. Campion, R.H. Heyn and T.D. Tilley, Inorg. Chem., 1990, **29**, 4356.

120. C. Floriani and G. Fachinetti, J. Chem. Soc. Chem. Commun., 1974, 615.

121. J.R. Pinkes, B.D. Steffey, J.C. Vites and A.R. Cutler, Organometallics, 1994, **13**, 21.

122. J.R. Pinkes, C.J. Masi, R. Chiulli, B.D. Steffey and A.R. Cutler, Inorg. Chem., 1997, **36**, 70.

123. Y. Gao, S. Iijima, H. Urabe and F. Sato, Inorg. Chim. Acta, 1994, **222**, 145.

124. H.G. Alt, G.S. Herrmann, M.D. Rausch and D.T. Mallin, J. Organomet. Chem., 1988, **356**, C53.

125. H.G. Alt and G.S. Herrmann, J. Organomet. Chem., 1990, **390**, 159.

126. B. Demerseman, R. Mahe and P.H. Dixneuf, J. Chem. Soc. Chem. Commun., 1984, 1394.

127. V.V. Burlakov, A.V. Polyakov, A.I. Yanovsky, Y. T. Struchkov, V.B. Shur, M.E. Vol'pin, U. Rosenthal and H. Gorls, J. Organomet. Chem., 1994, **476**, 197.

128. V.V. Burlakov, F.M. Dolgushin, A.I. Yanovsky, Y.T. Struchkov, V.B. Shur, U. Rosenthal and U. Thewalt, J. Organomet. Chem., 1996, **522**, 241.

129. V.V. Burlakov, U. Rosenthal, F.M. Dolgushin, A.I. Yanovskii, Y.T. Struchkov, O.G. Ellert, V.B. Shur and M.E. Vol'pin, Organometallic Chemistry in the USSR, 1992, **5**, 593.

130. U. Rosenthal, A. Ohff, M. Michalik, H. Görls, V.V. Burlakov and V.B. Shur, Organometallics, 1993, **12**, 5016.

131. D.A. Gately, J.R. Norton and P.A. Goodson, J. Am. Chem. Soc., 1995, **117**, 986.

132. H. Brand and J. Arnold, Organometallics, 1993, **12**, 3655.

133. F.R. Lemke and R.M. Bullock, Organometallics, 1992, **11**, 4261.

134. M. Vivanco, J. Ruiz, C. Floriani, A. Chiesi-Villa and C. Rizzoli, Organometallics, 1993, **12**, 1794.

135. J. Ruiz, M. Vivanco, C. Floriani, A. Chiesi-Villa and C. Rizzoli, Organometallics, 1993, **12**, 1811.

136. P. Fu, M.A. Khan and K.M. Nicholas, J. Organomet. Chem., 1996, **506**, 49.

137. P. Fu, M.A. Khan and K.M. Nicholas, J. Am. Chem. Soc., 1992, **114**, 6579.

138. P. Fu, M.A. Khan and K.M. Nicholas, Organometallics, 1991, **10**, 382.

139. P. Fu, M.A. Khan and K.M. Nicholas, Organometallics, 1992, **11**, 2607.

140. E.B. Brouwer, P. Legzdins, S.J. Rettig and K.J. Ross, Organometallics, 1993, **12**, 4234.

141. M. Aresta and E. Quaranta, J. Organomet. Chem., 1993, **463**, 215.

142. M.A. Bennett, D.C.R. Hockless and E. Wenger, Organometallics, 1995, **14**, 2091.

143. M.A. Bennett, J.A. Johnson and A.C. Willis, Organometallics, 1996, **15**, 68.

144. K. Osakada, R. Sato and T. Yamamoto, Organometallics, 1994, **13**, 4645.

Chapter 2

Synthesis, Characterization And Reactivity Of Long Chain Alkoxycarbonyl Complexes Of The Type [$Mn(CO)_5${C(O)OR}]

2.1 Introduction

The study of transition metal alkoxycarbonyl complexes [L_nM{C(O)OR}] (L_nM is the metal and associated ligands) is interesting, since alkoxycarbonyl complexes are the formal product of CO_2 insertion into the metal-carbon bond of alkyl complexes [L_nMR] as shown below:

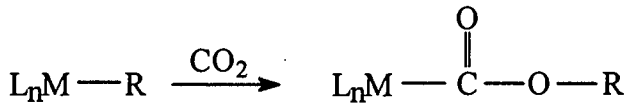

Scheme 2.1

Although the insertion of CO_2 into the M—C bond generally yields the "normal" insertion product (see Scheme 1.32 of Chapter 1), the "abnormal" insertion of CO_2 into the Co—ethyl bond of [$Co(PPh_3)_2(CO)(Et)$] to give the alkoxycarbonyl species, in additional to the "normal" insertion product, has also been postulated by Vol'pin and Kolomnikov [1]. These authors have reported that the reaction of the alkoxycarbonyl species, the "abnormal" insertion product, with methyl iodide affords ethyl acetate.

The insertion of CO_2 into the Mn—CH_2 bond of 2,2,2,2-tetracarbonyl-1,1-diphenyl-1-phospha-2-manganacyclobutane has been reported [2] to give the manganacarbonyl complex as shown in Scheme 2.2.

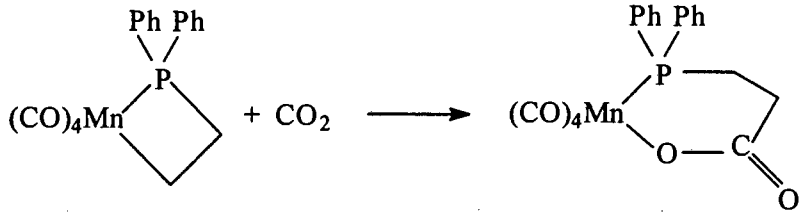

Scheme 2.2

The insertion of CO_2 into the metal-carbon bond of metal alkyl complexes is of great importance as this represents a means of CO_2 activation [1].

In addition, alkoxycarbonyl complexes have been proposed or identified as intermediates in the catalytic conversion of CO_2, H_2 and MeOH to give methyl formate HCO_2Me [3-6]. It has been reported that the anionic ruthenium complex $[Ru(CO)_3Cl_3]^-$ catalyzes the formation of methyl formate from CO_2, H_2 and MeOH in the presence of a strong base such as $KOCH_3$. From basic methanol solution, a dinuclear salt $[N(PPh_3)_2][Ru_2(CO)_4(CO_2CH_3)_2(OCH_3)Cl_2]$, which contains two μ_2-η^2-$OCOCH_3$ bridges, has been isolated [6].

The study of transition metal alkoxycarbonyl complexes $[L_nM\{C(O)OR\}]$ is also very important, because these complexes have been recognized as intermediates and/or products in a number of important heterogeneous and homogeneous catalytic processes [7-16], such as hydroformylation and hydrocarboxylation of olefins [7-11], carbonylation of alcohols and alkyl halides [7,12-16], homogeneous Fischer-Tropsch synthesis [8], synthesis of alkyl carbonates and of oxalate esters [14]. The formation of heptyl formate from hydroformylation of 1-hexene, catalyzed by $[Co_2(CO)_8]$ with added tertiary phosphine PR_3, has been reported to involve the alkoxycarbonyl cobalt intermediate $[Co(CO)_3(CO_2R)L]$ (L = PR_3) [9].

A few alkoxycarbonyl complexes $[Mn(CO)_5\{C(O)OR\}]$ have been reported in the literature [17-21]. The ethoxycarbonyl complex $[Mn(CO)_5\{C(O)OC_2H_5\}]$ was first prepared from $Na[Mn(CO)_5]$ and ethyl chloroformate $ClCO_2C_2H_5$ [17]. This complex was also synthesized by the reaction of $[Mn(CO)_5\{C(O)CH_3\}]$ with syngas (CO/H_2) [18]. The hexyloxycarbonyl complex $[Mn(CO)_5\{C(O)OC_6H_{13}\}]$ was similarly prepared by the reaction of $[Mn(CO)_5\{C(O)C_5H_{11}\}]$ with syngas [18]. The complexes $[Mn(CO)_5\{C(O)OR\}]$ (R = *n*-C_9H_{19} [20] and *n*-$C_{14}H_{29}$ [21]) were prepared by the reaction of $[Mn(CO)_5R]$ (R = *n*-C_8H_{17} and *n*-$C_{13}H_{27}$) with syngas in hexane but these complexes were not isolated pure and not fully characterized [20,21].

We now report our studies (1) on the synthesis of long chain alkoxycarbonyl complexes $[Mn(CO)_5\{C(O)OR\}]$ (R = CH_2R') by the reaction of the acyl complexes $[Mn(CO)_5\{C(O)R'\}]$ (R' = *n*-C_6H_{13} to *n*-C_9H_{19}, *n*-$C_{11}H_{23}$, and *n*-$C_{15}H_{31}$) with syngas; (2) on some reactions of $[Mn(CO)_5\{C(O)OR\}]$; and (3) on reactions of the alkyl complexes $[Mn(CO)_5R]$ and $[Re(CO)_5R]$ with CO_2 in attempts to prepare alkoxycarbonyl complexes directly by the insertion of CO_2 into the metal alkyl bond of $[Mn(CO)_5R]$.

2.2 Synthesis and characterization of acyl complexes $[Mn(CO)_5\{C(O)R'\}]$ and alkoxycarbonyl complexes $[Mn(CO)_5\{C(O)OR\}]$

2.2.1 Synthesis of acyl complexes $[Mn(CO)_5\{C(O)R'\}]$

The acyl complexes $[Mn(CO)_5\{C(O)R'\}]$ (where R' = *n*-C_6H_{13} to *n*-C_9H_{19}, *n*-$C_{11}H_{23}$, and *n*-$C_{15}H_{31}$) were synthesized according to the following route:

$$[Mn_2(CO)_{10}] \xrightarrow[THF]{Na/Hg} Na[Mn(CO)_5] \xrightarrow{ClC(O)R'} [Mn(CO)_5\{C(O)R'\}]$$

Scheme 2.3

These acyl complexes have been reported by Andersen and Moss [22]. A modification of the previous procedure was used for the synthesis of $[Mn(CO)_5\{C(O)C_{11}H_{23}\}]$ (see experimental section). The IR, ^1H and ^{13}C NMR data are in good agreement with the data reported [22]. In addition to the previous ^{13}C NMR data, we have also observed the carbon resonance of the acyl carbon (C=O) of these long chain acyl complexes at δ 257 ppm in $CDCl_3$. The thermal properties of the acyl complex $[Mn(CO)_5\{C(O)C_{11}H_{23}\}]$ have been studied by Differential Scanning Calorimetry (DSC) and Thermal Gravimetric Analysis (TGA). The DSC and TGA traces for the complex $[Mn(CO)_5\{C(O)C_{11}H_{23}\}]$ are shown in Figure 2.1.

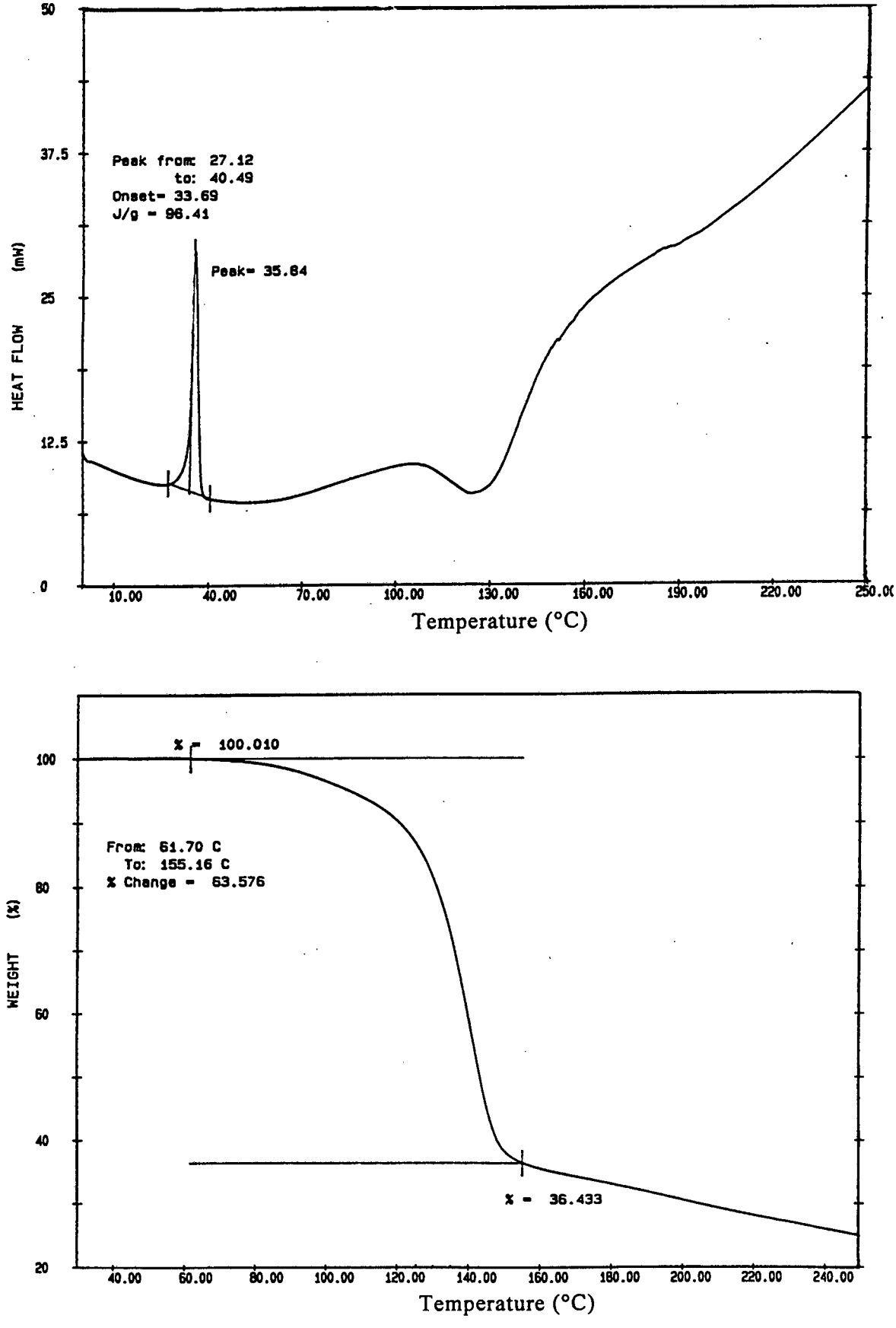

Figure 2.1 DSC (upper trace) and TGA (lower trace) for the acyl complex $[Mn(CO)_5\{C(O)C_{11}H_{23}\}]$ at a scan rate of 10 °C/minute.

The DSC trace of $[Mn(CO)_5\{C(O)C_{11}H_{23}\}]$ at a heating rate of 10°C/minute showed a sharp endothermic peak at T_{max}(endo) = 36 °C and a broad exothermic peak at T_{max}(exo) = 130 °C. The endothermic peak corresponds to the melting of the compound, by comparison with the hot-stage microscopy results (m.p. 27 - 30 °C). The exothermic peak is due to the decomposition of the complex, which is supported by the observation of a mass loss (64%) in the temperature range 110 - 155 °C in the TGA trace of the same compound. The mass remaining after heating to 250 °C corresponds to the decomposition of the complex to MnO_2.

2.2.2 Synthesis of the alkoxycarbonyl complexes $[Mn(CO)_5\{C(O)OR\}]$ (R = CH_2R') by the reaction of $[Mn(CO)_5\{C(O)R'\}]$ with syngas in hexane

The long chain alkoxycarbonyl manganese pentacarbonyl complexes of the type $[Mn(CO)_5\{C(O)OR\}]$ (R= *n*-C_7H_{15}, **1**; *n*-C_8H_{17}, **2**; *n*-C_9H_{19}, **3**; *n*-$C_{10}H_{21}$, **4**; *n*-$C_{12}H_{25}$, **5**; and *n*-$C_{16}H_{33}$, **6**) were synthesized by the reaction of the acyl complexes $[Mn(CO)_5\{C(O)R'\}]$ with syngas in hexane as described below:

$$[Mn(CO)_5\{C(O)R'\}] + CO/H_2 \xrightarrow{\text{hexane}} [Mn(CO)_5\{C(O)OR\}]$$

***n*-R'**	***n*-R**	**Compd. no. of alkoxycarbonyl product**
C_6H_{13}	C_7H_{15}	**1**
C_7H_{15}	C_8H_{17}	**2**
C_8H_{17}	C_9H_{19}	**3**
C_9H_{19}	$C_{10}H_{21}$	**4**
$C_{11}H_{23}$	$C_{12}H_{25}$	**5**
$C_{15}H_{31}$	$C_{16}H_{33}$	**6**

Scheme 2.4

This method is similar to that reported by Sheeran and Orchin [18] for the preparation of $[Mn(CO)_5\{C(O)OR\}]$ (R = C_2H_5 and *n*-C_6H_{13}). The complexes **1-6**

are new except for **3**. The complex **3** was previously prepared by the reaction of $[Mn(CO)_5(C_8H_{17})]$ with syngas in hexane but was not isolated pure and only partially characterized [20]. The complexes **1-6** were obtained as white or off-white crystalline solids with low-melting points. The complexes **1-6** have been fully characterized by IR, ^1H and ^{13}C NMR, mass spectroscopy, melting points and elemental analyses. Satisfactory elemental analysis results were obtained for complexes **1-5**, but no satisfactory data were obtained for complex **6**. The yields, melting points, elemental analyses and observed molecular ions (from mass spectra) of these compounds are given in Table 2.1. The IR, ^1H and ^{13}C NMR, and mass spectral results will be discussed in the following section.

2.2.3 Characterization of the alkoxycarbonyl complexes $[Mn(CO)_5\{C(O)OR\}]$

IR spectroscopy

The IR spectra of the new complexes **1-6** are in good agreement with the values reported for other related $[Mn(CO)_5\{C(O)OR\}]$ complexes [17,18,20,21] and show peaks (See Table 2.2) in hexane solution at about 2124w, (A_1); 2031s, (E); 2007s cm^{-1}, (A_1); for ν(CO) terminal carbonyls; and at about 1652m and 1021m cm^{-1} for ν(C=O) acyl and ν(C-O-C), respectively. There is no significant variation in the ν(CO) upon changing the length of the alkyl chain. Thus it appears that ν(CO) is relatively insensitive to the chain length of R. The IR spectrum of **3** was also recorded in CH_2Cl_2. The IR ν(CO) peaks were found at 2126w, 2028s and 1630m cm^{-1}. Similar absorptions for **3** were observed by using Nujol mull, *i.e.* ν(CO) 2124w, 2030s, 2006s, 1647m, 1629m and 1022m cm^{-1}. The two bands at 1647 and 1629 cm^{-1} seen in the Nujol mull spectrum of the complex **3** is likely to be due to solid state effects.

Table 2.1 Data for the alkoxycarbonyl complexes [$Mn(CO)_5\{C(O)OR\}$].

Compound no	*n*-R	M[a] calc.	M^{+b} observed	Yield (%)	M.p. (°C)	Elemental analysis (%)			
						C		H	
						calc.	found	calc.	found
1	C_7H_{15}	338	338	40	51 - 53	46.15	46.25	4.44	4.46
2	C_8H_{17}	352	352	44	52 - 54	47.73	47.31	4.83	4.78
3	C_9H_{19}	366	366	47	49 - 51	49.18	48.86	5.19	5.06
4	$C_{10}H_{21}$	380	380	45	48 - 51	50.53	50.23	5.53	5.60
5	$C_{12}H_{25}$	408	408	87	54 - 55	52.95	53.69	6.17	6.42
6	$C_{16}H_{33}$	464	464	44	49 - 52	c	c	c	c

[a]: M is the calculated molecular mass.

[b]: M^+ is the molecular ion observed in the mass spectrum of the compound.

[c]: No satisfactory data were obtained.

Table 2.2 IR spectroscopic data for the alkoxycarbonyl complexes $[Mn(CO)_5\{C(O)OR\}]$[a].

Compound no	*n*-R	IR (cm^{-1})		
		v(C≡O)	v(C=O)	v(C-O-C)
1	C_7H_{15}	2124w, 2031s, 2007s	1652m	1022m
2	C_8H_{17}	2124w, 2031s, 2007s	1652m	1022m
3	C_9H_{19}	2124w, 2031s, 2008s	1651m	1020m
4	$C_{10}H_{21}$	2124w, 2031s, 2007s	1652m	1022m
5	$C_{12}H_{25}$	2126w, 2033s, 2010s	1654m	1021m
6	$C_{16}H_{33}$	2125w, 2031s, 2008s	1654m	1024m

[a]: IR in hexane.

^{1}H NMR spectroscopy

The ^{1}H NMR data for the complexes **1-6** reported in Table 2.3 are in good agreement with the data reported for complexes of the type $[Mn(CO)_5\{C(O)OR\}]$ [17,18,20,21]. As an example of the results obtained, the ^{1}H NMR spectrum of **3** is shown in Figure 2.2.

From the ^{1}H NMR data, it can be seen that separate resonances are observed for the α (α to CO_2) and β protons and the methyl protons of the alkyl chain in these alkoxycarbonyl complexes. These resonances are not affected by the alkyl chain length. Thus integration is the only way to distinguish these complexes by ^{1}H NMR spectroscopy. The assignments were confirmed by a COSY experiment for the complex **3** (Figure 2.3). The resonances of the α and β protons of the alkyl chain in these alkoxycarbonyl complexes shift downfield compared with the α and β protons in the starting acyl complexes [22]. This is probably due to the deshielding effect of the electron-withdrawing C(O)O group.

^{13}C NMR spectroscopy

No ^{13}C NMR data have been previously reported for the alkoxycarbonyl complexes $[Mn(CO)_5\{C(O)OR\}]$ [17-21]. We have recorded the ^{13}C NMR spectra for all the new complexes and the data are presented in Table 2.4, with possible assignments. The assignments were made by comparisons with the related acyl complexes $[Mn(CO)_5\{C(O)R\}]$ [22] and the alkoxycarbonyl complexes *fac*-$[Mn(CO)_3(dppe)\{C(O)OC_2H_5\}]$ [23] as well as by means of a heteronuclear correlation (HETCOR) experiment. As an example, the ^{13}C NMR and the HETCOR spectra of **3** are shown in Figures 2.4 and 2.5, respectively. For all the complexes, the spectra show the terminal carbonyl resonance at δ 208 ppm and the alkoxycarbonyl carbon (C=O) resonance at δ 200 ppm in $CDCl_3$ solution. In C_6D_6 solution, the resonances of the terminal carbonyl and the acyl carbon atoms are found at δ 208 and 198 ppm, respectively. To assign the ^{13}C NMR resonances of the alkyl chain, a HETCOR experiment was performed for the

Table 2.3 ^{1}H NMR data for the alkoxycarbonyl complexes [$Mn(CO)_5${C(O)OR}] (400 MHz, $CDCl_3$).

Compound no	*n*-R	$C(O)OCH_2$ $^{3}J(HH)$	$C(O)OCH_2CH_2$ $^{3}J(HH)$	$C(O)OCH_2CH_2(CH_2)_n$	CH_3 $^{3}J(HH)$
1	C_7H_{15}	4.03, 2H, br	1.59, 2H, br	1.27, 8H, br	0.87, 3H, br
2[a]	C_8H_{17}	4.05, 2H, t 6.4 Hz	1.59, 2H, qn 6.1 Hz	1.27, 10H, br	0.87, 3H, t 6.6 Hz
3	C_9H_{19}	4.04, 2H, br	1.59, 2H, br	1.26, 12H, br	0.87, 3H, br
3[b]	C_9H_{19}	4.08, 2H, br	1.48, 2H, br	1.22, 12H, br	0.91, 3H, br
4	$C_{10}H_{21}$	4.04, 2H, br	1.58, 2H, br	1.26, 14H, br	0.87, 3H, br
5	$C_{12}H_{25}$	4.03, 2H, br	1.58, 2H, br	1.25, 18H, br	0.87, 3H, br
6	$C_{16}H_{33}$	4.04, 2H, br	1.58, 2H, br	1.25, 26H, br	0.87, 3H, br

[a]: The ^{1}H NMR spectrum for this compound was recorded at 200 MHz in $CDCl_3$.

[b]: In C_6D_6.

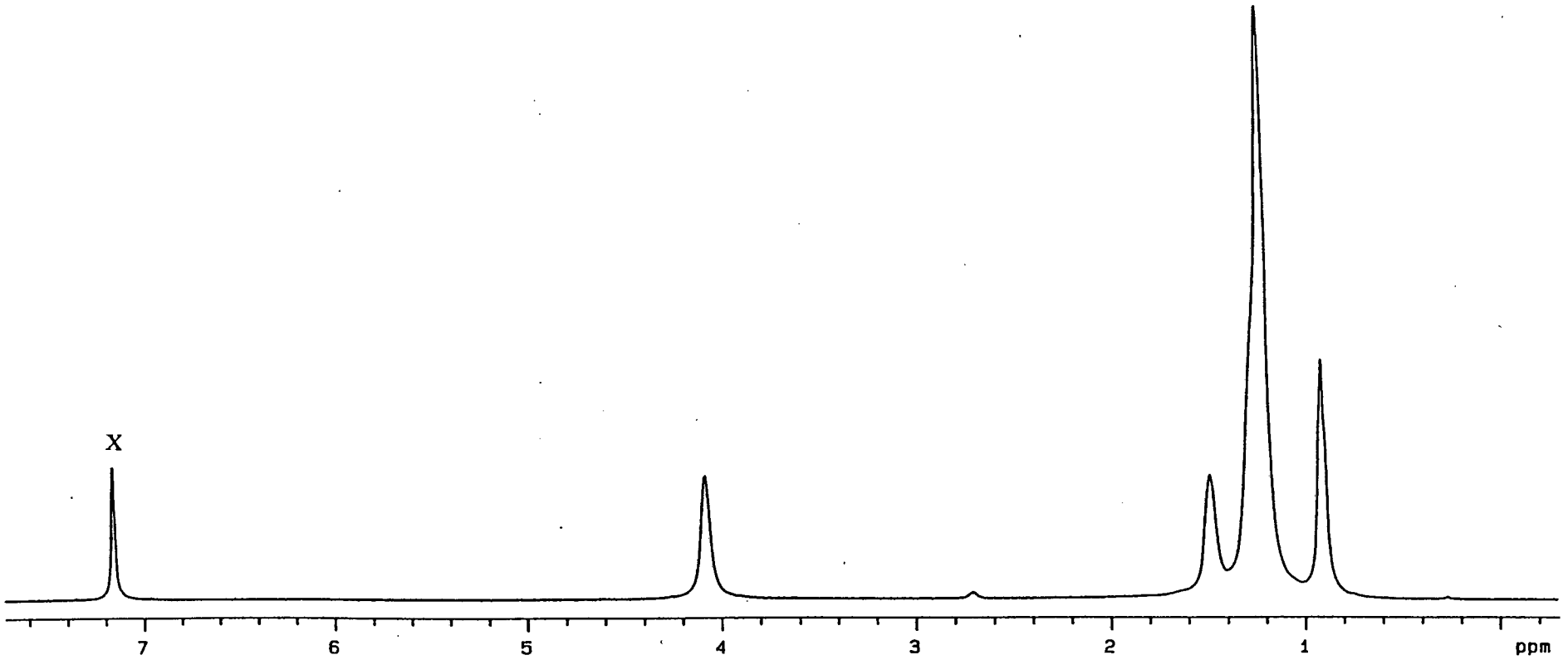

Figure 2.2 ^{1}H NMR spectrum of $[Mn(CO)_5\{C(O)OC_9H_{19}\}]$, 3 (400 MHz, C_6D_6, X = Solvent).

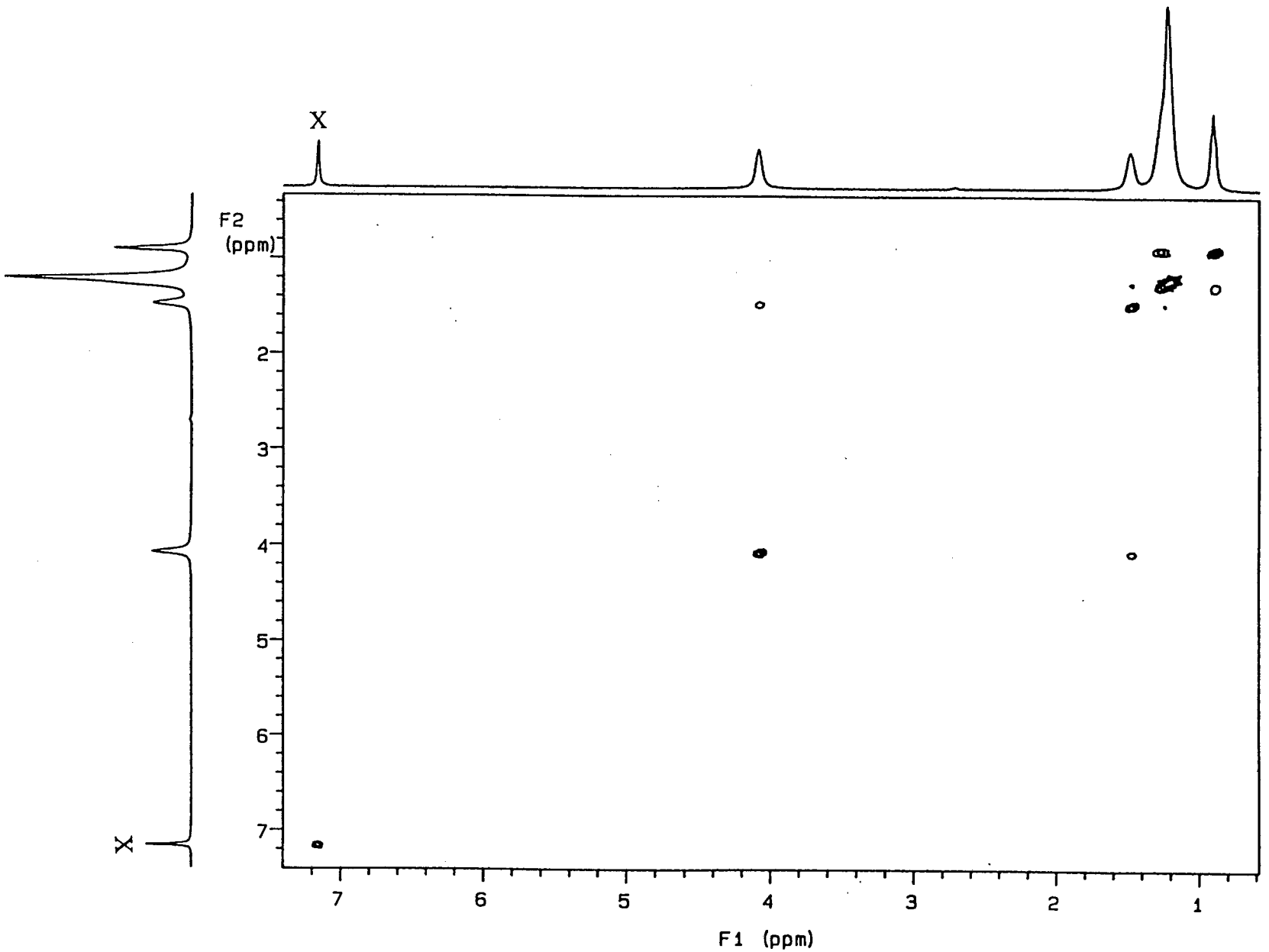

Figure 2.3 COSY spectrum of $[Mn(CO)_5\{C(O)OC_9H_{19}\}]$, 3 (400 MHz, C_6D_6, X = Solvent).

Table 2.4 ^{13}C NMR chemical shift (δ ppm) data for the alkoxycarbonyl complexes $[Mn(CO)_5\{C(O)OR\}]$ (100 MHz, $CDCl_3$).

Compd no.	*n*-R	CO *	C(O)O	OCH_2	OCH_2CH_2[a]	$OCH_2CH_2(CH_2)_n$[b]	$CH_2CH_2CH_3$	CH_2CH_3	CH_3
1	C_7H_{15}	207.84	200.30	64.54	31.75	29.08, 28.88	26.07	22.54	14.03
2[c]	C_8H_{17}	207.90	200.31	64.54	31.75	29.18, 29.09	26.11	22.61	14.01
3	C_9H_{19}	207.83	200.31	64.55	31.85	29.50, 29.20, 29.09	26.11	22.65	14.07
3[d]	C_9H_{19}	208.45	197.81	64.70	29.58	32.23, 29.91	26.45	23.06	14.31
4	$C_{10}H_{21}$	207.97	e	64.56	31.88	29.50, 29.29, 29.23, 29.09	26.12	22.66	14.08
5	$C_{12}H_{25}$	207.82	200.32	64.57	31.92	29.64, 29.56, 29.35, 29.25, 29.10	26.13	22.69	14.11
6	$C_{16}H_{33}$	207.86	200.33	64.57	31.92	29.68, 29.56, 29.35, 29.25, 29.10	26.13	22.68	14.10

[a]: The resonance for this carbon atom was assigned tentatively.

[b]: Peaks for these carbon atoms were not completely resolved or assigned.

[c]: The ^{13}C NMR spectrum for this compound was measured at 50 MHz.

[d]: In C_6D_6, the assignments were confirmed by a HETCOR experiment.

[e]: This peak was not observed.

* Two signals are observed for terminal CO's.

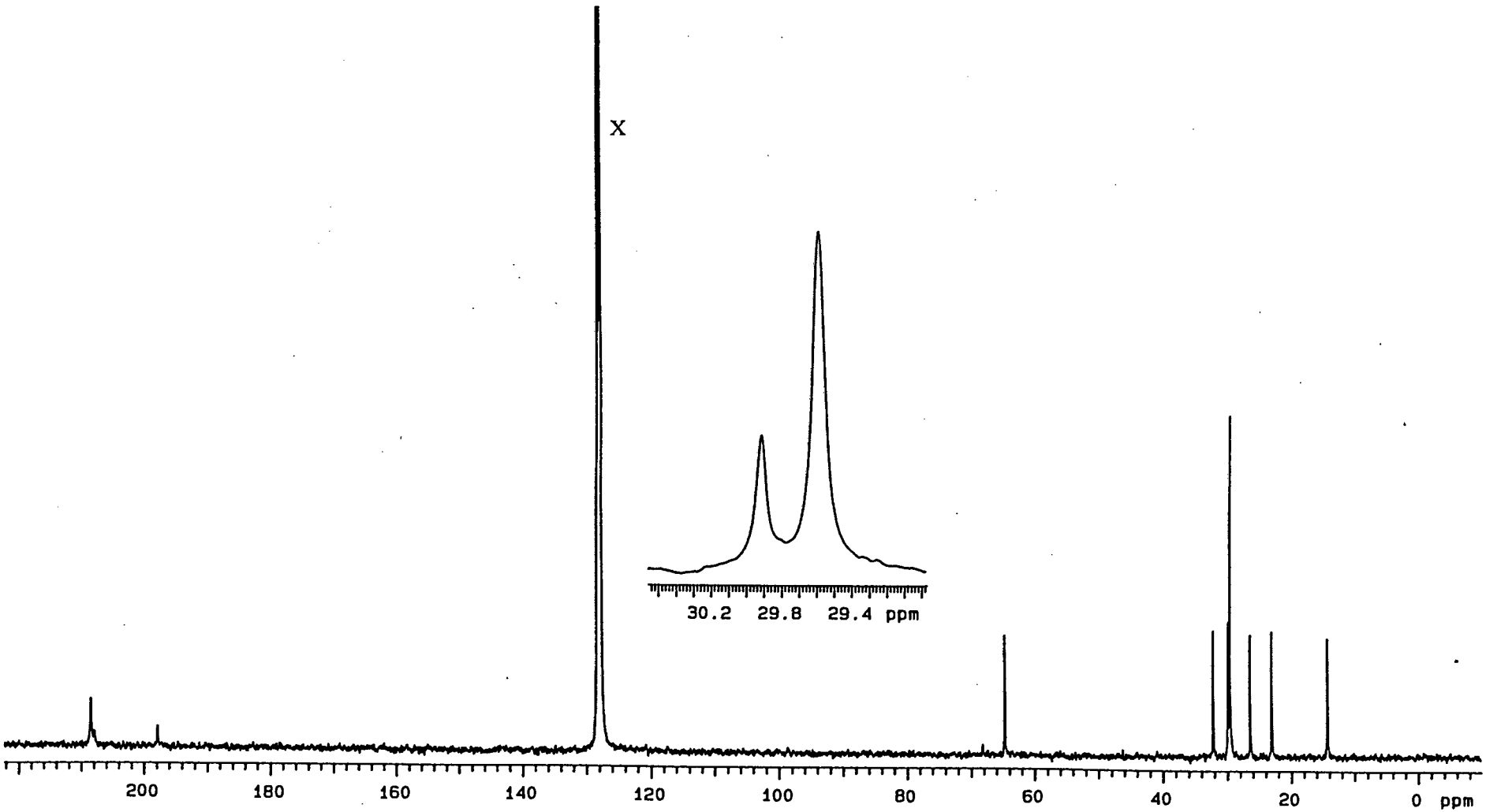

Figure 2.4 ^{13}C NMR spectrum of $[Mn(CO)_5\{C(O)OC_9H_{19}\}]$, 3 (100 MHz, C_6D_6, X = Solvent).

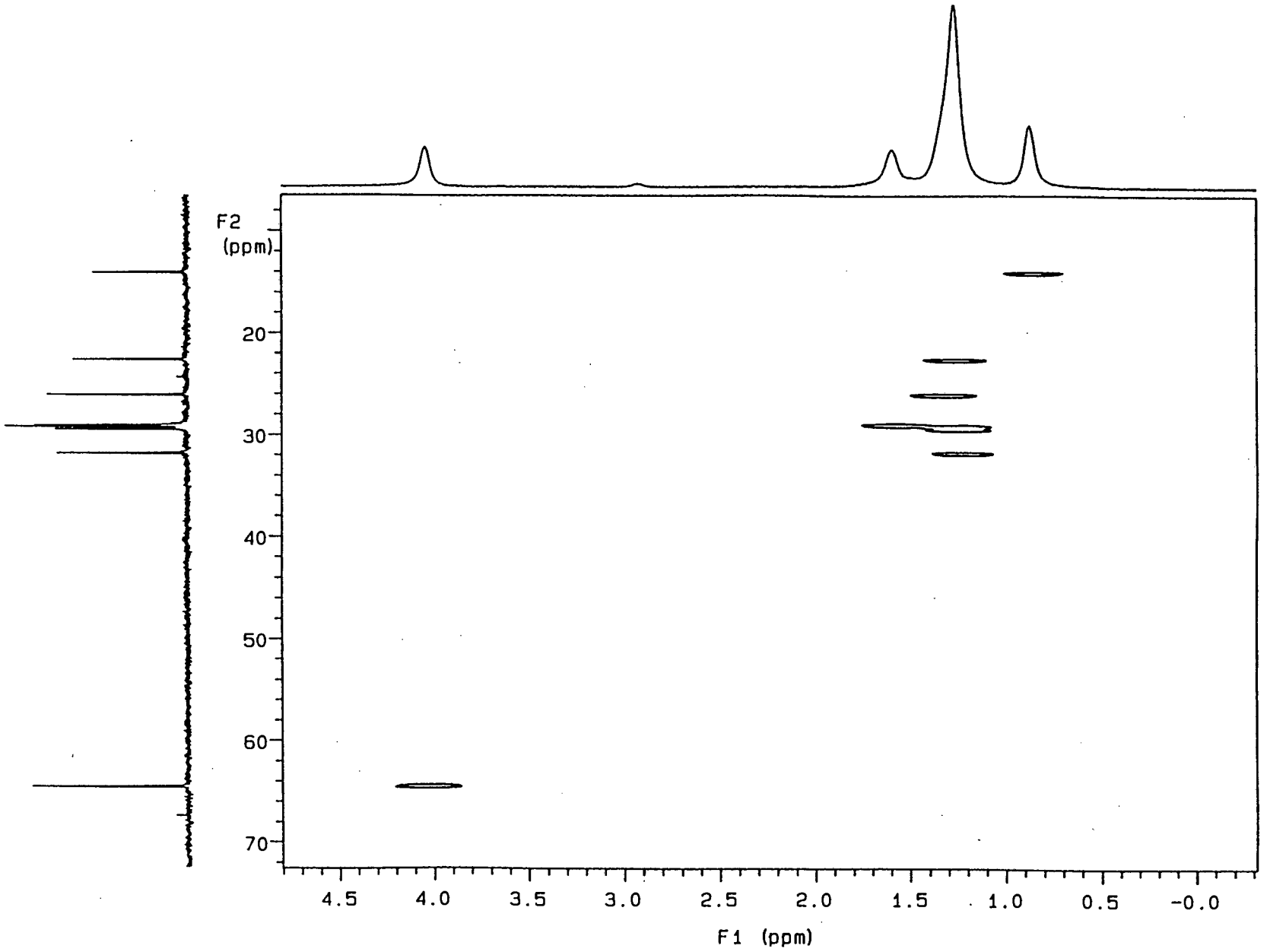

Figure 2.5 HETCOR NMR spectrum of $[Mn(CO)_5\{C(O)OC_9H_{19}\}]$, 3 ($C_6D_6$).

complex **3** in C_6D_6 solution. The HETCOR experiment confirms the assignments for the α-carbon (α to CO_2) and β-carbon as well as some other carbon atoms of the alkyl chain. The peaks due to the central methylene carbon atoms were not completely resolved and could not be assigned unambiguously, as was observed for the long chain acyl complexes [22].

The ^{13}C NMR resonances of the terminal carbonyl and alkoxycarbonyl carbons do not show any variation in chemical shift with increase in the length of the alkyl chain. By comparison with the ^{13}C NMR data of the starting acyl complexes [22], it appears that the manganese atom only affects the first two carbons of the alkyl chain.

Mass Spectra

The low resolution electron impact mass spectra for the complexes **1-6** were recorded. Molecular ions are observed for all the compounds under discussion, but are of low intensity. The intensities of the major organometallic peaks of the complexes **5** and **6** are reported in Table 2.5 with probable assignments.

All the complexes show similar fragmentation pathways. The fragmentation pathways for the complex **5** are given in Scheme 2.5. The predominant fragmentation pathway is sequential loss of carbonyl groups from the molecular ion, followed by loss of the OR group. The spectra of these complexes exhibit peaks corresponding to the ions $[Mn(CO)_6]^+$ (*m/z* 223), $[Mn(CO)_5]^+$ (*m/z* 195), $[Mn(CO)_4]^+$ (*m/z* 167) , $[Mn(CO)_3]^+$ (*m/z* 139), $[Mn(CO)_2]^+$ (*m/z* 111), $[Mn(CO)]^+$ (*m/z* 83), $[Mn]^+$ (*m/z* 55), $[CO_2]^+$ (*m/z* 44) and $[CO]^+$ (*m/z* 28).

Table 2.5 Some mass spectral data for $[Mn(CO)_5\{C(O)OR\}]$.

Ion[a]	Relative intensities[b] (%)	
	R = *n*-$C_{12}H_{25}$, **5**	R = *n*-$C_{16}H_{33}$, **6**
M	0.3	0.4
M - CO	3	2
M - 4CO	0	0.2
M - 5CO	2	1
M - 6CO	100	100
M - R	0.5	0.7
M - R - CO	1	0.2
M - R - 2CO	0.3	0.3
M - R - 3CO	0.4	0.4
M - R - 4CO	0.4	0.9
M - R - 5CO	0.5	1
M - OR	21	20
M - OR - CO	6	7
M - OR - 2CO	4	3
M - OR - 3CO	4	4
M - OR - 4CO	5	6
M - OR - 5CO	7	10
M - OR - 6CO (= Mn)	26	27

[a]: M = $[Mn(CO)_5\{C(O)OR\}]$; all ions have a single positive charge; ion refers to probable assignment.

[b]: Peak intensities are relative to [M - 6CO], *i.e.* [MnOR].

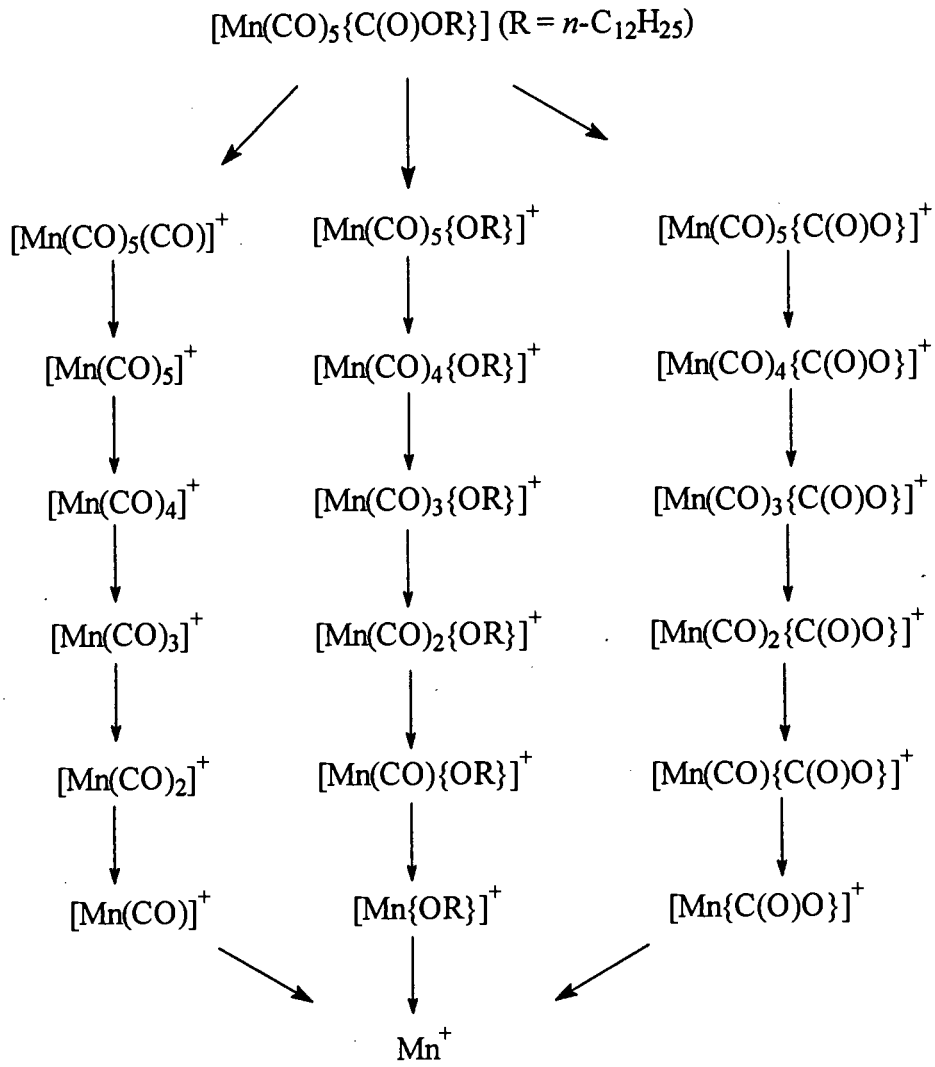

Scheme 2.5

2.2.4 Thermal properties of the alkoxycarbonyl complexes [Mn(CO)$_5${C(O)OR}]

The thermal behaviour of the complexes **1-4** and **6** were studied by DSC. The results are summarized in Table 2.6. The DSC traces of the complexes **2-4** are shown in Figure 2.6. Each trace shows a sharp endothermic peak in the temperature range which corresponds to the melting range measured by conventional means (Kofler hot stage microscope). A slight increase of the melting point (T_{max}) with the increase of alkyl chain length from n = 8 to 10 was observed. Another broad endothermic peak is observed in the DSC traces in the temperature range 103 to 140 °C, all with a maximum peak at 121-123 °C, which

corresponds to the decomposition of the complexes. This is supported by the observation of a significant mass loss in the TGA traces (Figure 2.7) of the complexes **2** and **4** over the temperature range 80-140 °C. The mass remaining after heating the complexes to 200 °C corresponds to the degradation of the alkoxycarbonyl complexes to MnO_2.

Table 2.6 Thermal analysis data for the complexes $[Mn(CO)_5\{C(O)OR\}]$.

Compound no	*n*-R	M.p. (°C)[a]	T_i (°C)[b]	T_{max} (°C)[c]	ΔH_{endo} (KJ/mol)[d]
1	C_7H_{15}	51 - 53	54.8	56.4	24.46
2	C_8H_{17}	52 - 54	52.7	54.5	21.72
3	C_9H_{19}	49 - 51	53.2	55.5	28.77
4	$C_{10}H_{21}$	48 - 51	53.5	58.0	27.46
6	$C_{16}H_{33}$	49 - 52	54.1	56.6	32.75

[a]: Determined on a Kofler hot stage microscope.

[b]: Temperature corresponding to the onset of a peak.

[c]: Temperature corresponding to the peak maximum.

[d]: Calculated by Perkin Elmer PC Series DSC7 machine (in J/g).

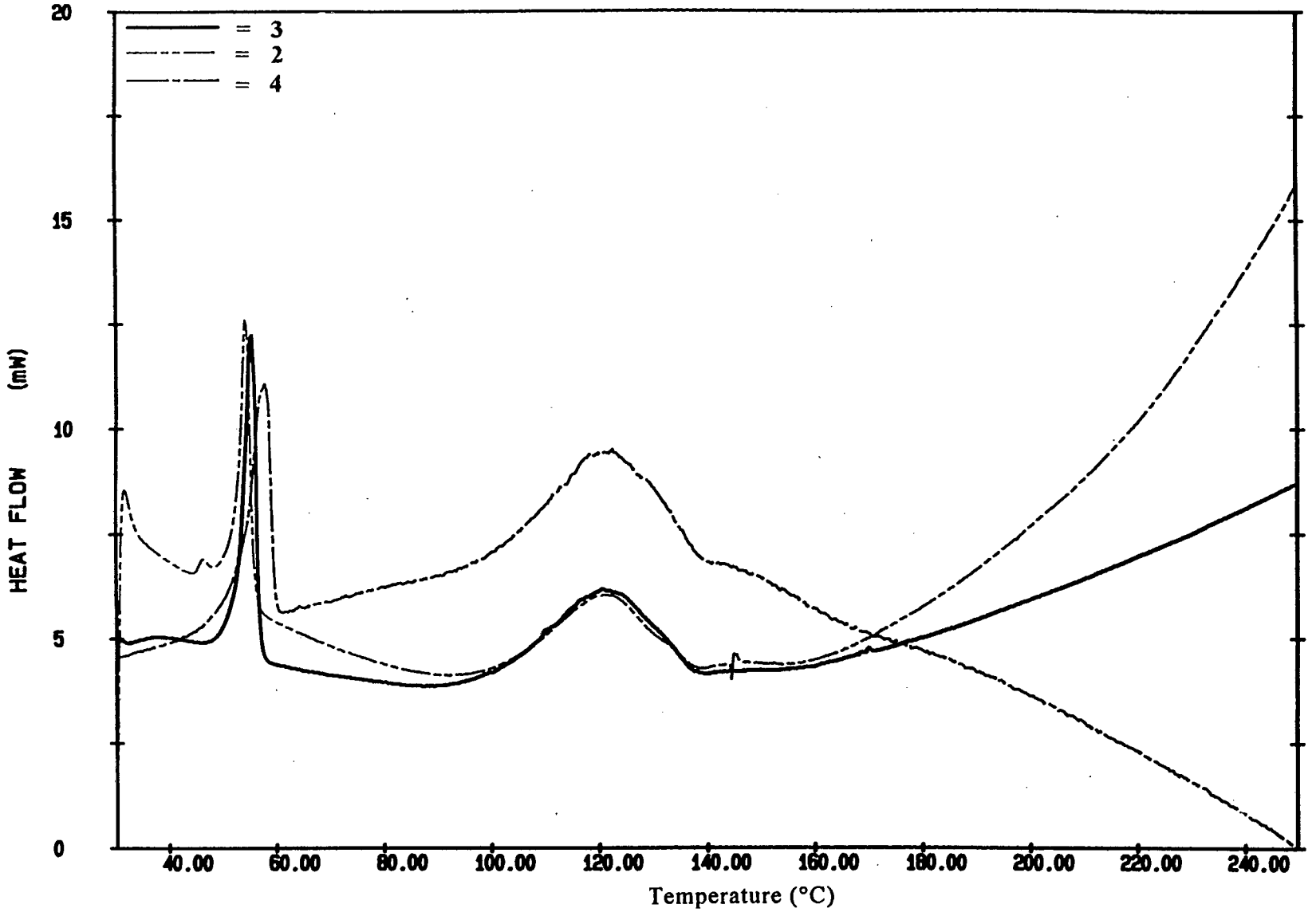

Figure 2.6 DSC traces for the alkoxycarbonyl complexes [Mn(CO)$_5${C(O)OR}] (R = *n*-C_8H_{17}, 2; *n*-C_9H_{19}, 3; and *n*-$C_{10}H_{21}$, 4) at a scan rate of 10 °C/minute.

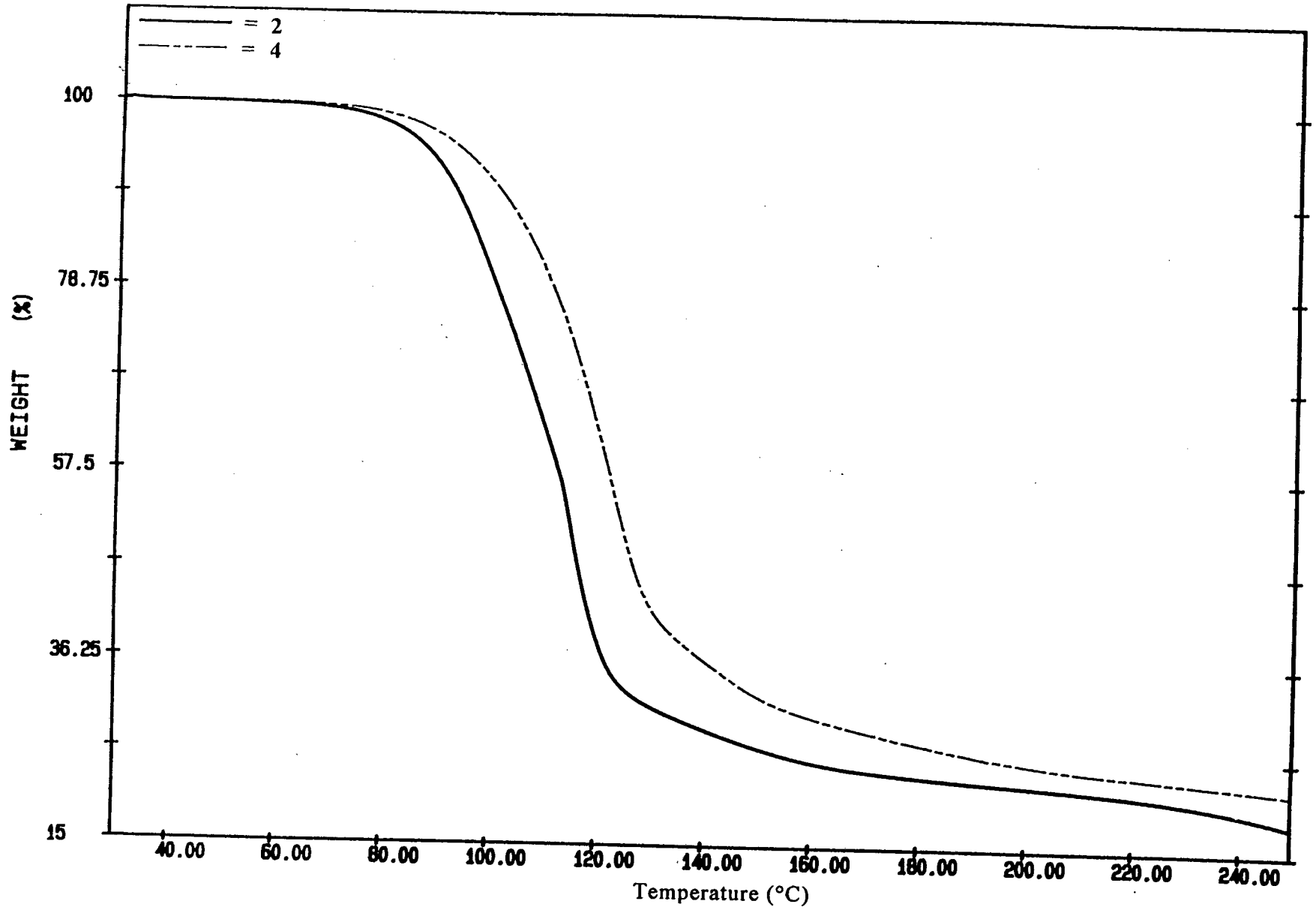

Figure 2.7 TGA traces for the alkoxycarbonyl complexes [$Mn(CO)_5\{C(O)OR\}$] (R = *n*-C_8H_{17}, 2; and *n*-$C_{10}H_{21}$, 4) at a scan rate of 10 °C/minute.

2.3 Reactivity of acyl complexes [$Mn(CO)_5\{C(O)R'\}$] and alkoxycarbonyl complexes [$Mn(CO)_5\{C(O)OR\}$]

2.3.1 Reactivity of the acyl complex [$Mn(CO)_5\{C(O)C_{11}H_{23}\}$] with syngas in THF — Synthesis of alcohol

It has been shown by us [24] and others [18,19] that the reaction of the acyl complexes [$Mn(CO)_5\{C(O)R'\}$] with syngas in hexane gives the alkoxycarbonyl complexes [$Mn(CO)_5\{C(O)OR\}$] (R = CH_2R'). The reaction of the acyl complexes [$Mn(CO)_5\{C(O)R'\}$] with syngas in the highly polar solvent sulfane gives exclusively aldehydes [25]. More recently, Moss and Andersen [21,26,27] have studied the reaction of the alkyl complexes [$Mn(CO)_5R$] with syngas in hexane, and found that alkoxycarbonyl complexes are the sole products. The reaction was repeated in THF and found to give exclusively alcohols. Therefore, Moss and Andersen have proposed that the nature of the solvent is crucial in determining the reaction product. These authors have also suggested that the acyl complexes [$Mn(CO)_5\{C(O)R\}$] are key intermediates for the reaction of alkyl complexes with syngas [26,27]. To confirm these results, we carried out the reaction of [$Mn(CO)_5\{C(O)C_{11}H_{23}\}$] with CO/H_2 in THF.

The reaction of [$Mn(CO)_5\{C(O)C_{11}H_{23}\}$] with CO/H_2 (48 bar) was carried out in freshly distilled THF in an autoclave at 60 °C for 8 hours. The reaction gave *n*-dodecanol in 92% yield as the only isolated organic product, which was identified by its melting point, mass spectrum, IR, ^1H and ^{13}C NMR. These characterization data are given in the experimental section 7.2.2. No aldehyde or formate was detected for this reaction. The organometallic product of this reaction, [$Mn_2(CO)_{10}$] was isolated by chromatographic separation (in 95% yield) and identified by IR spectroscopy.

$$2\,[Mn(CO)_5\{C(O)R\}] + 3\,H_2\,(CO) \xrightarrow{THF} [Mn_2(CO)_{10}] + 2\,RCH_2OH$$

Scheme 2.6

A small amount of $[HMn(CO)_5]$ was also detected by IR spectroscopy [28a,b]. However, this complex decomposed during separation and was not isolated.

The formation of alcohol from the reaction of $[Mn(CO)_5\{C(O)C_{11}H_{23}\}]$ with syngas in THF has provided further evidence for the previous proposal that the acyl complexes $[Mn(CO)_5\{C(O)R\}]$ are the most probable intermediates in the reactions of $[Mn(CO)_5R]$ with syngas [26,27], since the reaction of $[Mn(CO)_5R]$ with CO is known to give $[Mn(CO)_5\{C(O)R\}]$ [21].

Since different products were obtained from the reactions of acyl complexes $[Mn(CO)_5\{C(O)R\}]$ with syngas in different solvents, this suggests that the solvents play a crucial role in these reactions. The effect of the solvents could be rationalized as follows: (1) the polar, coordinating solvents such as THF might be able to protonate the acyl complex to give a hydroxycarbene species, as shown in step (a) of Scheme 2.7, which can then undergo reaction with H_2; (2) In non-polar solvents such as in hexane, the reaction might take place *via* another route, as shown in step (b) of the Scheme 2.7, to produce the alkoxycarbonyl species. The ruthenium complex (see below) containing a four-membered metallacycle similar to that of the key intermediate **A** in Scheme 2.7 has been reported [28c].

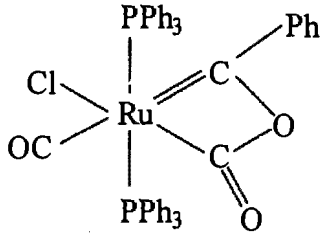

We have not yet carried out a mechanistic study of the reaction of acyl complexes $[Mn(CO)_5\{C(O)R\}]$ with syngas, however, our present results are in accordance with the proposed mechanism. This mechanism has been previously suggested by Andersen and Moss for the reaction of alkyl complexes $[Mn(CO)_5R]$ with syngas [26]. Orchin and co-workers have proposed another mechanism for the formation of $[Mn(CO)_5\{C(O)OR\}]$ [18,19]. These authors have suggested that the insertion of CO into the Mn—OR bond of intermediates $[Mn(CO)_5(OR)]$ might be the key step for the formation of $[Mn(CO)_5\{C(O)OR\}]$ [18,19]. It was not possible to

distinguish between these two mechanisms as we did not have sufficient information at this stage.

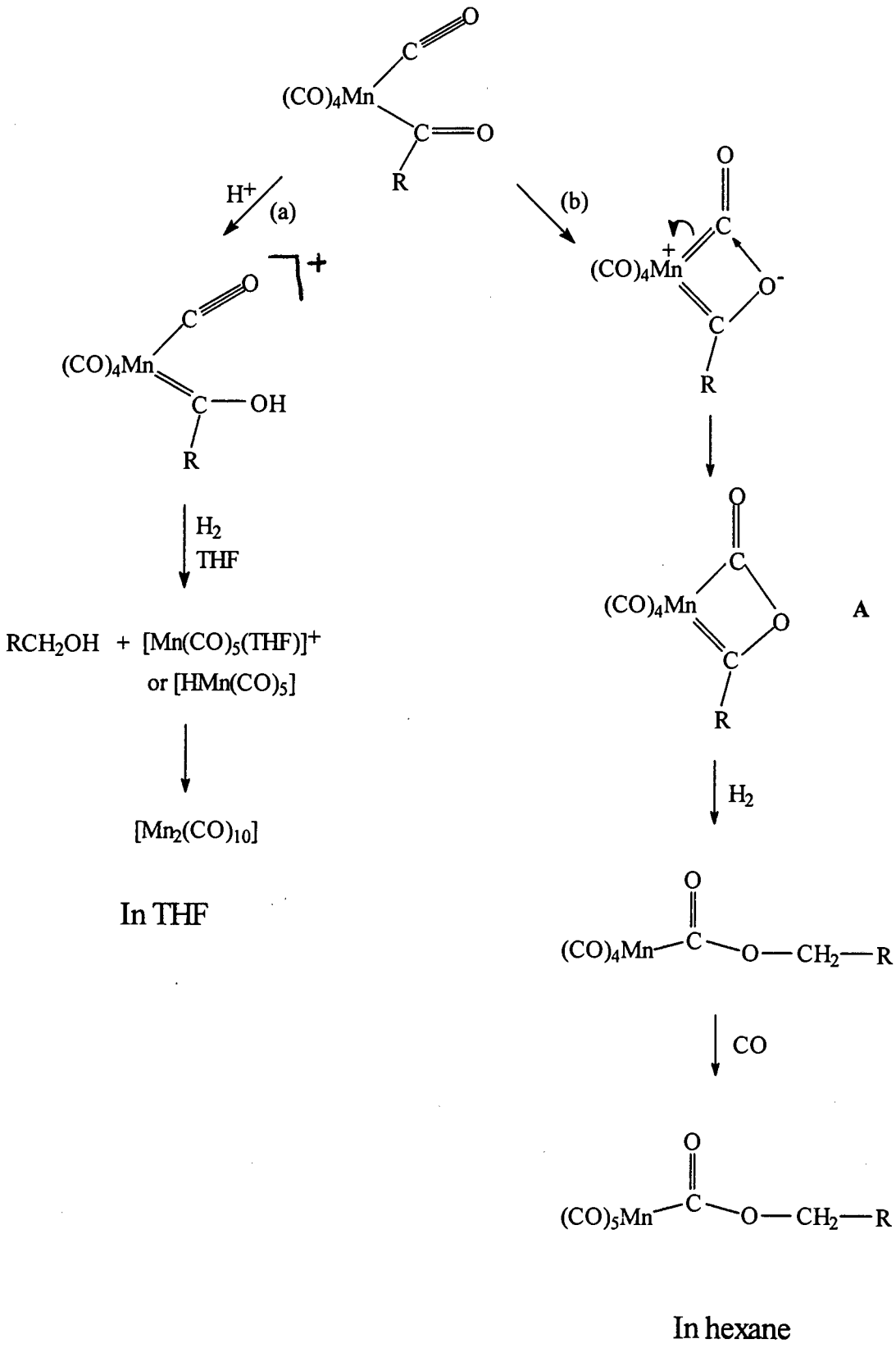

Scheme 2.7

In addition, it has been shown by Andersen and Moss that alcohols rather than aldehydes could be selectively obtained from the hydroformylation of α-olefin with $[Mn_2(CO)_{10}]$ in THF [26].

2.3.2 Reactivity of the alkoxycarbonyl complexes $[Mn(CO)_5\{C(O)OR\}]$

A general review on the reactivity of alkoxycarbonyl transition metal complexes has been published [29], which provides a broad perspective of earlier studies in this area. The reaction of the short chain alkoxycarbonyl complex $[Mn(CO)_5\{C(O)OC_2H_5\}]$ with acids is one of the more significant routes to the formation of cationic carbonyls such as $[Mn(CO)_6]^+$ (and C_2H_5OH as the organic product) [30]. It was later reported [31] that the reactions of $[Mn(CO)_5\{C(O)OC_2H_5\}]$ with $[HCo(CO)_4]$ and $[HMn(CO)_5]$ give ethyl formate and $[MnCo(CO)_9]$ and $[Mn_2(CO)_{10}]$, respectively. The reactivity of long chain $[Mn(CO)_5\{C(O)OR\}]$ complexes, especially the reactivity of these complexes under conditions similar to hydroformylation conditions, is unknown. We have studied the reaction of $[Mn(CO)_5\{C(O)OR\}]$ complexes with syngas in hexane and in THF. The reactivity of $[Mn(CO)_5\{C(O)OR\}]$ towards halogens and acids have also been investigated.

Reaction of $[Mn(CO)_5\{C(O)OC_{12}H_{25}\}]$, 5 with syngas in hexane

A solution of **5** in hexane was transferred to an autoclave pressurized with CO/H_2 to 48 bar. The reaction was carried out at 85 °C for 11 hours, and gave $[Mn_2(CO)_{10}]$ quantitatively, after column chromatography. The organic products isolated by chromatography were dodecyl formate *n*-$C_{12}H_{25}O_2CH$ in 33% yield, and dodecyl alcohol *n*-$C_{12}H_{25}OH$ in 66% yield. The identification of these organic products was made by their IR, ^1H and ^{13}C NMR, and mass spectra.

$$2\,[Mn(CO)_5\{C(O)OR\}] + H_2\,(CO) \xrightarrow{\text{hexane}} [Mn_2(CO)_{10}] + RO(O)CH + ROH$$

Scheme 2.8

The formation of the formate n-$C_{12}H_{25}O_2CH$ by the reaction of the alkoxycarbonyl complex under hydrofomylation conditions is not unexpected. In fact, formates have been reported as by-products in the Fischer-Tropsch synthesis [8,32], and alkoxycarbonyl complexes have been suggested as intermediates for the formate formation [7]. Hence, our manganese complexes may serve as model complexes for intermediates involved in the Fischer-Tropsch synthesis. The production of methyl formate from the reaction of CO_2, H_2 and MeOH might also involve the alkoxycarbonyl intermediates [6].

Reaction of $[Mn(CO)_5\{C(O)OC_{12}H_{25}\}]$, 5 with syngas in THF

Since solvents play a crucial role in product formation, we have also investigated the reaction of **5** with syngas in THF. The reaction was carried out at 60 °C for 23 hours under a pressure of 48 bar of CO/H_2. Chromatographic separation yielded $[Mn_2(CO)_{10}]$ in 63% yield. The hydride $[HMn(CO)_5]$ was detected by IR spectroscopy but this complex was not isolated owing to its decomposition. The organic products obtained by column chromatography were the alcohol n-$C_{12}H_{25}OH$ in 46% yield and the formate n-$C_{12}H_{25}O_2CH$ in 12% yield. Similar products were obtained for the reaction in hexane. In addition, another product was obtained in 43% yield. This product was identified as the ester $CH_3(CH_2)_3CO_2(CH_2)_{11}CH_3$, on the basis of its mass spectrum ($[M]^+$, 271), IR, ^1H and ^{13}C NMR.

$$2[Mn(CO)_5\{C(O)OR\}] + H_2\,(CO) \xrightarrow{THF}$$

$$[Mn_2(CO)_{10}] + RO(O)CH + ROH + CH_3(CH_2)_3C(O)OR$$

Scheme 2.9

The isolation of the ester product from the reaction of $[Mn(CO)_5\{C(O)OC_{12}H_{25}\}]$, **5** with syngas in THF strongly implied that the solvent THF reacted with **5** under these conditions. Our results show that the solvent indeed plays a crucial role in determining the nature of the products obtained from the reaction of alkoxycarbonyl complexes with syngas. We propose the following mechanism, as

shown in Scheme 2.10, to account for the products obtained in hexane and in THF. The routes (a) and (b) in Scheme 2.10 apply to the reaction in the non-polar solvent - hexane, whereas the routes (a), (b) and (c) for the reaction in the polar, coordinating solvent - THF.

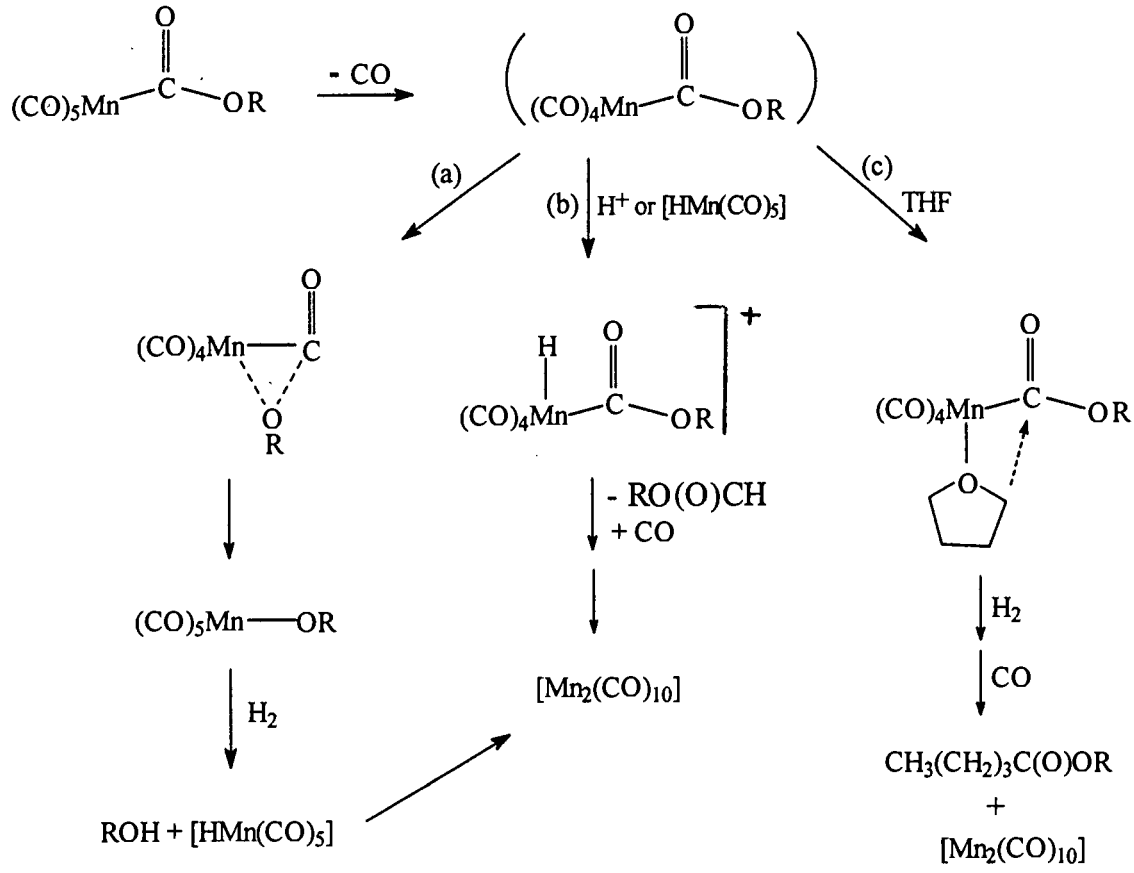

Scheme 2.10

The CO dissociation from the alkoxycarbonyl complex $[Mn(CO)_5\{C(O)OR\}]$ may form the 16-electron intermediate $[Mn(CO)_4\{C(O)OR\}]$. This species has been observed in the mass spectra of the alkoxycarbonyl complexes. The intermediate $[Mn(CO)_4\{C(O)OR\}]$ may undergo: (a) alkoxy group migration to form the alkoxy complex $[Mn(CO)_5(OR)]$, which can then be protonated; (b) proton coordination followed by elimination to yield the formate; and (c) in the presence of the coordinating ligand THF, the solvent might be coordinated to the manganese yielding the THF-coordinated intermediate $[Mn(CO)_4(THF)\{C(O)OR\}]$. The THF-coordinated species $[Mn(CO)_5(THF)]^+$ has been previously proposed [26]. Direct evidence for the formation of the

intermediate $[Mn(CO)_4(THF)\{C(O)OR\}]$ complex, however, has not been obtained.

Reaction of $[Mn(CO)_5\{C(O)OC_{12}H_{25}\}]$, 5 with tetrafluoroboric acid (HBF_4)

The reaction of **5** with HBF_4 (40% solution in water) was carried out in $CDCl_3$ in an NMR tube at room temperature. It was found that the reaction was complete in less than 5 minutes. ^1H NMR analysis of the reaction mixture showed that the characteristic peak at δ 4.04 ppm due to the CO_2CH_2 protons of the starting complex **5** had disappeared and a new peak at δ 3.63 ppm due to the OCH_2 protons had appeared. The peak at δ 3.63 ppm, together with others, suggests the formation of n-$C_{12}H_{25}OH$, and the integration suggests the quantitative conversion of **5** to the alcohol. No formate or formic acid was observed but a white precipitate was formed in the solution. After removing the solvent, the residue was analyzed by IR spectroscopy. Two products, $[Mn_2(CO)_{10}]$ and $[Mn(CO)_6][BF_4]$, were identified. A separate experiment was carried out in hexane by using boron trifluoride etherate $BF_3(OEt_2)$. It was found that a white precipitate was formed immediately after addition of $BF_3(OEt_2)$ to the hexane solution of **5**. The white precipitate was identified as $[Mn(CO)_6][BF_4]$ [30] by IR spectroscopy, which showed a ν(CO) band at 2094 cm^{-1}.

It has been reported that the reaction of $[Mn(CO)_5\{C(O)OC_2H_5\}]$ with gaseous BF_3 gives $[Mn(CO)_6][BF_4]$ [30]. The cation $[Mn(CO)_6]^+$ is very reactive towards water to give $[HMn(CO)_5]$ [29]. This complex could then undergo decomposition to give $[Mn_2(CO)_{10}]$ [33]. Thus our observation of the formation of $[Mn_2(CO)_{10}]$ and $[Mn(CO)_6][BF_4]$ in the reaction of **5** with HBF_4 (40% solution in water) is as expected. The reaction of **5** with HBF_4 thus could be described as follows:

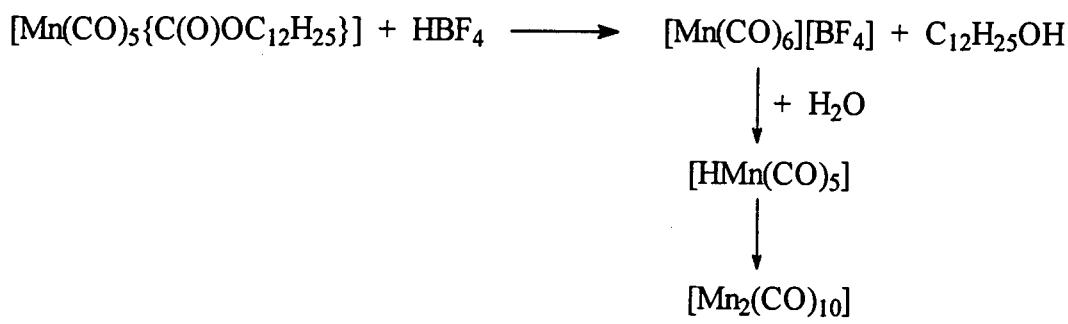

Scheme 2.11

Reaction of $[Mn(CO)_5\{C(O)OC_{12}H_{25}\}]$, 5 with HCl

The reaction of **5** with HCl (36% solution in water) was similarly carried out in $CDCl_3$. ^1H NMR analysis revealed the quantitative conversion of **5** into *n*-$C_{12}H_{25}OH$. In addition, a very small amount of formic acid HCO_2H was observed. IR analysis of the reaction product showed that $[Mn_2(CO)_{10}]$ was the only observable organometallic product. The formation of $[Mn_2(CO)_{10}]$ is most likely due to the reaction of $[Mn(CO)_6]^+$ with water. Previously, the reaction of $[Mn(CO)_5\{C(O)OC_2H_5\}]$ with dry HCl has been reported to give C_2H_5OH and $[Mn(CO)_6]^+HCl^-_2$, which can react with moisture from air to give $[HMn(CO)_5]$ [17]. The decomposition of this complex could give $[Mn_2(CO)_{10}]$ [33]. Thus the reaction of **5** with HCl in the presence of water could be proposed as follows:

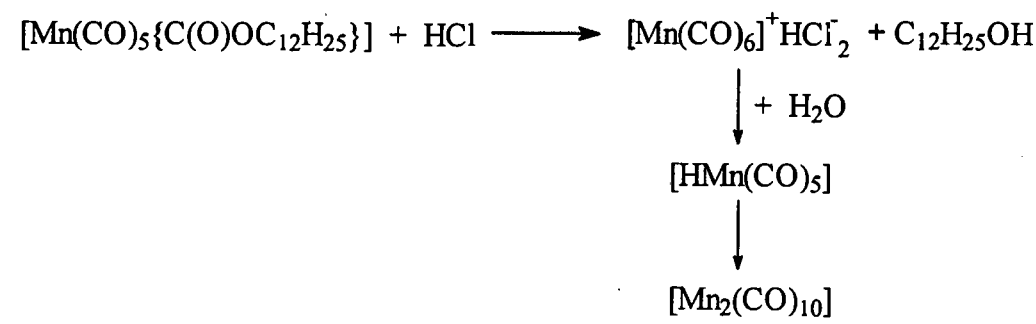

Scheme 2.12

Our results on the reaction of **5** with acids suggest that the oxygen atom of the alkoxy group is the preferential site of protonation. The reactivity of this long chain alkoxycarbonyl complex is similar to that of $[Mn(CO)_5\{C(O)OC_2H_5\}]$ [17].

Reaction of $[Mn(CO)_5\{C(O)OC_{12}H_{25}\}]$, 5 with Br_2

The reaction of **5** with Br_2 was carried out in C_6D_6 at room temperature. After 2 days, ^1H NMR monitoring of the reaction showed the disappearance of the peak at δ 4.09 ppm due to the CO_2CH_2 protons of the starting complex and the appearance of a new peak at δ 3.40 ppm, which suggested the possible formation of $C_{12}H_{25}OBr$ or $C_{12}H_{25}Br$. A white precipitate (presumably $[Mn(CO)_6]^+$) was formed during the reaction. A separate experiment of the same reaction was carried out in hexane at room temperature. It was found that the reaction completed in 17 hours and a white precipitate was formed in the solution. The white precipitate was identified as $[Mn(CO)_6]^+$ by IR spectroscopy.

Treatment of $[Mn(CO)_5\{C(O)OC_{12}H_{25}\}]$, 5 with CH_3I and H_2O

Treatment of **5** with CH_3I and with H_2O were carried out separately in $CHCl_3$ at room temperature. The reaction mixtures were shaken for 8 hours. IR monitoring of the reaction mixtures revealed that no reaction occurred (IR spectra of the resulting solution showed the same peaks with similar intensities as those of the starting solution). It is however known that the complex $[Mn(CO)_5\{C(O)OC_2H_5\}]$ can react with water at 75 °C in the presence of KCl to give $[HMn(CO)_5]$ and $[Mn_2(CO)_{10}]$ [34]. Thus the reaction temperature may be the key factor in the reaction of the alkoxycarbonyl complexes $[Mn(CO)_5\{C(O)OR\}]$ with water.

Thermal decomposition of $[Mn(CO)_5\{C(O)OC_9H_{19}\}]$, 3

The thermal decomposition of **3** was carried out in C_6D_6 in a sealed NMR tube at 70 ± 3 °C, and the process was monitored by ^1H NMR spectroscopy. A decrease in the concentration of the starting complex with time was observed. It was estimated that, after heating for about 8 hours, *ca.* 1/2 of the starting complex decomposed. The complete decomposition took about 55 hours. $[Mn_2(CO)_{10}]$ was

identified by GC-MS as the only organometallic product. No organic products from the decomposition were identified.

2.3.3 Attempted reactions of carbon dioxide with the complexes $[Mn(CO)_5(CH_3)]$ and $[Re(CO)_5(C_{16}H_{33})]$

Several experiments have been performed in order to investigate the possibility of insertion of CO_2 into the Mn-alkyl bond of $[Mn(CO)_5(CH_3)]$. Under the conditions used so far, no reaction occurred between CO_2 and $[Mn(CO)_5(CH_3)]$ in non-polar solvents (hexane and heptane) at 60 °C under 7 or 48 bar of CO_2 for 8 hours, with or without the presence of NEt_3. The IR spectra of the reaction solution showed exactly the same peaks as those of the starting reaction mixture except for an additional peak at 2333 cm^{-1} due to the dissolved CO_2 in solution. Treatment of $[Mn(CO)_5(CH_3)]$ with CO_2 (48 bar) in the presence of NEt_3 by increasing the reaction temperature to 75 °C and extending the reaction time to 24 hours resulted in the complete decomposition of $[Mn(CO)_5(CH_3)]$ to $[Mn_2(CO)_{10}]$.

An experiment was carried out for the reaction of $[Re(CO)_5(C_{16}H_{33})]$ with CO_2 (48 bar) at 50 °C in THF for 48 hours. After the reaction, only the starting complex was recovered in 89% yield.

It appears that insertion of CO_2 into the metal alkyl bond of the complexes $[Mn(CO)_5(CH_3)]$ and $[Re(CO)_5(C_{16}H_{33})]$ does not occur under the conditions that we investigated. It has been reported that the reaction of $[HMn(CO)_5]$ with olefins in supercritical CO_2 does not show any reaction between CO_2 and $[HMn(CO)_5]$ or related alkyl complexes [35]. It seems less likely to insert CO_2 into the M—C (M = Mn and Re) bond of the $[M(CO)_5R]$ complexes, although, as mentioned in section 2.1, the insertion of CO_2 into the Mn—C bond in the complex containing a four-membered ring is known [2]. However, the reactions of CO_2 with alkoxide complexes *fac*-$[M(CO)_3(P\text{-}P)OR]$ [where M = Mn or Re, P-P is either 1,2-bis(diphenylphosphino)ethane, or 1,3-bis(diphenylphosphino)-propane, and R is

CH_3, C_2H_5 or CF_3CH_2] have been reported to form the corresponding carbonato complexes *fac*-[$M(CO)_3(P\text{-}P)\{OC(O)OR\}$] [36]. These reactions involve the insertion of CO_2 into the M—O (M = Mn and Re) bond. It could be a general trend that the insertion of CO_2 into an M—C bond may be more difficult than the insertion of CO_2 into an M—O bond.

2.4 Conclusion

A series of new long chain alkoxycarbonyl manganese pentacarbonyl complexes [$Mn(CO)_5\{C(O)OR\}$] (R= *n*-C_7H_{15}, **1**; *n*-C_8H_{17}, **2**; *n*-C_9H_{19}, **3**; *n*-$C_{10}H_{21}$, **4**; *n*-$C_{12}H_{25}$, **5**; and *n*-$C_{16}H_{33}$, **6**) has been synthesized in 40-87% yields. All these complexes (except **6**) have been fully characterized by satisfactory elemental analysis, IR, ^1H and ^{13}C NMR spectroscopy as well as by mass spectroscopy. These complexes are relatively thermally stable. The results of the reactions of acyl and alkoxycarbonyl complexes with syngas in hexane and THF show solvent effects. The reactions of the alkoxycarbonyl complexes with syngas carried out in hexane gave formate and alcohols as products, while the same reaction in THF gave formate, alcohol and esters as products. The formation of the ester is probably due to the reaction of the alkoxycarbonyl complex with the solvent. The reaction of the acyl complex [$Mn(CO)_5\{C(O)C_{11}H_{23}$] with syngas in THF gave alcohol as the sole organic product. These reactions are relevant to catalytic reactions such as hydroformylation and the Fischer-Tropsch synthesis, where acyl and alkoxycarbonyl complexes have been recognized as key intermediates.

We have also investigated some chemistry of the long chain alkoxycarbonyl complex [$Mn(CO)_5\{C(O)OC_{12}H_{25}\}$]. Protonation of the complex takes place fast and gives [$Mn_2(CO)_{10}$] and the alcohol *n*-$C_{12}H_{25}OH$ as the main products. We would expect that the chemistry of other alkoxycarbonyl complexes should behave similarly.

In an attempt to synthesize complexes of the type [L_nMCO_2R] directly from CO_2 and [L_nMR], we have studied the reactions of CO_2 with metal alkyl complexes

$[Mn(CO)_5(CH_3)]$ and $[Re(CO)_5(C_{16}H_{33})]$ under various conditions. We obtained no evidence for insertion of CO_2 into the metal-alkyl σ bonds under the conditions investigated.

References

1. M. E. Vol'pin and I. S. Kolomnikov, Pure Appl. Chem., 1973, **33,** 567.
2. A. Behr, U Kanne and G. Thelen, J. Organomet. Chem., 1984, **269**, C1.
3. X. Yin and C. Wang, Shiyou Huagong, 1993, **22**, 557.
4. W. Leitner, Coord. Chem. Rev., 1996, **153**, 257.
5. P.G. Jessop, T. Ikariya and R. Noyori, Chem. Rev., 1995, **95**, 259.
6. G. Suss-Fink, J-M. Soulie, G. Rheinwald, H. Stoeckli-Evans and Y. Sasaki, Organometallics, 1996, **15**, 3416.
7. J. P. Collman, L. S. Hegedus, J. R. Norton and R.G. Finke, *Principles and Applications of Organotransition Metal Chemistry*, 2nd. ed., University Science Books: Mill Valley, CA, 1987, p 633.
8. J. B. Blackborow, R. J. Daroda and G. Wilkinson, Coord. Chem. Rev., 1982, **43,** 17.
9. C. D. Wood and P.E. Garrou, Organometallics, 1984, **3,** 170.
10. P.J. Stang and Z. Zhong, Organometallics, 1992, **11,** 1026.
11. D. Milstein and J.L. Huck, J. Am. Chem. Soc., 1982, **104**, 6150.
12. G. Vasapollo, L. Toniolo, G. Cavinato, F. Bigoli, M. Lanfranchi and M.A. Pellinghelli., J. Organomet. Chem., 1994, **481**, 173.
13. M. Tasi and G. Palyi, in *Organometallic Synthesis*, vol 4, Eds. R. B. King and J. J. Eisch, Academic Press: New York, 1988, p 266.
14. R. Bertani, G.Cavinato, L. Toniolo and G. Vasapollo, J. Mol. Catal., 1993, **84**, 165.
15. R. Bertani, G. Cavinato, G. Facchin, L. Toniolo and A. Vavasori, J. Organomet. Chem., 1994, **466**, 273.
16. D. Carmona, J. Ferrer, J. Reyes and L. A. Oro, Organometallics, 1993, **12**, 4241.
17. T. Kruck and M. Noack, Chem. Ber., 1964, **97**, 1693.
18. D. J. Sheeran, J. D. Arenivar and M. Orchin, J. Organomet. Chem., 1986, **316**, 139.
19. J. H. Freudenberger and M. Orchin, Organometallics, 1982, **1**, 1408.

20. A. Cotton (Supervisor Prof. J.R. Moss), B. Sc. Honour's Project Report, University of Cape Town, 1991.
21. J-A. M. Andersen, Ph.D. Thesis, University of Cape Town, 1994.
22. J-A. M. Andersen and J.R. Moss, Organometallics, 1994, **13**, 5013.
23. S.K. Mandal, D.H. Ho and M. Orchin, Polyhedron, 1992, **11**, 2055.
24. Section 2.2 of this chapter.
25. B. D. Dombek, J. Am. Chem. Soc., 1979, **101**, 6466.
26. J-A. M. Andersen and J.R. Moss, unpublished results.
27. S.F. Mapolie and J. R. Moss, J. Chem. Soc. Dalton Trans, 1990, 299.
28. (a): F. A. Cotton, J. A. Down and G. Wilkinson, J. Chem. Soc., 1959, 833.
(b): D.K. Huggins and H.D. Kaesz, J. Am. Chem. Soc., 1964, **86**, 2734.
(c): R.B. Bedford, A.F. Hill, A.J.P. White and D.J. Williams, Angew. Chem. Int. Ed. Engl., 1996, **35**, 95.
29. R. Angelici, Acc. Chem. Res., 1972, **5**, 335.
30. N. A. Beach and H. B. Gray, J. Am. Chem. Soc., 1968, **90**, 5713.
31. I. Kovacs, C. D. Hoff, F. Ungvary and L. Marko, Organometallics, 1985, **4**, 1347
32. M. E. Dry, Catalysis Today, 1990, **6**, 183.
33. R.M. Bullock and B. Rappoli, J. Organomet. Chem., 1992, **429**, 345.
34. H.C. Clark and W. J. Jacobs, Inorg. Chem., 1970, **9**, 1229.
35. P. G. Jessop, T. Ikariya and R. Noyori, Organometallics, 1995, **14**, 1510.
36. S.K. Mandal, D.H. Ho and M. Orchin, Organometallics, 1993, **12**, 1714.

Chapter 3

Synthesis, Characterization And Reactivity Of Long Chain Acyl And Alkyl Complexes Of The Type $[(\eta^5\text{-}C_5R'_5)Fe(CO)_2\{C(O)R\}]$ (R' = H, CH_3), $[CpW(CO)_3\{C(O)R\}]$ And $[CpW(CO)_3R]$ (R = *n*-alkyl) As Well As The Carbyne Complexes $[CpW(CO)_2(\equiv CR)]$

3.1. Introduction

We have, in a previous chapter, shown that the reactions of manganese acyl complexes $[Mn(CO)_5\{C(O)R\}]$ with syngas give $[Mn(CO)_5\{C(O)OCH_2R\}]$ or RCH_2OH, depending on whether the solvent is hexane or THF [1]. We were interested to see whether long chain acyl complexes of other metals would behave similarly. We were also interested to study the reactions of a range of complexes containing metal-carbon bonds with CO_2. Thus, we have investigated the reactions of alkyl complexes of iron and tungsten as well as the tungsten carbyne complexes with CO_2, in attempts to activate CO_2 using these organometallic complexes. The acyl and alkyl complexes of iron are of special interest since in the Fischer-Tropsch process, which is currently operated in SASOL, certain amounts of oxygenates (mainly formates, alcohols and ketones) are produced. The surface alkyl and acyl species are believed to play important roles in this process [2].

In heterogeneous reactions, the catalytic surfaces are difficult to study due to the lack of suitable methods for obtaining definitive information about the surface species [3]. One way to overcome this difficulty is to study the chemistry of model compounds, *i.e.* compounds that have many of the same features as the proposed intermediate species. Thus we can compare the surface alkyl and acyl species to the alkyl and acyl complexes of iron as shown below [3]:

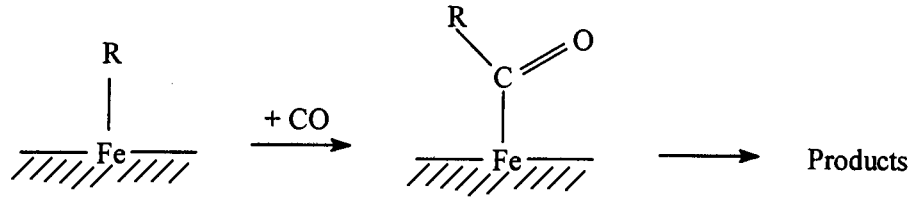

surface alkyl species surface acyl species

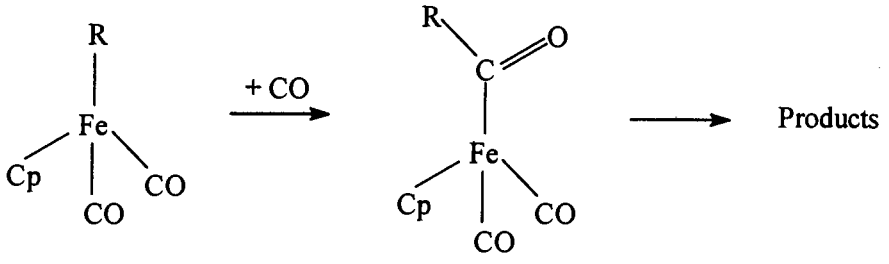

metal alkyl complex metal acyl complex

Metal alkyl complexes of the types $[Mn(CO)_5R]$ and $[CpM(CO)_2R]$ (M = Fe, Ru, Os), which can be used as models for catalytic intermediates, have recently been discussed by Moss [3]. The alkyl migration (or CO insertion) to give the corresponding acyl complexes in the above-mentioned systems have also been studied by Moss and co-workers [4-6]. We now extend this research to the acyl complexes of iron $[(\eta^5\text{-}C_5R'_5)Fe(CO)_2\{C(O)R\}]$ (R′ = H, CH_3) and tungsten $[CpW(CO)_3\{C(O)R\}]$, and the alkyl complexes of tungsten $[CpW(CO)_3R]$. These results should add to our knowledge of metal acyl complexes and may help to establish the role of the acyl intermediates in oxygenate formation in the Fischer-Tropsch process. This knowledge could also be useful in other catalytic reactions where acyl species have been recognized as key intermediates [7], such as the hydroformylation of alkenes, the Monsanto acetic acid synthesis and the co-polymerization of ethylene and CO.

We now report our results of (1) the synthesis, characterization and reactivity of acyl complexes $[(\eta^5\text{-}C_5R'_5)Fe(CO)_2\{C(O)R\}]$ (R′ = H, CH_3) and $[CpW(CO)_3\{C(O)R\}]$, (2) the synthesis and characterization of alkyl complexes $[CpW(CO)_3R]$, and (3) the reactions of CO_2 with some alkyl complexes of iron

and tungsten, and the tungsten carbyne complexes under various conditions. These results will be discussed in the following sections.

3.2 Synthesis, characterization and reactivity of the acyl complexes $[(\eta^5\text{-}C_5R'_5)Fe(CO)_2\{C(O)R\}]$ (R' = H, CH_3) and $[CpW(CO)_3\{C(O)R\}]$

3.2.1 Synthesis of the acyl complexes

The new iron acyl complexes of the type $[CpFe(CO)_2\{C(O)R\}]$ (R = *n*-C_5H_{11}, **1**; *n*-C_8H_{17}, **2**; *n*-$C_{11}H_{23}$, **3**; and *n*-$C_{17}H_{35}$, **4**) were prepared by the same general route as shown below:

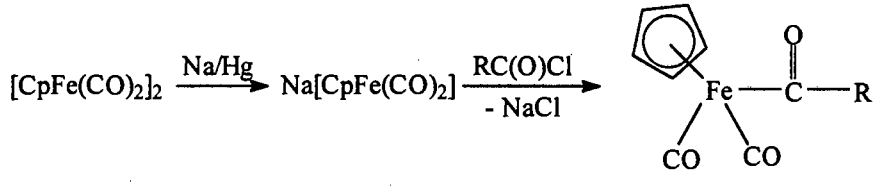

n-R	Compd no
C_5H_{11}	1
C_8H_{17}	2
$C_{11}H_{23}$	3
$C_{17}H_{35}$	4

Scheme 3.1

This method is similar to that reported for the synthesis of some short chain acyl complexes $[CpFe(CO)_2\{C(O)R\}]$ (R = Me [8], Et [9] and Pr [10]). The complex **3** has also been mentioned by Amiens and co-workers [11], but no detailed preparation and characterization data for the complex has been reported. The new complex $[Cp^*Fe(CO)_2\{C(O)R\}]$ (R = *n*-$C_{11}H_{23}$, **5**) has been similarly prepared from $Na[Cp^*Fe(CO)_2]$ and RC(O)Cl, and the new complex $[CpW(CO)_3\{C(O)R\}]$ (R = *n*-$C_{11}H_{23}$, **6**) prepared from RC(O)Cl and $Na[CpW(CO)_3]$. Some short chain acyl complexes of the types $[Cp^*Fe(CO)_2\{C(O)R\}]$ (R = Me [12], Et [13]) and $[CpW(CO)_3\{C(O)R\}]$ (R= Me [14] and Et [15]) have also been described in the literature.

The complexes **3-6** were obtained in good yields as low-melting yellow solids, whereas the complexes **1** and **2** were obtained as orange-red oils. The complexes **1-6** have been fully characterized by elemental analysis, m.p., IR, ^{1}H and ^{13}C NMR as well as mass spectroscopy. The results are given in Tables 3.1 - 3.5 and will be discussed below.

3.2.2 Characterization of the acyl complexes

IR spectroscopy

The IR spectra of complexes **1-6** were recorded in hexane solution in the range 2200 to 1600 cm^{-1}, and the data are given in Table 3.2. The results are in good agreement with the data reported for similar short chain acyl complexes [8-10,12-14]. All the iron complexes **1-5** show two bands for the terminal carbonyls and a characteristic band in the range 1645 to 1670 cm^{-1} due to the ν(C=O) acyl. There is no change in the position of ν(CO) as the carbon chain lengthens from *n*-C_5H_{11} to *n*-$C_{17}H_{35}$. ν(CO) for the Cp*Fe complexes are lower than those for the analogous CpFe complexes by about 15-20 cm^{-1}. This can be attributed to the increase in electron density on the iron (caused by the Cp* ligand), which results in increased back-bonding to the carbonyl groups, hence, a lower ν(CO) [15].

^{1}H NMR spectroscopy

The ^{1}H NMR data for complexes **1-6** are summarized in Table 3.3. The ^{1}H NMR spectrum of **3** is shown in Figure 3.1. Separate resonances are observed for the Cp, $COCH_2$ (and sometimes $COCH_2CH_2$), and methyl protons of the acyl group. The chemical shifts are found at similar positions to those reported for related short chain complexes [8-10,12-14]. These show no variation with alkyl chain length. The central methylene protons usually appear as a broad singlet. Thus, the integration is the only way to distinguish these complexes using ^{1}H NMR. The chemical shifts of the cyclopentadienyl protons for the iron complexes are found at higher field (δ 4.8 ppm) than for the tungsten complex (δ 5.5), as has been found previously in related compounds [9].

Table 3.1 Data for the acyl complexes [LM{C(O)R}].

Compound no	LM	*n*-R	Yield (%)	m.p. (°C)	Elemental analysis (%)			
					C		H	
					calc.	found	calc.	found
1	Fp[a]	C_5H_{11}	89	oil	56.55	57.06	5.84	6.14
2	Fp	C_8H_{17}	63	oil	60.39	60.63	6.97	7.11
3	Fp	$C_{11}H_{23}$	70	38 - 41	63.34	63.64	7.83	8.07
4	Fp	$C_{17}H_{35}$	58	57 - 59	67.56	67.71	9.07	9.30
5	Fp*[b]	$C_{11}H_{23}$	67	29 - 30	66.98	66.88	8.90	9.12
6	Wp[c]	$C_{11}H_{23}$	52	38 - 40	46.55	47.35	5.47	5.87

[a]: Fp = $CpFe(CO)_2$.
[b]: Fp* = $Cp^*Fe(CO)_2$.
[c]: Wp = $CpW(CO)_3$.

Table 3. 2 IR data for the acyl complexes [LM{C(O)R}].

Compound no	LM	*n*-R	IR (cm^{-1})[a]	
			v(CO)	v(C=O)
1	Fp[b]	C_5H_{11}	2017s, 1961vs,	1667m
2	Fp	C_8H_{17}	2017s, 1962vs,	1660m
3	Fp	$C_{11}H_{23}$	2016s, 1962vs,	1665m
4	Fp	$C_{17}H_{35}$	2017s, 1962vs,	1654m
5	Fp*[c]	$C_{11}H_{23}$	2002s, 1942s,	1647m
6	Wp[d]	$C_{11}H_{23}$	2017s, 1937s, 1922 vs, 1891w,	1650m

[a]: IR in hexane
[b]: Fp = $CpFe(CO)_2$.
[c]: Fp* = $Cp^*Fe(CO)_2$.
[d]: Wp = $CpW(CO)_3$.

Table 3.3 ^{1}H NMR data for the acyl complexes [LM{C(O)R}][a] (400 MHz, $CDCl_3$).

Compound no	LM	*n*-R	Cp	$C_5(CH_3)_5$	$COCH_2$ $^3J(HH)$	$COCH_2CH_2$ $^3J(HH)$	$(CH_2)_n$	CH_3 $^3J(HH)$
1[b]	Fp[c]	C_5H_{11}	4.14, 5H, s		2.81, 2H, t 7.2	1.57, 2H, qn 7.2	1.22, 6H, m	0.86, 3H, t 6.4
2	Fp	C_8H_{17}	4.80, 5H, s		2.84, 2H, br	1.20, 12H, br		0.84, 3H, br
3	Fp	$C_{11}H_{23}$	4.84, 5H, s		2.88, 2H, t 7.2	1.45, 2H, qn 7.2	1.23, 16H, m	0.86, 3H, t 7.2
4	Fp	$C_{17}H_{35}$	4.83, 5H, s		2.86, 2H, t 7.2	1.45, 2H, m	1.24, 30H, br	0.87, 3H, t 6.8
5	Fp*[d]	$C_{11}H_{23}$		1.76, 15H, s	2.79, 2H, t 7.2	1.42, 2H, qn, 7.2	1.22, 16H, m	0.86, 3H, t 6.8
6	Wp[e]	$C_{11}H_{23}$	5.54, 5H, s		2.93, 2H, t 7.2	1.38, 2H, qn 7.0	1.22, 16H, m	0.86, 3H, t 6.4

[a]: Coupling constants are given in Hz.
[b]: The complex **1** was measured in C_6D_6, all others were in $CDCl_3$.
[c]: Fp = $CpFe(CO)_2$.
[d]: Fp* = $Cp^*Fe(CO)_2$.
[e]: Wp = $CpW(CO)_3$.

Table 3.4 ^{13}C NMR chemical shift data (δ ppm) for the acyl complexes [LM{C(O)R}] (100 MHz, $CDCl_3$).

Compound no	LM	*n*-R	$C_5(CH_3)_5$	Cp	C=O	CO	$COCH_2$	$COCH_2(CH_2)_n$[a]	$CH_2CH_2CH_3$	CH_2CH_3	CH_3
1[b]	Fp[c]	C_5H_{11}		87.06	251.54	216.12	67.48	32.32	26.15	23.58	14.83
2	Fp	C_8H_{17}		86.32	256.84	214.44	66.74	31.82, 29.41, 29.14, 29.07	25.23	22.63	14.07
3	Fp	$C_{11}H_{23}$		86.35	256.86	214.45	66.78	31.92, 29.62, 29.51, 29.48, 29.34, 29.09	25.25	22.69	14.12
4	Fp	$C_{17}H_{35}$		86.35	256.86	214.45	66.78	31.93, 29.71, 29.52, 29.48, 29.37, 29.09	25.25	22.70	14.13
5	Fp*[d]	$C_{11}H_{23}$	97.03 9.56		264.42	216.32	66.27	31.92, 29.65, 29.55, 29.36, 29.25	25.33	22.70	14.14
6	Wp[e]	$C_{11}H_{23}$		95.26	f	226.70 220.07	67.31	31.87, 29.57, 29.45, 29.29, 28.87	25.14	22.65	14.08

[a]: Peaks for these carbon atoms were not completely resolved or assigned.
[b]: The complex **1** was measured in C_6D_6, all others were in $CDCl_3$.
[c]: Fp = $[CpFe(CO)_2]$.
[d]: Fp* = $[Cp^*Fe(CO)_2]$.
[e]: Wp = $[CpW(CO)_3]$.
[f]: not observed.

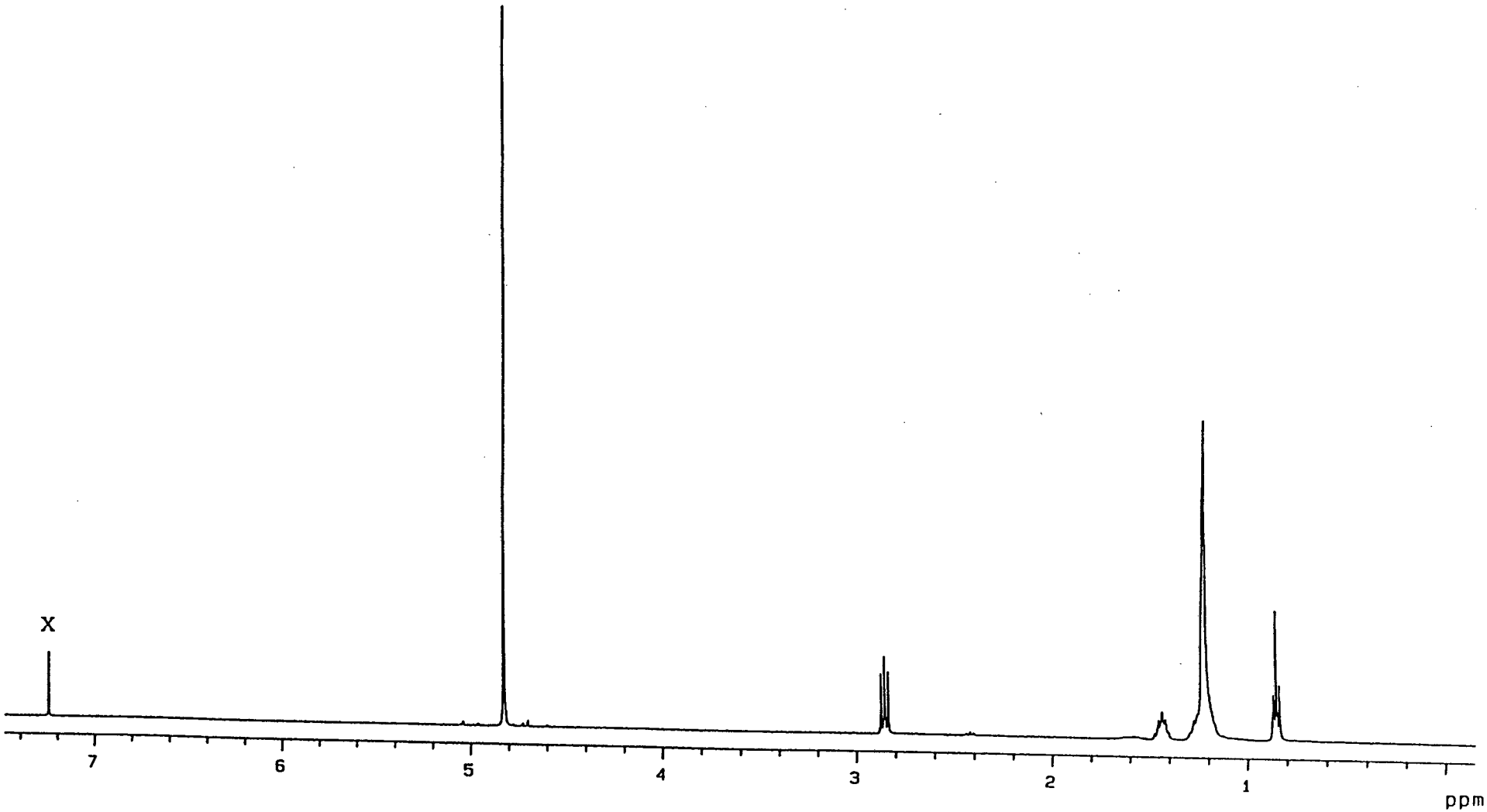

Figure 3.1 ^{1}H NMR spectrum of [$CpFe(CO)_2(COC_{11}H_{23})$], 3 (400 MHz, $CDCl_3$, X = Solvent)

^{13}C NMR spectroscopy

^{13}C NMR data for complexes **1-6** are given in Table 3.4. The ^{13}C NMR spectrum of **3** is shown in Figure 3.2 as an example. Assignments for the data were made as far as possible by comparison with the data reported for related short chain acyl complexes [10], and the binuclear acyl complexes [16] as well as with the manganese complexes $[Mn(CO)_5\{C(O)R\}]$ [4].

The Cp and CO resonances are dependent on the metal and the ligand, but independent of the alkyl chain length. The acyl carbon atom is more deshielded than the terminal carbonyl carbons and is observed at relatively lower field (see Table 3.4). Both the acyl carbon and the carbonyl carbons are more deshielded in the Cp*Fe complex than those in the CpFe complexes. For complex **1**, all the carbon atoms of the alkyl chain are assigned. For complexes with longer alkyl chain, the chemical shifts of the central carbon atoms are very close together and the assignments could not be made unambiguously, as has been found in other long chain acyl complexes [4].

Mass spectra

Low resolution electron impact mass spectra were obtained for all the compounds under discussion. The intensities of the major organometallic peaks of **1-6** are reported in Table 3.5, with possible assignments. The expected isotope pattern for the tungsten containing species was observed and the intensities of these species were based on the most abundant peaks observed.

Molecular ion peaks are observed for complexes **1-3**, but are of low intensity. For complexes **4-6**, the highest ion peaks observed correspond to [M-CO]. For all the iron complexes, the most abundant peaks observed correspond to [M-3CO-2H]. This could be due to the consecutive loss of the carbonyl groups and hydrogen from the molecular ion. The loss of (2CO and 2H) from $[CpFe(CO)_2R]$ complexes

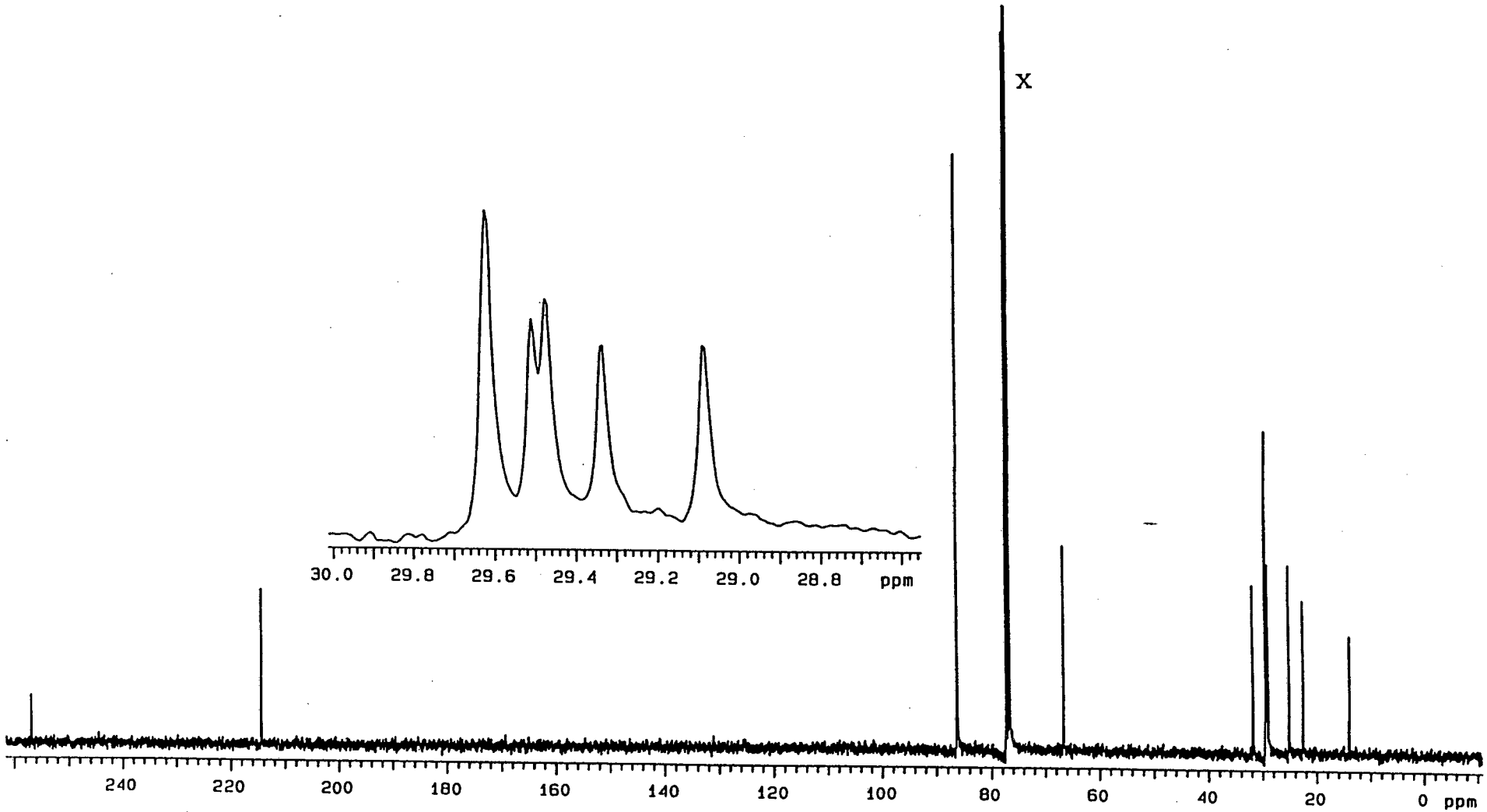

Figure 3.2 ^{13}C NMR spectrum of $[CpFe(CO)_2(COC_{11}H_{23})]$, 3 (100 MHz, $CDCl_3$, X = Solvent)

Table 3.5 Mass spectral data for the acyl complexes **1-6**.

Ion[a]	**Relative peak intensities**[b] **(%)**					
Compound no	**1**	**2**	**3**	**4**	**5**	**6**
M	3	0.3	2	0	0	0
M - CO	16	10	12	5	6	64
M - 2CO	4	0.8	4	0.6	5	65
M - 3CO	0	0	0	0	0	58
M - R	30	39	33	40	46	100
M - 3CO - 2H	100	100	100	100	100	54
M - COR	16	12	14	9	25	52
M - COR - O	13	2	5	0.4	0	4
M- COR - CO	15	12	12	7	40	54
M- COR - 2CO	68	41	52	30	44	39
M - COR - 3CO	0	0	0	0	0	41

[a]: M = $[(C_5R'_5)M(CO)_n\{C(O)R\}]$; all ions have a single positive charge; ion refers to probable assignment.

[b]: Peak intensities are relative to the base peak [M-3CO-2H] for the iron complexes **1 - 5**, and relative to $[CpW(CO)_3]$ for the complex **6**.

has been observed before [17]. This was suggested to be a result of remote functionalization [17] where the C-H bond of the methyl group of the alkyl chain could be activated by the coordinatively unsaturated metal atom to give a metallacycle after the initial loss of carbonyl groups from $[CpFe(CO)_2R]$. Further loss of hydrogen could then occur by β-hydrogen elimination, without loss of the alkyl residue [17]. The most abundant peak observed for complex **6** corresponds to [M-R].

All these complexes fragment similarly, and for complex **1**, the main fragmentation pathways are shown in Scheme 3.2 as an example.

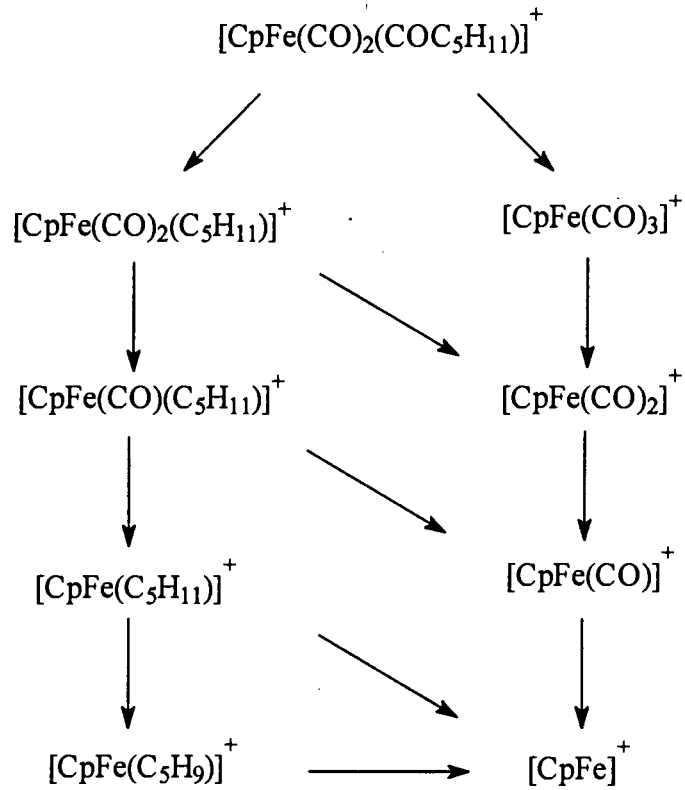

Scheme 3.2

The loss of Cp prior to the loss of other ligands from major fragments is not observed or is of very low intensity. The loss of Cp, possibly from $[CpFe]^+$ to give Fe^+ and Cp^+, is however observed.

3.2.3 A Comparison of the thermal properties of the acyl complexes

The thermal properties of the acyl complexes $[CpFe(CO)_2\{C(O)C_{11}H_{23}\}]$, **3**, $[Cp^*Fe(CO)_2\{C(O)C_{11}H_{23}\}]$, **5**, and $[CpW(CO)_3\{C(O)C_{11}H_{23}\}]$, **6** were studied by Differential Scanning Calorimetry (DSC) and Thermal Gravimetric Analysis (TGA). The DSC and TGA traces of the acyl complexes **3, 5** and **6** at a heating rate of 10 °C/min under nitrogen are shown in Figures 3.3 and 3.4 respectively. The data are summarized in Table 3.6. For all these complexes, the DSC traces exhibit sharp endothermic peaks in the range 35 to 45 °C, which correspond well with the melting of the samples determined using the hot-stage microscope. The melting points of these complexes increase slightly according to the following order:

$$[Mn(CO)_5\{C(O)C_{11}H_{23}\}] \cong [Cp^*Fe(CO)_2\{C(O)C_{11}H_{23}\}] <$$
$$[CpFe(CO)_2\{C(O)C_{11}H_{23}\}] < [CpW(CO)_3\{C(O)C_{11}H_{23}\}].$$

Broad peaks observed from the DSC traces over 170 °C may be due to the decomposition of the samples. This is supported by the observation that significant mass loss is seen in the TGA traces of these complexes over the temperature range 170 - 250 °C. The decomposition points (estimated from the peak maximum of the derivative of TGA curves) for **3** and **5** are estimated to be 210 and 241 °C respectively, suggesting that the Cp*Fe complex is more thermally stable than the CpFe complex. This could be assigned to the electronic and steric effect of the Cp* ligand. The acyl CpW complex is less stable than the CpFe complex. The decomposition points of these acyl complexes increase according to the following order:

$$[Mn(CO)_5\{C(O)C_{11}H_{23}\}] < [CpW(CO)_3\{C(O)C_{11}H_{23}\}] <$$
$$[CpFe(CO)_2\{C(O)C_{11}H_{23}\}] < [Cp^*Fe(CO)_2\{C(O)C_{11}H_{23}\}].$$

The mass remaining after heating the iron acyl complexes $[(\eta^5\text{-}C_5R_5)Fe(CO)_2\{C(O)C_{11}H_{23}\}]$ (R = H, CH_3) to 250 °C corresponds to the decomposition of the samples to $[(\eta^5\text{-}C_5R_5)_2Fe]$ (R = H, CH_3); whereas heating the complex $[CpW(CO)_3\{C(O)C_{11}H_{23}\}]$ leads to its decomposition to probable $[CpWO_2]$, indicated by the mass loss (47%) after heating the sample to 250 °C.

The acyl CpFe complex seems to be more stable than the long chain alkyl complex $[CpFe(CO)(C_6H_{13})]$ [18]. This could be the reason for the previous observation that the acyl iron complexes are difficult to decarbonylate to give the corresponding alkyl complexes [19].

Table 3.6 Thermal analysis data for the acyl complexes [LM{C(O)$C_{11}H_{23}$}]

Compd. no	LM	m.p. (°C)[a]	T_i (°C)[b]	T_{max} (°C)[c]	ΔH_{endo} (KJ/mol)[d]	T_{deriv} (°C)[e]
3	$CpFe(CO)_2$	38 - 41	38.1	40.1	12.91	210
5	$Cp^*Fe(CO)_2$	29 - 30	33.3	35.6	n.a.[f]	241
6	$CpW(CO)_3$	38 - 40	43.0	44.7	10.74	195
	$Mn(CO)_5$ [g]	27 - 30	33.7	35.8	9.23	135

[a]: Determined using a Kofler hot-stage microscope.

[b]: Temperature corresponding to the onset of a peak.

[c]: Temperature corresponding to the peak maximum.

[d]: Calculated by Perkin Elmer PC series DSC7 machine (in J/g).

[e]: Temperature determined from the peak maximum of the derivative curve of the TGA trace; derivative is the instantaneous slope of the first curve (or rate of change of the TGA curve).

[f]: Not available.

[g]: See section 2.2.1 of this thesis.

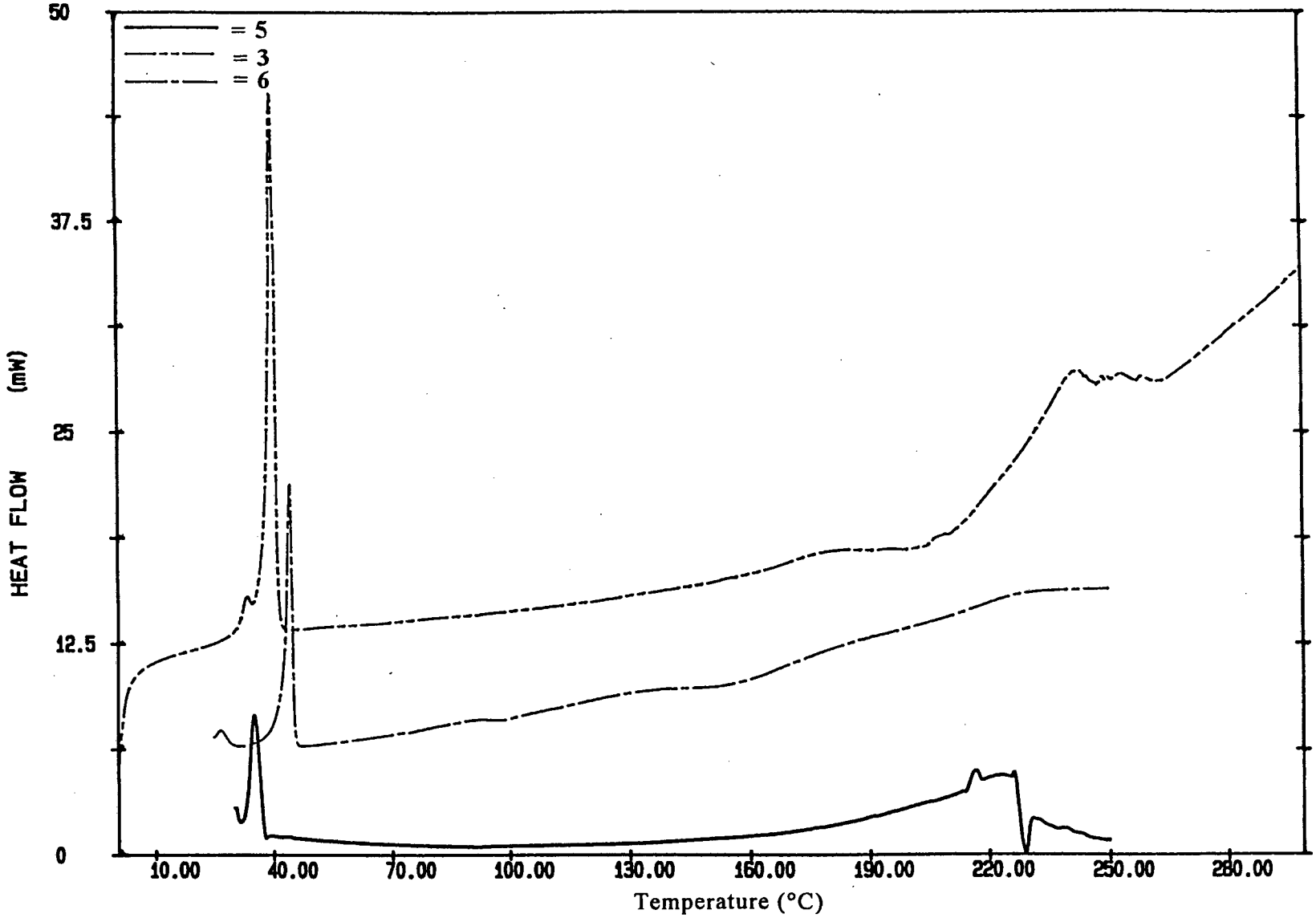

Figure 3.3 **DSC traces for the acyl complexes [$LM(COC_{11}H_{23})$] a: LM = $CpFe(CO)_2$, 3; b: LM = $Cp^*Fe(CO)_2$, 5; c: LM = $CpW(CO)_3$, 6; (Scan rate = 10 °C/min, traces offset for clarity).**

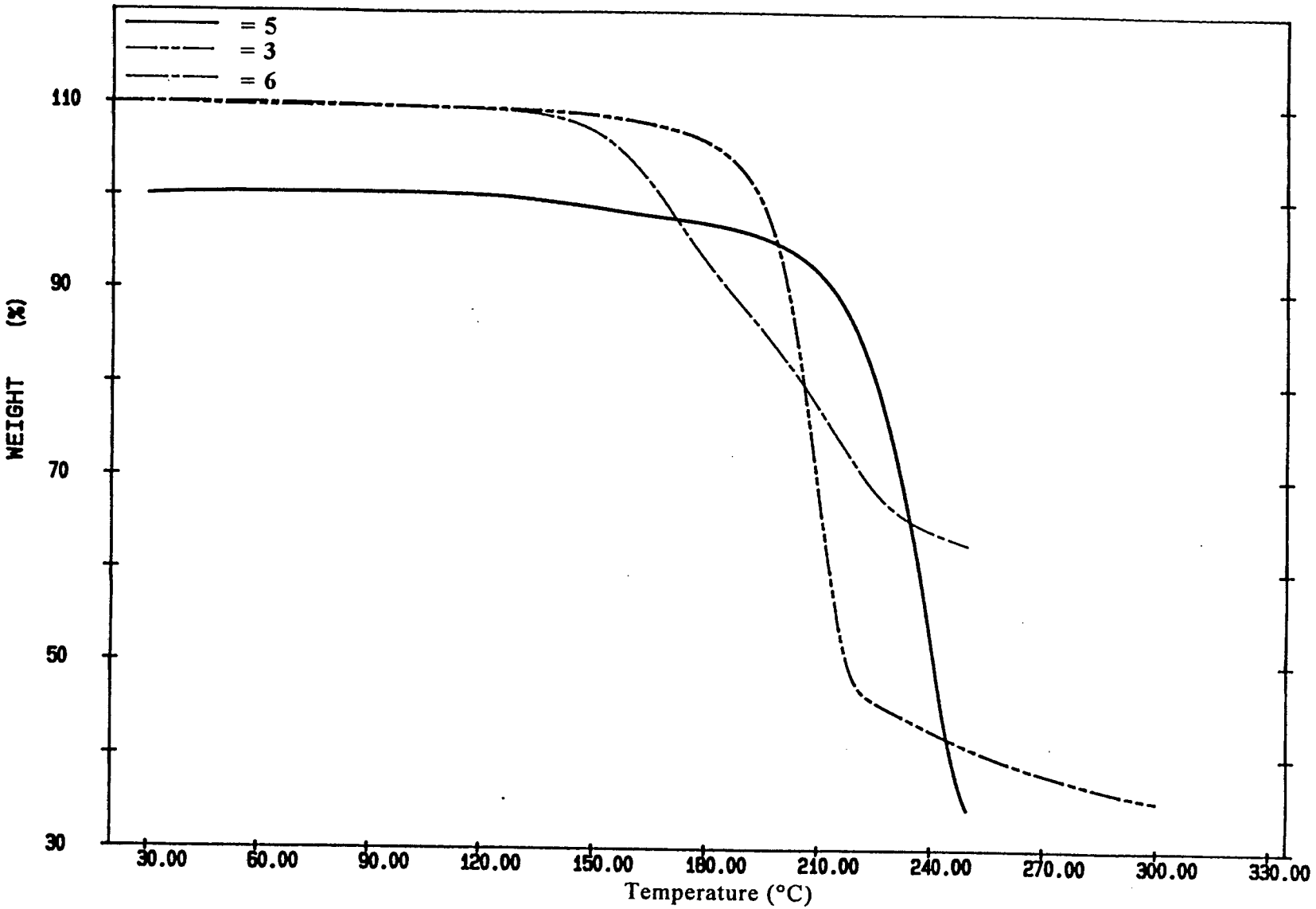

Figure 3.4 TGA traces for the acyl complexes [$LM(COC_{11}H_{23})$] a: LM = $CpFe(CO)_2$, 3; b: LM = $Cp^*Fe(CO)_2$, 5; c: LM = $CpW(CO)_3$, 6; (Scan rate = 10 °C/min, traces offset for clarity).

3.2.4 Reactivity of the acyl complexes with syngas

The reactivity of short chain acyl complexes [$CpFe(CO)_2\{C(O)R\}$] has been reviewed recently [20,21]. The reaction of **3** with cerium ammonium nitrate has also been reported [11]. However, there is no report of the reaction of the acyl complexes [$CpFe(CO)_2\{C(O)R\}$] with syngas. In Chapter 2, we have reported the reaction of the manganese acyl complex [$Mn(CO)_5\{C(O)C_{11}H_{23}\}$] with syngas. We have now carried out some reactions of the acyl complexes **3, 5** and **6** with syngas in hexane and THF.

The reaction of [$CpFe(CO)_2\{C(O)C_{11}H_{23}\}$], **3** with CO/H_2 (1:1, 45 bar) in hexane at 62 °C for 20 hours led to the formation of small amounts (less than 10%) of [$Fe(CO)_5$], identified by IR spectroscopy. No IR band due to aldehyde, formate or alcohol could be seen in the IR spectrum of the reaction solution. The starting complex **3** was recovered in 91% yield. The same reaction carried out with CO/H_2 (48 bar) in THF at 60 °C for 20 hours gave a mixture (crude yield 88%) of a formate HCO_2R, an ester and the starting complex in a ratio of 51:28:21, estimated by the integrations of their characteristic peaks in the ^1H NMR spectrum. The products were identified by their characteristic peaks in the ^1H and ^{13}C NMR as well as IR spectra. The exact composition of these products, however, could not be verified. The reaction could be described as below.

$$[CpFe(CO)_2\{C(O)R\}] + CO/H_2 \xrightarrow[20\ \text{hours, THF}]{48\ \text{bar, } 60^\circ C} \text{Formate} + \text{Ester} + [Fe(CO)_5]$$

Scheme 3.3

We expected that replacing the Cp ligand in the iron acyl complexes with a Cp* ligand may increase the binding between the Cp* and iron, thus this could affect the reaction pathway of the iron acyl complexes. This did not occur, since the reaction of [$Cp^*Fe(CO)_2\{C(O)C_{11}H_{23}\}$], **5** with CO/H_2 (48 bar) in hexane at 75 °C for 22 hours led similarly to the formation of small amounts (less than 7%) of

$[Fe(CO)_5]$. No IR band due to aldehyde, formate or alcohol could be detected by IR spectroscopy. The starting complex was recovered (recovery 93%).

Furthermore the reaction of $[CpW(CO)_3\{C(O)C_{11}H_{23}\}]$, **6** with CO/H_2 (42 bar) in hexane at 75 °C for 22 hours led only to the quantitative recovery of the starting complex. This suggests that the tungsten acyl complex is stable under these conditions.

The reactions of these iron and tungsten acyl complexes with syngas in hexane are unlike that of the $[Mn(CO)_5\{C(O)C_{11}H_{23}\}]$ which gives the alkoxycarbonyl complex $[Mn(CO)_5\{C(O)OC_{12}H_{25}\}]$ [1]. Instead, the Cp or Cp* ligand of the iron complexes is replaced by CO to form $[Fe(CO)_5]$. The formation of formates from the reaction of the iron acyl complexes with syngas may suggest that the alkoxycarbonyl complexes $[CpFe(CO)_2\{C(O)OR\}]$ might be a possible intermediate. The effect of solvent on the reactivity of the iron acyl complexes, like that found for the manganese acyl complexes [1], is also important. Our results show that the reactivity of the acyl complexes $[LM\{C(O)R\}]$ with syngas is metal, ligand and solvent dependent. The yield of the formate and ester from the reaction of iron acyl complexes with syngas may serve as indirect evidence for the involvement of the acyl species in the formation of oxygenates in the Fischer-Tropsch process.

3.3 Synthesis and characterization of the alkyl complexes $[CpW(CO)_3R]$

3.3.1 Synthesis of $[CpW(CO)_3R]$

The long chain alkyl complexes $[CpW(CO)_3R]$ (R = *n*-C_6H_{13}, **7**; *n*-C_7H_{15}, **8**; *n*-C_8H_{17}, **9**; and *n*-$C_{10}H_{21}$, **10**) were all prepared by the general route as shown in Scheme 3.4.

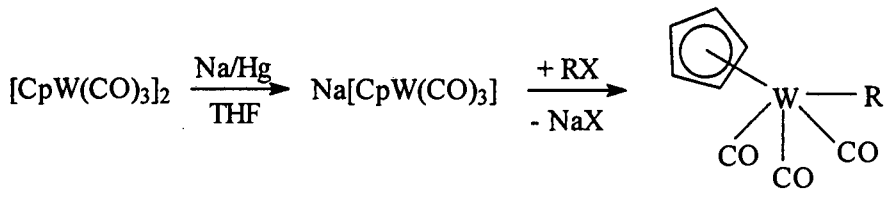

n-R	Compd no
C_6H_{13}	**7**
C_7H_{15}	**8**
C_8H_{17}	**9**
$C_{10}H_{21}$	**10**

Scheme 3.4

The preparative reaction was monitored by IR spectroscopy. It was found that a much longer reaction time was required to ensure complete conversion of $Na[CpW(CO)_3]$, even if a large excess of RBr (R = *n*-C_8H_{17}) was used. The complexes **7**, **9** and **10** were better prepared by using RI and relatively short reaction times could be used. The complexes **7-10** were obtained as low-melting yellow solids, which are stable in the solid state in air for short periods of time.

Previously the short chain complexes $[CpW(CO)_3R]$ [22] (R = Me [23], Et [23,24], *n*-Pr [24], *n*-Bu [24,25] and *n*-C_5H_{11} [24,25]) have been reported, along with some characterization data. The complex **10** has also been reported [24].

All the complexes **7-10** have been fully characterized by satisfactory elemental analysis, m.p., IR, ^1H and ^{13}C NMR as well as mass spectroscopy. The data are given in Tables 3.7 - 3.10, and the results are briefly discussed below.

Table 3.7 Data for [CpW(CO)$_3$R].

Compound no	*n*-R	Yield (%)	m. p. (°C)	IR ν(CO)[a] (cm^{-1})	Elemental analysis (%)			
					C		H	
					calc.	found	calc.	found
7	C_6H_{13}	50	97 - 99	2016s, 1927vs, 1894w	40.19	40.60	4.34	4.28
8	C_7H_{15}	62	40 - 42	2016s, 1926vs, 1894w	41.67	41.96	4.67	4.64
9	C_8H_{17}	31	35 - 37	2014s, 1924vs, 1890w	43.07	43.56	4.97	5.07
10	$C_{10}H_{21}$	62	40 - 42	2016s, 1927vs, 1894w	45.57	45.96	5.53	5.80

[a]: IR in hexane.

Table 3.8 ^{1}H NMR data for [CpW(CO)$_3$R] (400 MHz, $CDCl_3$).

Compound no	*n*-R	Cp	W-CH_2 and W-CH_2-CH_2	$(CH_2)_n$	CH_3 ^{3}J(HH) Hz
7	C_6H_{13}	5.36, 5H, s	1.54, 4H, br	1.27, 6H, m	0.87, 3H, t, 7.0
8	C_7H_{15}	5.35, 5H, s	1.53, 4H, br	1.26, 8H, br	0.86, 3H, t, 7.0
9	C_8H_{17}	5.36, 5H, s	1.54, 4H, br	1.26, 10H, br	0.88, 3H, t, 7.0
10	$C_{10}H_{21}$	5.37, 5H, s	1.54, 4H, br	1.26, 16H, br	0.88, 3H, t, 6.4

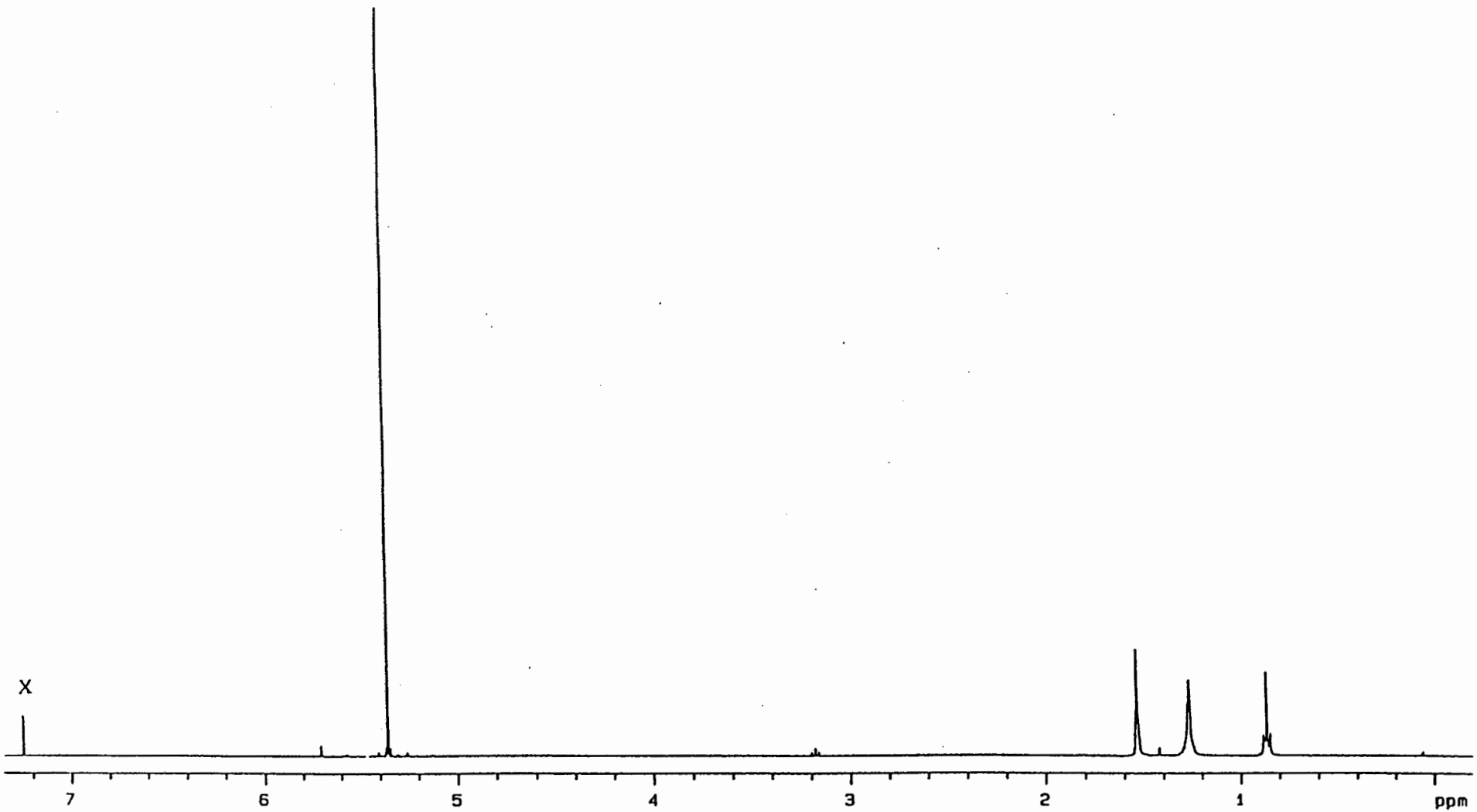

Figure 3.5 ^{1}H NMR spectrum of $[CpW(CO)_3(C_6H_{13})]$, 7 (400 MHz, $CDCl_3$, X = Solvent)

Table 3.9 ^{13}C NMR chemical shift data (δ ppm) for [$CpW(CO)_3R$] (100 MHz, $CDCl_3$).

Compound no	*n*-R	CO	Cp	W-C_1	C_2	C_3	C_4	C_5	C_6	C_7	C_8	C_9	C_{10}
7	C_6H_{13}	229.09, 217.52	91.48	-9.82	36.93	35.67	31.41	22.75	14.13				
8	C_7H_{15}	229.10, 217.52	91.48	-9.81	36.99	35.98	31.98	28.88	22.72	14.14			
9	C_8H_{17}	229.08, 217.50	91.47	-9.80	36.99	36.02	31.95[a]	29.41[a]	29.17[a]	22.70	14.14		
10	$C_{10}H_{21}$	229.07, 217.48	91.46	-9.81	36.98	36.00	31.93[a]	29.74[a]	29.66[a]	29.35[a]	29.20[a]	22.69	14.11

[a]: These peaks are tentatively assigned.

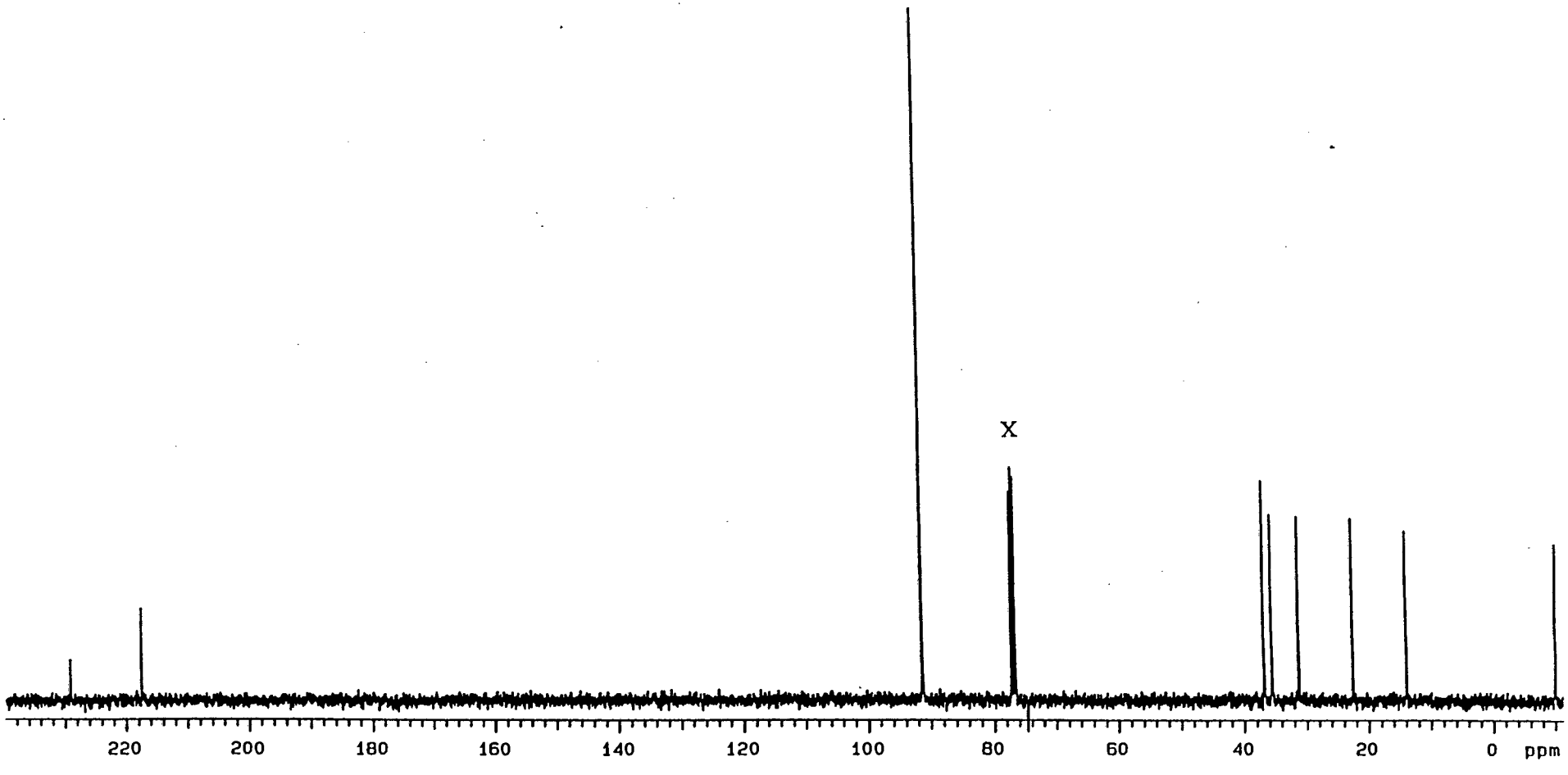

Figure 3.6 ^{13}C NMR spectrum of $[CpW(CO)_3(C_6H_{13})]$, 7 (100 MHz, $CDCl_3$, X = Solvent)

3.3.2 Characterization of [CpW(CO)$_3$R]

IR spectroscopy

The IR spectra of the complexes **7-10** were recorded in hexane solution in the range 2200 to 1600 cm^{-1}. Two strong ν(CO) bands are observed, which is in agreement with the data reported for related compounds [23-25]. In addition, we also observe a weak band at 1890 - 1894 cm^{-1} (about 30 cm^{-1} lower than the strongest peak), which could be assigned to the ν(^{13}CO). Similar observation has also been reported for the compound [CpW(CO)$_3$Pr] in CH_4 matrix [24]. No change in the positions of the carbonyl bands is observed as the carbon chain lengthens from *n*-C_6H_{13} to *n*-$C_{10}H_{23}$.

^{1}H NMR spectroscopy

The ^{1}H NMR data are given in Table 3.8, and the ^{1}H NMR spectrum of the complex **7** is shown in Figure 3.5. The data for complex **10** has been previously reported [24] and our results agree with the previous results. From the ^{1}H NMR data it can be seen that separate resonances are observed for the Cp and methyl group of the alkyl chain and these are not affected by the alkyl chain length. The methylene protons are observed as two broad peaks, thus integration is the only way to distinguish these complexes by ^{1}H NMR.

^{13}C NMR spectroscopy

The ^{13}C NMR data for the complexes **7-10** are summarized in Table 3.9, and the ^{13}C NMR spectrum of complex **7** is shown in Figure 3.6. Assignments were made by comparison with data reported for related compounds in particular the long chain alkyl complexes [CpM(CO)$_2$R] (R = Fe, Ru) [17] as well as with short chain alkyl complexes [CpW(CO)$_3$R] [23,24]. The data for complex **10** have been reported and our results are consistent with the literature [24].

The Cp, CO, W-CH_2 and W-CH_2CH_2 carbon resonances in the complexes **7-10** are found at the same positions regardless of the alkyl chain length. These resonances are dependent on the metal when they are compared to those of the complexes [$CpM(CO)_2R$] (R = Fe, Ru) [17]. Effects of the metal are evident on the first three carbon atoms of the alkyl chain. The remaining carbon resonances are found at the same positions as those found in [$CpM(CO)_2R$] (R = Fe, Ru) [17]. The assignments for the central carbon atoms are not unambiguous due to their similar chemical shifts, as is found for [$CpM(CO)_2R$] (R = Fe, Ru) [17].

Mass spectra

Low resolution electron impact mass spectra were obtained for the complexes **7-10**. The intensities of the major organometallic peaks of these complexes are reported in Table 3.10. The assignments of peaks in the mass spectra are complicated by the isotope pattern of tungsten, which makes the assignments ambiguous, especially for the assignments of the loss of protons.

All the complexes **7-10** show parent molecular ions with expected isotope patterns in their mass spectra. The most abundant peak for complexes **8-10** corresponds to the loss of (2CO and 2H) from molecular ions. This observation is similar to that reported for [$CpFe(CO)_2R$] by Moss and co-workers [17]. All spectra exhibit peaks which are characteristic of the complexes containing the [$CpW(CO)_3$] group, which gives rise to the ions $[CpW(CO)_n]^+$ (n = 0-3). The main fragmentation pathways begin as follows: (1) M, M-CO, M-2CO-2H, M-3CO-2H, M-3CO-6H; and (2) M-R, M-R-CO, M-R-2CO, M-R-3CO.

Table 3.10 Mass spectral data for $[CpW(CO)_3R]$

Ion[a] / Compound no	Relative intensities[b] (%)			
	7	**8**	**9**	**10**
M	11	17	8	8
M - H	7	0	5	6
M - CO	26	43	45	41
M - 2CO - 2H	56	100	100	100
M - 3CO - 2H	42	30	24	26
M - 3CO - 6H	100[c]	77	55	22
M - R	17	21	29	23
M - R - 5H	100[c]	61	67	33
M - CO - R	55	88	84	64
M - 2CO - R	40	61	55	46
M - 3CO - R	45	62	50	43

[a]: M = $[CpW(CO)_3R]$; all ions have a single positive charge; ion refers to probable assignment.
[b]: Peak intensities are relative to the base peak [M-2CO-2H] for complexes **8-10**.
[c]: These peaks could not be distinguished and they serve as the base peak for **7**.

3.3.3 Electrochemical behaviour of the complex $[CpW(CO)_3(C_7H_{15})]$

Cyclic voltammetry (CV) is perhaps the most versatile electroanalytical technique for the study of electroactive species [26-28]. The electrochemical behaviour of transition metal alkyl complexes are of current interest [29-31]. The electrochemical properties of some short chain alkyl complexes $[CpW(CO)_3(CH_3)]$ [32] and $[CpW(CO)_3(C_2H_5)]$ [33] have been investigated recently by Skagestad and Tilset. However, there are no reports of CV studies on longer chain alkyl tungsten complexes.

We have investigated the CV of the complex $[CpW(CO)_3(C_7H_{15})]$, **8**, in acetonitrile solution at room temperature under argon. The cyclic voltammogram of **8** is shown in Figure 3.7(a), measured at a Pt microelectrode and using a

voltage sweep rate of 200 mV/s. The CV analysis showed an irreversible oxidation peak at E_a = 0.56 ± 0.02 V (average of 3 measurements) *vs.* the ferrocene/ferrocenium (Fc/Fc^+) couple at the same scan rate, and at E_a = 0.60 V at a scan rate of 100 mV/s. There was no reduction peak observed for this complex over the range + 1 to -2.4 V.

The oxidation potential obtained for complex **8** is very similar to the values reported for $[CpW(CO)_3(CH_3)]$ (E_a = 0.55 V *vs.* Fc/Fc^+) and $[CpW(CO)_3(C_2H_5)]$ (E_a = 0.52 V). Thus we suggest that the complex **8** should behave similarly to the complexes $[CpW(CO)_3R]$ (R = CH_3, C_2H_5) [32,33]. Skagestad and Tilset have concluded that the oxidation of $[CpW(CO)_3R]$ (R = CH_3, C_2H_5) is an irreversible two-electron oxidation process [32,33]. By chemical oxidation of $[CpW(CO)_3R]$ (R = CH_3, C_2H_5) using acetylferrocenium tetrafluoroborate, they have isolated $[CpW(CO)_2(NCMe)_2(CH_3)]^{2+}$ and $[CpW(CO)_3(NCMe)(CH_3)]^{2+}$, or $[CpW(CO)(NCMe)_2(\eta^2\text{-}COC_2H_5)]^{2+}$ (*via* the intermediate $[CpW(CO)_2(NCMe)_2(C_2H_5)]^{2+}$), respectively. The different types of products obtained from these oxidations are believed to be due to the steric effects of the alkyl chains because the electronic effect difference should only be modest, as indirectly indicated by the nearly equal oxidation potentials measured for these complexes [33]. The longer chain complex **8** shows a similar oxidation potential to the shorter chain complexes, which may indicate that the electronic effect of the longer alkyl chain is similar to that of shorter chains. Considering the steric effect of the longer alkyl chain, we may expect that the complex **8** behaves similarly to the ethyl complex, for which the following electron oxidation mechanism has been suggested (Scheme 3.5) [33]:

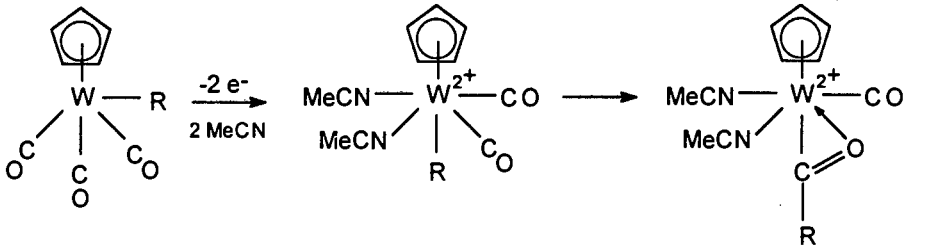

Scheme 3.5

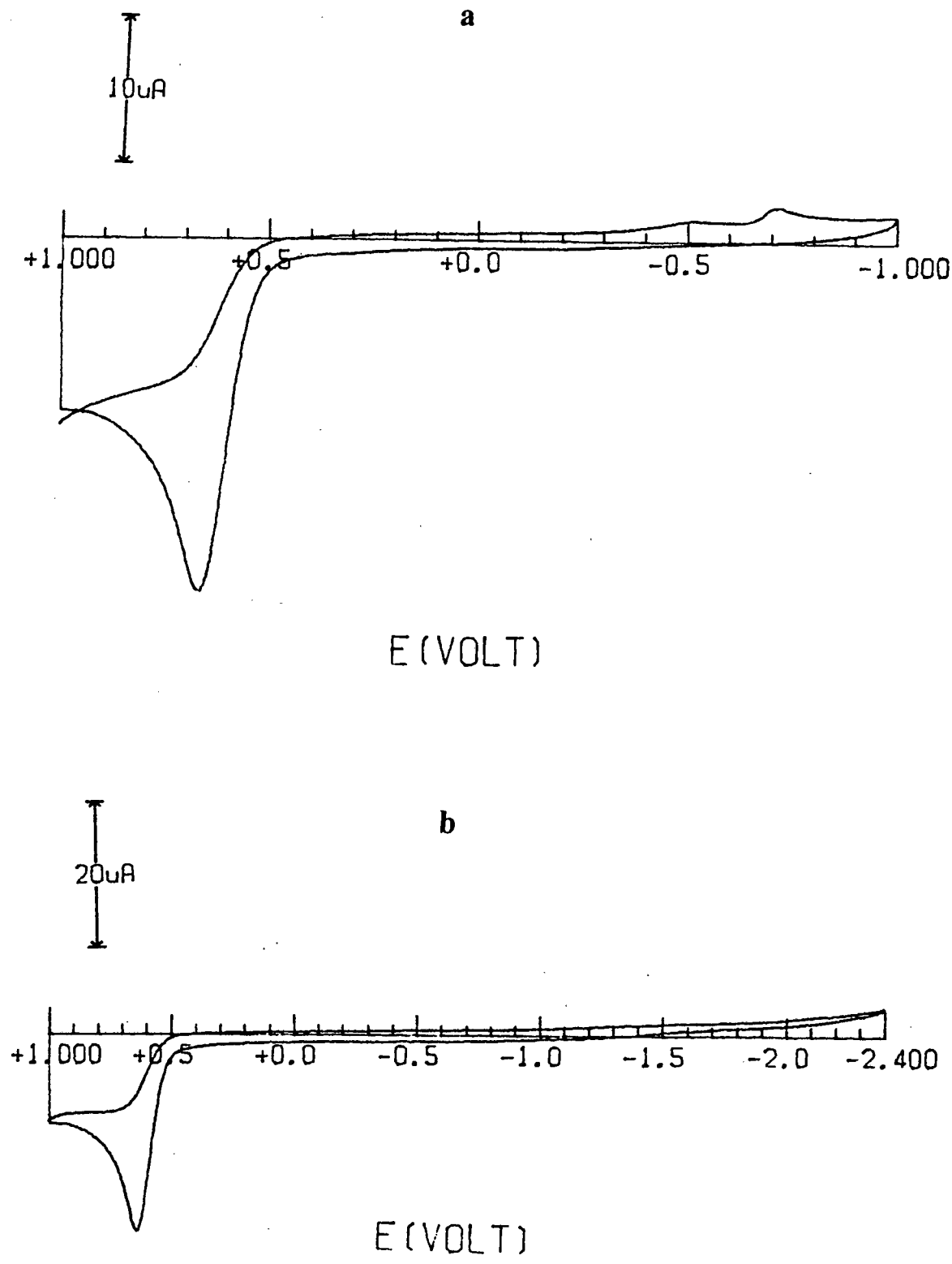

Figure 3.7 Cyclic voltammograms of 1.0 mM [CpW(CO)$_3$(C$_7$H$_{15}$)], 8, in acetonitrile containing 0.1 M [NBu$^n_4$]ClO$_4$ at a Pt microelectrode with a scan rate of 200 mV/s, a: under argon; b, under CO$_2$.

The electrochemical behaviour of **8** under an atmosphere of CO_2 has also been studied, employing similar conditions to those used under argon, and the resultant cyclic voltammogram is shown in Figure 3.7(b). The CV analysis showed an irreversible oxidation peak at 0.55 V *vs.* Fc/Fc^+, which is almost at the same potential as that observed when the CV study was carried out under argon. This result shows that the electrochemical behaviour of **8** under CO_2 is the same as that under argon. It appears that there is no interaction of CO_2 with the oxidized tungsten species.

3.3.4 Thermal behaviour of the complex $[CpW(CO)_3(C_7H_{15})]$ (8)

The thermal properties of complex **8** were studied by DSC and TGA. The DSC and TGA traces of **8** are shown in Figure 3.8. The first sharp endothermic peak at 53 °C of the DSC trace corresponds to the melting of the complex and the second broad endothermic peak at 192 °C corresponds to the decomposition of the complex, as is seen from the TGA trace that significant mass loss is observed over the temperature range 180 - 240 °C. The mass loss corresponds to the loss of all ligands from the complex. The decomposition point of the tungsten alkyl complex is slightly higher than that of the iron alkyl complexes $[CpFe(CO)_2(C_6H_{13})]$ which decomposes at about 160 °C [18]. This is in agreement with the earlier proposal for the short chain compounds that the tungsten complexes $[CpW(CO)_3R]$ are more thermally stable than the iron complexes $[CpFe(CO)_2R]$ [23]. The tungsten alkyl complex **8** seems to be more thermally stable than the tungsten acyl complex **6**. This is unlike the thermal properties observed for the related iron complexes (see section 3.2.3).

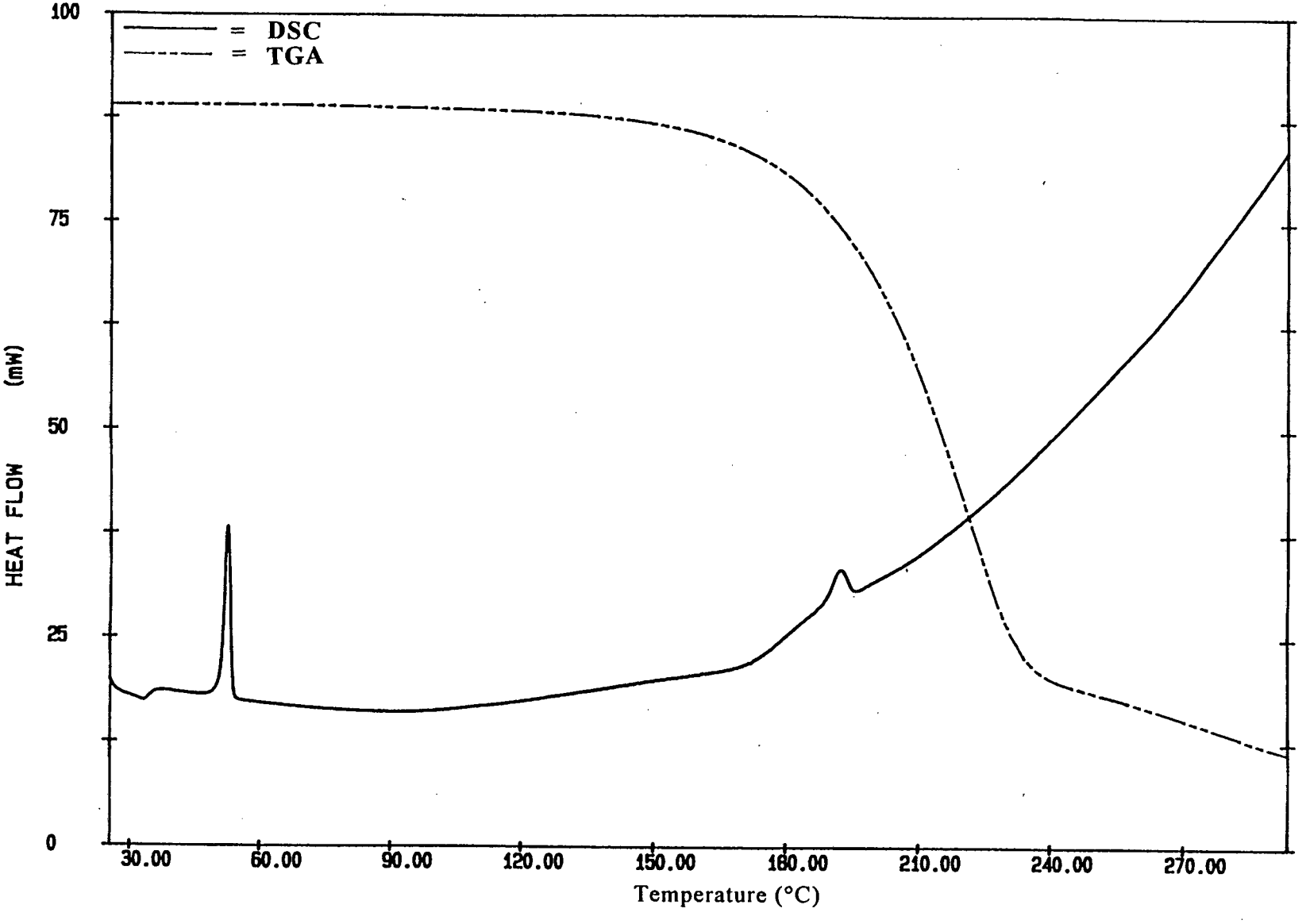

Figure 3.8 DSC and TGA traces for the complex [CpW(CO)$_3$(C$_7$H$_{15}$)], 8 (scan rate = 10 °C/min).

3.3.5 Reactions of CO_2 with the alkyl complexes $[CpFe(CO)_2R]$ and $[CpW(CO)_3R]$ as well as with the carbyne complexes $[CpW(CO)_2(\equiv CR)]$ [R = C_6H_5 and C_6H_4-OMe-(4)]

The reaction of anionic alkyl complexes $[PPN]^+[W(CO)_4(L)R]^-$ [R = Me, Et and Ph; L = CO, PMe_3 and $P(OMe)_3$] with CO_2 has been reported to give the CO_2 inserted product $[PPN]^+[W(CO)_4(L)(O_2CR)]^-$ [34]. The reaction of dialkyl complexes $[Cp^*W(NO)Ph_2]$ with CO_2 gives $[Cp^*W(NO)Ph(O_2CPh)]$ [35]. Fischer and co-workers [36] have also reported the reaction of the anionic carbyne complexes with CO_2 as shown below.

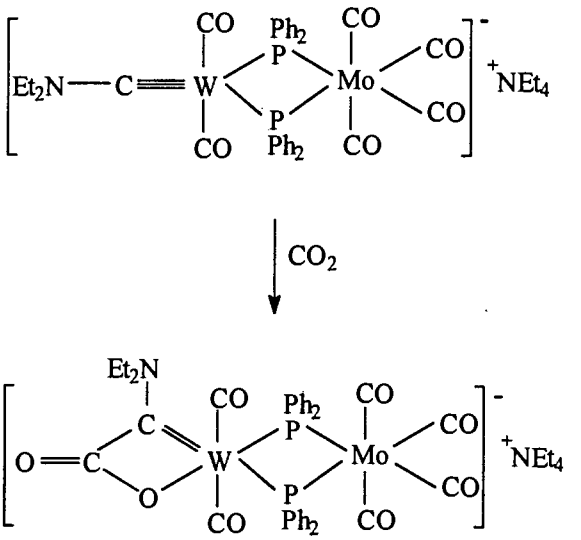

Scheme 3.6

These successful results have prompted us to investigate the reactions of some alkyl and carbyne complexes of tungsten with CO_2. Initially, we investigated the reaction of the alkyl complexes $[CpFe(CO)_2R]$ (R = CH_3, *n*-$C_{11}H_{23}$) with CO_2 (40 or 48 bar) at 50 °C in hexane or THF for two days and found that no reaction occurred. Similarly treatment of $[CpW(CO)_3R]$ (R = *n*-C_8H_{17}) with CO_2 (48 bar) at 50 °C in THF for two days showed no reaction and only the starting complex was recovered. This contrasts with the well-known reaction of $[CpFe(CO)_2R]$ and $[CpW(CO)_3R]$ with SO_2 to afford S-sulfinate $[CpFe(CO)_2(SO_2R)]$ [21] and $[CpW(CO)_3(SO_2R)]$ [22,37]. The lack of reactivity for these alkyl complexes with CO_2 could be due to the facts that these complexes are 18 electron species and are of poor nucleophilicity, thus inert to CO_2. The anionic alkyl complexes

$[PPN]^+[W(CO)_4(L)R]^-$ [34] and the dialkyl complexes $[Cp^*W(NO)Ph_2]$ [35] are probably better nucleophiles which are capable of undergoing reactions with CO_2. In fact, even the anion $[CpW(CO)_3]^-$ could not react with CO_2 in THF at room temperature. This is also due to its weak nucleophilicity, compared to the strong nucleophile $[CpFe(CO)_2]^-$. The latter has been reported to react with CO_2 at -78 °C to give $[CpFe(CO)_2(CO_2)]^-$ and subsequently to react with an alkylating reagent to give the alkoxycarbonyl complex $[CpFe(CO)_2(CO_2Me)]$ [38].

We were interested to investigate the reactions of compounds having different metal-carbon bond orders with CO_2. Thus, we subsequently investigated the reactions of two tungsten carbyne complexes with CO_2. The carbyne complexes **11** and **12** (as shown below) were first reported by Fischer and co-workers [39]. We used the procedure developed by Mayr and co-workers [40], which was later extended by Stone and co-workers [41], to prepare these carbyne complexes. The preparation scheme is shown below:

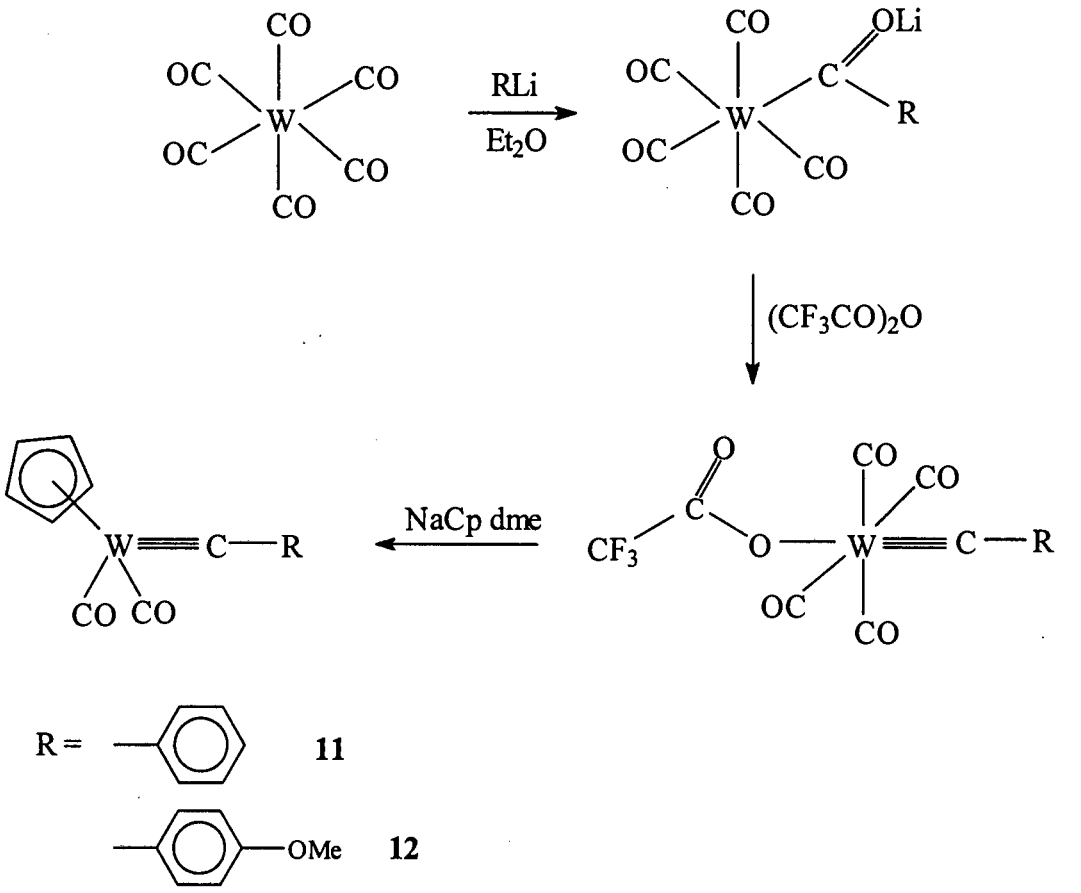

Scheme 3.7

The complexes **11** and **12** were characterized by IR, ^{1}H and ^{13}C NMR spectroscopy. The charaterization data are in good agreement with previously reported data [39]. In addition, new data on the thermal properties of **12** were obtained by DSC and TGA. The DSC trace of **12** shows a sharp endothermic peak at T_{max} = 95 °C due to the melting of the sample. The TGA trace of **12** shows significant mass loss over the range 190 - 250 °C due to the decomposition of the complex.

We reasoned that CO_2 could add to the W≡C bond of these complexes [42-44] to form cyclic species as postulated below:

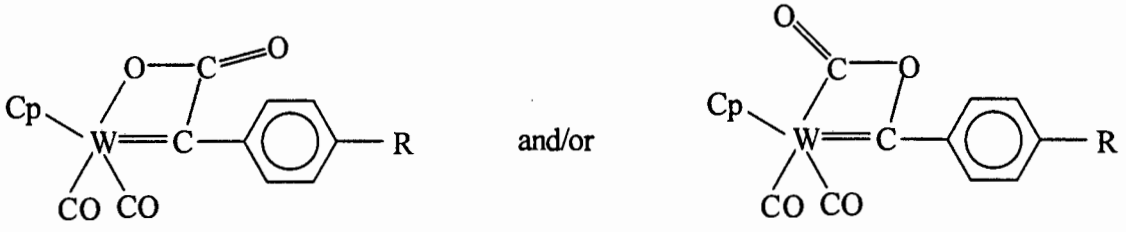

Thus we have attempted many experiments to investigate the reactions of the carbyne complexes **11** and **12** with CO_2 under various conditions. However, all the attempts to isolate the postulated products failed. For example, the reaction of **11** with CO_2 (50 bar) in CH_2Cl_2 at room temperature was carried out for 22 hours. The IR spectrum of the reaction mixture showed new peaks at 2020s and 1987s cm^{-1} as well as peaks due to the starting complex at 1977sh and 1908s cm^{-1}. The starting complex completely degraded in about 10 days under the same conditions as above-mentioned, to give a solution of which the IR spectrum showed bands at 2020s, 1993sh, 1976s, 1770w and 1713w cm^{-1}, suggesting that the reaction of **11** and CO_2 might have occurred. In contrast, keeping a solution of **11** in CH_2Cl_2 under 40 bar nitrogen for 22 hours at room temperature showed no change in the IR spectrum of the solution. The product(s) of the reaction of **11** and CO_2 could not be characterized due to the difficulties in obtaining a pure sample. Nevertheless, the ^{13}C NMR spectrum of the product(s) in DMF-d_7 showed peaks among others at δ 192 and 173 ppm, which are commonly seen for compounds

containing CO and CO_2 groups. This may provide additional evidence to that the reaction of **11** with CO_2 had indeed occurred.

The reaction of **11** with CO_2 (45 bar) was also carried out in benzene at 50 °C for 26 hours, which also showed the complete degradation of **11**. This is indicated by the disappearance of the IR bands at 1985 and 1911 cm^{-1} (in benzene) and the appearance of the new bands at 2016w, 1975m, 1916m and 1712s cm^{-1} in the IR spectrum of the reaction mixture. The final product(s) could again not be isolated. So far we have not been able to confirm the formation of the postulated products from the reaction of the carbyne complexes with CO_2. However, a recent report on the reaction of CO_2 with the ruthenium carbyne complex showed that the cycloaddition of C=O bond and Ru≡C is possible, as shown below [45].

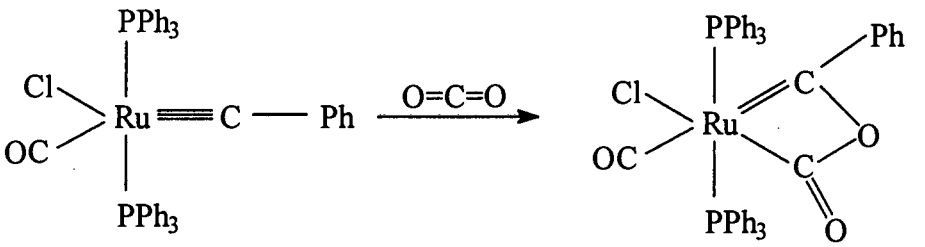

Scheme 3.8

3.4 Conclusion

The new long chain acyl complexes [$CpFe(CO)_2\{C(O)R\}$] (R = *n*-C_5H_{11}, **1**; *n*-C_8H_{17}, **2**; *n*-$C_{11}H_{23}$, **3**; and *n*-$C_{17}H_{35}$, **4**), [$Cp^*Fe(CO)_2\{C(O)R\}$] (R = *n*-$C_{11}H_{23}$, **5**) and [$CpW(CO)_3\{C(O)R\}$] (R = *n*-$C_{11}H_{23}$, **6**) have been prepared in good yields and fully characterized. The new long chain alkyl complexes [$CpW(CO)_3R$] (R = *n*-C_6H_{13}, **7**; *n*-C_7H_{15}, **8**; and *n*-C_8H_{17}, **9**) have also been prepared in moderate to good yields and fully characterized. These long chain acyl and alkyl complexes are relatively stable and can be conveniently handled. Thermal analysis of selected complexes have shown that these complexes are thermally stable up to 170 °C or higher temperature, although they are low-melting. The alkyl chain

length has little effect on the spectroscopic properties of the acyl or alkyl complexes.

The studies of the reactions of syngas with the iron acyl complexes have shown that formate and ester are the reaction products (albeit in low yields). The reactivity of the acyl complexes [LM{C(O)$C_{11}H_{23}$}] [L = $Mn(CO)_5$, $CpFe(CO)_2$, $Cp^*Fe(CO)_2$ and $CpW(CO)_3$] towards syngas is found to be dependent on the metal and ligand as well as solvent. These results may pertain to intermediates in catalytic reactions.

Attempted reactions of the alkyl complexes [$CpFe(CO)_2R$] and [$CpW(CO)_3R$] with CO_2 were unsuccessful under both thermal and electrochemical conditions investigated in this work. The reactions of the carbyne complexes [$CpW(CO)_2(\equiv CR)$] [R = C_6H_5 and C_6H_4-OMe-(4)] with CO_2 yield unidentified products and further investigation should be carried out.

References

1. Chapter 2 of this thesis.
2. M.E. Dry, Catalysis Today, 1990, **6**, 183.
3. J.R. Moss, J. Mol. Catal. A: Chemical, 1996, **107**, 169.
4. J-A. M. Andersen and J.R. Moss, Organometallics, 1994, **13**, 5013.
5. R. George, J-A. M. Andersen and J.R. Moss, J. Organomet. Chem., 1995, **505**, 131.
6. M.A. Gafoor, A.T. Hutton and J.R. Moss, J. Organomet. Chem., 1995, **515**, 233.
7. (a): F.A. Cotton and G. Wilkinson, *Advanced Inorganic Chemistry*, 5th ed., John Wiley & Sons Inc.: New York, 1988, chapter 28, p 1224;
   (b): J.P. Collman, L.S. Hegedus, J.R. Norton and R.G. Finke, *Principles and Applications of Organotransition Metal Chemistry*, 2nd ed.,University Science Books: Mill Valley, CA, 1987, chapter 12, p 619.
8. R.B. King, J. Am. Chem. Soc., 1963, **85**, 1918, and references therein.
9. J.A. McCleverty and G. Wilkinson, J. Chem. Soc., 1963, 4096.
10. R.S. Bly, G.S. Silverman, M.M. Hossain and R. K Bly, Organometallics, 1984, **3**, 642.
11. C. Amiens, G. Balavoine and F. Guibe, J. Chem. Soc. Chem. Commun., 1991, 1458.
12. R.B. King, W.M. Douglas and A. Efraty, J. Organomet. Chem., 1974, **69**, 131, and references therein.
13. J-P. Barras, S.G. Davies, M. R. Metzler, A.J. Edwards, V.M. Humphreys and K. Prout, J. Organomet. Chem., 1993, **461**, 157, and references therein.
14. R.D. Adams, D.F. Chodosh and N.M. Golembeski, Inorg. Chem., 1978, **17**, 266.
15. H.B. Friedrich, P.A. Makhesha, J.R. Moss and B.K. Williamson, J. Organomet. Chem., 1990, **384**,325.
16. S.J. Archer, G.A. Harvey, J.R. Moss and A.M. Crouch, Inorg. Chim. Acta, 1992, **201**, 43.

17. A. Emeran, M. A. Gafoor, J.K.I. Goslett, Y-H. Liao, L. Pimble and J.R. Moss, J. Organomet. Chem., 1991, **405**, 237, and references therein.
18. R.O. Hill (Supervisor Prof. J. R. Moss), B.Sc. Honour's Project Report, University of Cape Town, 1990.
19. R.B. King and M.B. Bisnette, J. Organomet. Chem., 1964, **2**, 15.
20. A.R. Cutler, P.K. Hanna and J.C. Vites, Chem. Rev., 1988, **88**, 1363.
21. R.C. Kerber in *Comprehensive Organometallic Chemistry II* , Eds. E.W. Abel, F.G.A. Stone and G. Wilkinson, Pergamon: New York, 1995, vol 7, p 101.
22. For a recent general review of tungsten alkyl compounds, M.J. Morris, in *Comprehensive Organometallic Chemistry II* , Eds. E.W. Abel, F.G.A. Stone and G. Wilkinson, Pergamon: New York, 1995, vol 5, p 393.
23. T.S. Piper and G. Wilkinson, J. Inorg. Nucl. Chem., 1956, **3**, 104.
24. K.A. Mahmoud, A.J. Rest, H.G. Alt, M.E. Eichner and B. M. Jansen, J. Chem. Soc. Dalton Trans., 1984, 175.
25. S.C. Tripathi, S.C. Srivastava and D.N. Pathak, J. Organomet. Chem., 1976, **107**, 315.
26. For a brief introduction of cyclic voltammetry, (a): P. T. Kissinger and W. R. Heineman, J. Chem. Educ., 1983, **60**, 702; (b): G. A. Mabbott, ibid, 1983, **60**, 697; (c): U. Loffler, Sensorik, 1994, **4** (Chemische Sensoren Heute und Morgen), 100-22, 174; Chem. Abstr., 1995, **123**:101385.
27. For a recent book of CO_2 activation by electrochemical method, Eds. B. P. Sullivan, K. Krist and H. E. Guard, *Electrochemical and Electrocatalytic Reactions of Carbon Dioxide*, Elsevier: Amsterdam, 1993.
28. For some recent papers of electrochemical activation of CO_2, (a): S. A. Wander, A. Miedaner, B. C. Noll, R. M. Barkley and D. L. DuBois, Organometallics, 1996, **15**, 3360; (b): F. P. A. Johnson, M. W. George, F. Hartl and J. J. Turner, Organometallics, **15**, 3374; (c): M. Hammouche, D. Lexa, M. Momenteau and J-M. Saveant, J. Am. Chem. Soc., 1991, **113**, 8455; (d): B. D. Steffey, C. J. Curtis and D. L. DuBois, Organometallics, 1995, **14**, 4937.

29. For electrochemical studies of complexes containing metal-carbon bonds, (a): S. Derien, J-C. Clinet, E. Dunach and J. Perichon, J. Org. Chem., 1993, **58**, 2578;
(b): C. Amatore and A. Jutand, J. Am. Chem. Soc., 1991, **113**, 2819; and references 30 and 31.

30. C. Amatore, A. Jutand, F. Khalil and M. F. Nielsen, J. Am. Chem. Soc., 1992, **114**, 7076.

31. A. L. Seligson and W. C. Trogler, J. Am. Chem. Soc., 1992, **114**, 7085.

32. V. Skagestad and M. Tilset, Organometallics, 1991, **10**, 2110.

33. V. Skagestad and M. Tilset, Organometallics, 1992, **11**, 3293.

34. D.J. Darensbourg, R.K. Hanckel, C.G. Bauch, M. Pala, D. Simmons and J.N. White, J. Am. Chem. Soc., 1985, **107**, 7463.

35. E.B. Brouwer, P. Legzdins, S.J. Rettig and K.J. Ross, Organometallics, 1993, **12**, 4234.

36. E.O. Fischer, A.C. Filippou, H.G. Alt and U. Thewalt, Angew. Chem. Int. Ed. Engl., 1985, **24**, 203.

37. R.G. Severson and A. Wojcicki, J. Am. Chem. Soc., 1979, **101**, 877.

38. T. Forschner, K. Menard, A.R. Culter, J. Chem. Soc. Chem. Commun., 1984, 121.

39. E.O. Fischer, T.L. Lindner, G. Huttner, P. Friedrich, F. R. Kreiβl and J.O Besenhard, Chem. Ber., 1977, **110**, 3397.

40. G.A. McDermott, A.M. Dorries and A. Mayr, Organometallics, 1987, **6**, 925.

41. S.J. Dossett, A.F. Hill, J.C. Jeffery, F. Marken, P. Sherwood and F.G.A. Stone, J. Chem. Soc. Dalton Trans., 1988, 2453.

42. F.G.A. Stone, Angew. Chem. Int. Ed. Engl., 1984, **23**, 89.

43. A. Mayr and H. Hoffmeister, Adv. Organomet. Chem., 1991, **32**, 227.

44. Y. Chi and D-K. Hwang, in *Comprehensive Organometallic Chemistry II*, Eds. E.W. Abel, F.G.A. Stone and G. Wilkinson, Pergamon: New York, 1995, vol. 10, p 85.

45. R.B. Bedford, A.F. Hill, A.J.P. White and D. J. Williams, Angew. Chem. Int. Ed. Engl., 1996, **35**, 95.

Chapter 4

Synthesis And Characterization Of Pt(II) And Pt(IV) Alkyl Complexes And Their Reactivity Towards Carbon Dioxide

4.1 Introduction

The group 10 metals Ni, Pd and Pt are electron rich late transition metals. These metals have been reported to form complexes with carbon dioxide. The nickel complexes $[Ni(CO_2)(PR_3)_2]$ (R = Et, Bu, Ph, Cy) [1] and the palladium complex $[Pd(CO_2)(PMePh_2)_2]$ [2] have been reported to be examples of η^2-CO_2 side-on coordination as shown below:

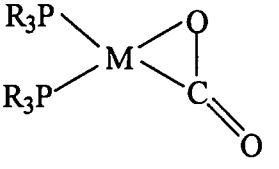

Vol'pin and Kolomnikov [3] have claimed the preparation of a similarly coordinated platinum complex $[Pt(CO_2)(PPh_3)_2]$ which has been characterized by IR and X-ray photoelectron spectroscopy (XPS). Wilkinson and co-workers [4,5] have also reported the reactions of $[Pt(PPh_3)_3]$ and $[Pd(PPh_3)_4]$ with O_2 and CO_2 to give the carbonate complexes $[M(CO_3)(PPh_3)_2]$ (M = Pt, Pd) *via* the insertion of CO_2 into the M-O bond as shown below.

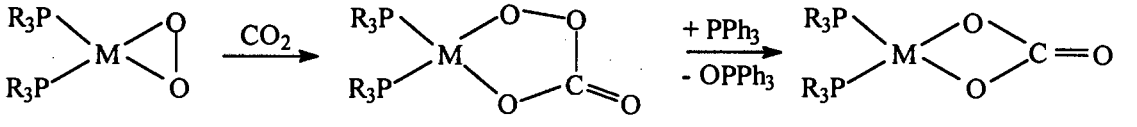

Scheme 4.1

The platinum carbonate complexes can be used as precursors for a wide range of Pt(0) and Pt(II) complexes [6-9].

The group 10 metals Ni [10-12] and Pd [12,13] have also been found to be reactive in the catalytic activation of CO_2. The insertion of CO_2 into a Ni-C bond [14,15], as shown in Scheme 4.2, has been reported.

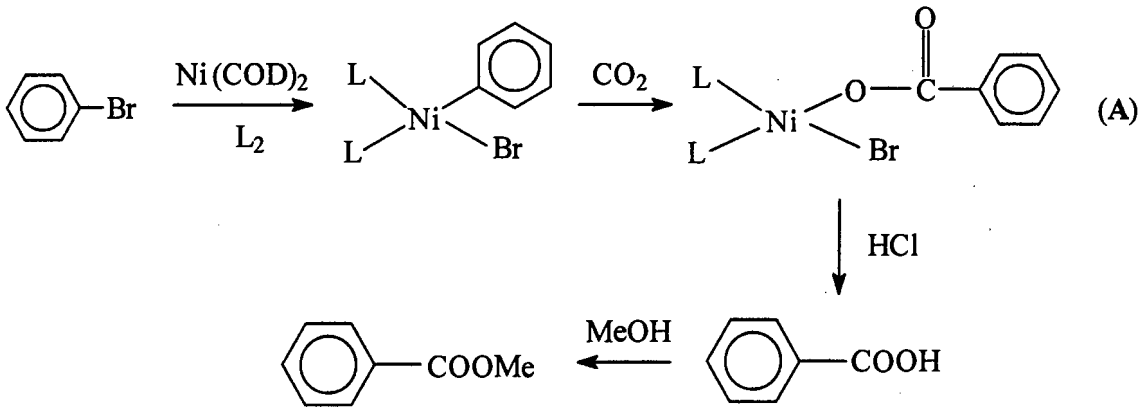

L = PPh_3, [15]; L_2 = bipy [14]

Scheme 4.2

It has been reported that the products obtained from the CO_2 insertion into the Ni-C bond are largely dependent on the ligand coordinated to Ni [14,15]. Thus 2,2′-bipyridine (bipy) is a better ligand than PPh_3 for the reaction shown in Scheme 4.2 [14,15]. This has also been confirmed by a preliminary experiment we have carried out using the bipy ligand. Unfortunately, the proposed key intermediate (A) could not be isolated. The electrochemical reduction of CO_2 by Ni and Pd complexes has also been studied extensively [16-18]. There are no reports however of the electrochemical reduction of CO_2 by Pt complexes.

The Pt(II) dialkyl complexes [PtR_2L_2] (R = alkyl, L = trialkylphosphine, or L_2 = bipy, phen) have been known for many years [19,20]. There are few reports on the reactivity of these complexes with CO_2, except that by Puddephatt and co-workers who reported the reaction of [$PtMe_2L_2$] (L_2 = bipy, phen) with CO_2 and epoxides to give cyclic carbonate complexes [21]. We envisaged that other Pt(II) dialkyl complexes may be reactive towards CO_2 under suitable conditions. Thus we have synthesized some new Pt(II) and Pt(IV) alkyl complexes with trialkylphosphine, bipy or 4,4′-dimethyl-2,2′-bipyridine (Me_2-bipy) ligands, and investigated their reactivity with CO_2 under various conditions. We have also prepared some Pt(II)

alkoxycarbonyl and carboxylate complexes, which could formally be derived from the insertion of CO_2 into the Pt-C bond of Pt(II) alkyl complexes. These results are discussed in the following sections.

4.2 Synthesis and reactivity of Pt(II) alkyl complexes with PR_3 ligands

4.2.1. Synthesis of Pt(II) alkyl complexes with PR_3 (R = Bu, Ph) ligands

The complexes *cis*-$[PtBu_2(PR_3)_2]$ (R= Bu, **1**; Ph, **2**) were prepared in good yields by the reaction of *cis*-$[PtCl_2(PR_3)_2]$ (R= Bu, Ph) with BuLi in dry ether (see Scheme 4.3). This method is similar to that reported for the preparation of **2** by Whitesides and co-workers [22].

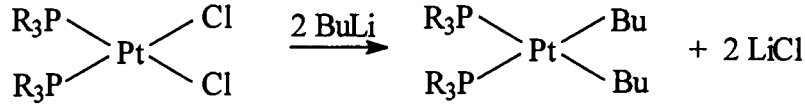

R = Bu, **1**
R = Ph, **2**

Scheme 4.3

The complex **1** is new and has been fully characterized by elemental analysis, melting point, IR, ^1H and ^{31}P NMR spectroscopy. The data are reported in the experimental section 7.4.1. The IR spectrum (recorded as Nujol mull) of **1** shows two weak bands at 454 and 393 cm^{-1} due to the ν(Pt-P), which indicates that the stereochemistry of the complex remains in the *cis* geometry [23]. For *trans* geometry, only one ν(Pt-P) band would be expected [23]. The ^{31}P NMR spectrum (recorded in C_6D_6) of **1** shows a peak at δ 1.95 ppm with $^1J(^{195}Pt\text{-}^{31}P)$ = 1704 Hz. The coupling constant $^1J(^{195}Pt\text{-}^{31}P)$ is very informative because this value is similar to those reported for *cis*-$[PtPh_2(PBu_3)_2]$ [$^1J(PtP)$= 1758 Hz][24] and *cis*-$[PtPr_2(PEt_3)_2]$ [$^1J(PtP)$ = 1701 Hz] [25]. The value of the coupling constant is further support that the geometry of complex **1** is *cis*.

The thermal properties of complex **1** were studied by DSC and TGA. The DSC trace of **1** shows a sharp endothermic peak (maximum) at 32 °C, which corresponds to the melting point (24 - 25 °C, Kofler hot stage microscope) of **1**, and another broad endothermic peak (maximum) at 133 °C, which corresponds to the decomposition of the sample. This is also supported by the mass loss over the range 81 - 161 °C in the TGA trace. The mass loss in this temperature range corresponds to the elimination of, presumably, butene and butane from complex **1** (see experimental section 7.4.1).

The complex **2** has been characterized by IR [22a] and ^{1}H NMR [22b] previously. We have recorded the ^{31}P NMR spectrum (in $CDCl_3$) of **2** which shows a peak at δ 27.36 ppm with $^{1}J(PtP)$ = 1719 Hz. This again confirms the *cis* geometry of the complex. The ^{13}C NMR spectrum of **2** was also recorded and the data are given in the experimental section 7.4.1.

The monoalkyl complex *trans*-[PtClBu(PBu_3)], **3**, was synthesized by the reaction of the dialkyl complex **1** with an equal molar amount of HCl in dry ether as shown in Scheme 4.4.

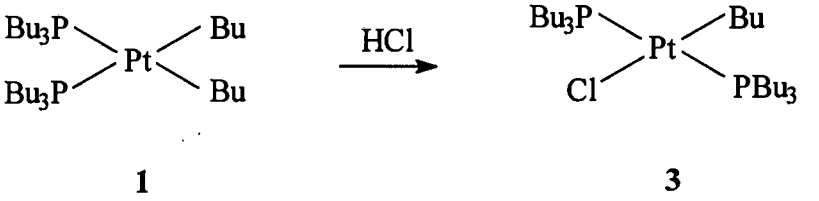

1 **3**

Scheme 4.4

This reaction is similar to that reported by Alibrandi and co-workers [23] for the preparation of *cis*- and *trans*-[PtClR(PEt_3)$_2$]. The new complex **3** was obtained as a pale-yellow oil and has been fully characterized by satisfactory elemental analysis, IR, ^{1}H, ^{13}C and ^{31}P NMR spectroscopy. The data can be found in the experimental section 7.4.1. The IR spectrum (neat film) of the complex **3** shows a peak at 264 cm^{-1} which is assigned to the ν(Pt-Cl). The ^{31}P NMR spectrum of **3** in C_6D_6 shows a single peak at δ 8.00 ppm with $^{1}J(PtP)$ = 2924 Hz, which indicates

that the complex **3** is *trans*. It has been reported that the *trans* monoalkyl complexes show only one phosphorus resonance with a coupling constant to ^{195}Pt centred at 2939 ± 90 Hz where the *cis* derivatives show two phosphorus resonances [23].

4.2.2 The reactivity of *cis*-[$PtBu_2(PR_3)_2$] (R = Bu, Ph) with CO_2

We envisaged that CO_2 might insert into the Pt-C bond of the dialkyl complexes to give either an alkoxycarbonyl complex (which contains the Pt-C bond) or a carboxylate complex (which contains the Pt-O bond) as shown below.

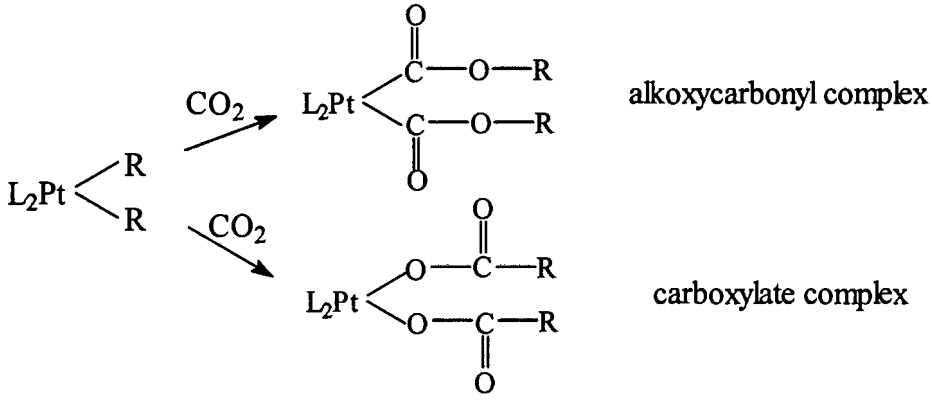

Scheme 4.5

Thus the reaction of *cis*-[$PtBu_2(PPh_3)_2$], **2** with CO_2 was carried out in an autoclave under CO_2 (50 bar) at 60 °C for 14 hours in triethylamine. The reaction produced a white solid product [$Pt(CO_3)(PPh_3)_2$], **4**, the IR spectrum (Nujol mull) of which shows two ν(C=O) bands at 1676s and 1625w cm^{-1}, and the ^{31}P NMR spectrum ($CDCl_3$) shows a peak at δ 6.61 ppm with $^1J(PtP)$ = 3711 Hz. These data are in good agreement with those obtained for an authentic sample of the carbonate complex [$Pt(CO_3)(PPh_3)_2$] prepared from *cis*-[$PtCl_2(PPh_3)_2$] and Ag_2CO_3 [9], and are also in good agreement with the data reported for [$Pt(CO_3)(PPh_3)_2$] prepared by another route [5].

Similarly, the reaction of [$PtBu_2(PBu_3)_2$], **1** and CO_2 gave a mixture of [$Pt(CO_3)(PBu_3)_2$], **5** and another product in a ratio of 75:25 (based on the

integration of the peaks in the ^{31}P NMR spectrum). The complex **5** shows IR peaks (CsI disc) at 1659s, 1633m cm^{-1}, and ^{31}P NMR (C_6D_6) at δ -4.84 ppm with $^1J(PtP)$ = 3417 Hz. The complex $[Pt(CO_3)(PBu_3)_2]$, **5** was also prepared from *cis*-$[PtCl_2(PBu_3)_2]$ and Ag_2CO_3. The ^{31}P NMR spectrum (C_6D_6) of the product prepared by this route shows a peak at δ -4.74 ppm with $^1J(PtP)$ = 3473 Hz. The other product was observed in the ^{31}P NMR spectrum (C_6D_6) at δ 15.18 ppm with $^1J(PtP)$ = 2714 Hz. This latter product may be $[Pt(PBu_3)_2]_n$, a decomposition product of the complexes $[Pt(CO_3)(PBu_3)_2]$ or $[Pt(CO_2)(PBu_3)_2]$, since no additional ν(C=O) band was seen in the IR spectrum of the product mixture.

The preparation of the carbonate complexes by the reactions of *cis*-$[PtBu_2(PR_3)_2]$ (R = Bu, Ph) with CO_2 has no advantage over previously reported methods using *cis*-$[PtCl_2(PR_3)_2]$ and Ag_2CO_3 [5,9]. However, the present work provides an additional route for the preparation of these carbonate complexes. The mechanism for the formation of the carbonate complexes could be as follows (Scheme 4.6):

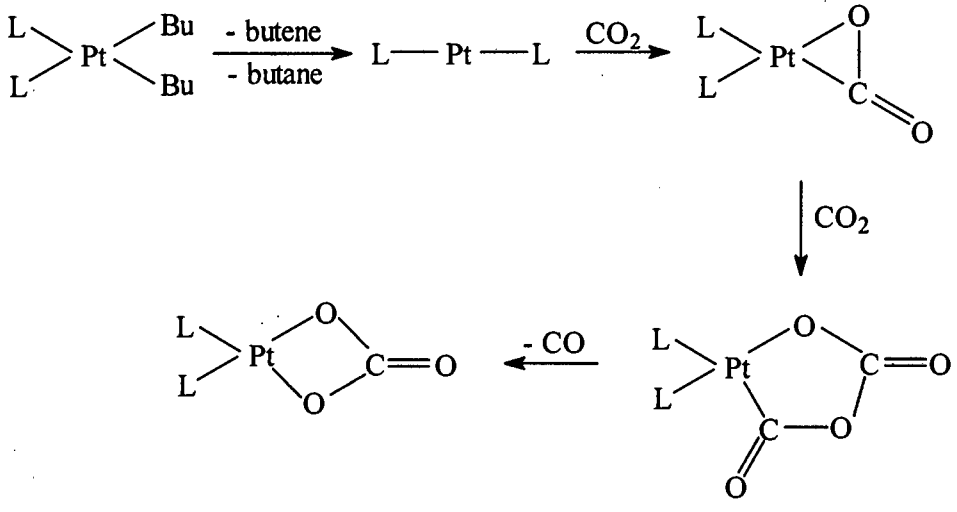

L = PPh_3, **4**; PBu_3, **5**

Scheme 4.6

The intermediate $[PtL_2]$ could be formed from thermal decomposition of the starting dialkyl complexes by elimination of butene and butane, as has been shown by Whitesides and co-workers [22] who have studied the thermal decomposition of *cis*-$[PtBu_2(PPh_3)_2]$. The η^2-CO_2 coordinated complex

$[Pt(CO_2)L_2]$ may be unstable and was not observed, however, analogous Ni [1] and Pd [2] complexes have been reported in the literature. The formation of the $[Pt(CO_2)L_2]$ intermediate is also supported by the isolation of the Pt(0) complex $[Pt(CH_2{=}CHCO_2Me)(PPh_3)_2]$, **6**, by the reaction of *cis*-$[PtBu_2(PPh_3)_2]$ with methylacrylate (see experimental section 7.4.1). Further CO_2 insertion into the Pt-C bond of the proposed complex $[Pt(CO_2)L_2]$ could give the platinum heterometallocyclic complex $[Pt(C_2O_4)L_2]$. This complex is similar to the iridium complex $[IrCl(C_2O_4)(PMe_3)_3]$ reported by Herskovitz and Guggenberger [26]. The carbonate complex $[Pt(CO_3)L_2]$ may result from the decarbonylation of $[Pt(C_2O_4)L_2]$. The formation of $[Pt(CO_3)(PPh_3)_2]$ by the reaction of $[Pt(CH_2{=}CH_2)(PPh_3)_2]$ with CO_2 *via* the intermediate $[Pt(C_2O_4)L_2]$ has also been suggested [27].

Another possible route for the formation of the carbonate complex $[Pt(CO_3)(PR_3)_2]$ by the reaction of $[PtR_2(PR_3)_2]$ with CO_2, though we believe less likely, could result from the existence of traces of water which could react with CO_2 to form carbonate anion and its subsequent reaction with $[PtL_2]$ could produce the carbonate complex.

Although the anticipated alkoxycarbonyl and carboxylate complexes have not been obtained by the reactions of the dialkyl complexes with CO_2, we have successfully prepared some alkoxycarbonyl and carboxylate complexes by other routes. These results will be discussed in the following section.

4.2.3 Alkoxycarbonyl, carboxylate and oxalate complexes

Alkoxycarbonyl and carboxylate complexes could be model complexes for the insertion of CO_2 into a Pt-C bond as shown in Scheme 4.5. We have synthesized some alkoxycarbonyl complexes of the type *trans*-$[Pt(CO_2R)_2(PPh_3)_2]$ (R = Me, **7**, Et, **8**) by a novel and simple route. We have also prepared the carboxylate complex *cis*-$[Pt(O_2CCH_3)_2(PPh_3)_2]$ and the oxalate complex $[Pt(C_2O_4)(PBu_3)_2]$ in order to compare their properties with the alkoxycarbonyl complexes.

Preparation of the alkoxycarbonyl complexes *trans*-[Pt(CO$_2$R)$_2$(PPh$_3$)$_2$]

The alkoxycarbonyl complexes *trans*-[Pt(CO$_2$R)$_2$(PPh$_3$)$_2$] (R = Me, **7**, Et, **8**) can be easily prepared in high yields by the reaction of *cis*-[PtCl$_2$(PPh$_3$)$_2$] with CO and ROH (R = Me, Et) in the presence of triethylamine, as shown below:

$$\textit{cis}\text{-}[PtCl_2(PPh_3)_2] + 2\,ROH + 2\,CO \xrightarrow{NEt_3} \textit{trans}\text{-}[Pt(CO_2R)_2(PPh_3)_2] + 2\,[NHEt_3]Cl$$

R = Me, **7**
R = Et, **8**

Scheme 4.7

The complexes *trans*-[Pt(CO$_2$R)$_2$(PPh$_3$)$_2$] (R = Me, Et) have been characterized by satisfactory elemental analysis and by IR and NMR spectroscopy. The data are in good agreement with the literature [28, 29]. In addition, we have characterized *trans*-[Pt(CO$_2$Me)$_2$(PPh$_3$)$_2$], **7** by ^{195}Pt NMR, which shows a peak at δ -4531.8 ppm (relative to external H_2PtCl_6) with $^1J(^{195}Pt\text{-}^{31}P)$ 3091 Hz. The stereochemistry of these complexes has previously been established by a single crystal X-ray structural determination of *trans*-[Pt(CO$_2$Et)$_2$(PPh$_3$)$_2$] [30]. The thermal properties of the complexes **7** and **8** have been studied by DSC and TGA, and the data can be found in the experimental section 7.4.2 of this thesis.

The method for the preparation of the alkoxycarbonyl complexes is very simple compared to the previous methods reported [28,29]. The previous methods required multistep reactions and gave low yields [28,29]. Although the complexes *trans*-[Pt(CO$_2$R)$_2$(PPh$_3$)$_2$] with R = Me and Et can be isolated analytically pure from the reaction of *cis*-[PtCl$_2$(PPh$_3$)$_2$] with CO/MeOH or CO/EtOH, similar reactions carried out with *n*-PrOH and *iso*-PrOH give a mixture of [Pt(CO)$_2$(PPh$_3$)$_2$], **9** [31] and *trans*-[Pt(CO$_2$R)$_2$(PPh$_3$)$_2$]. When *n*-BuOH was used, only [Pt(CO)$_2$(PPh$_3$)$_2$] was obtained. This can be attributed to the difference in the reactivity of these alcohols.

We have so far been unsuccessful in the preparation of the complex $[Pt(CO_2R)_2(PBu_3)_2]$ (R = Me). The reaction of *cis*-$[PtCl_2(PBu_3)_2]$ with CO/MeOH in the presence of NEt_3 gave only the known complex $[Pt(CO)_2(PBu_3)_2]$, **10** [31]. Furthermore, we found that no reaction took place if *trans*-$[PtCl_2(PCy_3)_2]$ was treated with CO/MeOH in the presence of NEt_3. The different reactivity of these complexes is presumably due to the steric and electronic effects of the PR'_3 (R′ = Ph, Bu and Cy) ligands.

It has been reported by Hidai and co-workers that *trans*-$[Pd(CO_2R)Cl(PPh_3)_2]$ can be prepared from *trans*-$[PdCl_2(PPh_3)_2]$ and CO/ROH in the presence of NEt_3 [32]. We have attempted a related reaction, *i.e.* the reaction of $[CuCl(PPh_3)_3]$ with $MeOH/NEt_3$ and CO, but we found that no reaction occurred. This demonstrates that the method for the preparation of alkoxycarbonyl complexes is dependent on the metal and its associated ligands as well as the alcohols used. The method shown in Scheme 4.7 can be conveniently used to prepare *trans*-$[Pt(CO_2R)_2(PPh_3)_2]$ (R = Me, Et).

Preparation of a carboxylate complex

The carboxylate complex *cis*-$[Pt(O_2CCH_3)_2(PPh_3)_2]$, **11** can be conveniently prepared by the reaction of *cis*-$[PtCl_2(PPh_3)_2]$ with CH_3CO_2Ag as shown below. This method has recently been independently reported by other workers [33].

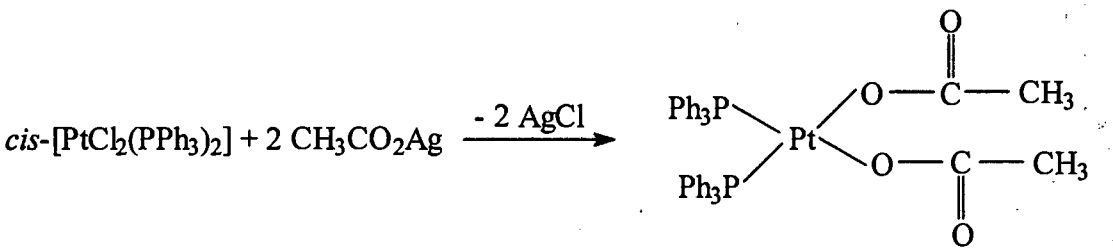

11

Scheme 4.8

Properties of the alkoxycarbonyl complex *trans*-[Pt(CO$_2$Me)$_2$(PPh$_3$)$_2$], 7 and the carboxylate complex *cis*-[Pt(O$_2$CCH$_3$)$_2$(PPh$_3$)$_2$], 11

We have found that the alkoxycarbonyl complex *trans*-[Pt(CO$_2$Me)$_2$(PPh$_3$)$_2$], 7 is stable in $CHCl_3$ under air but unstable when it is kept under a CO_2 atmosphere. The complex 7 in $CHCl_3$ under a CO_2 atmosphere decomposes to [Pt(CO$_3$)(PPh$_3$)$_2$] and [Pt(CO)$_n$(PPh$_3$)$_2$] [34]. Figure 4.1 shows the IR spectra of $CHCl_3$ solutions of *trans*-[Pt(CO$_2$Me)$_2$(PPh$_3$)$_2$] under air and CO_2 after various times. A comparison of the IR spectra shows that the C-bonded alkoxycarbonyl complexes are reactive towards CO_2. In contrast to this, the O-bonded carboxylate complex *cis*-[Pt(O$_2$CCH$_3$)$_2$(PPh$_3$)$_2$] is stable in $CHCl_3$ under both air and CO_2 atmospheres for several days. This may also be the reason for the isolation of the carbonate complex but not the [Pt(C$_2$O$_4$)(PR$_3$)$_2$] complex by the reaction of *cis*-[PtBu$_2$(PR$_3$)$_2$] with CO_2, because the Pt-O bond may be stronger than the Pt-C bond. We have also prepared the O-bonded oxalate complex **12** [35], as shown below, and found that this oxalate complex is stable in $CHCl_3$ under a CO_2 atmosphere.

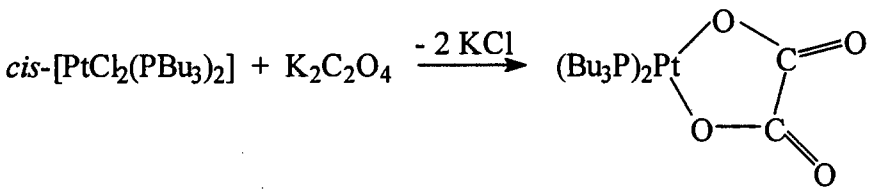

12

Scheme 4.8

From these studies, we have shown that the tertiary phosphine ligands have great influence over the reactivity of these alkoxycarbonyl complexes. Thus we were interested to see whether changing the tertiary phosphine ligands to nitrogen donor ligands would promote the insertion of CO_2 into the Pt-C bond of the Pt dialkyl complexes. Accordingly, we have synthesized some new nitrogen donor complexes [PtMe$_2$(R$_2$-bipy)] (R = H, CH_3) and [PtIMe$_2$(R′)(Me$_2$-bipy)] and investigated their reactivity with CO_2 under various conditions. These results are discussed in section 4.3.

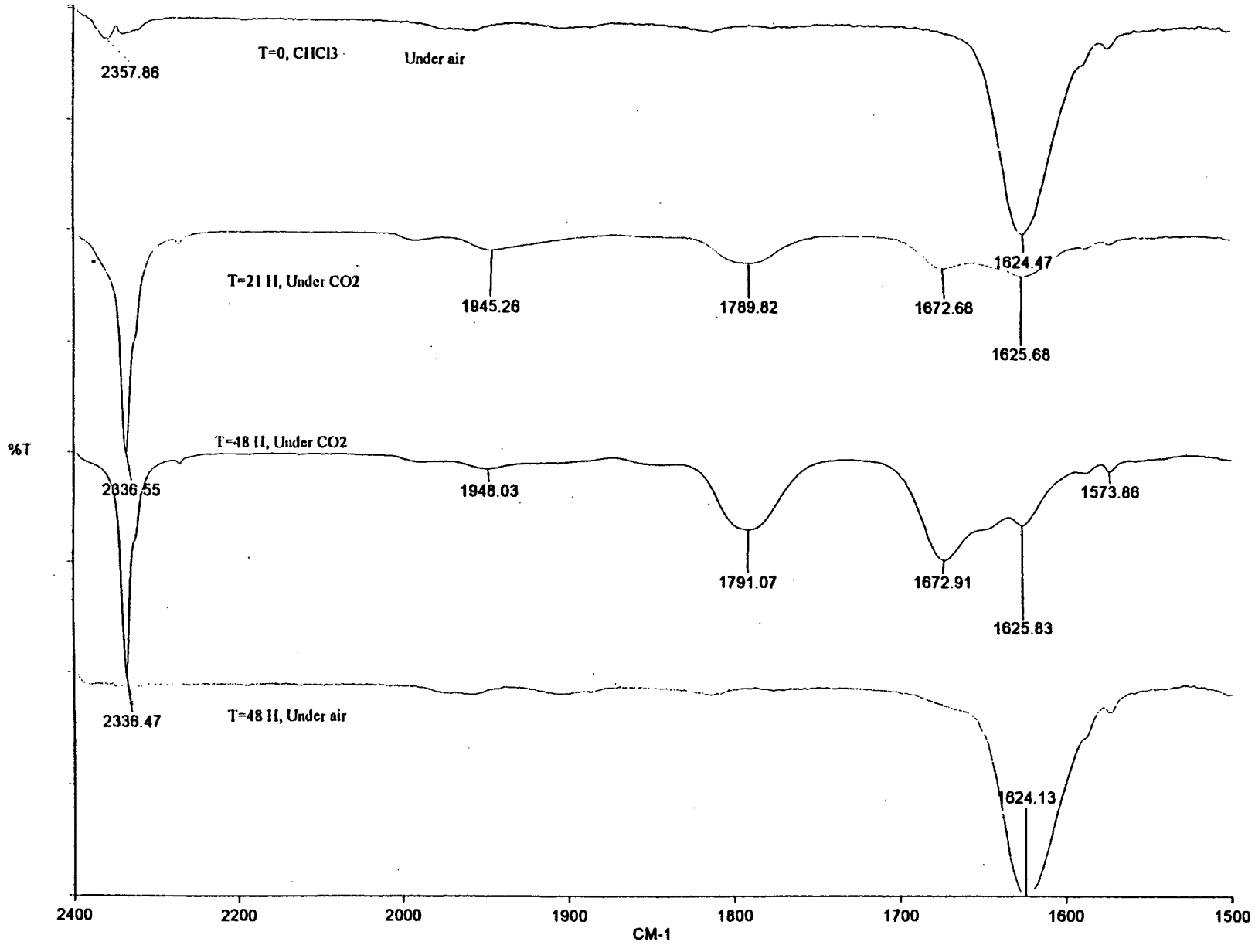

Figure 4.1 IR spectra of *trans*-$[Pt(CO_2Me)_2(PPh_3)_2]$, 7, in $CHCl_3$ under CO_2 or air.

4.3 Synthesis, characterizaton and reactivity of Pt(II) and Pt(IV) alkyl complexes with nitrogen-donor ligands

The square planar Pt(II) dialkyl complexes [$PtMe_2$(bipy)] and [$PtMe_2$(phen)] have been reported to be very reactive towards oxidative addition reactions [20,36]. A series of Pt(IV) alkyl complexes have been prepared by the oxidative addition of RI to [$PtMe_2$(phen)] [37,38]. We have previously mentioned that the complex [$PtMe_2$(bipy)] reacts with the epoxides (ethylene oxide or styrene oxide) and CO_2 to form cyclic carbonate complexes [21].

4.3.1 Synthesis and characterization of [$PtMe_2(R_2$-bipy)] (R = H, CH_3) and [$PtIMe_2$(R')(Me_2-bipy)]

a). Synthesis of the complexes

The complexes [$PtMe_2(R_2$-bipy)] (R = H, **13**, CH_3, **14**) were prepared according to scheme 4.9. The red complex, **13** has been reported previously [36,39a]. The new orange-red complex **14** [39b] has been characterized by satisfactory elemental analysis, UV-vis, ^1H, ^{13}C and ^{195}Pt NMR spectroscopy. The characterization data are given in Tables 4.1 - 4.3. The UV spectrum (as shown in Figure 4.2) of **14** in acetone shows an absorption band at λ_{max} = 464 nm due to the Pt(II) 5d-diimine π^* metal to ligand charge transfer (MLCT) [39a]. The MLCT band for the complex **13** is found at λ_{max} = 474 nm. This is in good agreement with the data reported for **13** and similar square planar Pt(II) alkyl complexes [39a,40]. The ^1H NMR spectrum of **14** shows a characteristic peak at 1.04 ppm with $^2J(^{195}Pt\text{-}^1H)$ = 86 Hz due to the Pt-Me groups, which confirms the formulation of the proposed product. The ^2J(PtH) value is similar to that reported for analogous compounds [36,40].

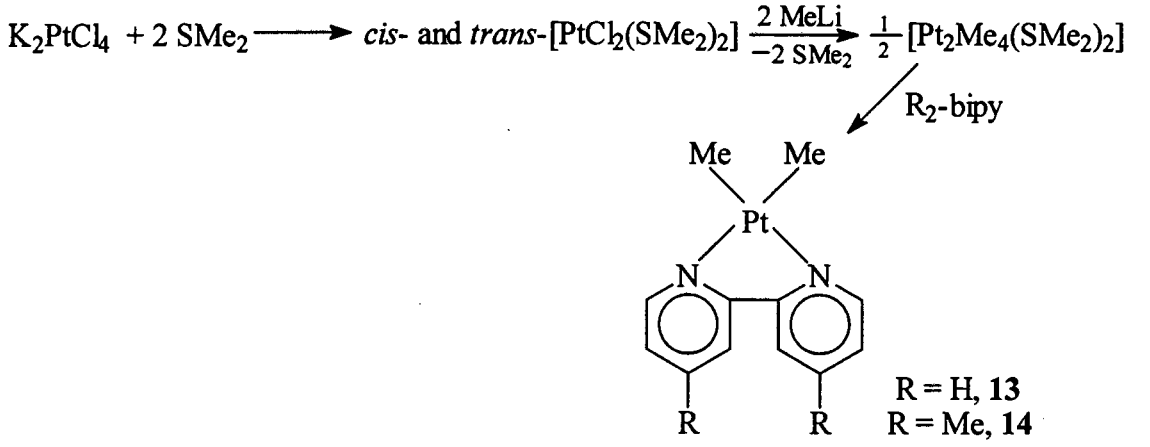

Scheme 4.9

The reaction of the complex [$PtMe_2(Me_2$-bipy)], **14** with alkyl iodides, R′I in acetone at room temperature gives a series of new Pt(IV) complexes [$PtIMe_2(R')(Me_2$-bipy)] (R′ = CH_3, **15**, Et, **16**, *n*-Pr, **17**, *n*-Bu, **18**, and *n*-pentyl, **19**) as shown below:

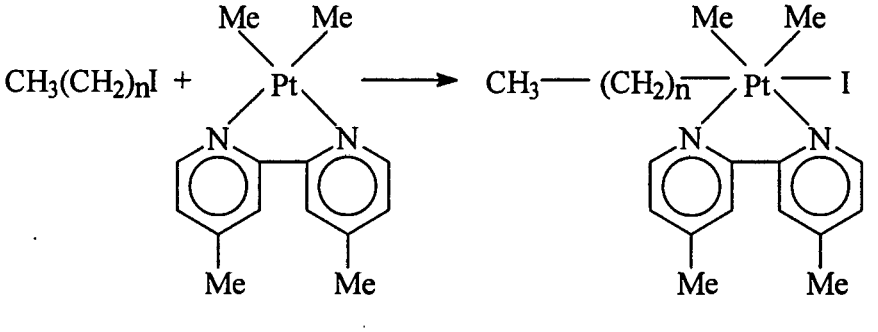

n	Compd no.
0	**15**
1	**16**
2	**17**
3	**18**
4	**19**

Scheme 4.10

The preparation of Pt(IV) complexes by the oxidative addition process has been widely used recently by Puddephatt and co-workers [20, 36-40]. We have observed that the reaction time of the oxidative addition of R′I to complex **14** is dependent on the R′ group of the R′I: the smaller the alkyl group the faster the reaction. Similar trends have been reported by Puddephatt and Monaghan on the reactions of alkyl iodides with [$PtMe_2$(phen)] [37,38]. These authors have also found that the oxidative addition reactions are overall second order and suggested an S_N2 mechanism for the oxidative addition. The solubility of the Pt(IV) alkyl

complexes with Me_2-bipy ligand prepared in our studies is better than that of similar complexes with the 1,10-phenanthrone ligand [37,38].

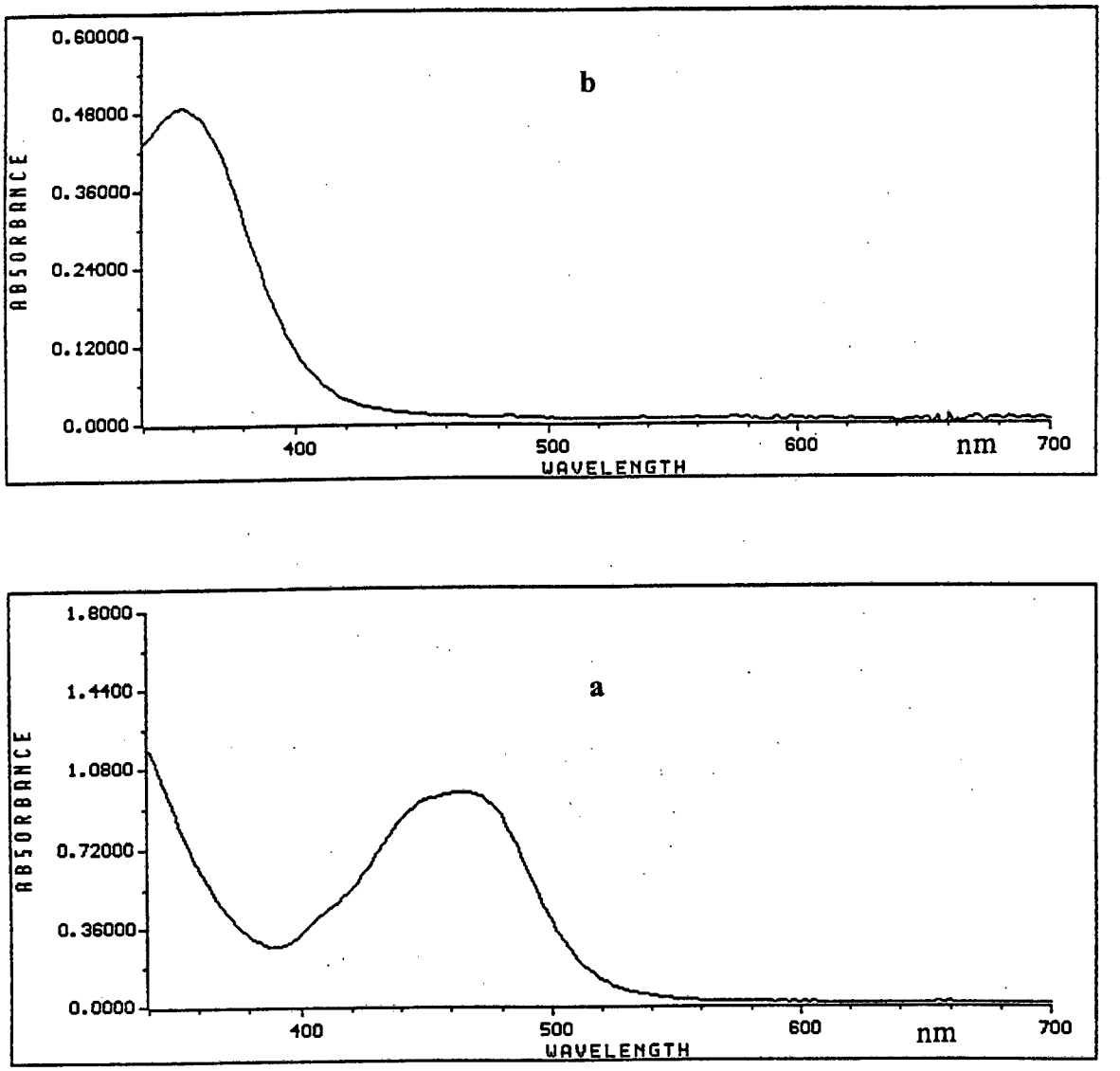

Figure 4.2 UV-visible spectra of (a): [$PtMe_2$(Me_2-bipy)], 14 and (b): [$PtIMe_2(C_4H_9)$(Me_2-bipy)], 18 in acetone.

b). Characterization of the complexes

The complexes **15 - 19** are yellow crystalline solids and have high melting points. They decompose on melting with gas evolution. These new complexes have been characterized by satisfactory elemental analysis, UV-vis, ^{1}H and ^{13}C NMR spectroscopy. The characterization data are listed in Tables 4.1 - 4.3 and the results are briefly discussed below.

UV-visible spectroscopy

The UV-vis spectra of the Pt(II) complex **14** and the Pt(IV) complex **19** in acetone are shown in Figure 4.2. The complex **19** shows a band at λ_{max} = 356 nm which is assigned to the Pt(IV)-diimine MLCT band [40]. This is a good evidence for the change of the oxidation state from Pt(II) to Pt(IV) in these complexes.

^{1}H NMR spectroscopy

The ^{1}H NMR spectra for complexes **15 - 19** were recorded in $CDCl_3$ and are reported in Table 4.2. The ^{1}H NMR spectrum of **16** is shown in Figure 4.3. The ^{1}H NMR data are conclusive in assigning the stereochemistry at the Pt centre. For each of the complexes, only one PtMe signal and one set of Me_2-bipy peaks are observed, indicating that the two PtMe groups are equivalent in these complexes, *i.e.* these complexes are the products of *trans* oxidative addition [38]. The decrease in the coupling constant $^{2}J(^{195}Pt\text{-}^{1}H)$, from 86 Hz for **14** to 70 - 72 Hz for **15 - 19**, is consistent with oxidation of Pt(II) to Pt(IV). Likewise, the coupling constant $^{3}J(^{195}Pt\text{-}^{1}H_6)$ is reduced from 22 Hz for **14** to 14 Hz for **15 - 19**. Changing the alkyl group R has no effect on the chemical shifts and coupling constants of the PtMe and Me_2-bipy groups. The resonances due to the alkyl group R are as expected, except that for **16**. For the complex **16**, a large coupling constant of the β-protons $^{3}J(^{195}Pt\text{-}^{1}H)$ = 69 Hz is observed, suggesting strong interaction between the β-protons and the platinum centre.

^{13}C NMR spectroscopy

The ^{13}C NMR data for **15 - 19** are summarized in Table 4.3. The assignments for the alkyl chain are made on the basis of the magnitude of the coupling constants $^{n}J(^{195}Pt\text{-}^{13}C)$, since the coupling decreases the further the carbon atom is from the Pt. The ^{13}C NMR spectrum of **16** is shown in Figure 4.4. Only one peak for the carbons of the two PtMe groups of **16** is observed, indicating that the two PtMe groups are equivalent. This again confirms the sterochemistry of the complex. Similarly, only one set of the Me_2-bipy peaks is observed. It is found that the alkyl groups R have no effect on the carbon δ values of the PtMe and Me_2-bipy groups except that for R = Me, for which the δ value of the PtMe groups *trans* to N is found at higher field, compared with those found in complexes **16 - 19**. The carbon resonance of the PtMe group *trans* to I is found at much lower field with larger coupling constant. This is most likely due to the *trans* influence of the iodine.

Table 4.1 Data for the complexes [$PtIMe_2(R')(Me_2\text{-bipy})$] and [$PtMe_2(Me_2\text{-bipy})$].

Compound no	R	Yield (%)	M.p. (°C)	Elemental Analysis (%)					
				C		H		N	
				calc.	found	calc.	found	Calc.	Found
14		71 - 88	260 - 266 dec.	41.07	41.32	4.43	4.48	6.84	6.85
15	Me	95	257 - 258 dec.	32.68	32.35	3.84	3.78	5.08	4.86
16	Et	68	257 - 262 dec.	33.99	34.12	4.10	3.98	4.96	4.83
17	*n*-Pr	77	260 - 262 dec.	35.24	35.35	4.35	4.32	4.84	4.83
18	*n*-Bu	96	248 - 250 dec.	36.43	36.75	4.59	4.58	5.19	4.71
19	*n*-pentyl	85	248 - 251 dec.	37.57	37.84	4.81	4.65	4.61	4.52

Table 4.2 ^{1}H NMR data for the complexes [PtIMe$_2$(R′)(Me$_2$-bipy)] and [PtMe$_2$(Me$_2$-bipy)] (400 MHz, $CDCl_3$, J in Hz)[a].

Compound no	R′	PtMe	R′	bipy-Me	Aromatic Ring
14		1.04, s, 6H, $^2J_{PtH}$ 86		2.36, s, 6H	9.01, d, J_{56} 5.6, 2H (H_6), $^3J_{PtH}$ 22.3 7.73, s, 2H (H_3) 7.27, d, J_{65} 5.6, 2H (H_5)
15	Me	1.51, s, 6H, $^2J_{PtH}$ 70	0.61, s, 3H, $^2J_{PtH}$ 74	2.54, s, 6H	8.81, d, J_{56} 5.6, 2H (H_6), $^3J_{PtH}$ 14 8.04, s, 2H (H_3) 7.39, d, J_{65} 5.6, 2H (H_5)
16	Et	1.44, s, 6H, $^2J_{PtH}$ 71	1.40, q., 2H, J_{HH} 7.6, $^2J_{PtH}$ 72, (CH_2) 0.01, t., 3H, J_{HH} 7.6, $^3J_{PtH}$ 69, (CH_3)	2.53, s, 6H	8.78, d, J_{56} 5.6, 2H (H_6), $^3J_{PtH}$ 14 8.02, s, 2H (H_3) 7.39, d, J_{65} 5.6, 2H (H_5)
17	*n*-Pr	1.46, s, 6H, $^2J_{PtH}$ 72	1.34, m, 2H, $^2J_{PtH}$ 72, (α-CH_2) 0.45, m, 2H, (β-CH_2) 0.61, t, 3H, J_{HH} 6.8, (CH_3)	2.55, s, 6H	8.79, d, J_{56} 5.6, 2H (H_6), $^3J_{PtH}$ 14 8.01, s, 2H (H_3) 7.41, d, J_{65} 5.6, 2H (H_5)
18	*n*-Bu	1.45, s, 6H, $^2J_{PtH}$ 71	1.35, m, 2H, $^2J_{PtH}$ 72, (α-CH_2) 0.41, m, 2H, (β-CH_2) 0.97, qn, 2H, J_{HH} 7.2, (γ-CH_2) 0.55, t, 2H, J_{HH} 7.6, (CH_3)	2.54, s, 6H	8.78, d, J_{56} 5.6, 2H (H_6), $^3J_{PtH}$ 14 8.01, s, 2H (H_3) 7.38, d, J_{65} 5.6, 2H (H_5)
19	*n*-pentyl	1.44, s, 6H, $^2J_{PtH}$ 71	1.35, m, 2H, $^2J_{PtH}$ 70, (α-CH_2) 0.43, m, 2H, (β-CH_2) 0.95, m, 4H, (γ-CH_2 + δ-CH_2) 0.62, t, 3H, J_{HH} 6.8, (CH_3)	2.54, s, 6H	8.78, d, J_{56} 5.6, 2H (H_6), $^3J_{PtH}$ 14 7.99, s, 2H (H_3) 7.38, d, J_{65} 5.6, 2H (H_5)

[a]: The diagram showing the carbon atom numbering is shown under Table 4.3.

Table 4.3 ^{13}C NMR chemical shift data (δ ppm, J in Hz) for the complexes $[PtIMe_2(R')(Me_2\text{-bipy})]$ and $[PtMe_2(Me_2\text{-bipy})]$ (100 MHz, $CDCl_3$).

Compd. no	R′	PtMe		R′			bipy-Me	Aromatic Ring		
		δ	$^1J_{PtC}$	δ	J_{PtC}	C. No.		δ	J_{PtC}	C. No.
14		- 17.53					21.81	156.19		2,2'
								147.95		4,4'
								146.52		6,6'
								127.43		5,5'
								122.92		3,3'
15	Me	-6.52	667	7.82	683	α	21.55	154.54		2,2'
								150.57		4,4'
								146.71	16	6,6'
								127.43	14	5,5'
								124.13	8	3,3'
16	Et	-4.93	695	20.02	669	α	21.56	154.74		2,2'
				14.88	37	β		150.51		4,4'
								146.71	15	6,6'
								127.48	14	5,5'
								124.02	9	3,3'
17	*n*-Pr	-5.07		23.24		α	21.59	154.76		2,2'
				28.98		β		150.45		4,4'
				14.96		γ		146.73	14	6,6'
								127.46	14	5,5'
								123.99	8	3,3'
18	*n*-Bu	-4.99	693	26.41	668	α	21.60	154.76		2,2'
				23.43	42	β		150.45		4,4'
				32.39	29	γ		146.73	14	6,6'
				13.67		δ		127.46	14	5,5'
								123.99	9	3,3'
19	*n*-Pe[a]	-5.01	692	26.63		α	21.59	154.77		2,2'
				32.64		β		150.44		4,4'
				29.75		γ		146.78	14	6,6'
				22.18		δ		127.45	14	5,5'
				13.82		ε		123.94	8	3,3'

[a]: *n*-pentyl.

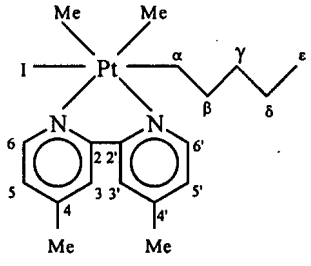

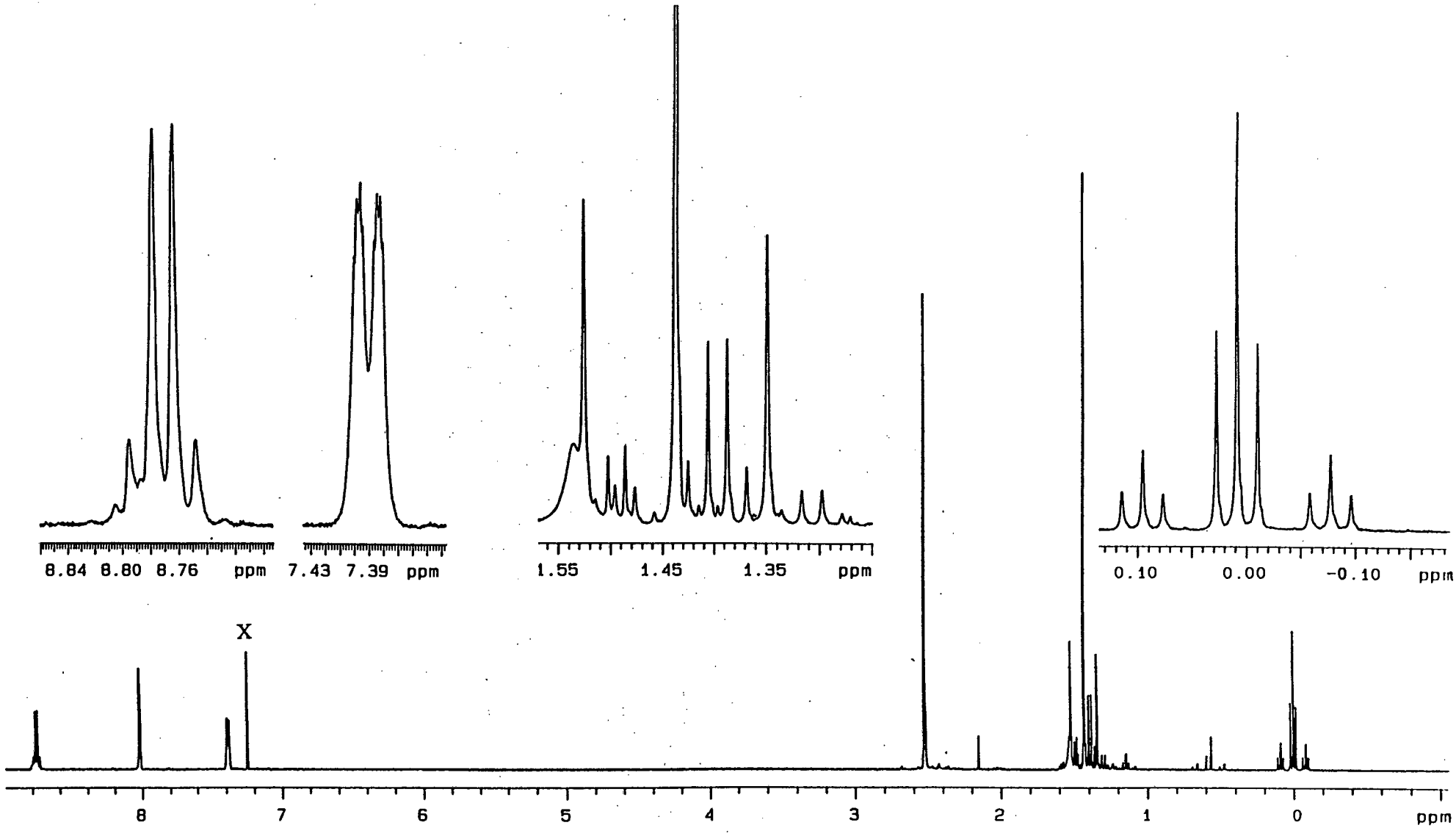

Figure 4.3 ^{1}**H NMR spectrum of [PtIMe$_2$(C$_2$H$_5$)(Me$_2$-bipy)], 16 (400 MHz, CDCl$_3$, X = solvent).**

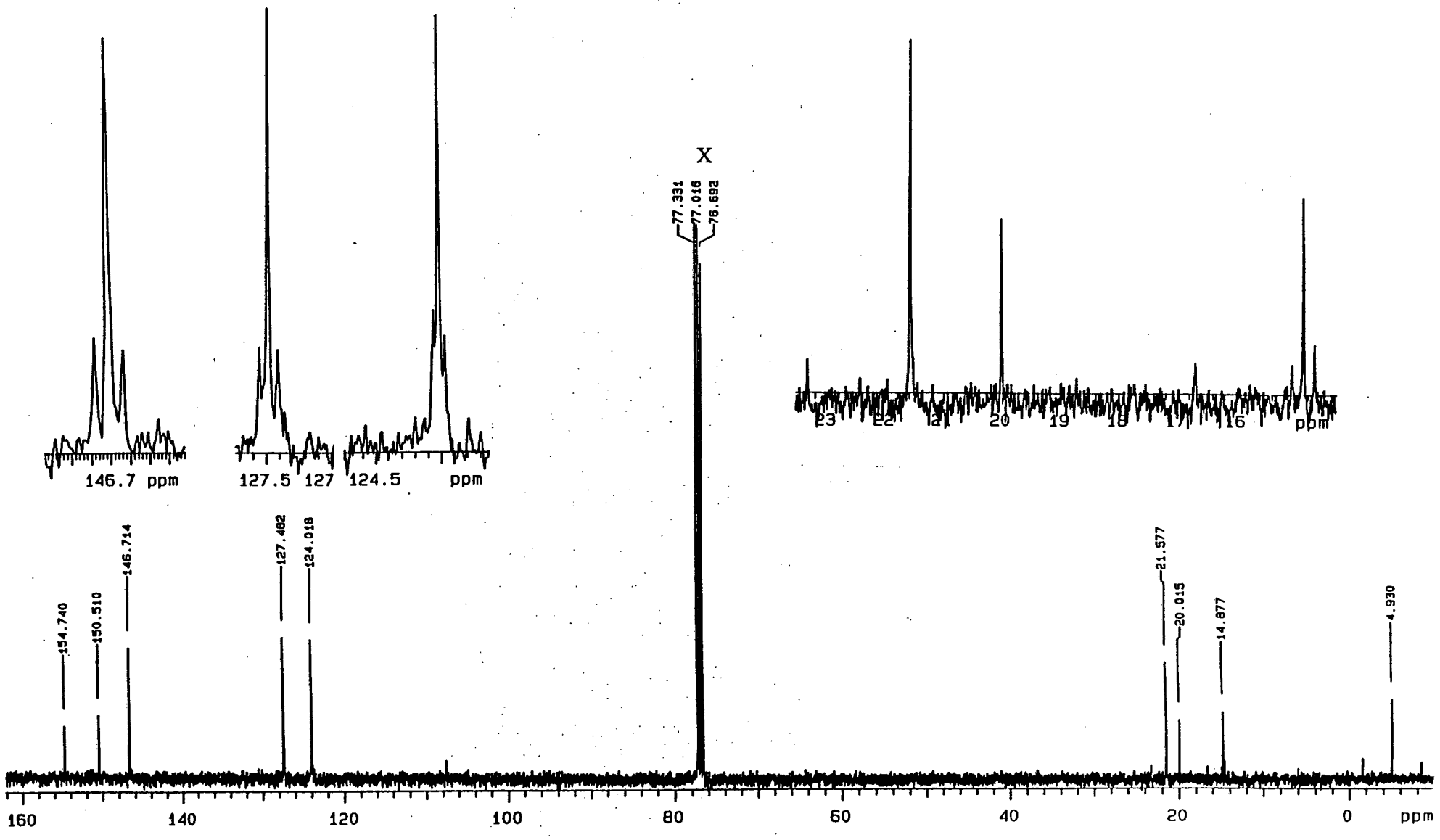

Figure 4.4 ^{13}C NMR spectrum of [$PtIMe_2(C_2H_5)(Me_2\text{-bipy})$], 16 (100 MHz, $CDCl_3$, X = solvent).

4.3.2 Reactivity of Pt(II) and Pt(IV) alkyl complexes with CO_2

The reactions of $[PtMe_2(R_2\text{-bipy})]$ (R = H, **13** and CH_3, **14**), $[PtIMe_2R'(Me_2\text{-bipy})]$ (R′ = Bu, **18**) and $[Pt_2Me_4(SMe_2)_2]$ with CO_2 under various conditions have been investigated.

Initially, we carried out the reaction of $[PtMe_2(Me_2\text{-bipy})]$, **14** with CO_2 (40 bar) at 60 °C for 41 hours in benzene. We found that only the starting complex was recovered and identified by IR, ^1H and ^{13}C NMR. Similarly, the reaction of **14** with $HNEt_2/NEt_3$ under CO_2 (40 bar) at 40 °C for 19 hours showed no reaction. However, the complexes $[PtMe_2(R_2\text{-bipy})]$ (R = H, **13**, CH_3, **14**) reacted with CO_2 (40 bar) at 40 °C for 22 hours in $MeOH/NEt_3$ or $EtOH/NEt_3$ and gave exclusively the new monoalkyl carbonate complexes $[PtMe\{OC(O)OMe\}(R_2\text{-bipy})]$ (R = CH_3, **21**), and $[PtMe\{OC(O)OEt\}(R_2\text{-bipy})]$ (R = H, **20**, CH_3, **22**) as shown below.

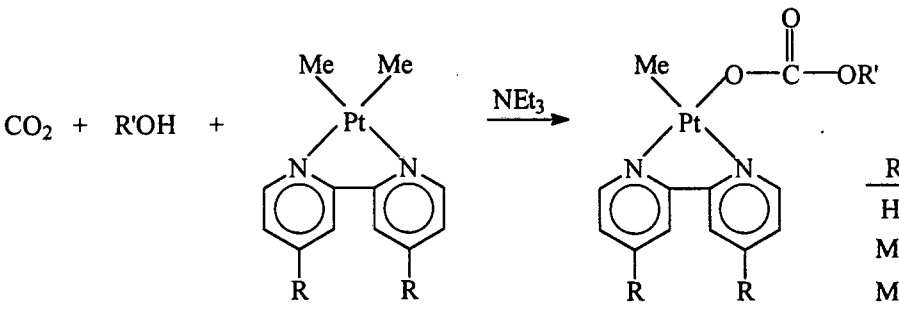

R	R'	Compd no.
H	Et	20
Me	Me	21
Me	Et	22

Scheme 4.11

Even though these complexes are quite unstable, we have been able to characterize one of them, namely $[PtMe\{OC(O)OEt\}(Me_2\text{-bipy})]$, **22**. This complex has been fully characterized by elemental analysis, IR, UV-vis, ^1H and ^{13}C NMR spectroscopy. The characterization data are given in the experimental section 7.4.3. The complexes **20** - **22** are the first examples of platinum monoalkyl carbonate complexes incorporating a diimine ligand. The platinum monoalkyl carbonate complexes with tertiary phosphine ligands have previously been reported in the literature [41]. Due to the instability of these complexes, **20** and **21** could not be obtained in a pure form. So far, the complexes **20** and **21**

have been characterized by IR and UV-vis spectroscopy. The data are tabulated in Table 4.4.

Table 4.4 IR and UV-visible spectroscopic data for the platinum monoalkyl carbonate complexes [PtMe{OC(O)OR'}(R_2-bipy)].

Compound no	R	R'	IR (Nujol) (cm^{-1})		UV (acetone) (λ_{max}/nm)
			ν(C=O)	ν(bipy)	
20	H	Et	1663s,	1614s	422
21	Me	Me	1653s,	1617s	424
22	Me	Et	1663s,	1617s	410

The Pt(II) 5d - π* diimine (MLCT) bands for the complexes **20** - **22** are found at lower λ values than that of [$PtMe_2$(R_2-bipy)] (R = H, **13**, CH_3, **14**), and higher than that of the Pt(IV) complexes. This indicates a decrease in the electron density at the Pt(II) centre of these complexes due to the electron-withdrawing effect of the monoalkyl carbonate ligand. The ν(C=O) position found in the IR spectra of these complexes is similar to that found in *trans*-[PtH{$OC(O)OCH_3$}(PCy_3)$_2$] [ν(C=O) = 1640 cm^{-1}] [41], [Cu{OC(O)OEt}(PPh_3)$_2$] [ν(C=O) = 1660 cm^{-1}] [42] and *fac*-[$Mn(CO)_3$(dppe){OC(O)OEt}] [ν(C=O) = 1651 cm^{-1}] [43], the crystal structures of which have showed that the monoalkyl carbonate ligand is mono-coordinated through one oxygen atom to the metal. The ν(C=O) values of the complexes **20** - **22** suggest that the monoalkyl carbonate ligand in these platinum complexes should have the same coordination mode as those found in other monoalkyl carbonate complexes [41-43], *i.e.* the monoalkyl carbonate ligand is bound through one oxygen atom to the platinum.

The stability of **22** in the chlorinated solvents, $CHCl_3$ and CH_2Cl_2 was investigated by IR spectroscopy at room temperature under an atmosphere of CO_2. It is found that in $CHCl_3$ or CH_2Cl_2, complex **22** decomposes completely in less than two hours. The IR spectra of the complex **22** in $CHCl_3$ and CH_2Cl_2 at various times are shown in Figure 4.5. It is also found that the decomposition gives

different products in different solvents. This is evidenced by the observation of a new peak at 1711 cm^{-1} in the IR spectrum of **22** in CH_2Cl_2, which increases with a decrease in the peak at 1660 cm^{-1} due to the starting complex in CH_2Cl_2. The decomposition of **22** in $CHCl_3$ gives no carbonyl-containing product.

The ^1H NMR spectrum of **22** measured in C_6D_6 is shown in Figure 4.6. Due to the inequivalence of the PtMe and Pt{OC(O)OEt} groups, the proton chemical shifts of the two pyridine rings are observed as two sets of resonances with equal integration. The two Me groups attached to the bipy ring are also observed as separate resonances at δ = 1.91 and 1.81 ppm. The PtMe proton resonance is observed at 1.46 ppm, but no ^2J(PtH) coupling was resolved due to the low intensity of the platinum satellites. The chemical shifts of the Pt{OC(O)OEt} group are observed at δ 4.38 [q, ^3J(HH) 6.8 Hz] and 1.32 (t, ^3J 7.2 Hz) ppm for the CH_2 and CH_3 protons respectively. Also seen from the ^1H NMR spectrum are the weak peaks at 3.28 (q, ^3J 7.2 Hz) and 0.90 (t, ^3J 7.2 Hz), which could result from an ethyl group of the ethyl carbonate ligand dissociated in the solution.

The ^{13}C NMR spectrum of **22** measured in CD_2Cl_2 under a CO_2 atmosphere is shown in Figure 4.7. Due to the inequivalence of the carbon atoms in the Me_2-bipy ligand, caused by the inequivalent *trans*-groups, separate resonances are observed for each carbon atom, thus 10 peaks are observed for the two rings and two peaks for the Me groups attached to the rings. The carbon resonance of the PtMe group of **22** is observed at δ -13.81 ppm, *ca.* 4 ppm deshielded than that of the starting dimethyl complex **14**. The carbon resonances of the ethyl group are found at 62.40 and 15.14 ppm.

The carbon resonance due to the carbonate carbon, CO_3, is found at 159.39 ppm. This is further confirmed by a DEPT experiment of the same solution. From the DEPT experiment, we deduced that five carbon resonances are due to tertiary carbons, four of which are assigned to the Me_2-bipy ligand, by comparison with the related Pt(II) complex. The chemical shift (159.39 ppm) of the carbonate carbon is at a similar position to that found in some monoalkyl carbonate

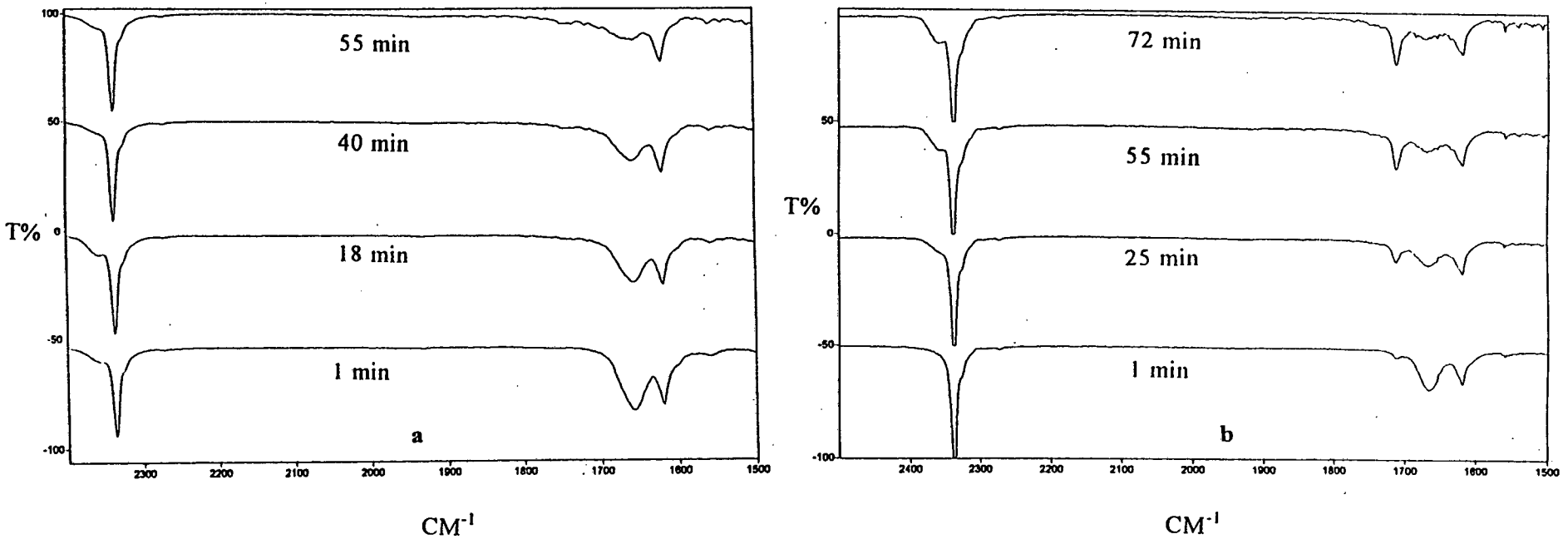

Figure 4.5 IR spectrum of [PtMe{OC(O)OC$_2$H$_5$}(Me$_2$-bipy)], 22, in (a): CHCl$_3$ and (b): in CH$_2$Cl$_2$ under a CO$_2$ atmosphere.

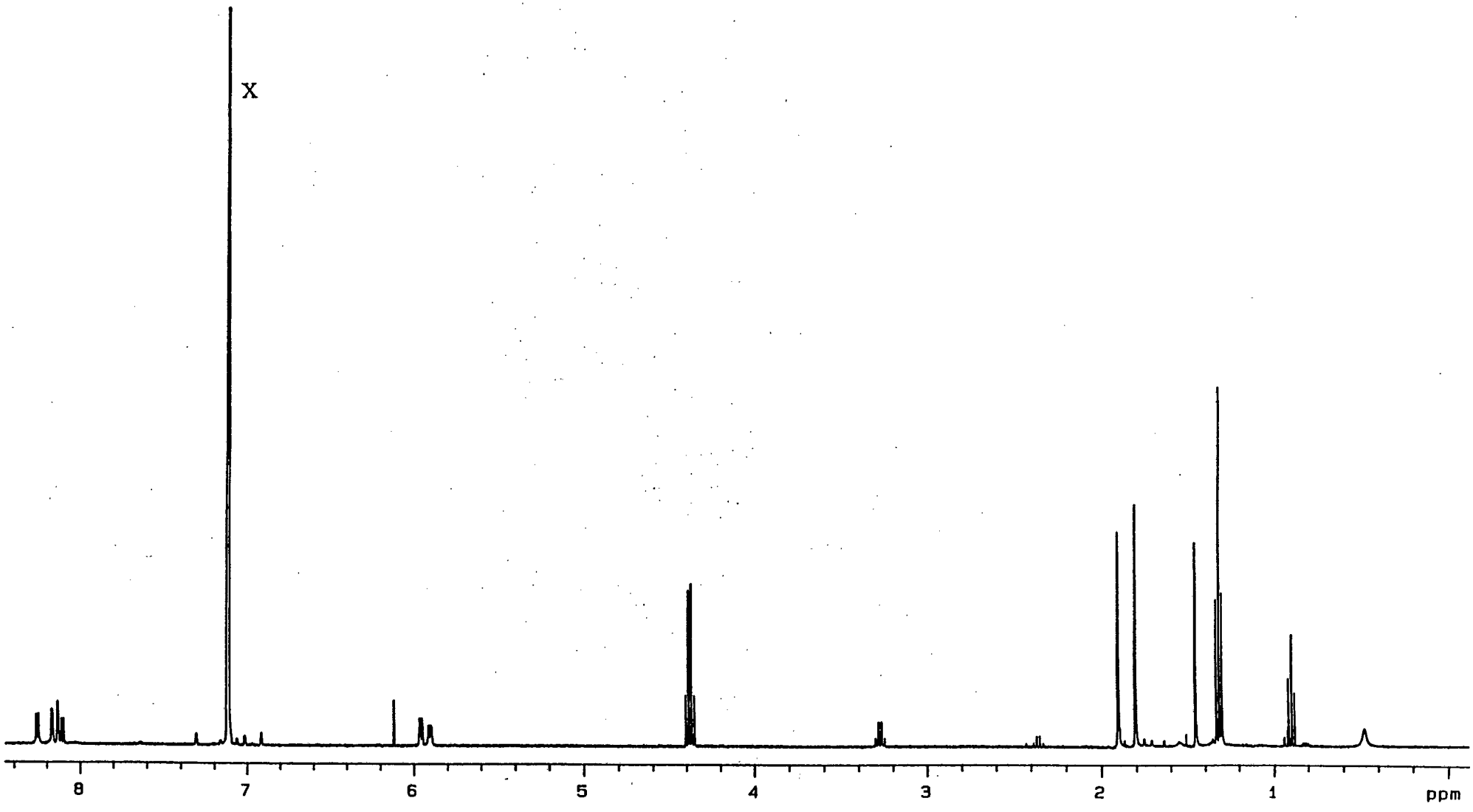

Figure 4.6 ^{1}**H NMR spectrum of [PtMe{OC(O)OC$_2$H$_5$}(Me$_2$-bipy)], 22 (400 MHz, C$_6$D$_6$, X = solvent).**

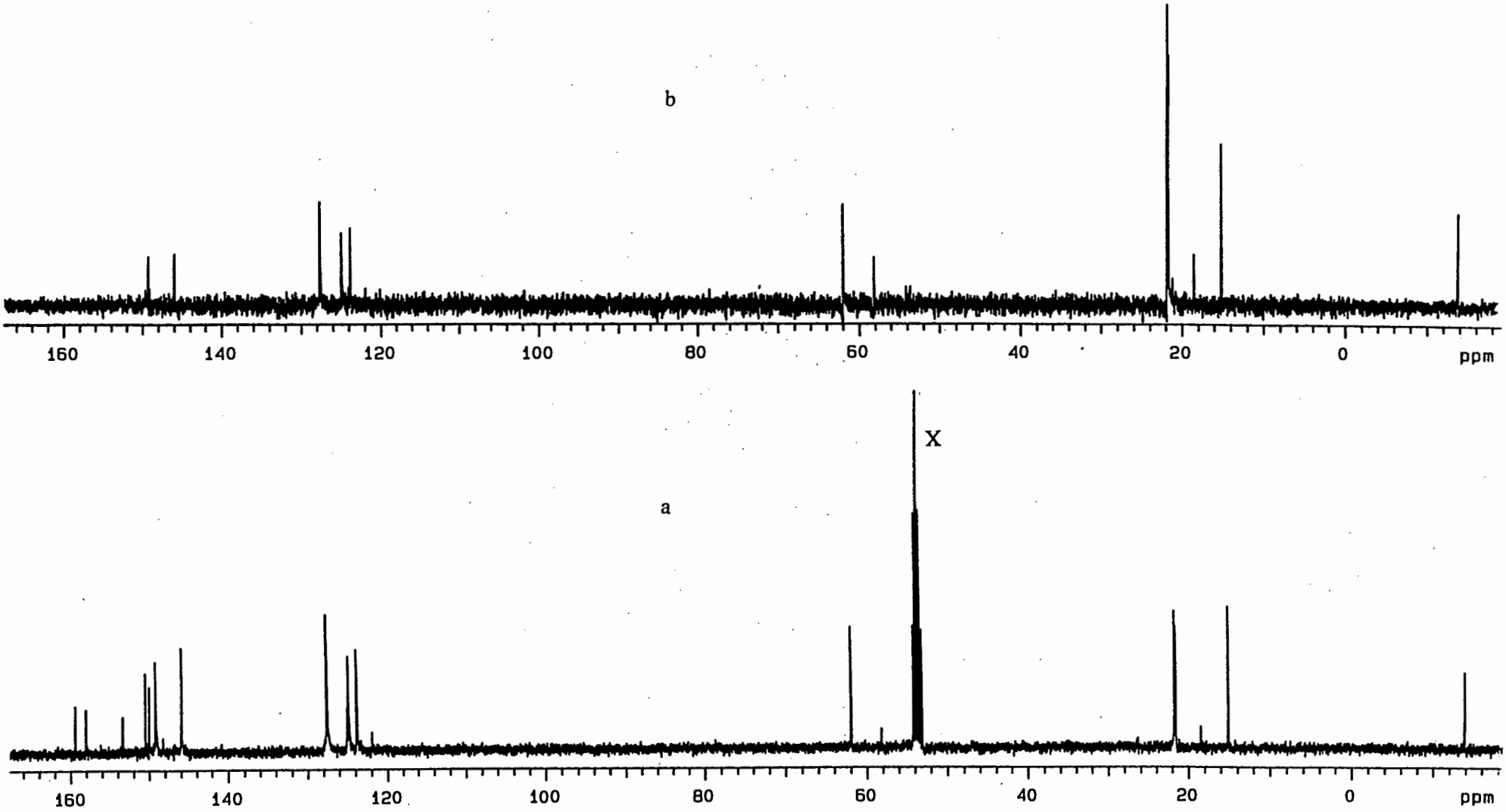

Figure 4.7 (a) ^{13}C NMR and (b) ^{13}C DEPT NMR spectra of [PtMe{OC(O)OC$_2$H$_5$}(Me$_2$-bipy)], 22 (100 MHz, C$_6$D$_6$, X = solvent) under a CO_2 atmosphere.

complexes of Mn and Re [43]. Two weak peaks found at δ 58.22 and 18.57 ppm are probably due to the ethyl carbonate ligand dissociated in the solution.

When the yellow complex [PtMe{OC(O)OEt}(Me_2-bipy)], **22** was dried under high vacuum at room temperature it turned into an orange-red solid, presumably due to the loss of CO_2 under high vacuum to form [PtMe(OEt)(Me_2-bipy)]. The orange-red solid absorbs CO_2 (1 bar) at room temperature to give the starting yellow complex. This process can be repeated several times. This suggests that the insertion of CO_2 may be reversible. Some manganese alkoxide complexes have also been reported to undergo reversible CO_2 insertion [43].

The reaction of the complex **22** with ethyl iodide at room temperature gives diethylcarbonate, which has been identified by GC analysis.

The mechanism for the formation of the monoalkyl carbonate complexes is proposed as follows:

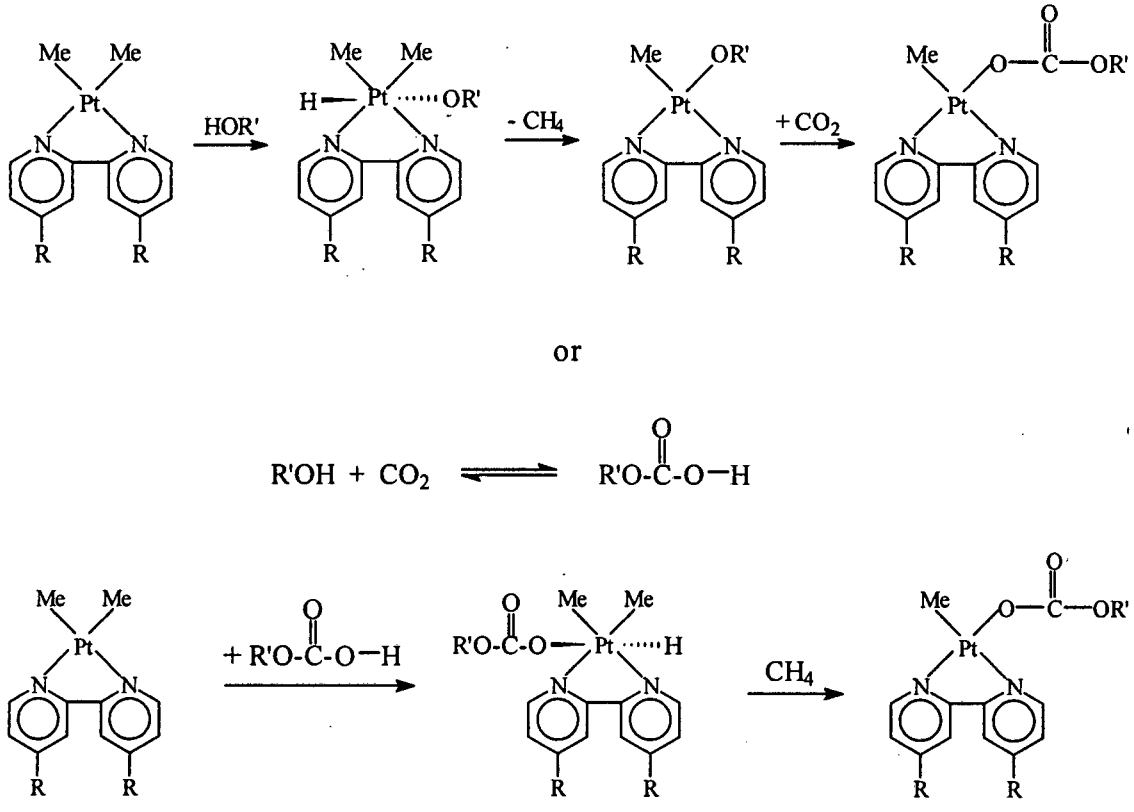

Scheme 4.12

It has been shown that the oxidative addition of R'O-H to [$PtMe_2$(bipy)], **13**, could give the Pt(IV) complex, [$PtHMe_2$(OR')(bipy)] (R' = Me, Et *etc.*), followed by a rapid reaction of the Pt-H group with a protic solvent [36]. By analogy, the reaction of R'O-H with [$PtMe_2$(Me_2-bipy)], **14** is expected to give [$PtHMe_2$(OR')(Me_2-bipy)], which could then undergo reductive elimination to give the Pt(II) alkoxide complex. The insertion of CO_2 into the Pt—OR' bond could afford the monoalkyl carbonate complex. The insertion of CO_2 into the M—OR' bond in some other alkoxide complexes has been reported for Mn [43], Re [43], Cu [42], Ir [44] and W [45]. The insertion may involve direct electrophilic attack of the CO_2 on the oxygen atom of the alkoxide, with or without prior M-CO_2 coordination [43].

Another possible mechanism is the initial formation of R'OC(O)OH from R'OH and CO_2, with subsequent oxidative addition of R'OC(O)O-H to **14** to give the Pt(IV) monoalkyl carbonate complex. The latter could undergo reductive elimination of CH_4 to give the Pt(II) monoalkyl carbonate complex.

We have also investigated the reaction of the Pt(II) alkyl complex containing bridged SMe_2 ligands with CO_2. Thus, treatment of [$Pt_2Me_4(SMe_2)_2$] with CO_2 in benzene at 30 °C and 50 °C led to either no reaction or decomposition of the starting complex respectively. The decomposition of [$Pt_2Me_4(SMe_2)_2$] at 50 °C yielded a black platinum metal which was coated on the wall of the reaction flask. This may suggest that the complex [$Pt_2Me_4(SMe_2)_2$] could be a good precursor for the MOCVD to prepare metallic Pt coating [46]. The reaction of [$PtIMe_2$(R')(Me_2-bipy)] (R' = Pr, Bu) with CO_2 (40 - 45 bar) in NEt_3 at 40 - 65 °C was also studied, however, no reaction was observed.

4.3.3 Electrochemical behaviour of [$PtIMe_2(C_5H_{13})(Me_2$-bipy)], 19

Although many Pt(IV) alkyl complexes have been reported [19,20], the electrochemical properties of Pt(IV) alkyl complexes have been less extensively studied [47]. We have investigated the electrochemical behaviour of

$[PtIMe_2(C_5H_{13})(Me_2\text{-bipy})]$, **19**. The cyclic voltammograms of **19** under both argon and CO_2 atmospheres, measured in an argon or CO_2 saturated acetonitrile solution at room temperature, using a Pt microelectrode and at a voltage sweep rate of 200 mV/s, are shown in Figure 4.8. The CV of **19**, over the range -1.0 to -2.4 V, exhibits an irreversible reduction peak at E_{c1} = -1.94 V, followed by a quasi-reversible couple at E_{c2} = -2.13 V (ΔE = 0.103 V), *vs.* the ferrocene/ferrocenium (Fc/Fc^+) couple (ΔE = 0.083 V) at the same sweep rate, although the anodic component is less clear in the CV run under CO_2 atmosphere. This result suggests that reduction of **19** did not generate reactive species which could react with CO_2 under CV conditions and within the CV measurement time scale. The reduction of the Pt(IV) alkyl complex could produce 16-electron Pt(II) and/or a Pt(I) species, as was suggested by Klingler and co-workers [47], who isolated a platinacyclobutane complex $[Pt(C_3H_6)bipy]$, by the electroreduction of the Pt(IV) complex $[PtCl_2(C_3H_6)bipy]$.

The electrochemical behaviour of $[PtIMe_2(C_5H_{13})(Me_2\text{-bipy})]$, **19**, was also studied from potentials -1.0 to 1.0 V under both argon and CO_2 atmospheres. Figure 4.8(a) shows the CV of **19** under argon, which exhibits an irreversible oxidation peak at E_{a1} = -0.01 V, followed by a quasi-reversible couple at E_{a2} = 0.26 V (ΔE = 0.103 V) *vs.* the Fc/Fc^+ couple at a voltage sweep rate of 200mV/s. When the CV was investigated under CO_2 atmosphere, a different cyclic voltammogram was obtained as shown in Figure 4.8(b). In addition to the irreversible oxidation peak at -0.03 V and the quasi-reversible couple at 0.27 V, an additional irreversible peak was observed at E_{a3} = 0.18 V *vs.* the Fc/Fc^+ couple. This could be due to a CO_2-containing species which might be formed after oxidation of $[PtIMe_2(C_5H_{13})(Me_2\text{-bipy})]$. Presumably the CO_2-containing species was oxidized at E_{a3} = 0.18 V. This was not observed when the CV of **19** was measured under argon. Further investigation would be helpful to understand the nature of the oxidation of $[PtIMe_2(C_5H_{13})(Me_2\text{-bipy})]$ under a CO_2 atmosphere. Nevertheless, in this preliminary study, we have observed a reactive species generated by electrochemical oxidation of the complex $[PtIMe_2(C_5H_{13})(Me_2\text{-bipy})]$ in acetonitrile, which may react with CO_2.

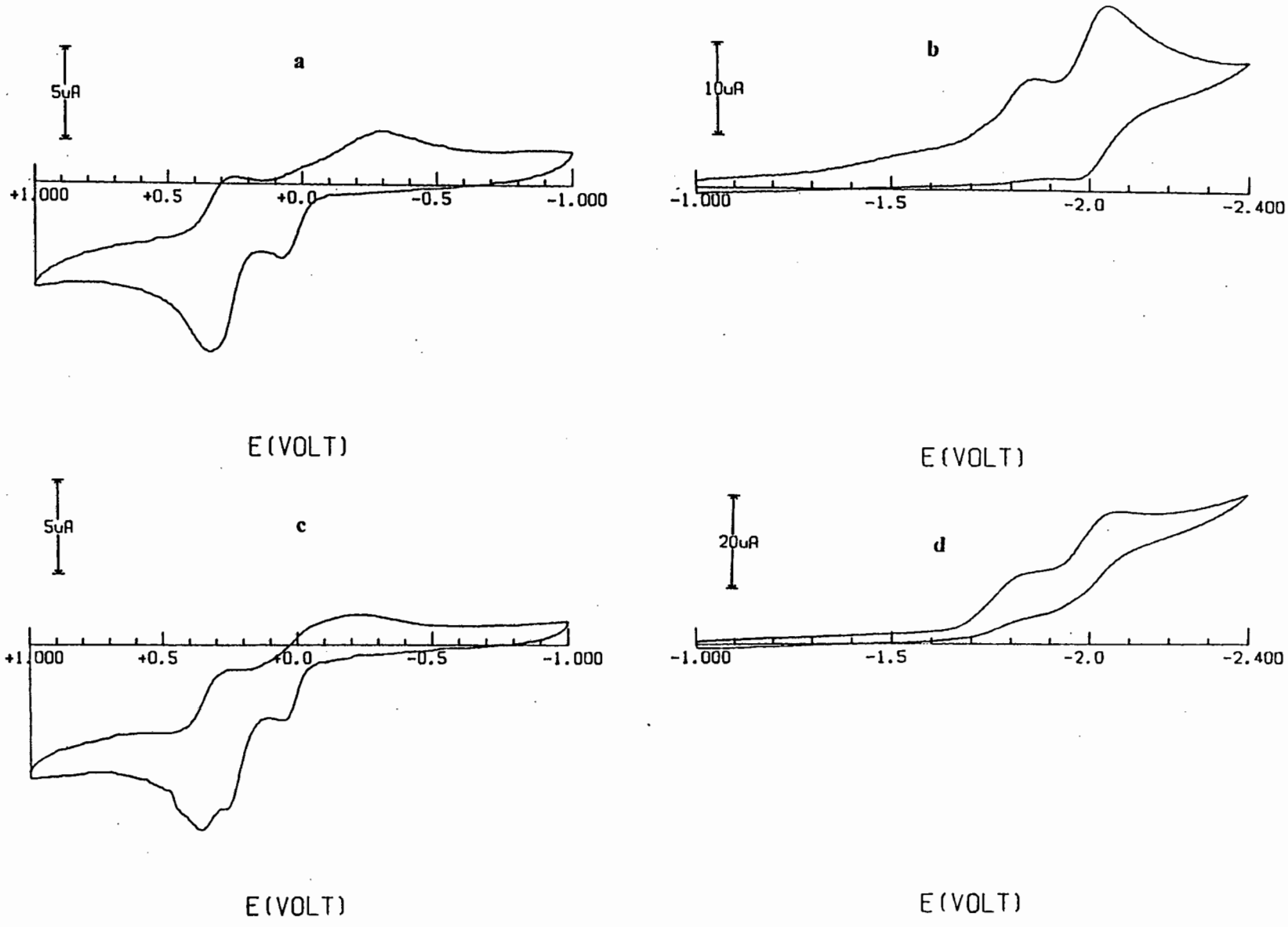

Figure 4.8 Cyclic voltammograms of 1.0 mM [$PtIMe_2(C_5H_{11})(Me_2\text{-bipy})$] in acetonitrile containing 0.1 M [NBu^n_4]ClO_4 at a Pt microelectrode with a scan rate of 200 mV/s, a and b: under argon; c and d: under CO_2.

4.3.4 Preparation of a Pt(II) complex with a bidentate nitrogen, phosphorus donor ligand [$Pt(NP)_2Cl_2$]

From previous studies, we have shown that different ligands may result in different chemistry. We were interested to see whether we could prepare complexes with a mixed nitrogen and phosphorus donor ligand and if so whether the reactivity of such complexes with CO_2 could be compared with that of the Me_2-bipy and PR_3 complexes. Initially, a mixed bidentate ligand containing both nitrogen and phosphorus, namely 1-(diphenylphosphino)-2-(2-pyridyl)ethane (NP), was synthesized according to the literature procedure [48]. The ligand was first used to prepare Ni complexes [48] and has recently been extensively used to prepare group 8 - 11 metal complexes [49]. However, there are no reports of the preparation of platinum complexes using this NP ligand. We have carried out the reaction of the ligand with [$Pt(COD)Cl_2$] in benzene at 50 °C for 10 hours. A white solid product was obtained. The product has a sharp melting point (214 - 216 °C), indicating that it is pure. The elemental analysis suggests the formula to be [$Pt(NP)_2Cl_2$], **23**. The IR spectrum of this product (CsI disc) shows two bands at 1630 and 1610 cm^{-1} due to the pyridine ring (the NP ligand has a band at 1591 cm^{-1} due to the pyridine ring), indicating that both the nitrogen and phosphorus atoms are bound to the platinum in the complex [49]. Thus the reaction could be postulated as follow:

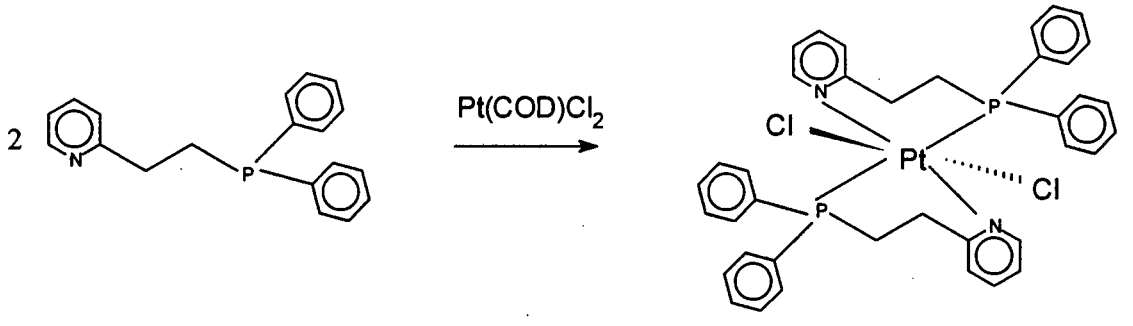

23

Due to the poor solubility of the complex, no ^1H and ^{31}P NMR measurements were obtained, thus no further information is available to confirm the stereochemistry at the platinum centre. The molar conductivity (Λ) of this

complex, measured in a 2.5 X 10^{-4} M solution in nitrobenzene, was Λ = 21 (Ω^{-1} cm^2 mol^{-1}), which suggests that the complex should be a 1:1 electrolyte. Thus the complex may be better postulated as $[Pt(NP)_2Cl]^+Cl^-$. It could not be confirmed whether this is due to the effect of the diluted solution or due to the dissociation of Cl^- from the complex in nitrobenzene.

The poor solubility of the complex **23** makes it difficult to study its chemistry further.

4.4 Conclusion

The new complexes *cis*-$[PtBu_2(PBu_3)_2]$, *trans*-$[PtBuCl(PBu_3)_2]$ and $[PtMe_2(Me_2$-bipy)] have been prepared and characterized. The reaction of $[PtMe_2(Me_2$-bipy)] with alkyl iodide leads to the *trans* oxidative addition of R'I to give the Pt(IV) complexes $[PtIMe_2(R')(Me_2$-bipy)] in good yields. A new platinum complex with the hybrid N and P ligand has also been prepared.

The platinum complexes containing PR_3 and Me_2-bipy ligands behave differently in the reactions of these complexes with CO_2. The reaction of *cis*-$[PtBu_2(PPh_3)_2]$ and *cis*-$[PtBu_2(PBu_3)_2]$ with CO_2 in NEt_3 gives the corresponding carbonate complexes $[Pt(CO_3)(PPh_3)_2]$ and $[Pt(CO_3)(PBu_3)_2]$. The reaction of $[PtMe_2(R_2$-bipy)] (R = H, CH_3) with CO_2 in R'OH/NEt_3 produces the new monoalkyl carbonate complexes $[PtMe\{OC(O)OR'\}(R_2$-bipy)]. The new complex $[PtMe\{OC(O)OEt\}(Me_2$-bipy)] has been fully characterized. The monoalkyl carbonate complexes are unstable both in solutions and in the solid state under vacuum, but can be kept in the solid state under a CO_2 atmosphere at -20 °C for several weeks. The reaction of the complex $[PtMe\{OC(O)OEt\}(Me_2$-bipy)] with ethyl iodide is found to give diethyl carbonate.

A new method has been developed for the synthesis of the alkoxycarbonyl complexes *trans*-$[Pt\{C(O)OR\}_2(PPh_3)_2]$ (R = Me, Et) by the reaction of *cis*-

$[PtCl_2(PPh_3)_2]$ with CO/ROH in NEt_3. Studies on the reactivity of the complexes $[PtCl_2(PR_3)_2]$ (R = Ph, Bu, Cy) and $[CuCl(PPh_3)_3]$ with CO/ROH in NEt_3 reveal that these reactions are dependent on the metal and ligands used for the reaction. The alkoxycarbonyl and carboxylate complexes serve as model complexes for the CO_2 insertion into the Pt-C bond of Pt(II) alkyl complexes. The alkoxycarbonyl complexes $[Pt\{C(O)OR\}_2(PPh_3)_2]$ (R = Me, Et) are unstable in $CHCl_3$ solution under a CO_2 atmosphere.

References

1. M. Aresta and C.F. Nobile, J. Chem. Soc. Dalton Trans., 1977, 708.
2. M. Sakamoto, I. Shimizu, and A. Yamamoto, Organometallics, 1994, **13**, 407.
3. M.E. Vol'pin and I.S. Kolomnikov, Pure. Appl. Chem., 1973, **33**, 567.
4. C.J. Nyman, C.E. Wymore and G. Wilkinson, J. Chem. Soc. (A), 1968, 561.
5. P.J. Hayward, D.M. Blake, G. Wilkinson and C.J. Nyman, J. Am. Chem. Soc., 1970, **92**, 5873.
6. D.M. Blake and D.M. Roundhill, Inorg. Synth., 1978, **18**, 120.
7. D.M. Blake and R. Mersecchi, J. Chem. Soc. Chem. Commun., 1971, 1045.
8. M.A. Andrews, G.L. Gould and E.J. Voss, Inorg. Chem., 1996, **35**, 5740.
9. M.A. Andrews, G.L. Gould, W.T. Klooster, K.S. Koenig and E.J. Voss, Inorg. Chem., 1996, **35**, 5478.
10. D. Walther, G. Bräunlich, U. Ritter, R. Fischer and B. Schönecker, in *Proceedings of the 3rd Symposium in Organic Synthesis via Organometallics*, Eds. K. H. Doetz and R. Hoffmann, 1990, p77.
11. C.P. Kubiak in *Comprehensive Organometallic Chemistry II*, Eds. E.W. Abel, F.G.A. Stone and G. Wilkinson, Pergamon: New York, 1995, Vol 9, Chapter 1, p1.
12. Chapter 1 of this thesis.
13. A. Behr and G.V. Ilsemann, J. Organomet. Chem., 1984, **276**, C77.
14. K. Osakada, R. Sato and T. Yamamoto, Organometallics, 1994, **13**, 4645.
15. A. Behr, W. Keim and G. Thelen, J. Organomet. Chem., 1983, **249**, C38.
16. a): D.L. Dubois, A. Miedaner, W. Bell and J.C. Smart in *Electrochemical and Electrocatalytic Reactions of CO_2*, Eds. B.P. Sullivan, K. Krist and H.E. Guard, Elsevier: Amsterdam, 1993, Chapter 4, p94;
    b): F.R. Keene and B.P. Sullivan, in *Electrochemical and Electrocatalytic Reactions of CO_2*, Eds. B.P. Sullivan, K. Krist and H.E. Guard, Elsevier: Amsterdam, 1993, Chapter 5, p118.

17. S. Dérien, J-C Clinet, E. Duñach and J. Périchon, Tetrahedron, 1992, **48**, 5235.

18. a): S. Dérien, E. Duñach and J. Périchon, J. Am. Chem. Soc., 1991, **113**, 8447.

b): C. Amatore and A. Jutand, J. Am. Chem. Soc., 1991, **113**, 2819.

19. G. K. Anderson in *Comprehensive Organometallic Chemistry II*, Eds. E.W. Abel, F.G.A. Stone and G. Wilkinson, Pergamon: New York, 1995, Chapter 8, p431.

20. F.R. Hartley in *Comprehensive Organometallic Chemistry*, Eds. G. Wilkinson, F.G.A. Stone and E.W. Abel, Pergamon: New York, 1982, Vol 6, Chapter 39, p471.

21. K-T. Aye, G. Ferguson, A.J. Lough and R.J. Puddephatt, Angew. Chem. Int. Ed. Engl., 1989, **28**, 767.

22. a): G.M. Whitesides, J.F. Gaasch and E.R. Stedronsky, J. Am. Chem. Soc., 1972, **94**, 5258.

b): G.M. Whitesides and J.F. Gaasch, J. Organomet. Chem., 1971, **33**, 24.

23. G. Alibrandi, M. Cusumano, D. Minniti, L.M. Scolaro and R. Romeo, Inorg. Chem., 1989, **28**, 342.

24. H.G. Alt, W-D Müller, J. Unsin and H.A. Brune, J. Organomet. Chem., 1986, **307**, 121.

25. T.J. McCarthy, R.G. Nuzzo and G.M. Whitesides, J. Am. Chem. Soc., 1981, **103**, 3396.

26. T. Herskovitz and L.J. Guggenberger, J. Am. Chem. Soc., 1976, **98**, 1615.

27. M. Ebner and H. Werner, Chem. Ber., 1986, **119**, 482.

28. a): R.K. Merwin and D.M. Roddick, J. Organomet. Chem., 1995, **487**, 69.

b): K. Werner and W. Beck, Chem. Ber., 1972, **105**, 3947.

c): G. Vasapollo, L. Toniolo, G. Cavinato, F. Bigoli, M. Lanfranchi and M.A. Pellinghelli, J. Organomet. Chem, 1994, **481**, 173.

29. D.M. Blake and L.M. Leung, Inorg. Chem., 1972, **11**, 2879.

30. P.L. Bellon, M. Manassero, F. Porta and M. Sansoni, J. Organomet. Chem., 1974, **80**, 139.

31. P. Chini and G. Longoni, J. Chem. Soc. (A), 1970, 1542.

32. M. Hidai, M. Kokura and Y. Uchida, J. Organomet. Chem., 1973, **52**, 431.

33. A.L. Tan, P.M.N. Low, Z-Y. Zhou, W. Zheng, B-M. Wu, T.C.W. Mak and T.S.A. Hor, J. Chem. Soc. Dalton Trans., 1996, 2207.

34. J. Chatt and P. Chini, J. Chem. Soc. (A), 1970, 1538.

35. R.S. Paonessa, A.L. Prignano and W.C. Trogler, Organometallics, 1985, **4**, 647.

36. P.K. Monaghan and R.J. Puddephatt, Organometallics, 1984, **3**, 444.

37. P.K. Monaghan and R.J. Puddephatt, J. Chem. Soc. Dalton Trans., 1988, 595.

38. P.K. Monaghan and R.J. Puddephatt, Organometallics, 1985, **4**, 1406.

39. (a) N. Chaudhury and R.J. Puddephatt, J. Organomet. Chem., 1975, **84**, 105.

(b) The crystal structure of this compound has recently been reported, independent of our work, see S. Achar and V.J. Catalano, *Polyhedron, 16*, (1997) 1555, but no other characterization data were given.

40. S. Achar, J.J. Vittal and R. J. Puddephatt, Organometallics, 1996, **15**, 43.

41. A. Immirzi and A. Musco, Inorg. Chimi. Acta, 1977, **22**, L35.

42. T. Yamamoto, M. Kubota and A. Yamamoto, Bull. Chem. Soc. Jpn., 1980, **53**, 680.

43. S.K. Mandal, D.M. Ho and M. Orchin, Organometallics, 1993, **12**, 1714.

44. D.J. Darensbourg, K.M. Sanchez and A.L. Rheingold, J. Am. Chem. Soc., 1987, **109**, 290.

45. J.L. Newman and R.G. Bergman, J. Am. Chem. Soc., 1985, **107**, 5314.

46. C.D. Tagge, R.D. Simpson, R.G. Bergman, M.J. Hostetler, G.S. Girolami and R.G. Nuzzo, J. Am. Chem. Soc., 1996, **118**, 2634.

47. R.J. Klingler, J.C. Huffman and J.K. Koch, J. Organomet. Chem., 1981, **206**, C7.

48. E. Uhlig and M. Maaser, Z. Anorg. Allg. Chem., 1966, **344**, 205.

49. a): A.D. Zotto, G. Nardin and P. Rigo, J. Chem. Soc. Dalton Trans., 1995, 3343 and references therein.

b): A.D. Zotto, A. Mezzetti and P. Rigo, J. Chem. Soc. Dalton Trans., 1994, 2257.

c): P. Rigo and M. Bressan, Inorg. Chem., 1975, **14**, 1491.

Chapter 5

Synthesis, Characterization And Reactivity Of ω-Haloalkyl And ω-Hydroxyalkyl Complexes Of The Type $[(\eta^5\text{-}C_5R_5)W(CO)_3\{(CH_2)_nX\}]$, $[Re(CO)_5\{(CH_2)_nX\}]$ And $[(\eta^5\text{-}C_5R_5)W(CO)_3\{(CH_2)_nOH\}]$ (R = H, CH_3)

5.1 Synthesis, characterization and reactivity of ω-haloalkyl complexes $[(\eta^5\text{-}C_5R_5)W(CO)_3\{(CH_2)_nX\}]$ (R = H, n = 3 - 7, X = Br, I; R = CH_3, n = 3, 4 and X = Br, I)

5.1.1 Introduction

Haloalkyl transition metal complexes of the type $[LyM\{(CH_2)_nX\}]$ (Ly = ligands, M = transition metal, X = halogen, $n \geq 1$), which were quite rare 30 years ago [1], are now well-known [2-10]. The synthesis and chemistry of some haloalkyl complexes have recently been extensively investigated [3-10] and comprehensively reviewed by Moss and Friedrich [2,11]. Haloalkyl complexes $[LyM\{(CH_2)_nX\}]$ can either be considered as simple examples of functionalized alkyl complexes of transition metals or as metal-substituted alkyl halides. Due to the functionality of the haloalkyl complexes, they have additional reactivity potential compared to the alkyl analogues. The haloalkyl complexes show interesting and novel chemistry and can be used, for example, as precursors for a wide range of useful compounds including acyclic and cyclic carbene complexes [12-14], homo- and hetero-bimetallic hydrocarbon-bridged complexes[13,15,16], dendrimers[17,18], as well as many other classes of functionalized alkyl compounds [9].

The wide application of haloalkyl complexes has prompted us to investigate the preparation of some hitherto unknown tungsten haloalkyl complexes of the type $[(\eta^5\text{-}C_5R_5)W(CO)_3\{(CH_2)_nX\}]$, which could be used to prepare potentially very useful heterobinuclear and polynuclear complexes. It might also be interesting to compare the properties of the haloalkyl complexes of tungsten with those of haloalkyl

complexes of other metals [3,5,6], for examples $[(\eta^5\text{-}C_5R_5)M(CO)_2\{(CH_2)_nX\}]$ (M = Fe, Ru, R = H, CH_3, $n \geq 3$, X = halogen), and to compare with that of the long chain alkyl complexes $[CpW(CO)_3\{(CH_2)_nCH_3\}]$, as some of them have been recently prepared by us [19].

The complexes $[(\eta^5\text{-}C_5R_5)W(CO)_3(CH_2X)]$ (R = H, CH_3, X = Cl, Br and I) have been reported [8], and the reactivity of these complexes have also been investigated, mainly by Moss and co-workers [8,9]. Some complexes of the type $[CpW(CO)_3\{(CH_2)_nBr\}]$ (n = 3 and 4) have been reported by King [1] in 1967, and these were the first examples of haloalkyl transition metal complexes $[LyM\{(CH_2)_nX\}]$ with $n \geq 1$. The complexes $[CpW(CO)_3\{(CH_2)_nBr\}]$ (n = 3 and 4) were prepared by the reaction of $Na[CpW(CO)_3]$ with 1,n-dibromoalkanes (n = 3, 4) in low yields [1]. The reaction of $Na[CpW(CO)_3]$ with 1,n-diiodoalkanes (n = 3, 4) was reported [13] to yield the hydrocarbon-bridged complexes $[Cp(CO)_3W(CH_2)_nW(CO)_3Cp]$ (n = 3, 4), and the iodoalkyl complexes $[CpW(CO)_3\{(CH_2)_nI\}]$ (n = 3 and 4) were suggested as intermediates in these reactions [13]. The intermediates could also be isolated under suitable conditions as was demonstrated by Scott and Moss [20], who successfully isolated $[CpW(CO)_3\{(CH_2)_nI\}]$ (n = 4 and 5) with only partial characterization. The complexes $[(\eta^5\text{-}C_5R_5)W(CO)_3\{(CH_2)_3I\}]$ (R = H, CH_3), however, were not obtained, either from the reaction of $Na[(\eta^5\text{-}C_5R_5)W(CO)_3]$ with 1,3-diiodopropane [20] or from the reaction of $[(\eta^5\text{-}C_5R_5)W(CO)_3\{(CH_2)_3Br\}]$ with LiI [13,14]: All of these conditions led to the formation of *trans*-2-oxacyclopentylidene tungsten complexes, as shown below:

$$[(\eta 5\text{-}C_5R_5)(CO)_2I\overline{W(COCH_2CH_2CH_2)}] \quad (R = H, CH_3)$$

Here, we report the synthesis and full characterization of an extensive series of haloalkyl complexes $[(\eta^5\text{-}C_5R_5)W(CO)_3\{(CH_2)_nX\}]$ (R = H, n = 3 - 7, X = Br, I; R = CH_3, n = 3, 4, X = Br and I). Furthermore, the reactions of these complexes leading to some bimetallic complexes have also been investigated and will be discussed in following sections.

5.1.2 Synthesis of $[(\eta^5\text{-}C_5R_5)W(CO)_3\{(CH_2)_nX\}]$

The bromoalkyl complexes $[(\eta^5\text{-}C_5R_5)W(CO)_3\{(CH_2)_nBr\}]$ (R = H, n = 3, **1**; 4, **2**; 5, **3**; 6, **4**; 7, **5**; R = CH_3, n = 3, **11**, 4, **12**) have been prepared in good yields by the reaction of $Na[(\eta^5\text{-}C_5R_5)W(CO)_3]$ with an excess 1,n-dibromoalkanes in THF as shown in Scheme 5.1.

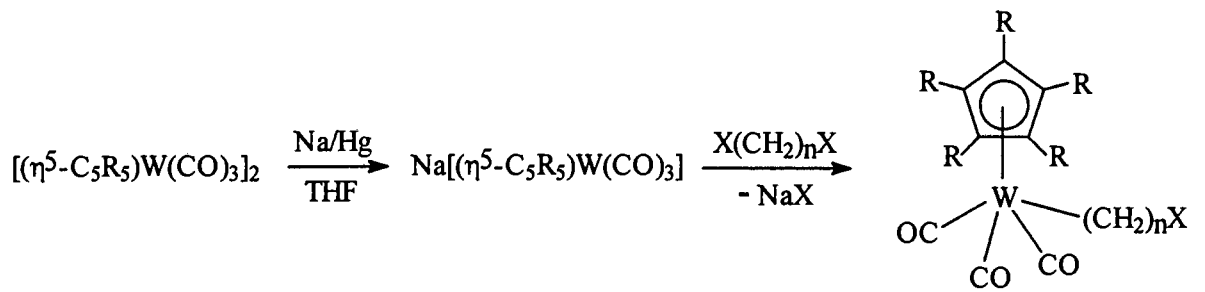

R	X	n	Compd. no
H	Br	3	**1**
H	Br	4	**2**
H	Br	5	**3**
H	Br	6	**4**
H	Br	7	**5**
H	I	4	**7**
CH_3	Br	3	**11**
CH_3	Br	4	**12**

Scheme 5.1

This method is similar to that reported by King and co-workers [1] for the preparation of **1** and **2** in low yields. Bailey and co-workers [14] have also applied this method to prepare **11**.

The reactions were monitored by IR spectroscopy, and stopped after all the $Na[(\eta^5\text{-}C_5R_5)W(CO)_3]$ was consumed. It is found that the reaction of $Na[CpW(CO)_3]$ with 1,n-dibromoalkanes is chain length dependent at room temperature. Thus, the longer the polymethylene chain, the longer the reaction time. Complexes **4** and **5** can only be prepared by refluxing the reaction mixture overnight. The relatively slow reaction rate of $Na[CpW(CO)_3]$ with 1,n-dibromoalkanes, compared with that of

$Na[CpFe(CO)_2]$, is due to the weak nucleophilicity of the tungsten anion [21]. The $Na[Cp^*W(CO)_3]$ is found to be more reactive than the Cp analogues due to the increased nucleophilicity caused by the Cp* ligand. It is also found, as expected, that the reaction of $Na[CpW(CO)_3]$ with 1,4-diiodobutane to give the complex **7** is completed faster than its reaction with 1,4-dibromobutane.

Complexes **1** - **5**, **7**, **11** and **12** were obtained in good yields as yellow solids after purification by chromatography and recrystallization. They are moderately air stable both in solutions and in the solid state for short periods of time.

The iodoalkyl complexes $[(\eta^5\text{-}C_5R_5)W(CO)_3\{(CH_2)_nI\}]$ (R = H, n = 3, **6**; 5, **8**; 6, **9**; and 7, **10**; R = CH_3, n = 3, **13**, 4, **14**) have been successfully prepared in high yields by the reaction of the corresponding bromoalkyl complexes with NaI in acetone at room temperature for 1 - 2 days, as shown in Scheme 5.2. Complexes **7** and **8** were prepared in this laboratory *via* a similar route, but were not fully characterized [20].

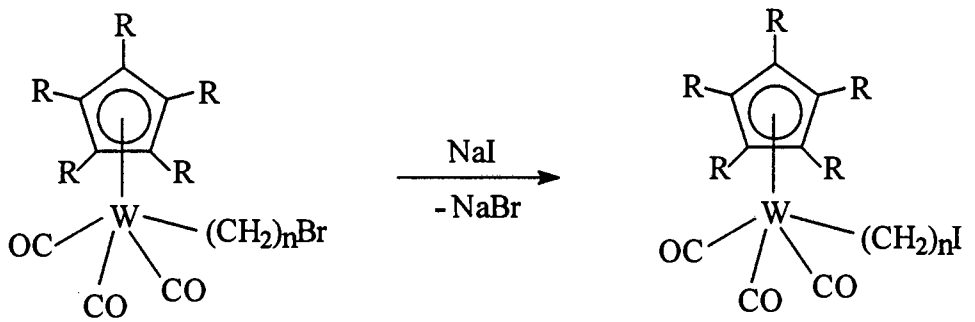

R	n	Compd. no
H	3	**6**
H	5	**8**
H	6	**9**
H	7	**10**
CH_3	3	**13**
CH_3	4	**14**

Scheme 5.2

The preparation of **6** and **13** from the reaction of **1** and **11** with NaI respectively are in contrast to the reports [12,14] that reaction of **1** and **11** with LiI in 1,2-

dimethoxyethane or THF, with refluxing, respectively gave the *trans*-2-oxacyclopentylidene tungsten complexes as shown below:

$$[(\eta 5\text{-}C_5R_5)(CO)_2I\overline{W(COCH_2CH_2CH_2)}] \quad (R = H, CH_3)$$

The different products obtained from the reactions of **1** and **11** with I^- under the above reaction conditions may be due to the reaction temperature. We suggest that complexes **6** and **13** could be the intermediates for the *trans*-2-oxacyclopentylidene complexes; the intermediates may be converted to the 2-oxacyclopentylidene complexes at high temperature.

This method (as shown in Scheme 5.2) had been previously used to convert bromoalkyl complexes of other metals to the corresponding iodoalkyl complexes [5,6].

The iodoalkyl complexes, like the bromoalkyl complexes, are yellow crystalline solids. They have similar melting points to the corresponding bromoalkyl complexes, except **6** which has much lower melting point than **1**. The iodoalkyl complexes are more sensitive to light and air than their bromoalkyl analogues.

5.1.3 Characterization of $[(\eta^5\text{-}C_5R_5)W(CO)_3\{(CH_2)_nX\}]$

The haloalkyl complexes (**1** - **14**) have been fully characterized by elemental analysis, melting point, IR, ^1H and ^{13}C NMR, as well as mass spectroscopy. The yields, melting points, and IR spectra, as well as elemental analysis data for the haloalkyl complexes (**1** - **14**) are summarized in Tables 5.1 and 5.2. All the complexes have been characterized by satisfactory C and H analyses. The ^1H and ^{13}C NMR, as well as mass spectral data are summarized in Tables 5.3 to 5.8.

Table 5.1 Data for $[CpW(CO)_3\{(CH_2)_nX\}]$.

Compound no	X	n	Yield (%)	M.p. (°C)	IR ν(CO)[a] (cm^{-1})	Elemental analysis (%)			
						C		H	
						calc.	found	calc.	found
1[b]	Br	3	66	108 - 110	2020s, 1929vs	29.00	29.30	2.40	2.42
2[c]	Br	4	45	58 - 66	2017s, 1927vs	30.70	31.12	2.77	2.75
3	Br	5	50	122 - 125	2017s, 1927vs	32.33	32.35	3.13	3.06
4	Br	6	49	61 - 63	2017s, 1927vs	33.83	34.08	3.45	3.47
5	Br	7	37	44 - 48	2017s, 1927vs	35.25	35.73	3.75	3.79
6	I	3	70	81 - 84	2020s, 1929vs	26.32	26.92	2.21	2.21
7[d]	I	4	56	67 - 69	2018s, 1927vs	27.91	28.11	2.51	2.45
8[e]	I	5	63	127 - 130	2017s, 1927vs	29.46	29.97	2.85	2.65
9	I	6	62	57 - 58	2017s, 1927vs	30.91	31.46	3.15	3.14
10	I	7	57	49 - 51	2016s, 1927vs	32.28	32.57	3.43	3.44

[a]: IR in hexane, [b]: Literature [1], m.p. 109 - 112 °C, [c]: Literature [1], m.p. 66 - 68 °C, DSC studies showed that this complex might exist in different crystal forms (see discussion in text), [d]: Literature [20], m.p. 69 - 71 °C, [e]: Literature [20], m.p. 129 - 131 °C.

Table 5.2 Data for $[Cp^*W(CO)_3\{(CH_2)_nX\}]$.

Compound no	X	n	Yield (%)	M.p. (°C)	IR ν(CO)[a] (cm^{-1})	Elemental analysis (%)			
						C		H	
						calc.	found	calc.	found
11[b]	Br	3	68	83 - 85	2007s, 1914vs	36.60	36.93	4.03	4.05
12	Br	4	62	53 - 55	2005s, 1913vs	37.87	38.09	4.30	4.33
13	I	3	78	83 - 85	2006s, 1914vs	33.59	34.26	3.70	3.76
14	I	4	71	63 -65	2005s, 1913vs	34.84	35.30	3.96	4.00

[a]: IR in hexane, [b]: Literature [14], m.p. 80 - 82 °C.

IR spectroscopy

The IR spectra of complexes **1** to **14** were recorded in hexane solution in the range 2200 to 1600 cm^{-1}. The data are given in Tables 5.1 and 5.2. The results are in good agreement with the data reported for some known compounds [1,14,20]. It can be seen that there is no significant change in the positions of the carbonyl bands in the IR spectra between the bromoalkyl and corresponding iodoalkyl complexes, and there is only a very slight trend towards lower wavenumbers as the carbon chain lengthens from n = 3 to n = 5. No change is seen in the positions of the carbonyl bands beyond n = 5. The IR spectra of the Cp complexes are also very similar to that of the long chain alkyl complexes $[CpW(CO)_3(CH_2)_nCH_3]$ (n = 5 to 9) [19], which implies that the halogen group in these haloalkyl complexes has little or no effect on the positions of the carbonyl bands.

The ν(CO) for the Cp* complexes is lower than that for the analogous Cp complexes by about 13 cm^{-1}. This is believed to be due to the increase in electron density on the metal (caused by the Cp* group) which results in increased back-bonding to the carbonyl groups, and hence, a lower ν(CO) [5].

^{1}H NMR Spectroscopy

The ^{1}H NMR data for complexes **1** - **14** are summarized in Tables 5.3 and 5.4. Assignments for the data were made as far as possible by comparison with literature data [14], with similar haloalkyl complexes $[CpFe(CO)_2\{(CH_2)_nX\}]$ (n = 3 - 7, X = Br and I) [3,5], and with $[CpW(CO)_3R]$ (R = various alkyl groups) [19], as well as by comparison with alkyl halides RX [22]. The ^{1}H NMR spectra of complexes **6** and **14** are shown in Figures 5.1 and 5.3 as examples.

The ^{1}H NMR data for **11** have been reported by Bailey [14] and we found that our results for the same compound agree well with the reported data. Although complexes **1**, **2**, **7** and **8** have also been characterized by ^{1}H NMR, it is found, however, that previous data were either unresolved [1] or incorrectly assigned

[20]. Thus we fully characterized the haloalkyl complexes **1** - **14** by ^{1}H NMR spectroscopy.

From Tables 5.3. and 5.4, it can be seen that the α-CH_2 (α to tungsten) proton peaks appear at about 1.5 ppm for the Cp complexes and at about 0.8 ppm for the Cp* complexes. No coupling between tungsten and α-CH_2 protons is observed. The fact that the α-CH_2 protons of the Cp* complexes are much more shielded than those of the Cp analogues is probably due to the increased electron density at the tungsten centre in these Cp* complexes. Noteworthy features for the α-CH_2 and β-CH_2 protons are observed in the complexes with n = 3, *i.e.* complexes **1**, **6**, **11** and **13**. An example is shown in the insets of Figure 5.1 for complex **6**. The rather complicated feature of the α-CH_2 and β-CH_2 protons in the ^{1}H NMR spectra of the complexes with n = 3 could possibly be due to the complex spin system. The CH_2X (X = Br, I) protons for complexes with n = 3 are also found slightly more shielded than the CH_2X protons for complexes with n greater than 4. However, the CH_2X and CH_2CH_2X protons show no further shift on increasing the chain length beyond n = 5, suggesting that the inductive or steric effect of the tungsten group on the other chain end is no longer detectable in these complexes. Similar trends were also observed in the haloalkyl iron complexes [5]. The up-field shift of 0.2 - 0.3 ppm of the CH_2X peaks, as X changes from Br to I, is as expected because of the difference in their electronegativities, however the effect of the halogen diminishes quickly along the carbon chain.

^{13}C NMR Spectroscopy

No ^{13}C NMR data have previously been reported for complexes **1** - **14** in the literature [1,13,20]. The ^{13}C NMR data for complexes **1** - **14** are given in Tables 5.5 and 5.6. Assignments for the data were made as far as possible by comparison with the ^{13}C NMR of the haloalkyl complexes $[CpFe(CO)_2\{(CH_2)_nX\}]$ (n = 3 - 7, X = Br, I) [5], and $[CpW(CO)_3R]$ (R = various alkyl group) [19], as well as alkyl halides RX [23], and also by HETCOR experiments. As examples, the ^{13}C NMR spectra of **6** and **14** are shown in Figure 5.2 and 5.4.

Table 5.3 ^{1}H NMR data for [CpW(CO)$_3${(CH$_2$)$_n$X}] (400 MHz, CDCl$_3$)[a].

Compd no	X	n	Cp	CH_2X ^3J(HH)	CH_2CH_2X ^3J(HH)	α-CH_2	β-CH_2	γ-CH_2 ^3J(HH)	δ-CH_2 ^3J(HH)	ε-CH_2
1	Br	3	5.41, 5H, s	3.33, 2H, t, 7.2	2.06, 2H, qn, 7.2	1.49, 2H, m				
2	Br	4	5.41, 5H, s	3.45, 2H, t, 7.2	1.87, 2H, qn, 7.2	1.50, 2H, m	1.67, 2H, m			
3	Br	5	5.37, 5H, s	3.40, 2H, t, 6.7	1.88, 2H, qn, 6.9	1.54, 4H, m		1.43, 2H, m		
4	Br	6	5.37, 5H, s	3.40, 2H, t, 6.8	1.84, 2H, qn, 7.2	1.55, 4H, m		1.42, 2H, m	1.32, 2H, qn, 7.2	
5	Br	7	5.37, 5H, s	3.40, 2H, t, 7.2	1.85, 2H, qn, 7.2	1.54, 4H, m		1.41, 2H, m	1.32, 4H, m	
6	I	3	5.39, 5H, s	3.11, 2H, t, 7.2	2.02, 2H, d-qn, 7.6	1.47, 2H, d-t				
7	I	4	5.40, 5H, s	3.22, 2H, t, 7.2	1.83, 2H, qn, 6.8	1.48, 2H, m	1.65, 2H, m			
8	I	5	5.37, 5H, s	3.17, 2H, t, 7.2	1.83, 2H, qn, 7.2	1.52, 4H, m		1.39, 2H, qn, 7.6		
9	I	6	5.37, 5H, s	3.18, 2H, t, 7.2	1.81, 2H, qn, 7.2	1.54, 4H, m		1.40, 2H, qn, 7.2	1.31, 2H, m	
10	I	7	5.37, 5H, s	3.19, 2H, t, 7.2	1.82, 2H, qn, 7.2	1.53, 4H, m		1.35, 2H, m	1.31, 4H, m	

[a]: Coupling constants are given in Hz; α-CH_2 refers to the protons on the CH_2 α to tungsten etc.

Table 5.4 ^{1}H NMR data for [Cp*W(CO)$_3${(CH$_2$)$_n$X}] (400 MHz, $CDCl_3$)[a].

Compound no	X	n	$C_5(CH_3)_5$	CH_2X $^{3}J(HH)$	CH_2CH_2X $^{3}J(HH)$	α-CH_2	β-CH_2
11[b]	Br	3	1.97, 15H, s	3.35, 2H, t, 7.2	2.07, 2H, m	0.75, 2H, m	
12	Br	4	1.97, 15H, s	3.42, 2H, t, 7.2	1.91, 2H, qn, 7.2	0.79, 2H, m	1.70, 2H, m
13	I	3	1.98, 15H, s	3.16, 2H, t, 7.2	2.04, 2H, m	0.76, 2H, m	
14	I	4	1.96, 15H, s	3.19, 2H, t, 7.2	1.89, 2H, qn, 7.2	0.78, 2H, m	1.66, 2H, m

[a]:Coupling constants are given in Hz, α-CH_2 refers to the protons on the CH_2 α to tungsten etc.
[b]: These data are in good agreement with literature values [14].

Table 5.5 ^{13}C NMR chemical shift data (δ ppm) for $[CpW(CO)_3\{(CH_2)_nX\}]$ (100 MHz, $CDCl_3$).

Compd no	X	n	CO	Cp	CH_2X	CH_2CH_2X	α-CH_2[a]	β-CH_2	γ-CH_2	δ-CH_2	ε-CH_2
1	Br	3	228.17, 217.36	91.53	37.77	40.09	-14.66				
2	Br	4	228.53, 217.47	91.47	33.49	35.05	-12.44	38.35			
3	Br	5	228.62, 217.60	91.47	32.28	34.11	-10.91	35.88	34.29		
4	Br	6	228.83, 217.57	91.47	32.88	34.09	-10.46	36.62	34.98	27.66	
5	Br	7	228.90, 217.55	91.46	32.84	34.06	-10.21	36.72	35.65	28.20	28.18
6	I	3	228.15, 217.38	91.49	11.70	41.00	-11.92				
7	I	4	228.52, 217.47	91.47	6.99	37.49	-12.61	39.03			
8	I	5	228.68, 217.59	91.47	7.40	33.02	-10.91	36.64	35.66		
9	I	6	228.86, 217.57	91.46	7.36	33.60	-10.45	36.61	34.76	29.99	
10	I	7	228.91, 217.55	91.47	7.37	33.58	-10.21	36.73	35.62	30.50	27.99

[a]: α-CH_2 refers to the CH_2 carbon α to tungsten, etc.

Table 5.6. ^{13}C NMR chemical shift data (δ ppm) for [Cp*W(CO)$_3${(CH$_2$)$_n$X}] (100 MHz, $CDCl_3$).

Compound no	X	n	CO	$C_5(CH_3)_5$	CH_2X	CH_2CH_2X	α-CH_2[a]	β-CH_2	$C_5(CH_3)_5$
11	Br	3	232.01, 223.01	102.89	38.92	39.88	-3.41		10.36
12	Br	4	232.29, 223.10	102.77	33.49	35.10	-1.02	39.82	10.36
13	I	3	231.97, 223.03	102.91	13.47	40.74	-0.46		10.37
14	I	4	232.30, 223.07	102.77	6.63	37.48	-1.25	40.64	10.36

[a]: α-CH_2 refers to the CH_2 carbon α to tungsten, etc.

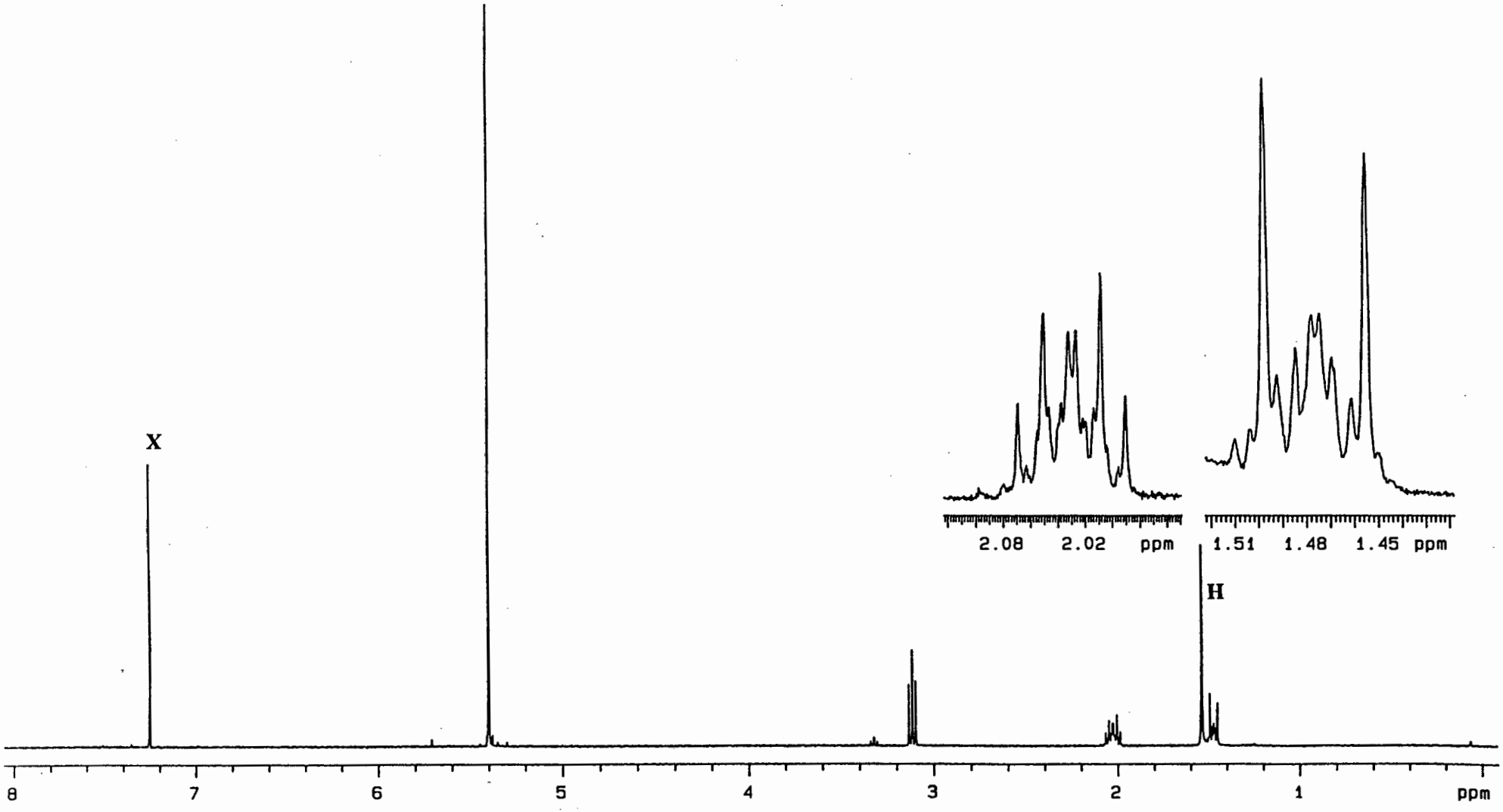

Figure 5.1 ^{1}H NMR spectrum of [$CpW(CO)_3\{(CH_2)_3I\}$], 6 (400 MHz, $CDCl_3$) (X = $CDCl_3$, H = H_2O).

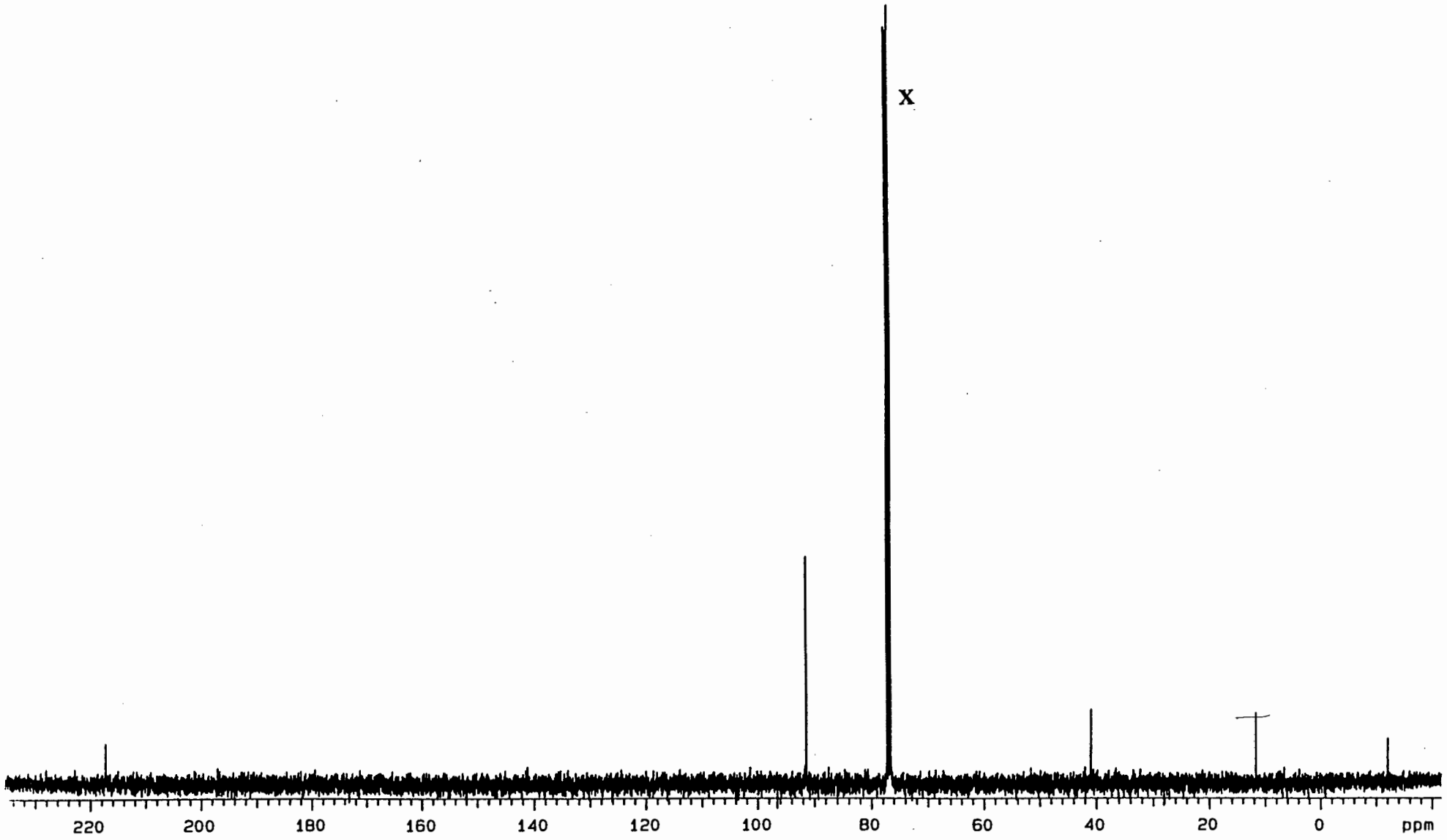

Figure 5.2 ^{13}C **NMR spectrum of** $[CpW(CO)_3\{(CH_2)_3I\}]$, **6 (100 MHz,** $CDCl_3$**) (X =** $CDCl_3$**).**

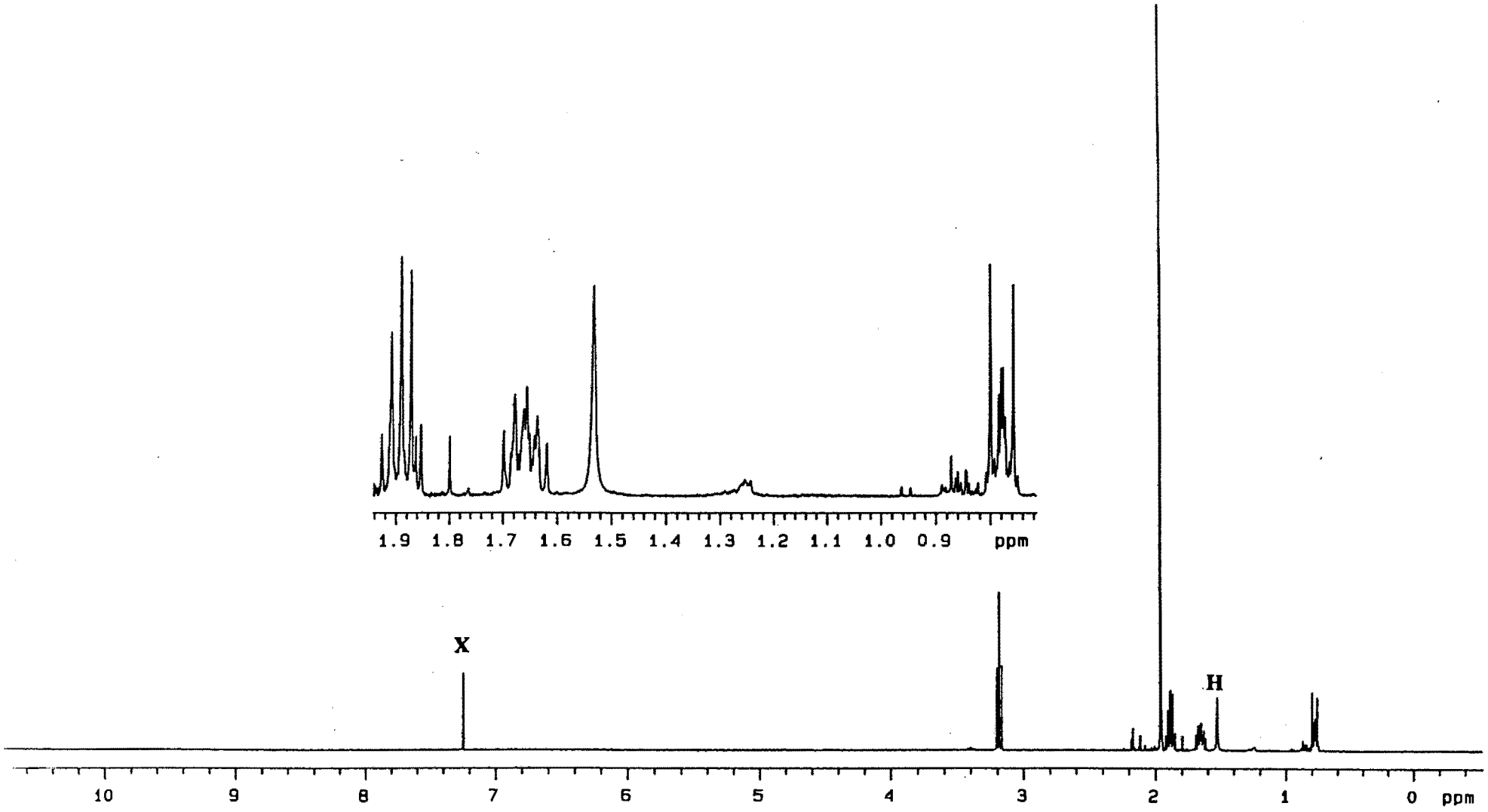

Figure 5.3 ^{1}H NMR spectrum of [Cp*W(CO)$_3${(CH$_2$)$_4$I}], 14 (400 MHz, CDCl$_3$) (X = CDCl$_3$, H = H$_2$O).

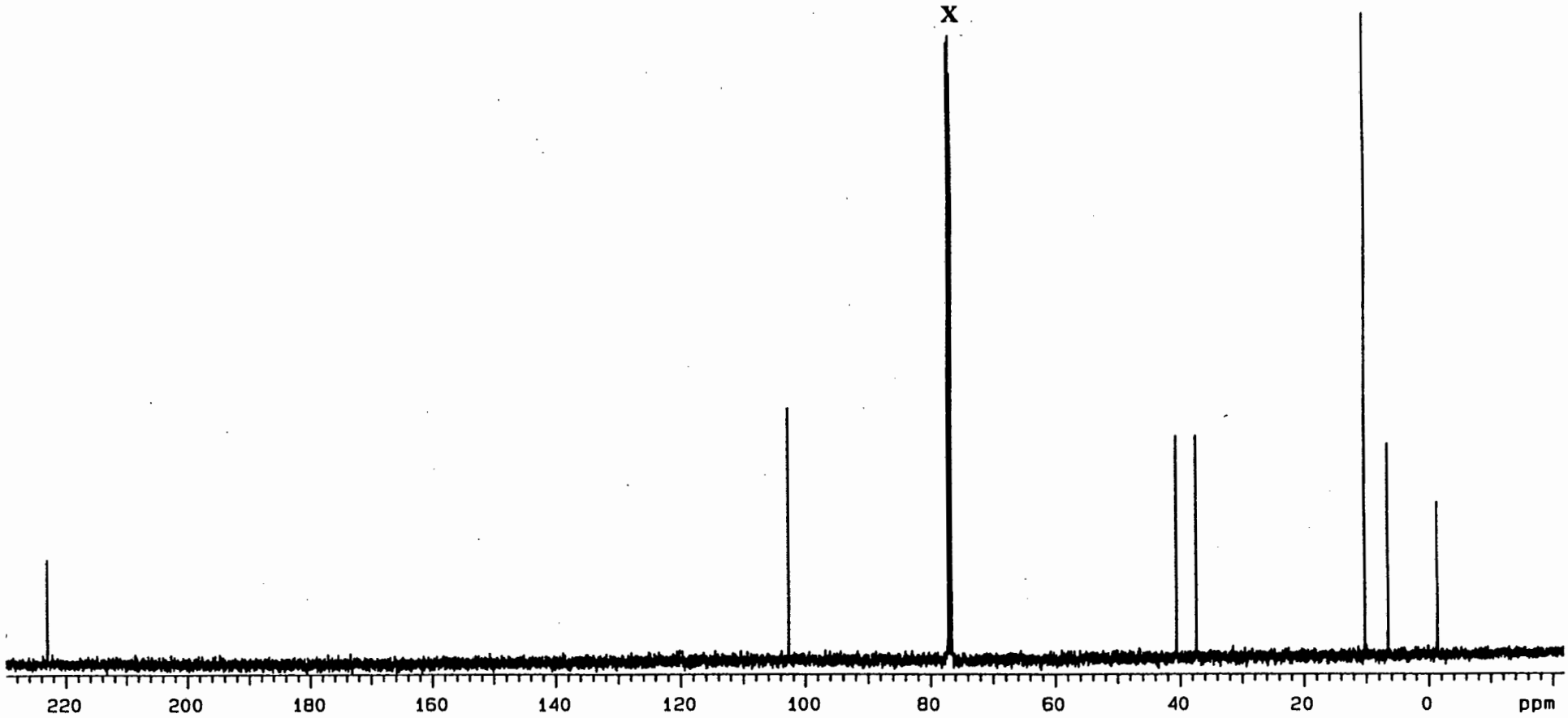

Figure 5.4 ^{13}C **NMR spectrum of [Cp*W(CO)$_3${(CH$_2$)$_4$I}], 14 (100 MHz, CDCl$_3$) (X = CDCl$_3$).**

The chain length or the nature of the halogen have no significant effect on the positions of the CO peaks. Similarly, the chain length and the halogen do not appear to affect the position of Cp or Cp* peaks very much, although for complexes with n = 3 the CO peaks are found at slightly higher field and the Cp or Cp* peaks at slightly lower field, compared to those for complexes with n greater than 3. The methylene α-CH_2 carbons in the Cp* complexes are significantly (~ 10 ppm) more deshielded than those in the corresponding Cp complexes. So too are the carbonyl carbon peaks, though to a lesser degree (~ 4 ppm). The deshielding effect is no longer apparent for the β-carbons of the methylene chain.

The effect of the halogen on the δ value of the α-CH_2 carbon, for the complexes where n = 3 and n = 4, is very apparent, and diminishes gradually with increasing n from 5 to 7. The peak due to the α-carbon is shifted upfield for those complexes with smaller values of n. This is in contrast with what one would expect considering the inductive effect of the halogens. For both the Cp and the Cp* complexes, the complexes with n = 3 are of particular interest, as the peak for the α-carbon is at a much higher field for X = Br than for X = I. These observations could possibly be explained in terms of a weak interaction between the halogen and tungsten, as has been suggested for the iron complexes $[CpFe(CO)_2\{(CH_2)_nX\}]$ [5]. The interaction between tungsten and halogen is also shown by the *ca.* 4 ppm downfield shift of the peaks of the CH_2X carbon for n = 3, relative to the corresponding peaks for compounds with n = 4 to 7. Thus as n increases, the distance between X and tungsten increases, and the effect of their interaction would decrease. Also apparent from the ^{13}C NMR data is the large chemical shift difference (*ca.* 25 ppm) between the CH_2X carbons (X = Br and I), reflecting the different electron withdrawing abilities of the halogens.

Mass spectra

Low resolution electron impact mass spectra were obtained for all the compounds under discussion. The intensities of the major organometallic peaks of

Table 5.7. Mass spectral data for $[CpW(CO)_3\{(CH_2)_nX\}]$.

Ion[a]	Relative peak intensities[b] (%)									
n =	3		4		5		6		7	
X =	Br	I	Br	I	Br	I	Br	I	Br	I
M	11	15	23	31	23	20	14	5	3	9
M - CO	12	24	0	0	2	4	5	0	4	7
M - 3CO[c]	12	7	80	73	0	0	0	0	0	0
M - $(CH_2)_n$	0	2	0	0	30	0	28	0	0	0
M - HX	0	0	27	3	5	58	0	0	0	0
M - $(CH_2)_nX$	60	24	12	61	17	20	81	60	49	16
M - CO - $(CH_2)_n$	52	100	80	82	100	60	100	100	100	69
M - CO - $(CH_2)_nX$	37	41	53	71	56	45	56	83	62	48
M - CO - HX	12	22	0	41	0	0	0	66	0	100[d]
M - 2CO - $(CH_2)_n$	65	46	93	73	0	54	84	99	79	100[d]
M - 2CO - $(CH_2)_nX$	0	37	46	58	55	46	52	82	57	42
M - 2CO - HX	10	44	0	61	8	43	0	89	0	88[e]
M - 3CO - $(CH_2)_nX$	40	66	61	79	74	65	59	94	59	46
M - 3CO - HX	18	20	0	0	4	0	13	0	24	5
M - $(CH_2)_n$ - CO_2	13	11	0	0	17	11	2	0	0	0
M - $(CH_2)_n$ - X - CO_2	24	37	0	0	9	16	2	0	0	0
M - $(CH_2)_nX$ - CO_2 - CO	15	29	4	3	13	0	8	0	0	0
M - $(CH_2)_nX$ - CO_2 - CpH	28	33	0	27	24	15	0	0	0	0
M - $(CH_2)_nX$ - CO_2 - CO - CpH	10	14	0	0	6	8	0	0	0	0
CpWX	100	91	100	100	0	100	81	93	56	88[e]
WX	12	0	4	0	9	0	5	0	0	0

[a]: M = $[CpW(CO)_3\{(CH_2)_nX\}]$; all ions have a single positive charge; ion refers to probable assignment. [b]: Peak intensities are relative to the base peak at *m/z* 328/330 due to $[CpWBr]^+$ (calculations based on the most abundant peaks for all ions) for complexes X = Br, n = 3 and 4, *m/z* 376 $[CpWI]^+$ for X = I, n = 4 and 5; *m/z* 384/386 due to $[CpW(CO)_2Br]^+$ for complexes X = Br, n = 5 - 7, *m/z* 432 due to $[CpW(CO)_2I]^+$ for complexes X = I, n = 3 and 6; *m/z* 403 for X= I, n = 7. [c]: No ions corresponding to M - 2CO, M - 2CO -Cp, M - CO - Cp or M - 3CO - Cp observed. [d] and [e]: These ions can not be distinguished.

Table 5.8 Mass spectral data for $[Cp^*W(CO)_3\{(CH_2)_nX\}]$.

Ion[a]	Relative intensity[b] (%)			
n =	3		4	
X =	Br	I	Br	I
M	100	48	100	99
M - CO	46	34	0	1
M - 2CO	17	8	2[c]	1[d]
M - 3CO	0	10	0	100[e]
M - HX	10	0	0	6
$M - (CH_2)_n$	3	11	2[c]	1[d]
$M - (CH_2)_nX$	0	45	0	0
$M - CO - (CH_2)_n$	0	0	0	100[e]
M - CO - HX	44	78	0	0
$M - CO - (CH_2)_nX$	18	100	11	0
$M - 2CO - (CH_2)_n$	0	0	0	84
M - 2CO - HX	0	0	0	0
$M - 2CO - (CH_2)_nX$	67	73	11	8
M - 3CO -HX	27	79	0	0
$M - 3CO - (CH_2)_nX$	38	19	13	10
Cp*WX	0	20	0	7

[a]: M = $[Cp^*W(CO)_3\{(CH_2)_nX\}]$; all ions have a single positive charge; ion refers to probable assignment. [b]: Peak intensities are relative to the parent peak for complexes with n = 3, 4 and X = Br, relative to $[Cp^*W(CO)_2]$ for n = 3, X = I, and relative to $[Cp^*W(CH_2)_4I]$ for n = 4, X = I, [c, d] and [e] : These ions can not be distinguished.

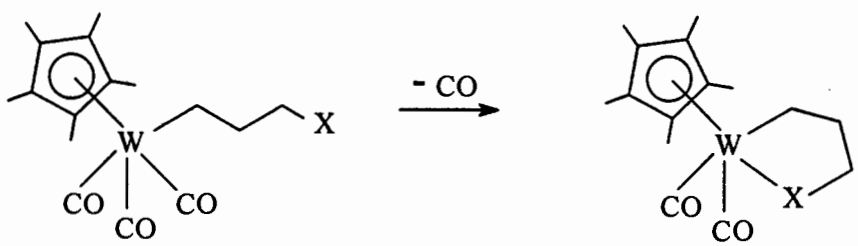

Scheme 5.3

All the complexes fragment according to three main pathways illustrated in Scheme 5.4. The possible fragmentation pathways for complex **6** are discussed in detail below.

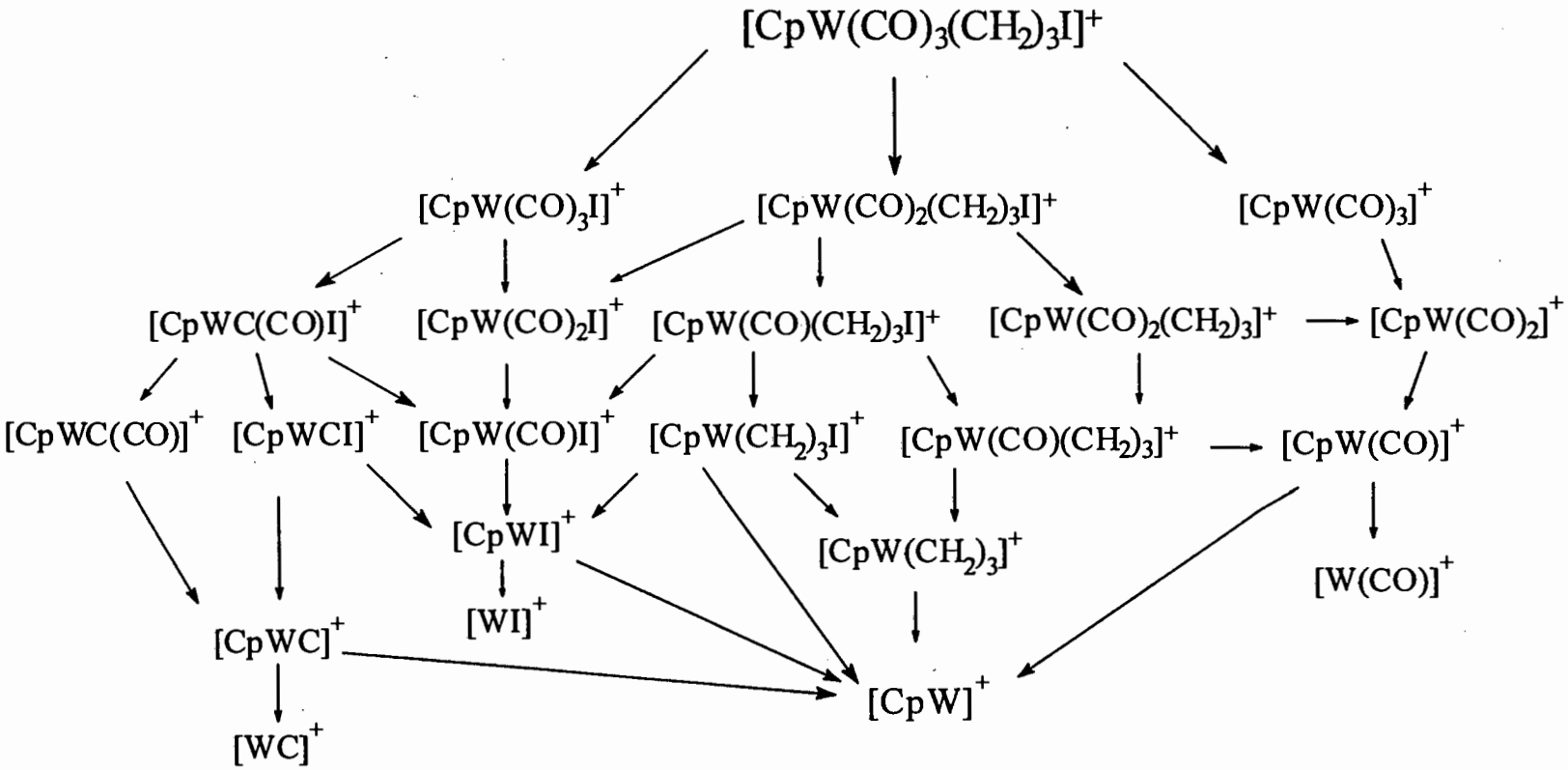
[CpW(CO)3(CH2)3I]+
[CpW(CO)3I]+
[CpW(CO)2(CH2)3I]+
[CpW(CO)3]+
[CpWC(CO)I]+
[CpW(CO)2I]+
[CpW(CO)(CH2)3I]+
[CpW(CO)2(CH2)3]+
[CpW(CO)2]+
[CpWC(CO)]+
[CpWCI]+
[CpW(CO)I]+
[CpW(CH2)3I]+
[CpW(CO)(CH2)3]+
[CpW(CO)]+
[CpWI]+
[CpW(CH2)3]+
[W(CO)]+
[WI]+
[CpWC]+
[CpW]+
[WC]+

Scheme 5.4

The first pathway involves the loss of $(CH_2)_3$ from the molecular ion and migration of I to tungsten to give $[CpW(CO)_3I]^+$, sequential loss of CO from this species gives $[CpW(CO)_2I]^+$, $[CpW(CO)I]^+$ and then $[CpWI]^+$. This is good evidence for a W-I interaction. The ion $[CpW(CO)_2I]^+$ could also be possibly formed by the loss of $CO(CH_2)_3$ from molecular ion *via* the formation of cyclic carbene species. The most abundant peak observed for this complex and most other complexes, corresponds to a halogen containing species, suggesting that the interaction between halogen and tungsten may be strong under the electron impact conditions.

The second fragmentation pathway, common to all the complexes containing CO, involves the sequential loss of CO from the molecular ion to give $[CpW(CO)_2(CH_2)_3I]^+$, $[CpW(CO)(CH_2)_3I]^+$ and $[CpW(CH_2)_3I]^+$. $[CpW(CO)_2(CH_2)_3I]^+$ could itself fragment in three ways: (a) by losing $(CH_2)_3I$ to give $[CpW(CO)_2]^+$, (b) by losing I to give $[CpW(CO)_2(CH_2)_3]^+$ or (c) by losing $(CH_2)_3$ with migration of I to tungsten to give $[CpW(CO)_2I]^+$. Further fragmentation pathways are illustrated in Scheme 5.4. The third pathway involves the formation of $[CpW(CO)_3]^+$ by the loss of $(CH_2)_3I$ from molecular ion. The further fragmentation of this species has been discussed above.

5.1.4 Thermal properties of $[CpW(CO)_3\{(CH_2)_nBr\}]$

The thermal properties of complexes $[CpW(CO)_3\{(CH_2)_nBr\}]$ (n = 3, **1**; and 4, **2**) were studied by DSC and TGA. The DSC traces of **1** and **2** recorded over the range 40 to 300 °C under nitrogen are shown in Figure 5.5. The upper trace for **1** shows an endothermic peak at 109 °C, which corresponds to the melting of the sample, by comparison with the hot-stage microscopy results. The exothermic peak at 194 °C corresponds to the decomposition of the complex. This can be seen from the TGA results (Figure 5.6), which show a significant mass loss at this temperature. The mass remaining after heating the sample to 290 °C corresponds to the decomposition of the sample to probable [WOBr] (suggested by mass percentage).

The DSC trace for complex **2** shows three endothermic peaks at 62, 68 and 72 °C, which, by comparison with the hot-stage microscopy results, are assigned to the melting points of the sample. The presence of more than one peak in the melting range of **2** suggests that this complex may exist in several crystalline forms or phases. This is confirmed by repeated experiments, and by checking the IR and ^{1}H NMR spectra of the sample after heating the sample to melting under nitrogen. The IR and ^{1}H NMR spectra of the melted sample are the same as the IR and ^{1}H NMR spectra of the pre-heating sample, although the colour of the melted sample is slightly darker. In addition, the TGA also shows no decomposition over the range 40 - 190 °C. The exothermic peak at 213 °C on the DSC trace of **2** is assigned to the decomposition of the complex. This is seen from the TGA results which show a significant mass loss at this temperature. The mass remaining after heating the sample to 290 °C corresponds to the degradation of **2** to tungsten metal.

The decomposition temperature for **2** is *ca.* 10 °C higher than that of **1**. The thermal decomposition of **1** gave different products to that of the decomposition of **2**. The different thermal behaviour of these complexes could be due to the alkyl chain length and the interaction between the tungsten and halogen as discussed in previous sections.

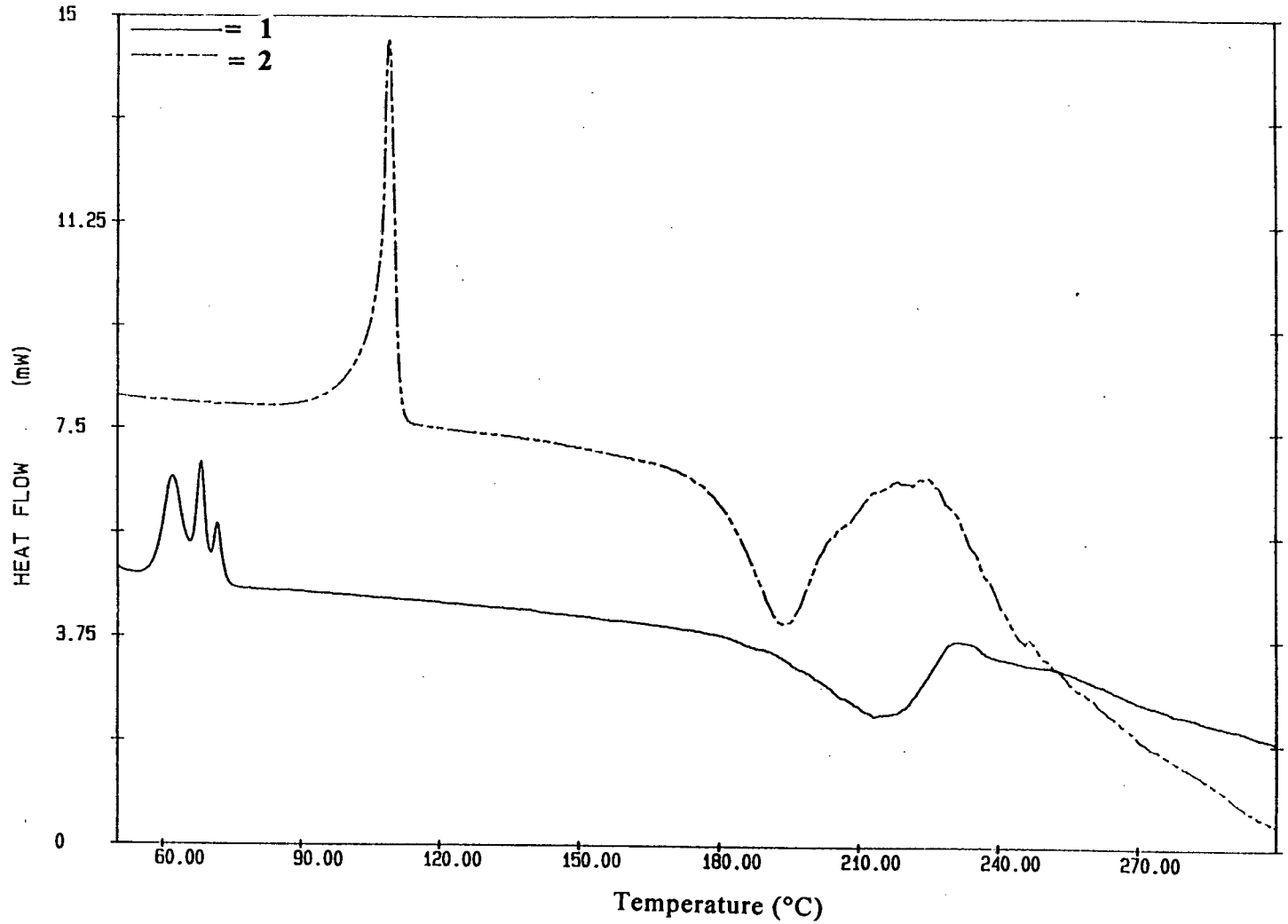

Figure 5.5 DSC traces for the complexes [CpW(CO)$_3${(CH$_2$)$_3$Br}], 1 and [CpW(CO)$_3${(CH$_2$)$_4$Br}], 2 (Scan rate = 20 °C/min).

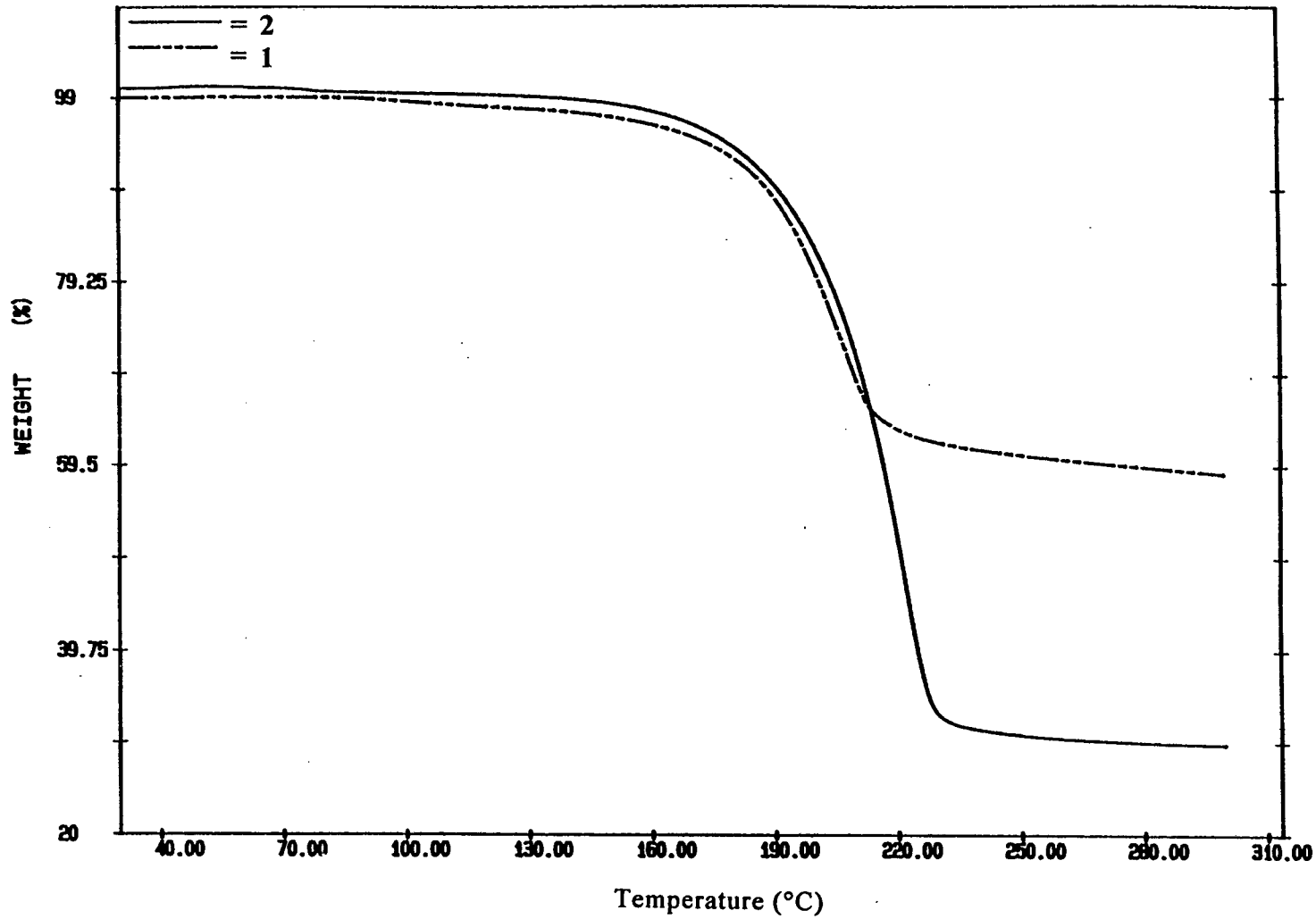

Figure 5.6 TGA traces for the complexes [CpW(CO)$_3${(CH$_2$)$_3$Br}], 1 and [CpW(CO)$_3${(CH$_2$)$_4$Br}], 2 (Scan rate = 20 °C/min).

5.1.5 Reactivity of $[CpW(CO)_3\{(CH_2)_nX\}]$

Introduction

Although some reactivity studies for $[(\eta^5\text{-}C_5R_5)W(CO)_3(CH_2X)]$ have been reported [8,9], the complexes $[(\eta^5\text{-}C_5R_5)W(CO)_3\{(CH_2)_nX\}]$ (n > 1) are less documented with the exception of the reports of the reaction of $[(\eta^5\text{-}C_5R_5)W(CO)_3\{(CH_2)_nX\}]$ (n = 3) with I^- or CN^- to form the 2-oxacyclopentylidene complexes [12-14]. An early attempt to prepare heterobinuclear complexes of the type $[CpMo(CO)_3(CH_2)_3ML]$ (ML = $CpFe(CO)_2$ or $Mn(CO)_5$) by the reaction of $[CpMo(CO)_3\{(CH_2)_3Br\}]$ with $Na[CpFe(CO)_2]$ or $Na[Mn(CO)_5]$ failed, due to the replacement of both the Br and the $CpMo(CO)_3$ groups by the $CpFe(CO)_2$ group [1]. However, no similar attempt has been made for the analogous tungsten complexes. Instead, heterobinuclear complexes $[CpM'(CO)_3(CH_2)_3ML]$ [M' = Mo, W; ML = $CpFe(CO)_2$ or $Mn(CO)_5$] have been synthesized by the reaction of $Na[CpM'(CO)_3]$ (M' = Mo, W) with $[CpFe(CO)_2\{(CH_2)_nX\}]$ (X = Br, I) [15,20].

A recent study of $[CpFe(CO)_2\{(CH_2)_6Br\}]$ has demonstrated [10] that it is possible to direct reactions selectively to either the metal or the bromo group. It is also possible to convert the haloalkyl complexes to other complexes with a new functionality, which then could be further used, for example in the preparation of dendrimers [17,18]. Since there is no report of the use of $[(\eta^5\text{-}C_5R_5)W(CO)_3\{(CH_2)_nX\}]$ (n > 1) as precursors for the preparation of binuclear and polynuclear complexes, we decided to explore the preparation of binuclear and polynuclear complexes from $[(\eta^5\text{-}C_5R_5)W(CO)_3\{(CH_2)_nX\}]$ (n > 1).

Reaction of $[CpW(CO)_3\{(CH_2)_3Br\}]$, 1 and $[CpW(CO)_3\{(CH_2)_4I\}]$, 7 with 3,5-dihydroxybenzyl alcohol

The reaction of $[CpRu(CO)_2\{(CH_2)_3Br\}]$ with 3,5-dihydroxybenzyl alcohol has been reported as the first step for the preparation of large ruthenium dendrimers

[17,18]. We have carried out similar reactions with tungsten haloalkyl complexes. The reaction of $[CpW(CO)_3\{(CH_2)_3Br\}]$, **1** with 3,5-dihydroxybenzyl alcohol in refluxing acetone for 3 days, in the presence of K_2CO_3 and 18-crown-6, gave predominately the bis-substituted product **15**, (51% yield) and a small amount of the mono-substituted product **16**, (3%). Both complexes were obtained as yellow solids after purification by column chromatography and recrystallization.

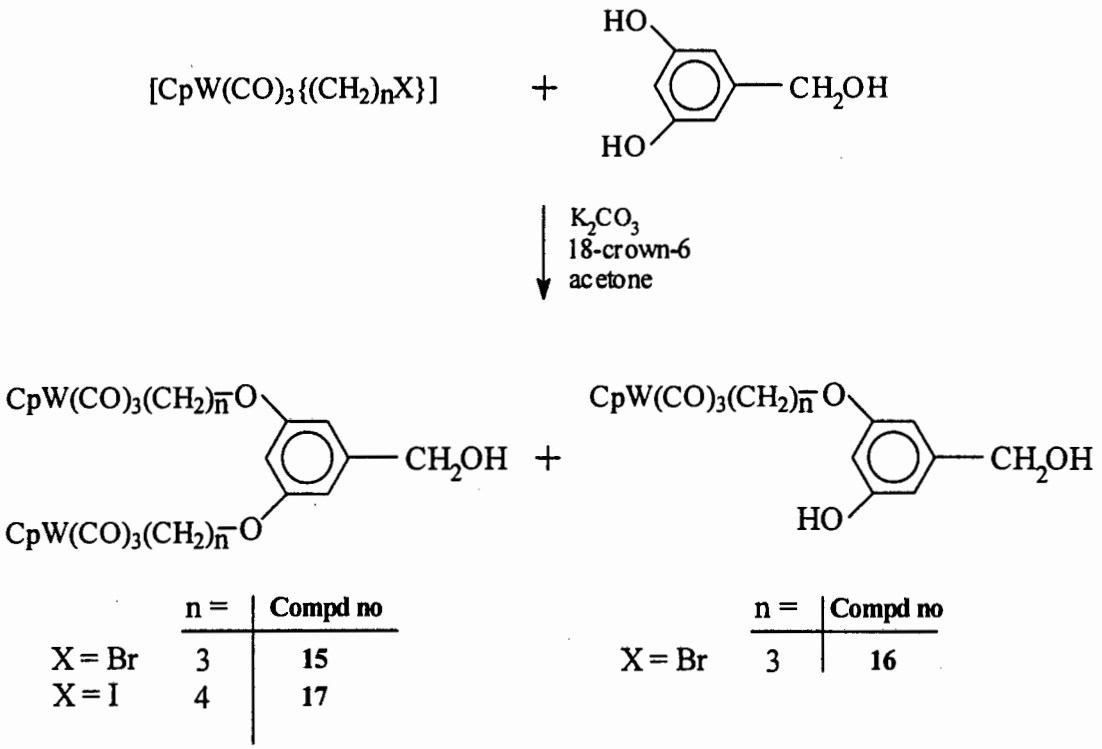

	n =	Compd no
X = Br	3	**15**
X = I	4	**17**

	n =	Compd no
X = Br	3	**16**

Scheme 5.5

The reaction of $[CpW(CO)_3(CH_2)_4I]$, **7** with 3,5-dihydroxybenzyl alcohol was carried out similarly in refluxing acetone for 2 days, but gave only a low yield (24%) of the bis-substituted product, **17**.

Complexes **15** - **17** have been characterized by elemental analysis, IR, and ^1H NMR, and the complexes **15** and **17** have also been characterized by ^{13}C NMR. The characterization results are given in the section 7.5.1. Two bands are observed in the IR spectra of **15** - **17** at similar positions to those observed for the corresponding haloalkyl complexes. This suggests that the metal centre is not affected by the reaction. The ^1H NMR spectra of **15** - **17** show a CH_2O proton triplet peaks at about δ 3.9 ppm which confirms the conversion from the haloalkyl to the anticipated products.

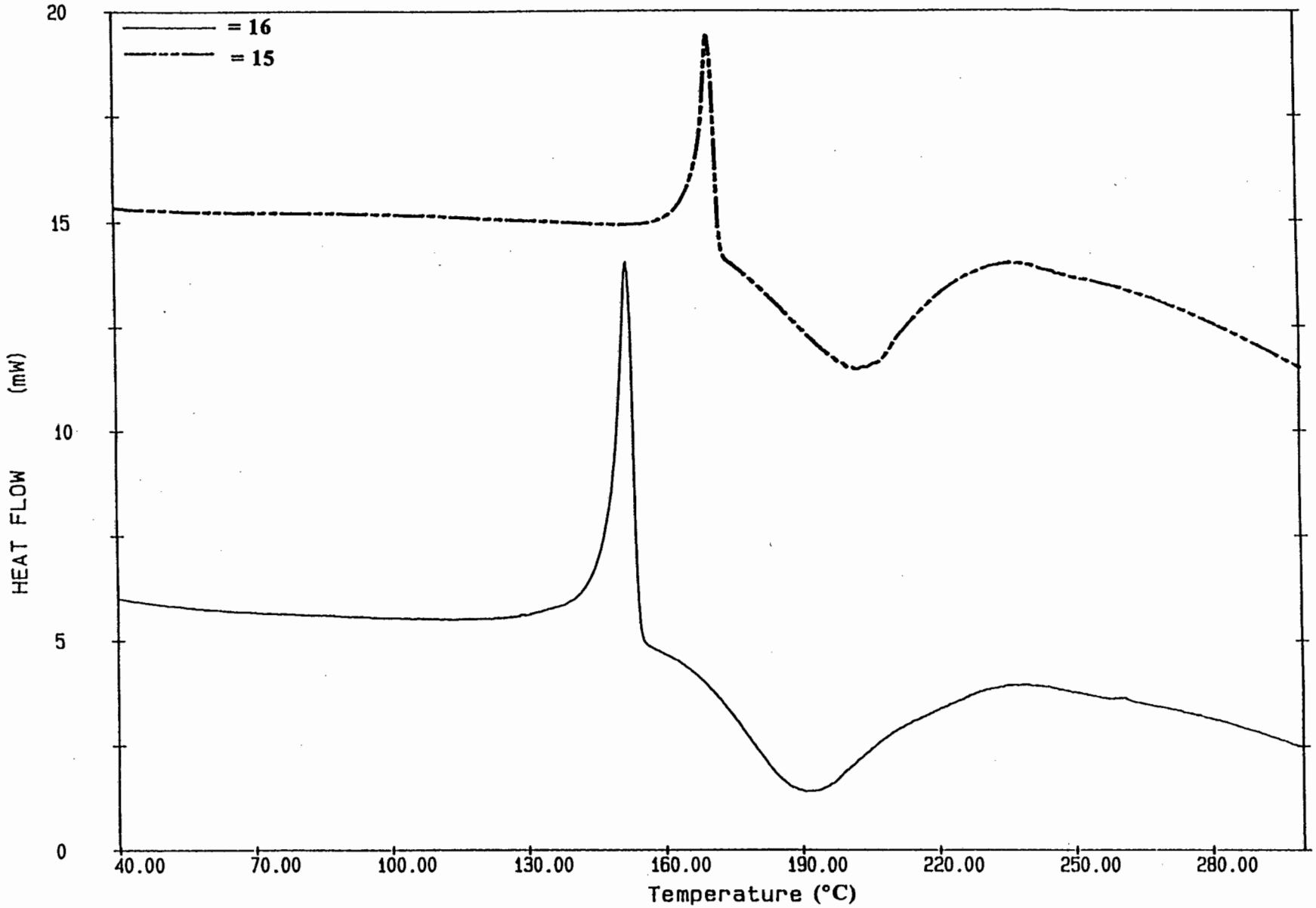

Figure 5.7 DSC traces for the complexes 15 and 16 (Scan rate = 10 °C/min).

The complexes **15** and **16** can be easily distinguished by observation of the aromatic proton resonances and by integration, and also by observation of the phenolic OH proton peak at 4.7 ppm in the ^{1}H NMR spectrum of **16**. Three separate proton resonances with equal integration are observed, in the region 6.2 - 6.4 ppm, in the ^{1}H NMR spectrum of **16,** due to the inequivalence of these aromatic protons in the mononuclear complex. Two separate proton peaks with integration of 2:1 due to the aromatic protons are observed in the ^{1}H NMR spectrum of **15**. Elemental analysis results confirm the formulae of the proposed complexes **15** and **16**.

The thermal properties of **15** and **16** have also been studied. The DSC traces of the mono- and bi-nuclear complexes **15** and **16** are shown in Figure 5.7. It is found that the mononuclear complex **16** is less thermally stable than the binuclear complex **15**. The melting points [DSC T_{max}(endo)] for **15** and **16** are 171 and 152 °C, respectively, in agreement with the melting points observed on the hot-stage microscope. The decomposition points [DSC T_{max}(exo)] measured for **15** and **16** are 203 and 190 °C, respectively.

Reaction of [CpW(CO)$_3${(CH$_2$)$_3$Br}], 1 with 1,1,1-tris(4'-hydroxy-phenyl)ethane

The reaction of **1** with 1,1,1-tris(4'-hydroxyphenyl)ethane was also carried out in refluxing acetone for 3 days, in the presence of K_2CO_3 and 18-crown-6, which gave the product **18** as shown below in good yield (61%).

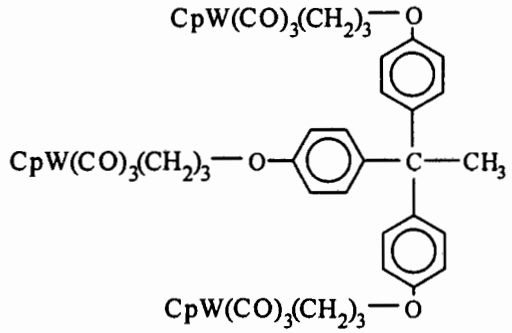

18

The complex **18** has been characterized by elemental analysis, IR, ^{1}H and ^{13}C NMR (see section 7.5.1). The IR spectrum of **18** shows two ν(CO) bands at 2012 and 1913 cm^{-1}, very similar to those observed in the IR spectra of **15** - **17**. The ^{1}H NMR spectrum of **18** shows a triplet at δ 3.85 ppm which corresponds to the CH_2 attached to a phenoxy group. The integration of the protons also indicates the formula of the product being as anticipated.

Conversion of 15 to the benzyl bromide complex 19

The benzyl alcohol complex **15** was reacted with CBr_4 and PPh_3 in THF at room temperature. After purification by column chromatography and recrystallization, the bromide complex **19** was obtained in low yield (10%). This is in contrast to the similar reactions carried out for the iron and ruthenium complexes [10,17,18], which generally give benzyl bromide complexes in high yields (70 - 90%). This could be due to the different metal employed. The complex **19** has also been characterized by IR and ^{1}H NMR. The IR spectrum of **19** shows the same bands as those for complex **15**. The ^{1}H NMR spectrum of **19** shows a characteristic single peak at δ 4.39 ppm, while all other peaks are found at the same positions as those in the ^{1}H NMR spectrum of **15**, which indicates the conversion of **15** to the anticipated product. The low yield of the bromide complex **19** makes it difficult to further study reactions of this complex.

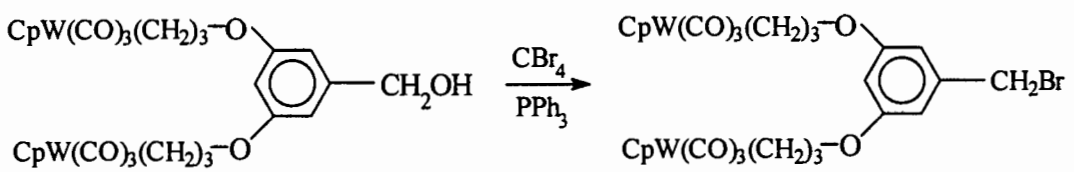

19

Scheme 5.6

Attempted preparation of a heterobimetallic complex containing W and Rh

A procedure reported [24] for the preparation of $[RhR(DH)_2(py)]$ from $[RhCl_2(DH_2)(DH)]$ and RX, in the presence of $NaBH_4$, was followed in an

attempt to prepare a heterobimetallic complex containing W and Rh. Thus, the reaction of $[CpW(CO)_3\{(CH_2)_4I\}]$ and $[RhCl_2(DH_2)(DH)]$ in the presence of $NaBH_4$ was conducted in a mixed solvent system of methanol/water/KOH/pyridine. After the reaction, none of the anticipated heterobimetallic complex could be observed. However, a yellow product was isolated in low yield (13%) in addition to some unreacted starting tungsten complex. This yellow product was identified as a new tungsten complex $[CpW(CO)_3\{(CH_2)_4OCH_3\}]$, **20**, by elemental analysis, IR, ^1H and ^{13}C NMR as well as mass spectroscopy. The characterization data are given in the experimental section 7.5.1. Parent ions (*m/z* 420, 422) are observed in the mass spectrum of **20**.

Attempts were also made to prepare heterobinuclear complexes of W and Pt by the reaction of $[CpW(CO)_3\{(CH_2)_4I\}]$ with $[Pt(CH_2{=}CH_2)(PPh_3)_2]$, but were unsuccessful. However, the reaction of $[(\eta^5\text{-}C_5R_5)W(CO)_3\{(CH_2)_nI\}]$ with $[PtMe_2(R_2\text{-bipy})]$ (R = H, CH_3) gave rise to a series of heterobinuclear W/Pt complexes which will be the subject of chapter 6 of this thesis.

5.2 Synthesis, characterization and reactivity of the ω-hydroxyalkyl complexes $[CpW(CO)_3\{(CH_2)_nOH\}]$ (n = 3, 6 and 7)

5.2.1 Introduction

Hydroxyalkyl metal complexes can be regarded as a new class of functionalized alkyl complexes, in which the metal centre and the hydroxy functional group are bridged by a polymethylene chain $[LyM\{(CH_2)_nOH\}]$. Hydroxyalkyl metal complexes with n = 1 and 2 have been recognized and/or proposed as model complexes for intermediates on catalyst surfaces, such as the Wacker process [25]. A brief survey of hydroxyalkyl metal complexes has been reported [10]. Hydroxyalkyl complexes $[LyM\{(CH_2)_nOH\}]$ (n > 2) are far less well known, compared to hydroxymethyl and hydroxyethyl complexes. Recently, Liao and Moss [10] have reported the synthesis of a series of new ω-hydroxyalkyl

complexes of the type $[LyM\{(CH_2)_nOH\}]$ (where LyM = $CpFe(CO)_2$, $Cp^*Fe(CO)_2$, and $CpRu(CO)_2$; n = 2 - 4). However, no hydroxyalkyl complex of the type $[CpW(CO)_3\{(CH_2)_nOH\}]$ is known with the exception of $[CpW(CO)_3\{(CH_2)_2OH\}]$ [26]. We have been successful in the synthesis of a series of new complexes of the type $[CpW(CO)_3\{(CH_2)_nOH\}]$ (n = 3, 6 and 7). The results are summarized below.

5.2.2 Synthesis of $[CpW(CO)_3\{(CH_2)_nOH\}]$

A series of new complexes of the type $[CpW(CO)_3\{(CH_2)_nOH\}]$ (n = 3, 6 and 7). have been prepared by the general method from $Na[CpW(CO)_3]$ and $Br(CH_2)_nOH$ in refluxing THF as shown in Scheme 5.7.

$$Na[CpW(CO)_3] + Br(CH_2)_nOH \longrightarrow [CpW(CO)_3\{(CH_2)_nOH\}] + NaBr$$

n	Compd. no
3	**21**
6	**22**
7	**23**

Scheme 5.7

The complexes **21** and **22** were isolated as yellow crystalline solids and **23** as a yellow oil. It is found that the hydroxyalkyl complexes are less stable to air and light than the haloalkyl complexes $[CpW(CO)_3\{(CH_2)_nX\}]$, both in solutions and in the solid state. Futhermore, they are extremely unstable when dissolved in chlorinated solvents.

5.2.3 Characterization of $[CpW(CO)_3\{(CH_2)_nOH\}]$

The complexes **21** - **23** have been characterized by elemental analysis, melting points, IR, ^1H and ^{13}C NMR. Mass spectra of these compounds show the parent molecular ions except **21**. The physical and spectroscopic data have been tabulated in Tables 5.9 - 5.11.

Table 5.9 Data for $[CpW(CO)_3\{(CH_2)_nOH\}]$.

Compound no	n	Yield (%)	M.p. (°C)	[a]M calc.	[b]M^+ observed	IR ν(CO)[c] (cm^{-1})	Elemental analysis (%)			
							C		H	
							calc.	found	calc.	found
11	3	27	71 - 73	392	364[d]	2018s, 1927vs	33.70	33.99	3.06	3.09
12	6	29	69 - 72	434	434/436	2016s, 1927vs	38.73	38.99	4.18	4.23
13	7	46	oil	448	448	2016s, 1927vs	40.20	40.89	4.50	4.94

[a]: The calculated molecular mass.

[b]: The molecular ion observed in the mass spectrum of the compound, with expected isotope patterns.

[c]: IR in hexane.

[d]: This ion corresponds to $[M\text{-}CO]^+$.

Table 5.10 ^{1}H NMR data for $[CpW(CO)_3\{(CH_2)_nOH\}]$[a] (400 MHz, $CDCl_3$).

Compound no	n	Cp	CH_2OH $^{3}J(HH)$	CH_2CH_2OH	α-CH_2[b]	β-CH_2	γ-CH_2	δ-CH_2	ε-CH_2
21	3	5.39, 5H, s	3,55, 2H, t, 6.4	1.82, 2H, m	1.49, 2H, m				
22	6	5.36, 5H, s	3.62, 2H, t, 6.8	1.54, 6H, m			1.34, 4H, m		
23	7	5.35, 5H, s	3.62, 2H, t, 6.8	1.53, 6H, m			1.31, 6H, m		

[a]: Coupling constants are given in Hz. [b]: Protons of the methylene chain α to tungsten etc.

Table 5.11 ^{13}C NMR chemical shift data (δ ppm) for $[CpW(CO)_3\{(CH_2)_nOH\}]$(100 MHz, $CDCl_3$).

Compound no	n	CO	Cp	CH_2OH	CH_2CH_2OH	α-CH_2[a]	β-CH_2	γ-CH_2	δ-CH_2	ε-CH_2
21	3	228.56, 217.47	91.54	67.10	39.73	-16.48				
22	6	228.93, 217.56	91.46	63.08	32.83	-10.24	36.79	35.63	25.19	
23	7	228.98, 217.56	91.47	63.06	32.80	-10.04	36.81	35.88	28.90	25.76

[a]: Carbon of the methylene chain α to tungsten etc.

IR spectroscopy

The IR spectra of **21 - 23** were recorded in hexane solution in the range 2200 to 1600 cm^{-1}, and the data are given in Table 5.9. Generally, there is no change in the positions of the carbonyl bands in the IR spectra, although a very slightly higher wavenumber is observed for the complex with n = 3 than that for complexes with n = 6 and 7. The IR spectra of these complexes show almost identical ν(CO) to that of the alkyl complexes $[CpW(CO)_3R]$ and haloalkyl complexes $[CpW(CO)_3\{(CH_2)_nX\}]$, suggesting that the hydroxy group has little or no effect on the ν(CO).

^{1}H NMR spectroscopy

The ^{1}H NMR data for complexes **21 - 23** are summarized in Table 5.10. Assignments for the data were made by integration and comparison with $[CpW(CO)_3\{(CH_2)_nX\}]$ and ROH. It can be seen that the alkyl chain length has no effect on the chemical shift of the Cp ring. Separate resonances for the C*H*$_2$OH protons are observed for **21 - 23** at positions similar to those found in organic alcohols [22]. The C*H*$_2$OH protons for the complex with n = 3 show a small shift compared with the complexes with n = 6 and 7, which could be due to either the inductive or steric effect of tungsten.

^{13}C NMR spectroscopy

The ^{13}C NMR data for complexes **21 - 23** are listed in Table 5.11. Assignments were made by comparison with $[CpW(CO)_3\{(CH_2)_nX\}]$ and ROH. The chain length and the hydroxy group appear to have no effect on the positions of the CO peaks and the position of the Cp peak. The effect of the hydroxy group on the chemical shift of the α-CH_2 carbon for the complex with n = 3 is very apparent, compared with that for the complexes with n = 6 and 7. The peak due to the α-carbon is shifted upfield for the complex with n = 3, with $\Delta\delta = \delta_{n=6} - \delta_{n=3} = 6.2$ ppm. This difference is much larger than that found for the similar haloalkyl

complexes, *eg.* for $[CpW(CO)_3\{(CH_2)_nBr\}]$ $\Delta\delta = \delta_{n=6} - \delta_{n=3} = 4.2$ ppm. This may be explained in terms of a weak binding interaction between the functional hydroxy group and the tungsten. The larger $\Delta\delta$ in the hydroxyalkyl complexes than that in the haloalkyl complexes is due to the larger electronegativity of oxygen than that of the bromine. The peak of the carbon α to OH group for the complex with n = 3 shifts downfield *ca.* 4 ppm, relative to the corresponding peak for complexes with n = 6 and 7.

Mass spectra

All the complexes **21** - **23** have been characterized by low resolution electron impact mass spectroscopy. Molecular ions are observed for all the complexes except **21**. It is found that the fragmentation pathways of these hydroxyalkyl complexes are similar to those of haloalkyl complexes discussed in section 5.1.2. The fragmentation schemes for **21** are illustrated in Scheme 5.8.

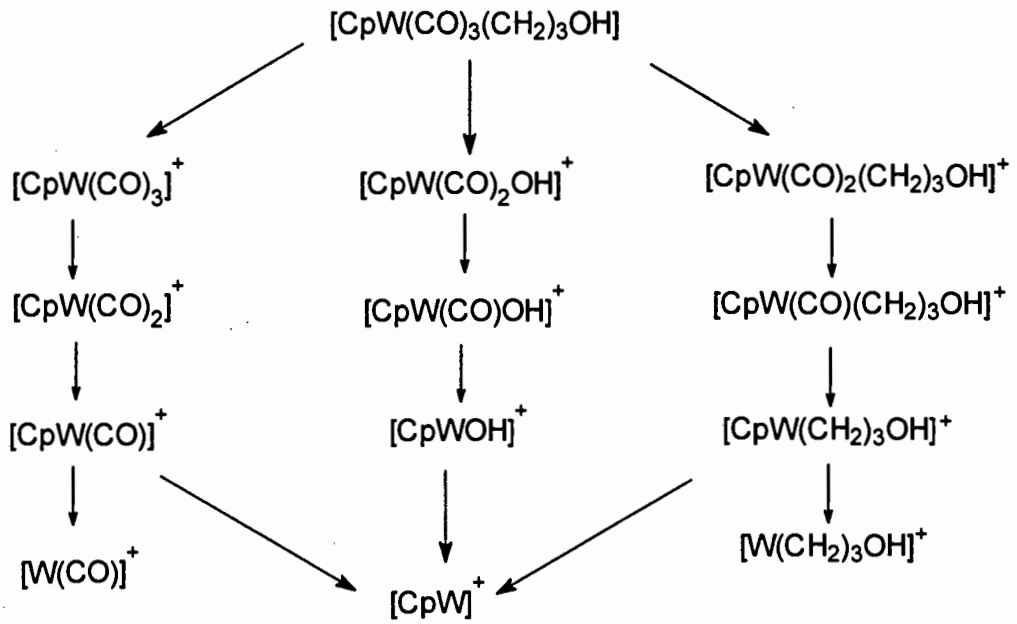

Scheme 5.8

5.2.4 Reactivity of $[CpW(CO)_3\{(CH_2)_nOH\}]$

Reaction of $[CpW(CO)_3\{(CH_2)_7OH\}]$ with *p*-anisoyl chloride

This was an attempt to elaborate the -OH function, as similar reactions have been performed successfully with $[CpFe(CO)_2\{(CH_2)_nOH\}]$ [10]. The reaction of $[CpW(CO)_3\{(CH_2)_7OH\}]$ with BuLi at -78 °C followed by adding *p*-anisoyl chloride was found to yield an ester complex $[CpW(CO)_3\{(CH_2)_7OC(O)(C_6H_4)OMe\}]$, **24**, in 33 % yield (see below).

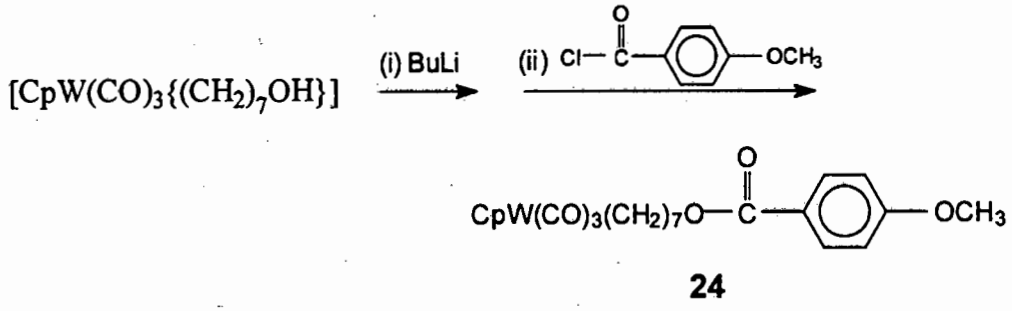

24

Scheme 5.9

The complex **24** is a yellow crystalline solid and has been fully characterized (see experimental section 7.5.2). The IR spectrum of **24** in hexane shows two strong bands at 2016 and 1926 cm^{-1} for the CO groups bonding to the metal and two medium bands at 1723 and 1608 cm^{-1} for the ester C=O group. The ^1H NMR spectrum shows a triplet at δ 4.28 ppm which corresponds to the $CH_2OC(O)$ protons, which, together with expected integrations confirms the formation of the anticipated product. The mass spectrum of **24** also shows molecular ion peaks at *m/z* 580 and 581. Satisfactory elemental analysis results further confirm the formula of **24**.

Direct reaction of $[CpW(CO)_3\{(CH_2)_7OH\}]$ with *p*-anisoyl chloride in THF/NEt_3 did not yield a similar ester product. This is in contrast to the result obtained for a similar reaction carried out with $[CpFe(CO)_2\{(CH_2)_3OH\}]$ and 4-nonyloxy-benzoyl chloride, to yield the ester $[CpFe(CO)_2\{(CH_2)_3OC(O)(C_6H_4)OC_9H_{19}\}]$ [10].

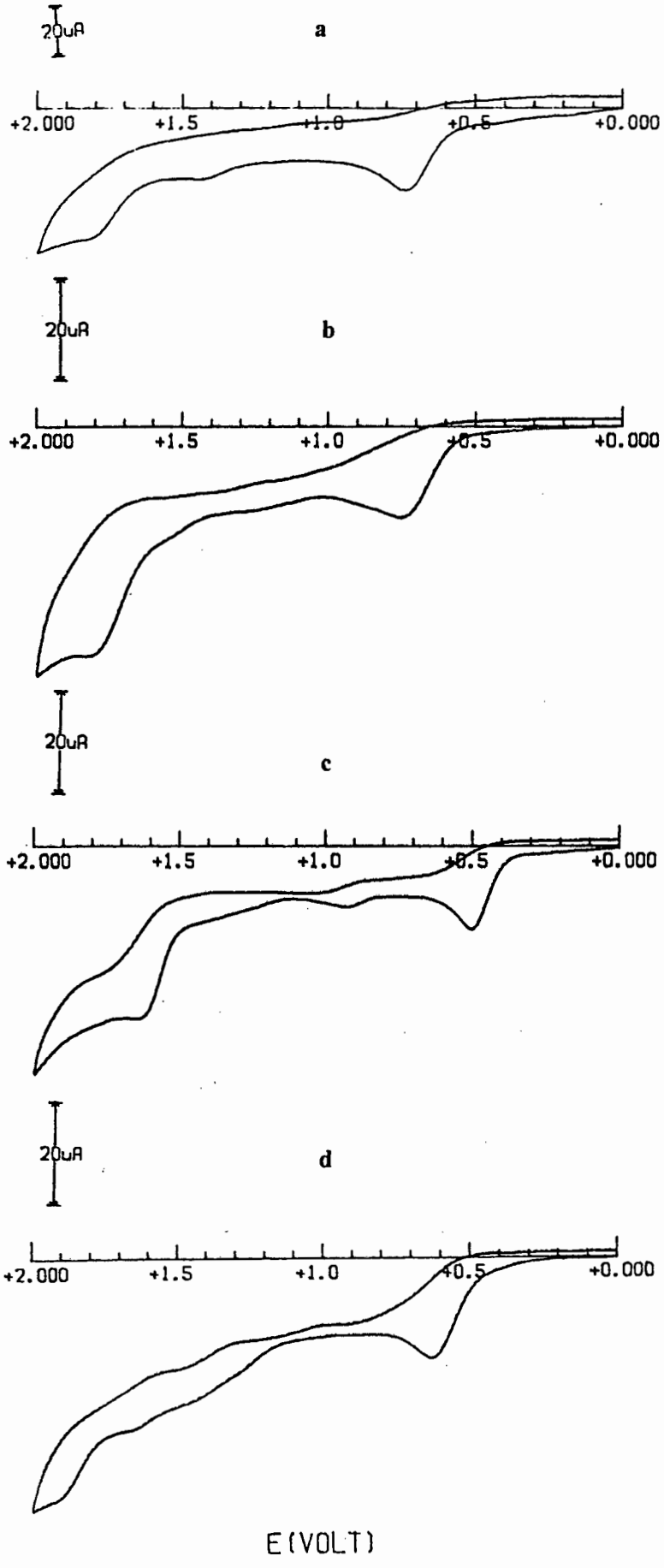

Figure 5.8 Cyclic voltammograms of 1.0 mM solutions of (a): [Wp{$(CH_2)_3Br$}] (at a scan rate of 500 mV/s); (b): [Wp{$(CH_2)_5I$}]; (c): [Wp*{$(CH_2)_4I$}]; and (d): [Wp{$(CH_2)_3OH$}]; in acetonitrile containing 0.1 M [NBu^n_4]ClO_4 at a Pt microelectrode with a scan rate of 100 mV/s, under argon.

A difference between the complexes with the Cp ligand and the complexes with the Cp* ligand is observed. The complex with the Cp* ligand, $[Cp^*W(CO)_3\{(CH_2)_4I\}]$, was oxidized at much less positive potential than similar complexes containing the Cp ligand, which is a direct indication that the tungsten centre in the Cp* complex is more electron rich than in the Cp complexes. This is due to the strong electron donating effect of the Cp* ligand. Similar studies on the iron complexes $[CpFe(CO)_2(CH_2)_5CH_3]$, $[CpFe(CO)_2\{(CH_2)_6Br\}]$ and $[CpFe(CO)_2\{(CH_2)_3OH\}]$ have shown [10] that their electrochemical behaviour and redox potentials are affected neither by the hydrocarbon chain length nor by the nature of the functional groups. Given the fact that these tungsten complexes show similar chemistry in a range of reactions to that of the iron complexes [10], it is expected that the electrochemical behaviour of these tungsten complexes $[CpW(CO)_3\{(CH_2)_nX\}]$ is not likely to be affected by the alkyl chain length or the nature of the functional groups.

5.4 Synthesis and characterization of $[Re(CO)_5\{(CH_2)_nX\}]$

Introduction

Although the complexes $[Re(CO)_5\{(CH_2)_nX\}]$ (n = 1, X = F, Cl, Br, I; n = 4, X = I) have been reported [4,27], to date no other haloalkyl rhenium complexes $[Re(CO)_5\{(CH_2)_nX\}]$ have been reported. To complete our studies of haloalkyl complexes, we have synthesized a series of $[Re(CO)_5\{(CH_2)_nX\}]$ complexes using the methodology which we developed for the preparation of other haloalkyl complexes.

Synthesis of $[Re(CO)_5\{(CH_2)_nX\}]$

The complexes $[Re(CO)_5\{(CH_2)_nX\}]$ (n = 3 - 5, X = Br, **25** - **27**) were prepared by reacting $Na[Re(CO)_5]$ with excess $Br(CH_2)_nBr$ in THF at low temperature as shown in Scheme 5.10.

$$Na[Re(CO)_5] + Br(CH_2)_nBr \longrightarrow [Re(CO)_5\{(CH_2)_nBr\}] + NaBr$$

n	Compd no
3	**25**
4	**26**
5	**27**

Scheme 5.10

Complexes **25** and **26** were isolated in low yields by column chromatography and recrystallization, as low melting off-white solids. The complex **27** could only be obtained as a mixture of **27** and $Br(CH_2)_5Br$. It was also found that low temperature and an excess of the dibromoalkanes are necessary to prevent the formation of $[(CO)_5Re(CH_2)_nRe(CO)_5]$.

Like the bromoalkyl tungsten complexes, the $[Re(CO)_5\{(CH_2)_nBr\}]$ complexes react with NaI to form $[Re(CO)_5\{(CH_2)_nI\}]$ as shown in Scheme 5.11.

$$[Re(CO)_5\{(CH_2)_nBr\}] + NaI \longrightarrow [Re(CO)_5\{(CH_2)_nI\}] + NaBr$$

n	Compd no
3	**28**
4	**29**
5	**30**

Scheme 5.11

Complexes **28** and **29** were obtained as colourless oils in reasonable yields. The complex **29** has been previously prepared by the reaction of $Na[Re(CO)_5]$ with a large excess of $I(CH_2)_4I$ [27]. Complex **30** was obtained as a mixture with $I(CH_2)_5I$ which could not be purified by column chromatography or recrystallization. The physical and characterization data for the haloalkyl rhenium complexes are reported in Tables 5.13 - 5.15.

IR spectroscopy

The IR spectra of **25** - **30** were recorded in hexane solution in the range 2200 to 1600 cm^{-1}. The IR spectrum of **29** was also recorded in CH_2Cl_2, in order to compare with the literature data [27]. Our results are in good agreement with the

literature. No significant change in the ν(CO) band positions is observed upon variation of either the chain length or the halogens.

^{1}H and ^{13}C NMR spectroscopy

Assignment of the ^{1}H and ^{13}C NMR data of these complexes were made by comparison with literature data [27], [$Re(CO)_5R$] [28] and RX [22]. The ^{1}H and ^{13}C NMR data for complexes **25**, **26**, **28** and **29** are given in Tables 5.14 and 5.15, respectively. It can be seen that the halogen and n affect the chemical shifts of the CH_2X peaks. Thus these peaks are shifted 0.2 ppm up-field as X changes from Br to I, reflecting the electronegativity difference of the halogens. As n changes from 3 to 4, the CH_2X triplet moves down-field by 0.1 ppm, presumably reflecting a decrease in the influence of Re.

In the ^{13}C NMR spectra, no significant change of the positions of CO peaks is observed by varying either the halogen or n. The effect of the halogen on the chemical shift of the Re-CH_2 carbon is apparent. The Re-CH_2 peak for the complexes with n = 3 is at a higher field for X = Br than for X = I. This may imply an interaction between the metal and the γ-C-X bond, with this interaction being stronger for the iodoalkyl complexes. Also apparent is the large chemical shift difference between the carbon α to Br and I respectively, reflecting the different electron withdrawing abilities of the halogens.

Mass Spectra

No molecular ions were observed in the mass spectra of these haloalkyl complexes by low resolution electron impact mass spectrometry. The highest mass peak for all complexes corresponds to [M - 2CO]. This may be due to the instability of these complexes under electron impact conditions. Previous studies of the mass spectra of the alkyl complexes [$Re(CO)_5R$] in this laboratory have also shown that no parent ion could be observed for these alkyl complexes [28].

Table 5.13 Data for $[Re(CO)_5\{(CH_2)_nX\}]$.

Compound no	X	n	Yield (%)	M. p. (°C)	IR ν(CO)[a] (cm^{-1})	Elemental analysis (%)			
						C		H	
						calc.	found	calc.	found
25	Br	3	29	29 - 31	2128w, 2013s, 1987m	[b]	[b]	[b]	[b]
26	Br	4	38	27 - 28	2124w, 2013s, 1985m	23.38	23.63	1.74	1.65
27[c]	Br	5	17	oil	2124w, 2012s, 1984m	25.22	25.03	2.12	1.78
28	I	3	31	oil	2126w, 2013s, 1987m	[b]	[b]	[b]	[b]
29[d]	I	4	58	oil	2126w, 2012s, 1986m	[d]	[d]	[d]	[d]
30[e]	I	5	-	oil	2125w, 2012s, 1985m	[b]	[b]	[b]	[b]

[a]: IR in hexane

[b]: No satisfactory elemental analysis results were obtained due to the instability of these complexes.

[c]: Obtained as a mixture of **27** and $Br(CH_2)_5Br$.

[d]: IR (in CH_2Cl_2) ν(CO): 2127w, 2009s, 1977m cm^{-1}, these results are in good agreement with the literature [27].

[e]: Obtained as a mixture of **30** and $I(CH_2)_5I$.

Table 5.14 ^{1}H NMR data for $[Re(CO)_5\{(CH_2)_nX\}]$ (400 MHz, $CDCl_3$)[a].

Compound no	X	n	CH_2X $^{3}J(HH)$	CH_2CH_2X	β-CH_2	α-CH_2
25	Br	3	3.30, 2H, t, 7.2	2.29, 2H, m		0.91, 2H, m
26	Br	4	3.45, 2H, t, 6.4	1.89, 4H, m		0.92, 2H, m
28	I	3	3.11, 2H, t, 7.6	2.22, 2H, m		0.91, 2H, m
29[b]	I	4	3.22, 2H, t, 6.8	1.83, 4H, m		0.91, 2H, m

[a]: Coupling constants are given in Hz, α-CH_2 refers to the protons on the CH_2 α to rhenium etc.
[b]: These data are in good agreement with literature [27].

Table 5.15. ^{13}C NMR chemical shift data (δ ppm) for $[Re(CO)_5\{(CH_2)_nX\}]$ (100 MHz, $CDCl_3$).

Compound no	X	n	CO	CH_2X	CH_2CH_2X	α-CH_2[a]	β-CH_2
25	Br	3	184.95, 180.70	39.03	42.17	-12.84	
26	Br	4	185.50, 181.09	33.41	37.27	-11.25	40.05
28	I	3	184.98, 180.66	13.27	43.20	-9.69	
29[b]	I	4	185.5, 181.1	6.8	39.7	-11.6	40.7

[a]: α-CH_2 refers to the CH_2 carbon α to rhenium, etc.[b]: Data from literature [27].

5.4 Conclusion

The new ω-bromoalkyl tungsten complexes $[CpW(CO)_3\{(CH_2)_nBr\}]$ (n = 5-7) and $[Cp^*W(CO)_3\{(CH_2)_nBr\}]$ (n =4) are easily prepared in good yields by the reaction of $Na[CpW(CO)_3]$ or $Na[Cp^*W(CO)_3]$ with $Br(CH_2)_nBr$. The iodoalkyl complexes $[CpW(CO)_3\{(CH_2)_nI\}]$ (n = 3-7) and $[Cp^*W(CO)_3\{(CH_2)_nI\}]$ (n =3 and 4) can be prepared by reacting $[CpW(CO)_3\{(CH_2)_nBr\}]$ and $[Cp^*W(CO)_3\{(CH_2)_nBr\}]$ with NaI or by reacting $Na[CpW(CO)_3]$ with $I(CH_2)_nI$.

All these haloalkyl complexes are obtained as yellow solids and have been fully characterized. The Cp* complexes are more stable than their Cp analogues, while the bromoalkyl complexes are more stable than their iodoalkyl analogues.

Both similarities and differences are observed in the IR, ^1H and ^{13}C NMR and mass spectra of the respective Cp and Cp* complexes. The effects of the chain length and the halogens on the spectroscopic properties are discussed.

The haloalkyl complexes $[CpW(CO)_3\{(CH_2)_3Br\}]$ reacts with 1,1,1-tris(4'-hydroxyphenyl)ethane and 3,5-dihydroxybenzyl alcohol to give tri-nuclear and bi-nuclear complexes respectively.

The ω-hydroxyalkyl tungsten complexes $[CpW(CO)_3\{(CH_2)_nOH\}]$ (n = 3, 6 and 7) are synthesized by the reaction of $Na[CpW(CO)_3]$ with $Br(CH_2)_nOH$ in good yields. These complexes are less stable than the analogous haloalkyl complexes. The reaction of the hydroxyalkyl complex $[CpW(CO)_3\{(CH_2)_7OH\}]$ with BuLi followed by *p*-anisoyl chloride gives the complex $[CpW(CO)_3\{(CH_2)_7O_2C(C_6H_4)$-OMe-(4)$\}]$.

In a similar way, the new bromoalkyl rhenium complexes $[Re(CO)_5\{(CH_2)_nBr\}]$ (n = 3 and 4) are prepared by the reaction of $Na[Re(CO)_5]$ with $Br(CH_2)_nBr$ at low temperature to prevent competing reactions. The bromoalkyl complexes $[Re(CO)_5(CH_2)_nBr]$ react with NaI to yield $[Re(CO)_5\{(CH_2)_nI\}]$. The haloalkyl

rhenium complexes appear to be less stable than the haloalkyl tungsten complexes.

The characterization data obtained for these haloalkyl and hydroxyalkyl complexes support previous observations by other workers that there is an interaction between the metal and the γ-C-X bond in halopropyl and hydroxypropyl transition metal complexes.

The reactivity of the iodoalkyl complexes to give polymethylene bridged heterobinuclear complexes is discussed in Chapter 6.

References

1. R. B. King and M. B. Bisnette, J. Organomet. Chem., 1967, **7**, 311.
2. H. B. Friedrich and J. R. Moss, Adv. Organomet. Chem., 1991, **33**, 235.
3. J. R. Moss, J. Organomet. Chem., 1982, **231**, 229.
4. J. R. Moss and S. Pelling, J. Organomet. Chem., 1982, **236**, 221.
5. H. B. Friedrich, P. A. Makhesha, J. R. Moss and B. K. Williamson, J. Organomet. Chem., 1990, **384**, 325.
6. H. B. Friedrich, K. P. Finch, M. A. Gafoor and J. R. Moss, Inorg. Chim. Acta, 1993, **206**, 225.
7. S. Pelling, C. Botha and J. R. Moss, J. Chem. Soc. Dalton Trans., 1983, 1495.
8. H. B. Friedrich and J. R. Moss, J. Organomet. Chem., 1993, **453**, 85.
9. J. R. Moss, M. L. Niven and P. M. Stretch, Inorg. Chim. Acta, 1986, **119**, 177.
10. Y-H. Liao, Ph D. Thesis, University of Cape Town, 1994.
11. J. R. Moss, Trends in Organomet. Chem., 1994, **1**, 211.
12. N. A. Bailey, P. L. Chell, C. P. Manuel, A. Mukhopadhyay, D. Rogers, H. E. Tabbron and M. J. Winter, J. Chem. Soc. Dalton Trans., 1983, 2397.
13. H. Adams, N. A. Bailey and M. J. Winter, J. Chem. Soc. Dalton Trans., 1984, 273.
14. N. A. Bailey, D. A. Dunn, C. N. Foxcroft, G. R. Harrison, M. J. Winter and S. Woodward, J. Chem. Soc. Dalton Trans., 1988, 1449.
15. H. B. Friedrich, J. R. Moss and B. K. Williamson, J. Organomet. Chem., 1990, **394**, 313.
16. S. F. Mapolie, Ph. D. Thesis, University of Cape Town, 1988.
17. Y-H. Liao and J. R. Moss, J. Chem. Soc. Chem. Commun., 1993, 1774.
18. Y-H. Liao and J. R. Moss, Organometallics, 1995, **14**, 2130; 1996, **15**, 4307.
19. See Chapter 3 of this Thesis.
20. L. G. Scott, M. Sc. Thesis, University of Cape Town, 1984.

21. R. E. Dessy, R. L. Pohl and R. B. King, J. Am. Chem. Soc., 1966, **88**, 5121.

22. C. J. Pouchert, *The Aldrich Library Of NMR Spectra*, 3rd ed., vol 1, 1983, USA.

23. E. Breitmaier and W. Voelter, *Carbon-13 NMR Spectroscopy: High-Resolution Methods And Applications In Organic Chemistry And Biochemistry*, 3rd ed., VCH: Weinheim, 1987.

24. B. Giese, J. Hartung, C. Kesselheim, H. J. Lindner and I. Svoboda, Chem. Ber., 1993, **126**, 1193.

25. P. M. Henry, Adv. Organomet. Chem., 1975, **13**, 363.

26. W. H. Knoth, Inorg. Chem., 1975, **14**, 1566.

27. Y. Zhou and J. A. Gladysz, Organometallics, 1993, **12**, 1073.

28. (a) J-A.M. Andersen, Ph. D. Thesis, University of Cape Town, 1993.
(b) J-A.M. Andersen and J.R. Moss, J. Organomet. Chem., 1995, **494**, 105.

Chapter 6

Synthesis And Characterization Of Polymethylene Bridged Heterobimetallic Complexes And Dendritic Polynuclear Pt(II) Alkyl Complexes

6.1 Synthesis and characterization of polymethylene bridged heterobimetallic complexes of the type $[LM(CH_2)_nPtIMe_2(R_2\text{-bipy})]$

6.1.1 Introduction

Transition metal complexes incorporating hydrocarbons as bridges between metal atoms are of great interest as they play a pivotal role in the development of binuclear and polynuclear organometallic chemistry [1-8]. Complexes with bridging μ-alkanediyl ligands $[LM(CH_2)_nM'L']$, where ML and M'L' are the metals with their associated ligands, are of particular interest [1,3,6-8] since they could serve as models for intermediates in the Fischer-Tropsch reaction [1,9], in the polymerization of alkenes and alkynes [1,6], in hydrocarbon reforming [10] and for unsaturated hydrocarbons chemisorbed on metal surfaces [1].

Because of the great importance of these complexes, much effort has been devoted to developing methods for the preparation of transition metal complexes with bridging hydrocarbon groups [1-8]. For example, Moss and co-workers [6,11-13] have developed strategies for building up homo- and hetero-binuclear complexes where the metal centres are bridged by an alkanediyl ligand. The earlier synthesis of polymethylene bridged homobinuclear complexes of the general formula $[LM(CH_2)_nML]$ (where ML is the metal with associated ligands) was limited to the reactions of transition metal anions $[ML]^-$ with 1,n-dihaloalkanes [14]. The ability to isolate monometalated intermediates, $[LM\{(CH_2)_nX\}]$ (where X is a halogen) [15,16] in these reactions allowed the

synthesis of heterobimetallic complexes with saturated hydrocarbon bridges $[LM(CH_2)_nM'L']$ [11-13], by the reactions of metal anions $[L'M']^-$ with the haloalkyl metal complexes $[LM\{(CH_2)_nX\}]$.

Oxidative additions of 1,n-dihaloalkanes to late transition metal complexes for the preparation of polymethylene bridged homobinuclear complexes have been reported for Rh [17], Co [18,19], Pd and Pt [20-23]. Recent studies by Canty and co-workers [23] have demonstrated that oxidative addition can also be used to prepare the mixed Pd(IV) and Pt(IV) complex, by treatment of $[PdMe_2(bipy)]$ with α,α-dibromo-*m*-xylene followed by addition of $[PtMe_2(bipy)]$, as shown below [23]:

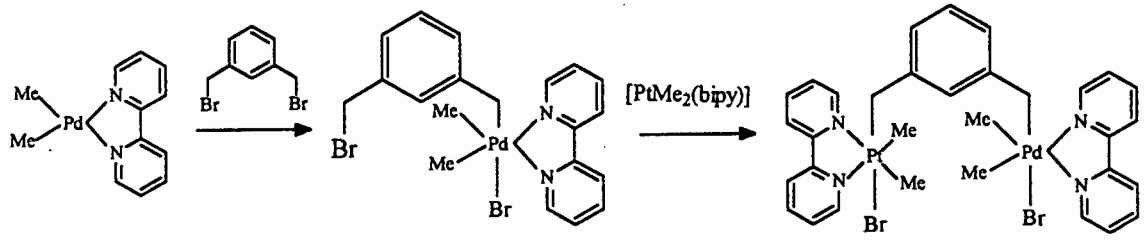

Scheme 6.1

Scott and Puddephatt [24] have developed methods for the synthesis of tetranuclear Pt(II) and Pt(IV) species (as shown below) based on the oxidative addition reactions [24].

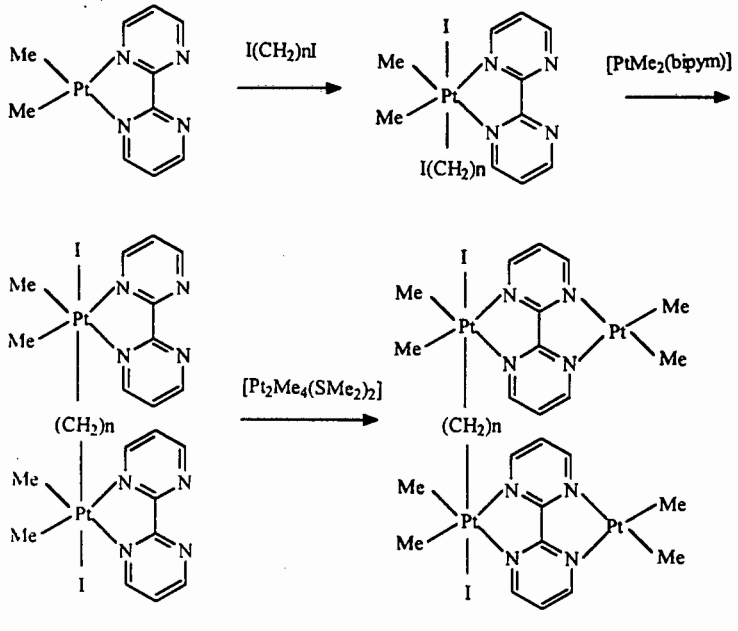

Scheme 6.2

An interesting example has shown that oxidative addition can also be used for the synthesis of methylene bridged heterobinuclear complexes $[PtClMe_2(CH_2MPPh_3)(bipy)]$ (M = Au, Hg) from the chloromethyl complexes $[M(CH_2Cl)(PPh_3)]$ and $[PtMe_2bipy]$, reported by Puddephatt and co-workers [3,25]. However, there is so far, to our knowledge, no literature of polymethylene bridged heterobimetallic complexes prepared by the oxidative addition reaction.

Recently, numerous studies have described complexes containing both early, oxophilic and late, electron rich transition metals [2,26]. The very different electronic character of the two metals raises the possibility that their complementary interaction with substrates might result in new chemistry that cannot be achieved by using a single metal system [2,27]. These early-late metal combinations have been used for CO_2 activation [28-30]. For example, CO_2 inserts into the Zr-C bond of $[Cp(PMe_3)_2RuCH{=}CHZrClCp_2]$, producing the carboxylate complex $[Cp(PMe_3)_2RuCH{=}CHCO_2ZrClCp_2]$ [28]; Bergman and co-workers have reported the insertion of CO_2 into the Zr-Ir bond of $[Cp_2Zr(\mu\text{-}N^tBu)IrCp^*]$ to yield $[Cp_2Zr(\mu\text{-}N^tBu)\{\mu\text{-}OC(O)\}IrCp^*]$ [29]. Another example is the insertion of CO_2 into the M-Zr bond of $[Cp(CO)_2M\text{-}Zr(Cl)Cp_2]$ (M = Fe, Ru) to give $[Cp(CO)_2M\{\mu\text{-}OC(O)\}Zr(Cl)Cp_2]$ [30].

We anticipated that early and late transition metal pairings which combine the Lewis acidity of the early metals and the known ability of late metal centres to activate hydrocarbons could have the potential for CO_2 activation and reduction. One of our aims is to incorporate CO_2 into hydrocarbons, for instance α-olefins which are produced by SASOL, to produce useful organic products. Thus we are interested in the preparation of polymethylene bridged early-late transition metal complexes containing W/Pt, Re/Pt or other metal combinations and their subsequent reactions with CO_2. These polymethylene bridged complexes could be models for dienes absorbed on an early-late heterobimetallic catalyst. They may also find applications in catalysis [1,10,31], either as models or as precursors for bimetallic catalysts [31b]. For example, oxide-supported Pt-Re bimetallic

catalysts have used extensively in the naphtha reforming for the production of gasoline with high octane number [31c].

We now report our results of developing a novel, general method for the preparation of polymethylene bridged heterobimetallic complexes of the type $[LM(CH_2)_nPtIMe_2(R_2\text{-bipy})]$. These complexes are prepared by oxidative addition of iodoalkyl complexes of W, Ru, Re and Fe $[LM\{(CH_2)_nI\}]$ [LM = $(\eta^5\text{-}C_5R'_5)W(CO)_3$, R′ = H and CH_3, n = 3-5; LM = $(\eta^5\text{-}C_5R'_5)Fe(CO)_2$, R′ = H and CH_3, n = 3 and 4; LM = $CpRu(CO)_2$, n = 4; and LM = $Re(CO)_5$, n = 4] [32] to $[PtMe_2(R_2\text{-bipy})]$ (R = H and CH_3) [33,34]. The oxidative addition reaction occurs in a *trans* sense and has been proved to be effective and versatile for the synthesis of a wide range of polymethylene bridged heterobimetallic complexes. We have also attempted some reactions of these heterobimetallic complexes with CO_2 under various conditions and the results are discussed below.

6.1.2 Synthesis of $[LM(CH_2)_nPtIMe_2(R_2\text{-bipy})]$

The complexes $[PtMe_2(R_2\text{-bipy})]$ (R = H, CH_3) are electron rich and among the most active of noble-metal complexes in oxidative addition reactions [34]. We envisaged that oxidative addition reactions of iodoalkyl complexes to $[PtMe_2(R_2\text{-bipy})]$ (R = H, CH_3) might produce heterobimetallic complexes. An initial experiment showed that the iodoalkyl complex $[CpW(CO)_3\{(CH_2)_4I\}]$ reacted with $[PtMe_2(bipy)]$ in dry benzene at room temperature for 17 hours to give the desired heterobimetallic W/Pt complex (Scheme 6.3). This reaction was characterized by a colour change from a red solution to a pale yellow solution

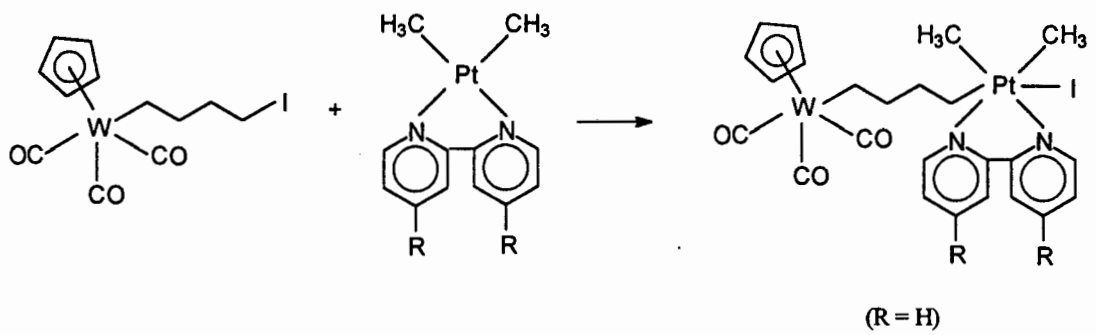

Scheme 6.3

after the reaction was complete, and a yellow product precipitated. The product was purified by recrystallization from CH_2Cl_2/ether and obtained in high yield (92%).

This was subsequently shown to be a general route to a series of new heterobimetallic W/Pt alkanediyl complexes as shown in Scheme 6.4, by *trans* oxidative addition of the iodoalkyl complexes to the Pt(II) centre. It was found that when the reactions were carried out in dry benzene, for longer chain haloalkyl complexes, the reaction required a longer time to run to completion. Therefore, acetone being a more polar solvent was chosen for subsequent reactions. The reaction was complete within 30 hours in acetone at room temperature.

$$[(\eta^5\text{-}C_5R'_5)W(CO)_3\{(CH_2)_nI\}] + [PtMe_2(R_2\text{-bipy})] \longrightarrow$$

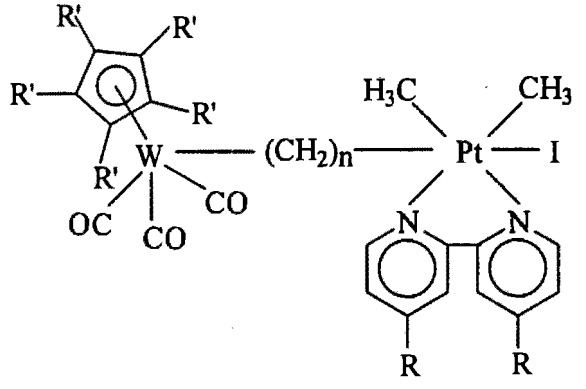

R′	R	n	Compound no	Reaction conditions	
				solvent	time (hour)
H	H	3	**1**	benzene	22
H	H	4	**2**	benzene	16
H	H	5	**3**	benzene	240
H	CH_3	3	**4**	benzene	26
H	CH_3	4	**5**	benzene	144
H	CH_3	5	**6**	acetone	26
CH_3	H	3	**7**	acetone	30
CH_3	H	4	**8**	acetone	30
CH_3	CH_3	3	**9**	acetone	27
CH_3	CH_3	4	**10**	acetone	27

Scheme 6.4

This was found to be a general route for the preparation of other polymethylene bridged heterobimetallic complexes, containing the metals Fe/Pt, Re/Pt and

Ru/Pt, from the corresponding iodoalkyl complexes and $[PtMe_2(R_2\text{-bipy})]$ (R = H, CH_3), as shown in Scheme 6.5.

$[LM\{(CH_2)_nI\}] + [PtMe_2(R_2\text{-bipy})] \longrightarrow$

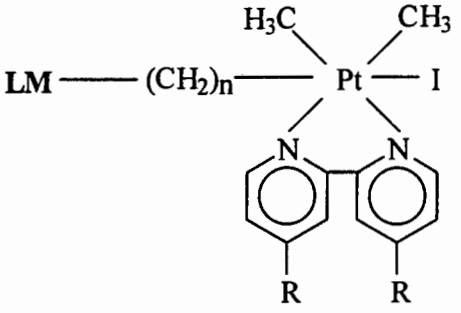

LM	R	n	Compound no	Reaction conditions	
				solvent	time (hour)
Fp	H	4	**11**	benzene	24
Fp	CH_3	4	**12**	acetone	26
Rp	H	4	**13**	acetone	17
Rp	CH_3	4	**14**	acetone	22
Fp*	H	3	**15**	acetone	24
Fp*	CH_3	3	**16**	acetone	24
Fp*	H	4	**17**	acetone	24
Fp*	CH_3	4	**18**	acetone	24
$Re(CO)_5$	CH_3	4	**19**	acetone	29

Scheme 6.5

6.1.3 Characterization of $[LM(CH_2)_nPtIMe_2(R_2\text{-bipy})]$

All these new complexes **1 - 19** were obtained in high yields as yellow solids which are moderately stable in air. Yields, melting points, elemental analyses, IR and other characterization data for these complexes are given in Tables 6.1 and 6.2. These complexes have also been characterized by ^1H and ^{13}C NMR spectroscopy. Fast atom bombardment (FAB) or electrospray (ES) mass spectroscopy and conductivity studies of selected complexes confirm the postulated structures of the complexes. Cyclic voltammetry studies were also carried out for selected complexes. These results will be discussed below.

Table 6.1 Data for the heterobinuclear complexes $[LM(CH_2)_nPtIMe_2(R_2\text{-bipy})]$ {LM = Wp, $[CpW(CO)_3]$; Wp*, $[Cp^*W(CO)_3]$; R = H and CH_3}.

Compd. no	LM	R_2-bipy	n	Yield (%)	M.p.[a] (°C)	IR[b] ν(CO) (cm^{-1})	Elemental analysis (%)					
							C		H		N	
							calc.	found	calc.	found	calc.	found
1	Wp	bipy	3	79	192 - 194	2008s, 1910s	31.29	31.18	2.85	2.82	3.17	3.11
2[c]	Wp	bipy	4	92	185 - 190	2009s, 1909s	30.58	30.52	2.98	2.98	2.83	2.83
3	Wp	bipy	5	74	168 - 172	2009s, 1910s	32.95	33.06	3.21	3.29	3.07	3.09
4[d]	Wp	Me_2-bipy	3	69	200 - 203	2008s, 1910s	32.59	33.24	3.17	3.27	3.04	3.10
5[c,d]	Wp	Me_2-bipy	4	52	131 - 135[e]	2009s, 1909s	32.10	32.55	3.29	3.37	2.77	2.78
6	Wp	Me_2-bipy	5	78	155 - 158[e]	2008s, 1909s	34.52	34.86	3.54	3.58	2.98	2.70
7	Wp*	bipy	3	72	247 -249	1996s, 1901s	35.27	35.13	3.70	3.63	2.94	2.88
8[d,f]	Wp*	bipy	4	85	223 - 225	1995s, 1896s	36.00	36.21	3.86	3.81	2.89	2.87
9[d]	Wp*	Me_2-bipy	3	82	236 - 239	1995s, 1897s	36.71	36.58	4.01	3.97	2.85	2.80
10[d]	Wp*	Me_2-bipy	4	83	138 -140	1995s, 1896s	37.40	37.55	4.12	3.79	2.81	3.06

[a]: melt with decomposition; [b]: in CH_2Cl_2 ; [c]: crystallized with 1 molecule CH_2Cl_2; [d]: UV-vis measured for these complexes in acetone, λ_{max}/nm = 350 - 360; [e]: melts without decomposition; [f]: conductivity in nitrobenzene (1×10^{-3} mol/L) $\Lambda = 0.77\ \Omega^{-1}\ cm^2\ mol^{-1}$.

Table 6.2. Data for the heterobinuclear complexes $[LM(CH_2)_nPtIMe_2(R_2\text{-bipy})]$ {LM = Fp, $[CpFe(CO)_2]$; Fp*, $[Cp^*Fe(CO)_2]$; Rp, $[CpRu(CO)_2]$; and $Re(CO)_5$; R = H, CH_3}.

Compd. no	LM	R_2-bipy	n	Yield (%)	M.p.[a] (°C)	IR[b] ν(CO) (cm^{-1})	Elemental analysis (%)					
							C		H		N	
							calc.	found	calc.	found	calc.	found
11	Fp	bipy	4	64	156 - 161	2001s, 1938s	37.27	35.45	3.67	3.61	3.78	3.83
12[c]	Fp	Me_2-bipy	4	67	178 - 180	1999s, 1938s	39.02	38.53	4.06	4.04	3.64	3.67
13	Rp	bipy	4	53	191 - 194	2010s, 1944s	35.12	35.03	3.46	3.47	3.56	3.55
14[c]	Rp	Me_2-bipy	4	63	181 - 185	2010s, 1945s	36.86	36.29	3.84	3.90	.3.43	3.67
15	Fp*	bipy	3	88	250 - 270[d]	1981s, 1915s	40.67	40.52	4.42	4.35	3.51	3.46
16[c]	Fp*	bipy	4	98	229 - 231	1978s, 1914s	41.45	41.27	4.59	4.58	3.45	3.35
17[c,e]	Fp*	Me_2-bipy	3	98	219 - 221	1977s, 1915s	40.79	41.35	4.64	4.70	3.22	2.71
18[c]	Fp*	Me_2-bipy	4	92	203 - 205	1978s, 1914s	42.92	42.71	4.92	4.83	3.34	3.10
19[c]	Re	Me_2-bipy	4	78	108 - 112	2124w, 2007s, 1976m, sh	30.07	30.06	2.85	2.77	3.05	2.92

[a]: melt with decomposition; [b]: in CH_2Cl_2; [c]: UV-vis measured for these complexes in acetone, λ_{max}/nm = 350 - 360; [d]: decomposed without melting; [e]: crystallized with 0.5 molecule CH_2Cl_2.

Elemental analysis

As shown in Tables 6.1 and 6.2, satisfactory elemental analysis (C, H and N) results were obtained for all these complexes except **11**, which might result from the instability of the complex. It has been shown that the complexes with [$Cp(CO)_2Fe$-CH_2] units are much less stable than the analogous ruthenium complexes [35].

Physical properties

It is found that these new heterobimetallic complexes (except **5** and **6**) generally melt with decomposition to give off gas when viewed under the hot-stage microscope. The melting points of these complexes are dependent on the metal, ligand and chain length. The melting point, for the complexes containing the same ligands (except Re/Pt **19**) and the same chain length, decreases according to the following order:

W/Pt > Ru/Pt > Fe/Pt (> Re/Pt).

The complexes with the Cp^* ligand generally have higher melting points than the analogous complexes with the Cp ligand. For the complexes with the same metal and ligand system, the melting point decreases as the chain length increases (except **5**). For both W/Pt and Fe/Pt complexes, the Cp^* complexes show greater thermal stability than their Cp analogues. This is believed to be due to a combination of steric and electronic factors, because the substitution of the hydrogens of the Cp ring with methyl groups can be expected to lead to a stronger bond between the η-C_5R_5 ring and the metal, as well as an increase in the steric bulk of the complex [12].

It is also found that the complexes with higher melting points (*eg.* **7** and **8**) usually have lower solubility. Thus, the short chain complexes (with n = 3 and bipy ligand) are less soluble (even in $CHCl_3$), and these complexes were not characterized by NMR spectroscopy. The low solubility of these complexes might be due to their rigid structure. In contrast to this, the complexes with n greater than 4 and with Me_2-bipy ligands are more soluble in polar solvents such as acetone, CH_2Cl_2 and $CHCl_3$ but

insoluble in hexane and ether. Thus recrystallization from CH_2Cl_2/ether is a general way to purify most of these complexes.

UV-visible spectroscopy

UV-vis spectroscopy was used to characterize both the starting mononuclear complexes and the heterobinuclear complexes. The measurements were carried out in acetone solution at room temperature in the range 340 - 800 nm. Figure 6.1 shows typical spectra obtained for the starting complexes and the heterobinuclear complexes. It is found that each of the heterobimetallic complexes investigated shows an absorption band in the range λ_{max} = 350 - 360 nm, which might be due to the Pt(IV)-diimine metal to ligand charge transfer (MLCT) [36]. The starting square planar Pt(II) complexes shows an absorption band at λ_{max} = 464 nm due to the Pt(II) 5d-diimine (π^*) MLCT [33,34]. The UV-vis absorption band shifts from the visible region to the UV region is characteristic of the change from Pt(II) to Pt(IV) [20-22]. It is also found that for the complexes with different metals and ligands, the UV-vis absorption band appears at a similar position, suggesting that the metal and ligands in the one polymethylene chain end have little effect on the UV-vis absorption at the other end, *i.e.* at the Pt(IV) centre.

IR spectroscopy

The IR spectra of all the complexes were recorded in CH_2Cl_2 in the range 1600 cm^{-1} to 2200 cm^{-1}, and the data are listed in Tables 6.1 and 6.2. All the spectra of these complexes show the expected ν(CO) peaks in the expected positions, comparing with the data for the corresponding starting iodoalkyl complexes measured under identical conditions [16,32]. Little shift of the ν(CO) peaks suggests that the structure around the metal centre (M ≠ Pt) in these heterobinuclear complexes is similar to that in the starting iodoalkyl complexes [LM{$(CH_2)_nI$}]. It is also notable that the ν(CO) for the Cp^* complexes is lower than that for the analogous Cp complexes (13 cm^{-1} for the tungsten complexes and *ca.* 20 cm^{-1} for the iron complexes). This is due to the

increase in electron density on the metal (caused by the Cp^* group), which results in increased back-bonding to the carbonyl groups, and hence, a lower ν(CO) [12].

^{1}H NMR spectroscopy

^{1}H NMR spectra were recorded for all the complexes except **7** and **15** in $CDCl_3$ at room temperature. The complexes **7** and **15** were not soluble enough to run the spectra. Assignments of the ^{1}H NMR data were made by comparison of all the NMR data for the heterobinuclear complexes and by comparison of these data with those of the mononuclear complexes, and by using HETCOR experiments. The ^{195}Pt-^{1}H coupling constants were also used for assigning peaks. As examples of the results obtained, the ^{1}H and ^{13}C NMR, as well as HECTOR spectra of complex **3** are shown in Figures 6.2 - 6.4.

The ^{1}H NMR data with assignments are summarized in Table 6.3 for the W/Pt complexes **1** - **10** and Table 6.4 for the heterobinuclear complexes **11** - **19**. From the ^{1}H NMR data, it can be seen that only one strong resonance is observed at δ 1.4 - 1.5 ppm with platinum satellites ^{2}J(PtH) 71 Hz for the PtMe protons (except **9**), and also that only one set of four chemical shifts due to the bipy or Me_2-bipy ligands are observed. This is characteristic of the methyl groups *trans* to bipy or Me_2-bipy [20-22]. This suggests that the heterobinuclear complexes are the products of *trans* oxidative addition of iodoalkyl complexes to the square planar Pt(II) complexes. The ^{2}J(PtH) observed is about the same range as reported by Puddephatt and co-workers for other polymethylene bridged platinum complexes [20-22]. The protons for the PtMe groups of **9** is more shielded than those for other complexes, and the proton resonance of the PtMe groups for **9** are observed at δ 1.32 ppm with ^{2}J(PtH) 70Hz. This could be due to the influence of the bulky [$Cp^*W(CO)_3$] group and the short chain n = 3.

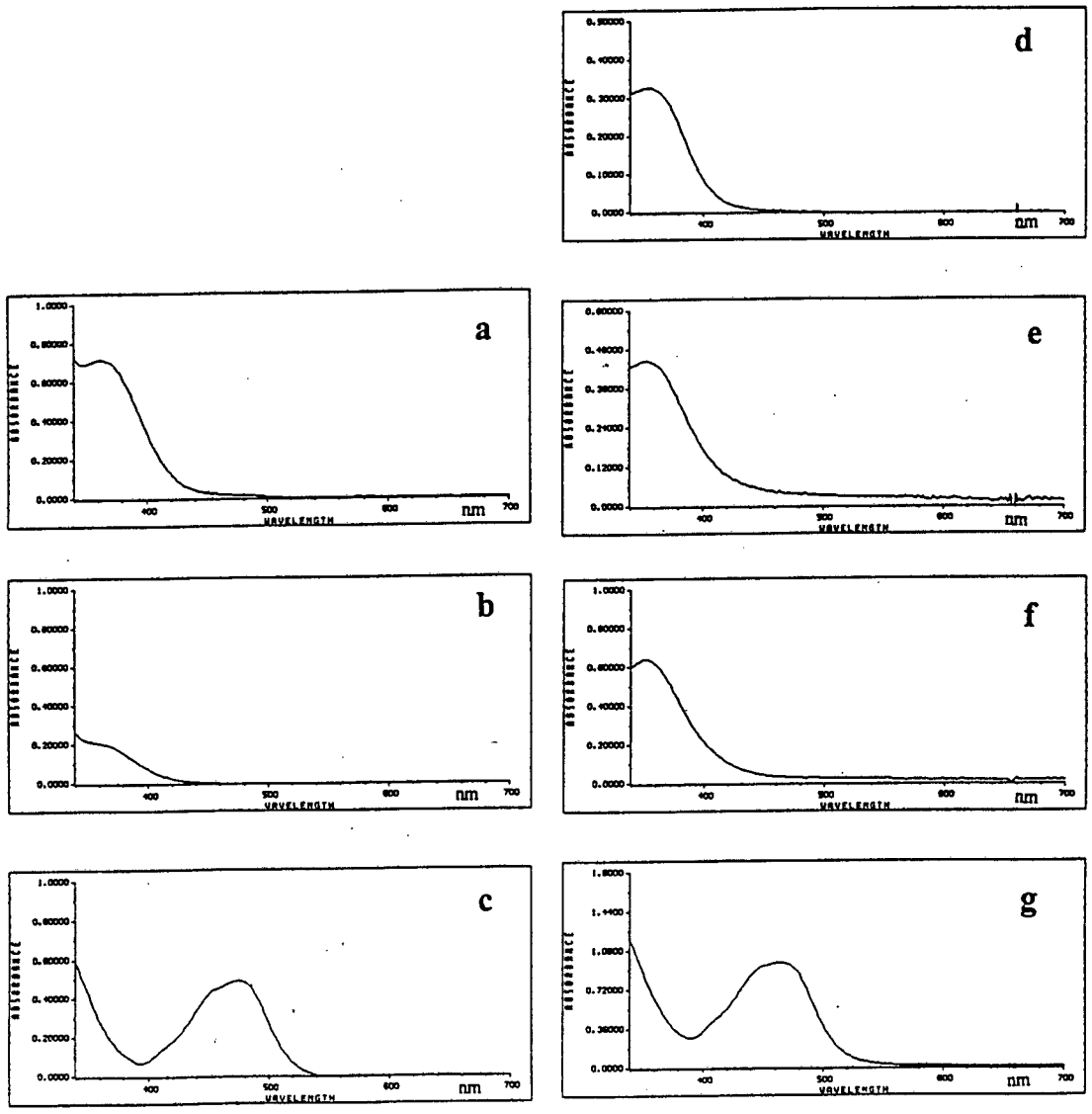

Figure 6.1 UV-vis spectra of the following complexes in acetone:

a: $[Wp(CH_2)_4PtIMe_2(bipy)]$, **2**; b: $[Wp\{(CH_2)_4I\}]$; c: $[PtMe_2(bipy)]$;

d: $[Re(CO)_5(CH_2)_4PtIMe_2(Me_2\text{-}bipy)]$, **19**; e: $[Fp^*(CH_2)_4PtIMe_2(Me_2\text{-}bipy)]$, **18**;

f: $[Fp(CH_2)_4PtIMe_2(Me_2\text{-}bipy)]$, **12**; g: $[PtMe_2(Me_2\text{-}bipy)]$.

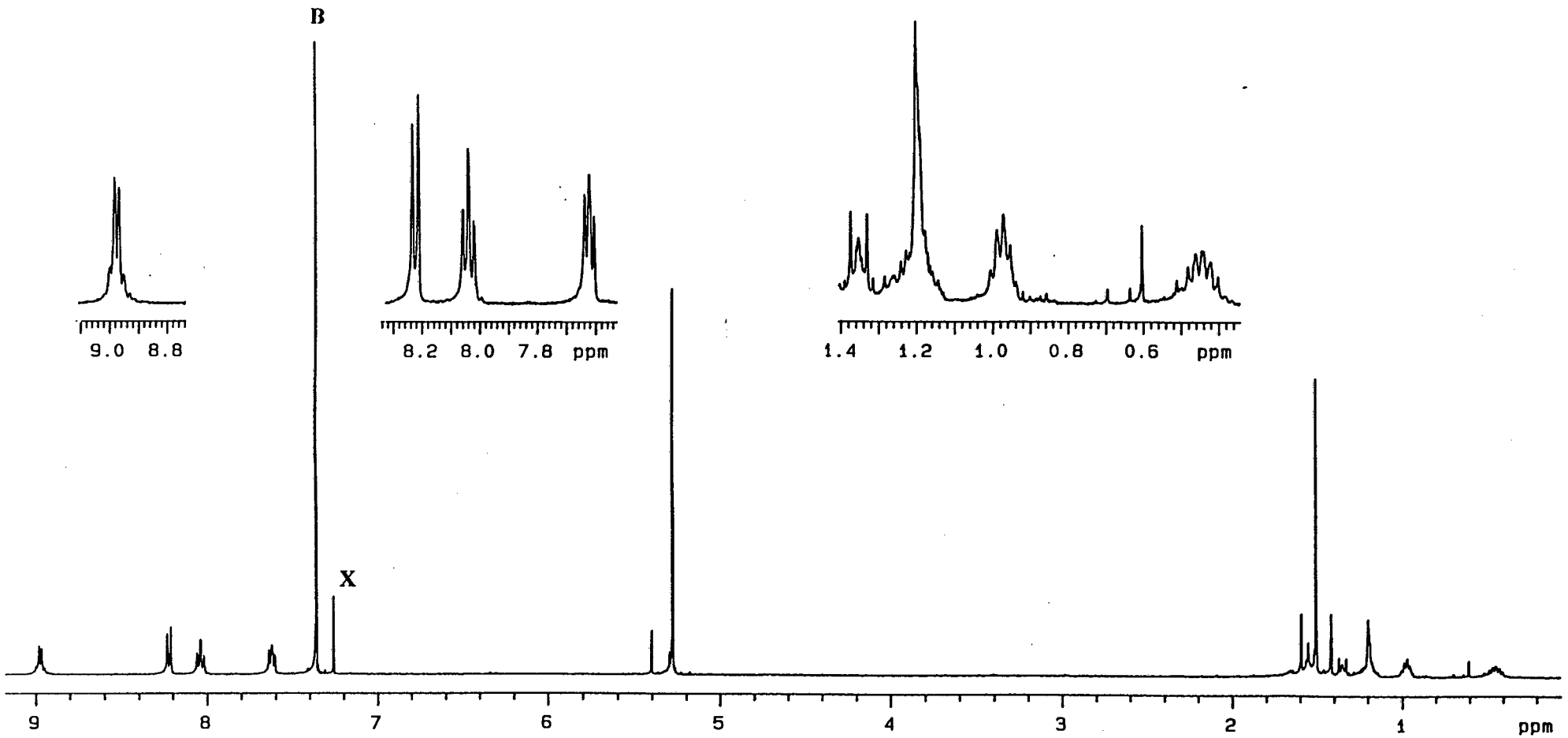

Figure 6.2 ^{1}H **NMR spectrum of** $[Wp(CH_2)_5PtIMe_2(bipy)]\bullet C_6H_6$ **(400 MHz, X =** $CDCl_3$**, B =** C_6H_6**).**
(C_6H_6 **is the solvent of recrystallization)**

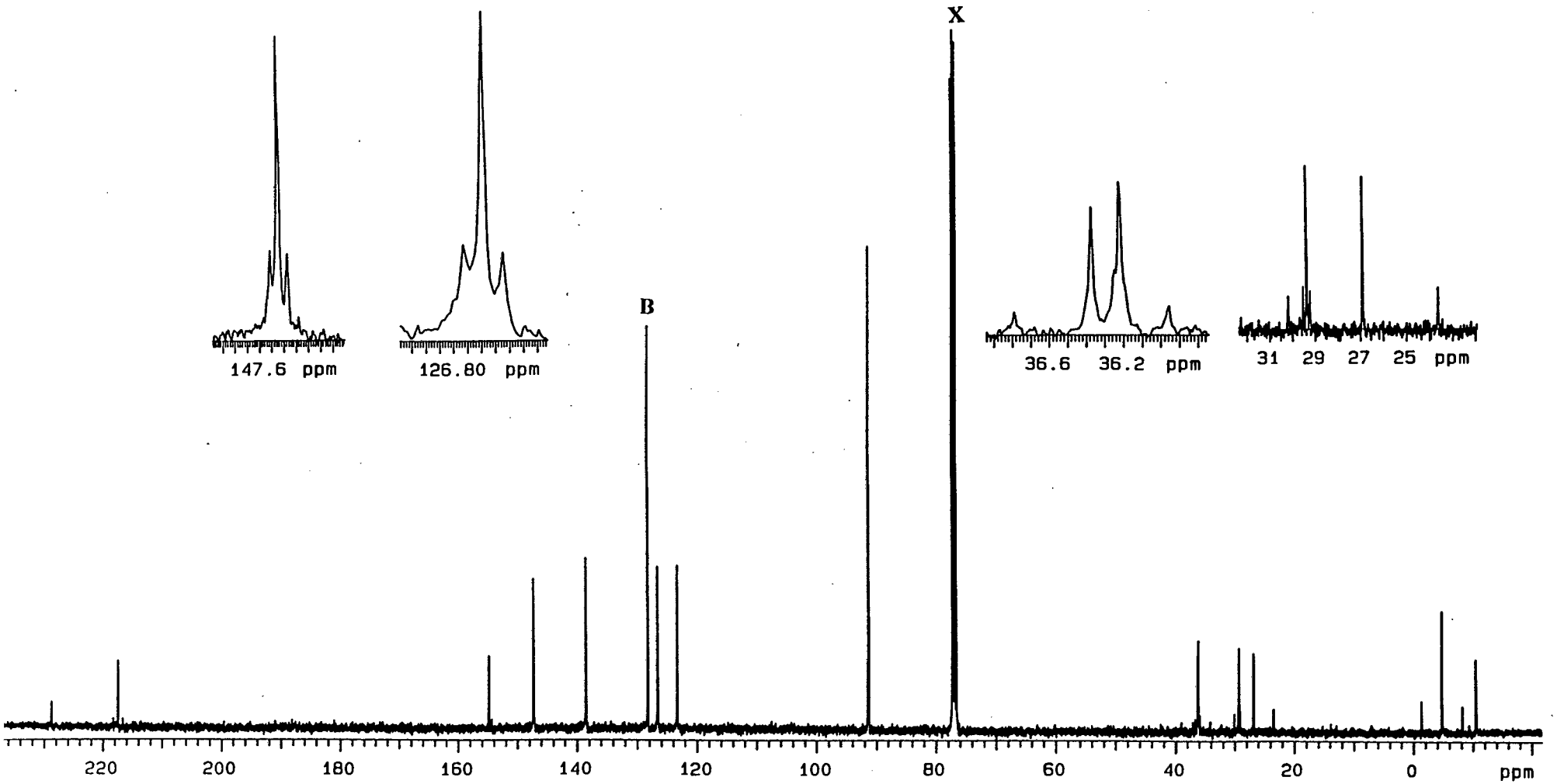

Figure 6.3 ^{13}C **NMR spectrum of** $[Wp(CH_2)_5PtIMe_2(bipy)]\bullet C_6H_6$ **(100 MHz, X =** $CDCl_3$**, B =** C_6H_6**).**

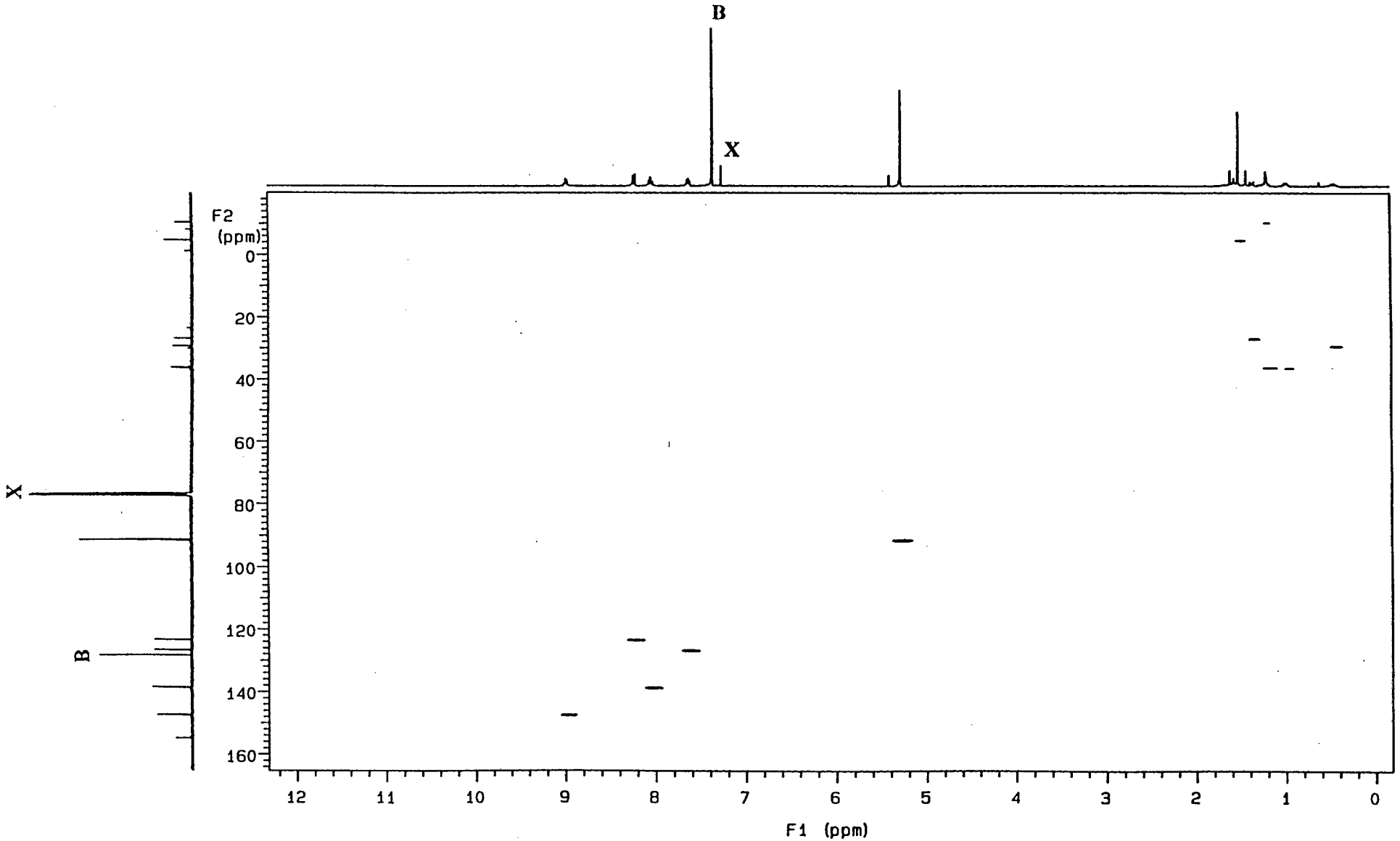

Figure 6.4 HECTOR NMR spectrum of $[Wp(CH_2)_5PtIMe_2(bipy)]\bullet C_6H_6$ (X = $CDCl_3$, B = C_6H_6).

Table 6.3 ^{1}H NMR data for the heterobinuclear complexes [LM$(CH_2)_n$PtIMe$_2$(R_2-bipy)] {LM = Wp, [CpW$(CO)_3$]; Wp*, [Cp*W$(CO)_3$]; R = H and CH_3}, (400 MHz, $CDCl_3$).

Compd no	LM	R_2-bipy	n	C_5R_5 R = H, or CH_3	bipy-CH_3	PtMe$_2$ ^{2}J(PtH)	Pt-αCH_2	βCH_2	γCH_2	δCH_2	εCH_2	$H^{3,3'}$ a	$H^{4,4'}$ b	$H^{5,5'}$ c	$H^{6,6'}$ d
1	Wp	bipy	3	5.15, 5H s	-	1.50, 6H, s 71 Hz	1.34, 2H m	0.65, 2H m	1.17, 2H m	-	-	8.20	8.09	7.65	9.00
2[e]	Wp	bipy	4	5.27, 5H s	-	1.50, 6H, s 71 Hz	1.39, 2H m	0.45, 2H m	1.22, 4H m		-	8.20	8.09	7.65	9.00
3[f]	Wp	bipy	5	5.28, 5H s	-	1.51, 6H, s 71 Hz	1.36, 2H m	0.44, 2H m	0.97, 2H qn, 7 Hz	1.20, 4H m		8.23	8.04	7.63	8.98
4	Wp	Me_2-bipy	3	5.15, 5H s	2.55, 6H s	1.45, 6H, s 71 Hz	1.31, 2H m	0.64, 2H m	1.17, 2H m	-	-	7.97 g	-	7.40	8.78
5[e]	Wp	Me_2-bipy	4	5.27, 5H s	2.57, 6H s	1.45, 6H, s 71 Hz	1.36, 2H m	0.46, 2H m	1.22, 4H m		-	7.99 g	-	7.41	8.78
6	Wp	Me_2-bipy	5	5.28, 5H s	2.55, 6H s	1.45, 6H, s 71 Hz	1.34, 2H m	0.44, 2H m	0.99, 2H qn, 7 Hz	1.18, 4H m		8.00 g	-	7.41	8.78
8	Wp*	bipy	4	1.87, 15H, s	-	1.49, 6H	1.40, 2H m	0.50, 2H m	1.26, 2H m	0.51, 2H, m	-	8.20	8.04	7.61	8.98
9	Wp*	Me_2-bipy	3	1.76, 15H, s	2.46, 6H s	1.32, 6H, s 70 Hz	1.20, 2H m	0.50, 4H m		-	-	7.92 g	-	7.32	8.68
10	Wp*	Me_2-bipy	4	1.89, 15H, s	2.51, 6H s	1.45, 6H, s 71Hz	1.40, 2H m	0.50, 2H m	1.23, 2H m	0.54, 2H, m	-	8.00 g	-	7.39	8.80

[a]: 2H, d, J(HH) 8 Hz; [b]: 2H, m; [c]: 2H, m; [d]: 2H, m; [e]: peak observed at 5.28 ppm due to the solvent CH_2Cl_2 (1 mol.) of crystallization; [f]: peak observed at 7.36 ppm due to the solvent benzene (1 mol.) of crystallization; [g]: 2H, s.

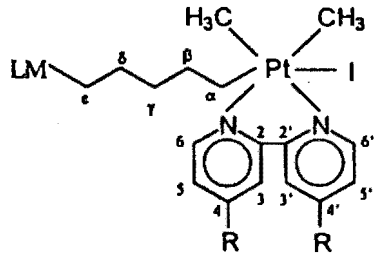

Table 6.5 ^{13}C NMR chemical shift data (δ ppm) for the heterobinuclear complexes $[LM(CH_2)_nPtIMe_2(R_2\text{-bipy})]$ {LM = Wp, $[CpW(CO)_3]$; Wp*, $[Cp^*W(CO)_3]$; R = H and CH_3}, (100 MHz, $CDCl_3$).

Compd No	CO	CO	C_5R_5	$C_5(CH_3)_5$	bipy-CH_3	$PtMe_2$ $^1J(PtC)$ Hz	Pt-αCH₂ $^1J(PtC)$ Hz	βCH₂ $^2J(PtC)$ Hz	γ CH₂ $^3J(PtC)$ Hz	δ CH₂	ε CH₂	$C^{2,2'}$	$C^{3,3'}$ J(PtC) Hz	$C^{4,4'}$	$C^{5,5'}$ J(PtC) Hz	$C^{6,6'}$ J(PtC) Hz
2[a]	228.77	217.46	91.41	-	-	-4.65 693	26.51 662	37.95 87	36.47 29	-10.42	-	154.91	123.36 8	138.59	126.73 14	147.47 14
3[b]	228.85	217.60	91.41	-	-	-4.71 694	26.93 661	36.37 84	29.40 30	36.22	-10.43	154.90	123.39 8	138.63	126.69 14	147.44 14
4	c	217.25	91.24	-	21.55	-5.40	31.32	37.12	-11.38	-	-	154.78	123.90	150.47	127.35	146.78
5[a]	c	217.47	91.42	-	21.62	-4.99	26.24	38.06	36.46	-10.25	-	154.76	121.96	150.41	127.52	146.77
6	228.90	217.57	91.43	-	21.59	-5.06 694	26.67 666	36.33 84	29.35 29	36.22	-10.33	154.75	124.00	150.49	127.48 14	146.71 14
8	232.76	222.96	102.66	10.29	-	-4.64 698	27.20	36.74	36.92	0.43	-	154.94	123.34	138.49	126.64	147.46
10	232.79	222.96	102.66	10.30	21.58	-4.95 696	26.90 663	36.75 82	36.92 29	0.47	-	154.80	124.04	150.35	127.42	146.73

[a]: peak found at 53.41 ppm due to the solvent CH_2Cl_2 of crystallization.

[b]: peak found at 128.33 ppm due to the solvent C_6H_6 of crystallization.

[c]: not observed

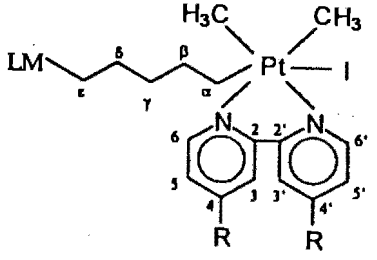

The methylene α-CH_2 (α to Pt) protons for all complexes except **9** have a chemical shift of δ 1.3 - 1.4 ppm, which is little affected by the metal at the other chain end. The β-CH_2 protons have a chemical shift of 0.50 ppm. These are characteristic of the polymethylene chain attached to the Pt centre [20-22], as has been found for the mononuclear complexes [$PtIMe_2(R')(Me_2$-bipy)] discussed in Chapter 4 of this thesis. The ^{195}Pt-^{1}H coupling constant is difficult to resolve in most cases because it is of low intensity and often complicated by other proton resonances in this region.

The methylene protons on the carbon α to the metal M (M other than Pt) have chemical shifts characteristic of the metal and its associated ligands [12,32]. The Cp peaks or the methyl proton peaks of the Cp* ligand do not show significant shifts with changing either the chain length, or the ligand on the Pt centre. Similarly, the chemical shifts of the bipy and Me_2-bipy protons do not show any shift with changing the chain length, the metal and the ligands (LM).

^{13}C NMR spectroscopy

^{13}C NMR data are summarized in Tables 6.5 - 6.6 for all complexes except **1, 7, 14** and **15**, with possible assignments. Assignments were made by comparison of all the NMR data for the heterodinuclear complexes and by comparison of these data with those of the mononuclear complexes, and by using HETCOR experiments. The ^{195}Pt-^{13}C coupling constants were also used for assigning peaks. The ^{13}C NMR spectroscopy provided the most important information regarding the structures of these complexes. The carbon resonance of the PtMe groups is found at δ -4.6 to -5.4 ppm as a single peak with platinum satellites ^{1}J(PtC) 693 ~ 698 Hz, for the complexes **2, 3, 6, 8, 9, 13** and **16**. This indicates that the methyl (PtMe) groups of these heterobinuclear complexes are *trans* to the bipy [20-22] or Me_2-bipy ligands as they are in the [$PtMe_2$(bipy)] or [$PtMe_2(Me_2$-bipy)] complexes. This observation is similar to those reported for the polymethylene bridged Pt(IV) complexes [20,22]. The Pt(II) complex [$PtMe_2(Me_2$-bipy)] shows a chemical shift for the PtMe groups at -17.5 ppm as a single peak [33]. The *ca.* 12

ppm shift of the carbon resonance of the PtMe groups from Pt(II) to Pt(IV) complexes is probably due to the deshielding effect of the reduced electron density on the methyl carbon. The ligand bipy or Me_2-bipy has little influence on the chemical shift and J(PtC) of the PtMe groups. The chemical shifts of the carbons of the bipy or Me_2-bipy ligands are found virtually in the same positions regardless of the metal and ligands at the other end of the polymethylene chain, and are also not affected by the chain length from n = 3 or 6. The carbon resonances of CO and $C_5R'_5$ (R' = H and CH_3) groups are observed at expected positions and are characteristic of that metal and ligand system. They are found at similar positions to those found in the corresponding haloalkyl complexes [16,32] and some other heterobinuclear complexes [12].

The carbon resonances of the $PtCH_2$ group of the polymethylene chain are observed at 26 - 27 ppm with ^{1}J(PtC) *ca.* 665 Hz for complexes with n = 4 and 5. Those for n = 3 are observed at 31 - 32 ppm with ^{1}J(PtC) *ca.* 637 Hz. The differences in the chemical shift and coupling constant for complexes with n = 3, and n = 4 and 5 may be due to the fact that in complexes with n = 3, the two metals are situated in closer proximity than those in the complexes with n = 4 and 5 and thus the interaction between the two metals are expected to be stronger when the polymethylene chains are shorter. It is also noted that the MCH_2 carbon resonances of the polymethylene chain are observed at different positions for complexes with n = 4 and 5, to those observed for complexes with n = 3 (for W/Pt complexes $\Delta\delta$ = 1 ppm and for Fe/Pt complexes $\Delta\delta$ = 0.6 ppm). The chemical shift of the MCH_2 group is found at the characteristic position for that particular metal and ligand system, and is similar to that reported for the corresponding haloalkyl complexes [16,32] and other heterobinuclear complexes [12].

For all the complexes studied, the chemical shift of the β-CH_2 group (β to Pt) is observed at higher frequency with much smaller ^{2}J(PtC) (81 - 87 Hz) than that of the α-CH_2. The ^{3}J(PtC) (ca. 30 Hz) of the γ-CH_2 is observed but ^{4}J(PtC) was not detected at all. These coupling constants are similar to those reported for the polymethylene bridged Pt(IV) complexes [20,22]. The observation of ^{3}J(PtC) is a

good indication that the metal (Pt) influences the γ carbon of the chain, although previous observations suggested that the metal could have influence on the α and β carbons [12]. The detection of the $^{1}J(PtC)$, $^{2}J(PtC)$ and $^{3}J(PtC)$ confirms that the two metal centres are bridged by the polymethylene chain in these complexes. The values of the coupling constants decrease from α to γ carbon along the polymethylene chain because the effect of the platinum diminishes along the chain.

Fast Atom Bombardment (FAB) and Electrospray (ES) Mass Spectroscopy

FAB-MS and ES-MS have proved to be versatile and sensitive methods for the analysis of organometallic compounds [37-39]. Selected heterobimetallic complexes were studied by FAB-MS, using *m*-nitrobenzyl alcohol (NBA) as matrix. The positive ion FAB mass spectral data for the complexes **3** and **5** are given in Table 6.7, and those for **12** and **14** in Table 6.8.

It is found that the molecular ions M^+ for these complexes can not be observed. However, in most cases, $[M-I]^+$ ions are observed as major peaks with expected isotope patterns in the FAB mass spectra of all compounds studied. The $[M-I]^+$ ions could be formed by the cleavage of the weak Pt-I bond, either in solutions before bombardment or in the mass spectrometer. For the $[M-I]^+$ ions, there is good agreement between the calculated and observed isotope distributions.

As shown in Tables 6.7 and 6.8, ions corresponding to $[2M-I]^+$ are observed in low intensity in all the spectra. The formation of the $[2M-I]^+$ ion could be due to the formation of an iodo bridged dimeric complex as shown in Scheme 6.6.

Table 6.7 Mass spectral data for the heterobinuclear W/Pt complexes†.

Ion[a]	Relative intensities[b] (%)	
	$[Wp(CH_2)_5PtIMe_2(bipy)]$ **3**	$[Wp(CH_2)_4PtIMe_2(Me_2\text{-bipy})]$ **5**
M - I	35	85
M - I - CO	7	4
M - I - 2CO	5	12
M - I - 3CO	0	0
M - I - $CpW(CO)_3$	100	100
M - I - CO - R_2-bipy	6	0
M - I - 2CO - R_2-bipy	11	0
M - I - 3CO - R_2-bipy	11	0
M - I - CO - Cp - R_2-bipy	7	7
M - I - CO - Cp - R_2-bipy - Me	7	38
M - I - 2CO - Cp - R_2-bipy - Me	14	6
M - I - 2CO - Cp - R_2-bipy - 2Me	16	6
M - I - $CpW(CO)_3$ - Me	9	48
M - I - $CpW(CO)_3$ - 2Me	16	27
M - I - $CpW(CO)_3$ - $(CH_2)_n$	6	11
M - I - $CpW(CO)_3$ - Me - $(CH_2)_n$	40	73
M - I - $CpW(CO)_3$ -2Me-$(CH_2)_n$	31	67
2M - I	2	6
2M - I - $CpW(CO)_3$	2	9

† For complexes $[Wp(CH_2)_3PtIMe_2(bipy)]$, **1** and $[Wp(CH_2)_4PtIMe_2(bipy)]$, **2**, $[M - I]^+$ ions were observed. Complex $[Wp^*(CH_2)_4PtIMe_2(Me_2\text{-bipy})]$, **10** was characterized by ES-MS, and the $[M - I]^+$ ion was observed.

[a]: M = parent ion; all ions have a single positive charge; ion refers to probable assignment.

[b]: Peak intensities are relative to the base peak due to $[M\text{-}I\text{-}CpW(CO)_3]$; the intensity is based on the most abundant peak.

Table 6.8 Mass spectral data for the heterobinuclear complexes $[Mp(CH_2)_4PtIMe_2(Me_2\text{-bipy})]$ (Mp = Fp, Rp).

Ion[a]	**Relative intensities**[b] **(%)**	
	$[Rp(CH_2)_4PtIMe_2(Me_2\text{-bipy})]$ **14**	$[Fp(CH_2)_4PtIMe_2(Me_2\text{-bipy})]$[b] **12**
M - I	100	80
M - I -CO	9	5
M - I - 2CO	0	0
M - I - 2CO - Cp	0	5
M - I - 2CO - Cp - Me	5	28
M - I - 2CO - Cp - 2Me	6	0
M - Mp	83	66
M - Mp - I	15	28
M - Mp - I - Me	21	36
M - Mp - I - 2Me	23	11
M - Mp - I - $(CH_2)_4$ -2Me	79	36
M - Mp - I - $(CH_2)_4$	10	8
MpI	30	100
Mp	14	3
2M - I	3	5
2M - Mp	3	5
2M - I - Mp - $Mp(CH_2)_4$	0	6
2M - I + Mp	11	0

[a]: M = parent ion; all ions have a single positive charge; ion refers to probable assignment. [b]: Peak intensities are relative to the base peak due to $[M\text{-}I]^+$ for complex **14**, and relative to $[CpFe(CO)_2I]^+$ for **15**; the intensity is based on the most abundant peak.

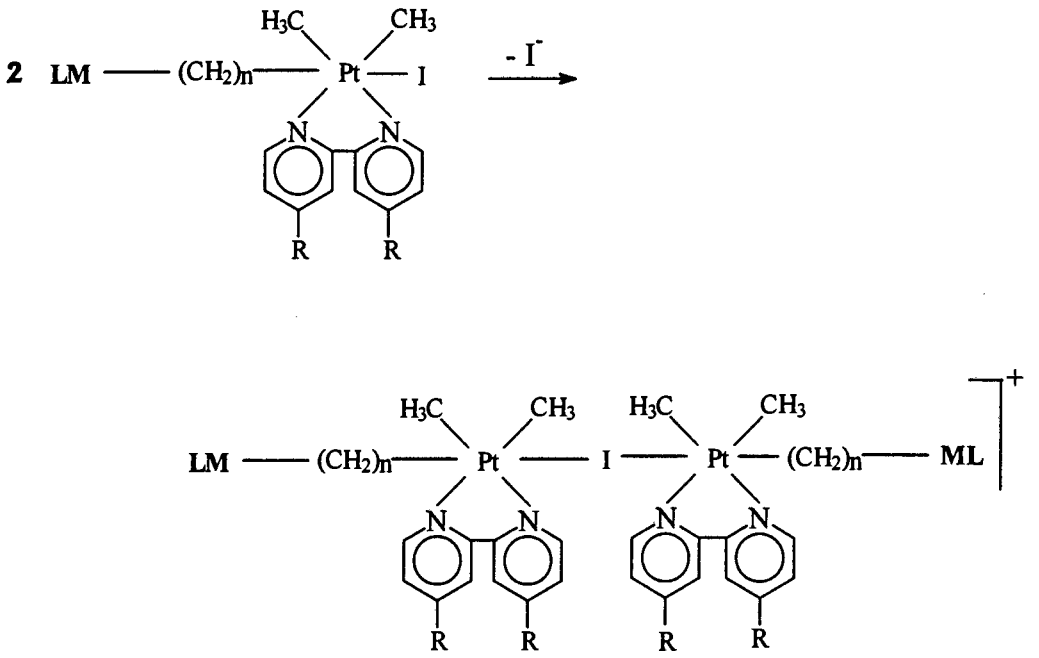

Scheme 6.6

Similar iodo bridged dimeric complexes of the types $[PtIMe_2(Me_3Sn)(^tBu_2\text{-bipy})]Me_3SnI$ [40], $[Me_3Pt(\mu\text{-}I)(\mu\text{-}Me_2PCH_2PMe_2)_2PtMe_3]I$ [41], and $[(R\text{-}C_5H_4)(CO)_2Fe\text{-}I\text{-}Fe(R\text{-}C_5H_4)(CO)_2]X$ (R = H, CH_3, X = Br and Cl) [42] were previously reported. Puddephatt and co-workers [40] have characterized the complex $[PtIMe_2(Me_3Sn)(^tBu_2\text{-bipy})]Me_3SnI$ by X-ray diffraction, and the structure is shown below [41].

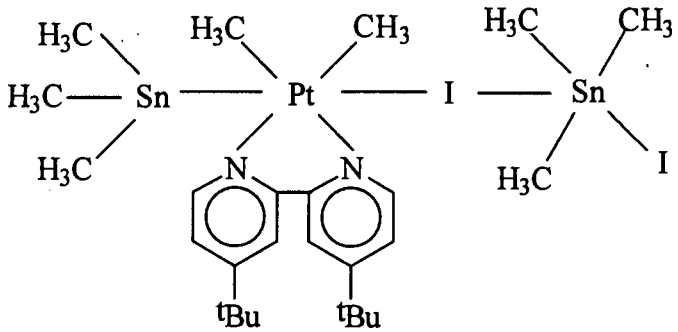

In the mass spectra of the W/Pt complexes, ions corresponding to $[2M\text{-}I\text{-}Wp]^+$ are also observed in low intensity, while for Fe/Pt and Ru/Pt complexes, ions corresponding to $[2M\text{-}Mp]^+$ (Mp = Fp or Rp) are observed in low intensity. Differences between W/Pt, Fe/Pt and Ru/Pt complexes are also observed at lower mass region. Thus for the W/Pt complexes, the most abundant peaks are found to

correspond to $[M\text{-}I\text{-}Wp]^+$, whereas for the Fe/Pt and Ru/Pt complexes, the most abundant peaks are found to correspond to $[CpFe(CO)_2I]^+$ and $[M\text{-}Rp]^+$. The difference may be due to the nature of the early transition metal tungsten which differs from the late transition metals.

The fragmentation pathways giving rise to the ions observed for the Fe/Pt complex **12** are shown in Scheme 6.7 as an example.

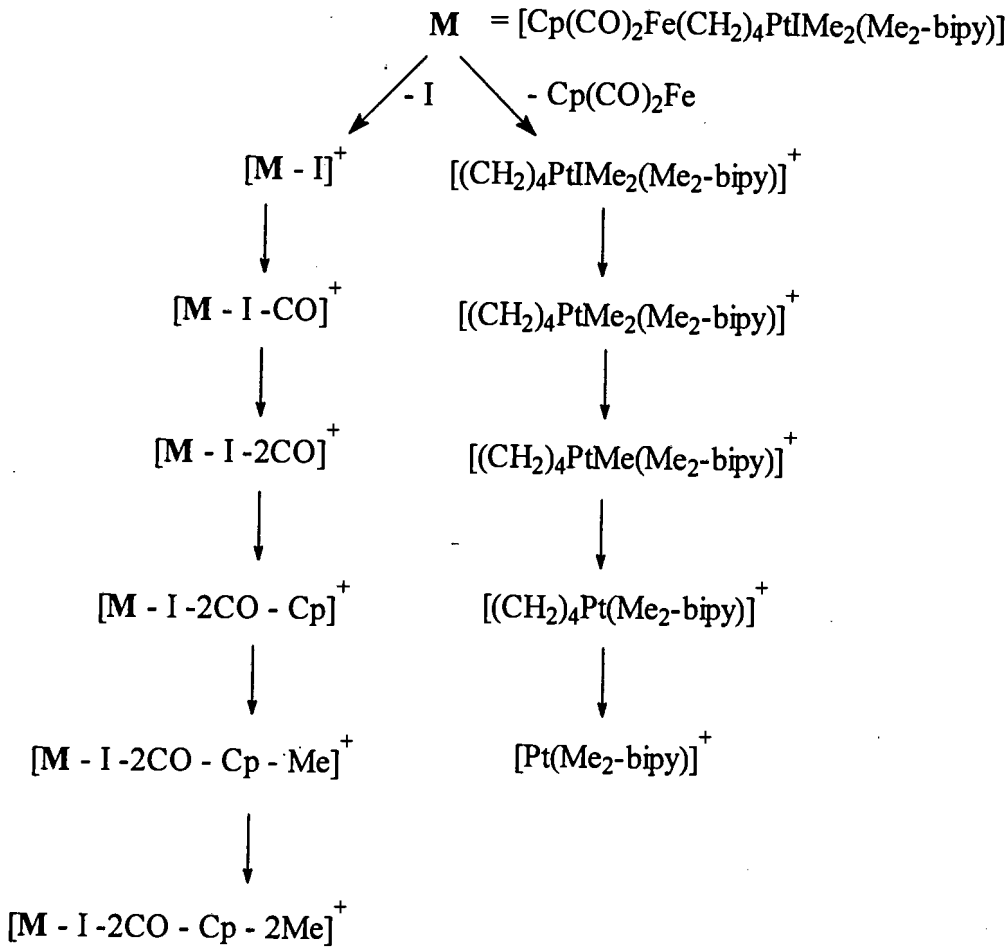

Scheme 6.7

Two important fragmentation pathways occur. The first fragmentation pathway is the loss of iodine followed by subsequent loss of CO, 2CO and (2CO+Cp), which is characteristic for $CpFe(CO)_2$ containing complexes [12]. This gives the fragment $[(CH_2)_4PtMe_2(Me_2\text{-bipy})]^+$. Further loss of Me, 2Me, and $(CH_2)_4$ from the fragment $[(CH_2)_4PtMe_2(Me_2\text{-bipy})]^+$ is also observed. The second pathway

involves the loss of $CpFe(CO)_2$ followed by subsequent loss of iodine, Me, 2Me and the $(CH_2)_4$ chain to form the $[Pt(Me_2\text{-bipy})]^+$ ion. It is also noted that the ion corresponding to the cleavage of Pt-CH_2 bond, forming the $[Fp(CH_2)_4]^+$, $[Rp(CH_2)_4]^+$ or $[Wp(CH_2)_n]^+$ ions, were not observed at all. This could imply that the Pt-CH_2 bond is much stronger than the Fe-CH_2, Ru-CH_2 and W-CH_2 bonds.

Since no molecular ion was observed using FAB-MS, ES-MS was chosen as an alternative technique to characterize these compounds. Complex **10** was investigated under various conditions (temperature, solvent, and cone voltage) in attempts to observe the molecular ion. No parent ion however was observed under the conditions we investigated. The experiment was conducted in acetonitrile solution at source temperature = 60 °C and cone voltage = 50 V. The most abundant peaks observed are a cluster of peaks in the mass range 865 - 872, which correspond to the $[M\text{-}I]^+$ ion, with expected isotope distributions as calculated. In order to get more information that could corroborate the postulated structure of the compound, the fragmentation of the peak $[M\text{-}I]^+$, *i.e.* $[D]^+$ at m/z = 867 was studied. The fragmentation of the $[D]^+$ ion gives major peaks which correspond to $[D\text{-}Wp^*]^+$, $[D\text{-}Wp^*\text{-}Me]^+$, $[D\text{-}Wp^*\text{-}2Me]^+$, $[D\text{-}Wp^*\text{-}Me\text{-}(CH_2)_4]^+$, $[D\text{-}Wp^*\text{-}2Me\text{-}(CH_2)_4]^+$, and $[Wp^*]^+$ ions. Peaks due to $[D\text{-}nCO\text{-}mMe]^+$ and $[D\text{-}Me_2\text{-}bipy)\text{-}nCO\text{-}mMe]^+$ (n = 1 to 3, m = 1 to 5) are also observed, but are of very low intensities (< 3%).

Although no parent ion was observed by using either FAB-MS or ES-MS techniques, the fragment ions we observed in these studies help to confirm the postulated structures of these compounds. Because in all cases, $[M\text{-}I]^+$ ions were observed, there is a possibility that these complexes might exist as ionic species, *i.e.* $[LM(CH_2)_nPtMe_2(R_2\text{-bipy})]^+I^-$. To eliminate such a possibility, the conductivity for complex **9** was measured in nitrobenzene at a concentration of 1×10^{-3} mol/L at room temperature. The molar conductivity (Λ) of this complex is 0.77 Ω^{-1} cm^2 mol^{-1}, which confirms that the complex is a non-electrolyte [43].

Attempted reactions of $[Cp^*W(CO)_3(CH_2)_3PtIMe_2(Me_2\text{-bipy})]$, 9 and $[Cp^*Fe(CO)_2(CH_2)_4PtIMe_2(Me_2\text{-bipy})]$, 18 with CO_2

The reactions of **9** and **18** with CO_2 were investigated in attempts to activate CO_2 using these heterobimetallic complexes. The reaction of **9** with CO_2 (40 bar) in a mixture of NEt_3 and EtOH at 25 °C for 24 hours and then 45 °C for 43 hours did not yield any CO_2-containing product. Only the starting complex was recovered quantitatively. We also investigated the reaction of **18** with CO_2 (43 bar) in toluene at 80 °C for 42 hours. After this time, the starting complex was recovered quantitatively.

It appeared to us that the attempted reactions for incorporating CO_2 by these heterobinuclear complexes under these conditions did not yield any new products. This could be due to the fact that the metal centres in these complexes are all 18-electron species which are stable and inert to CO_2. In order to generate reactive species, some methods for the activation of these complexes are required. Therefore, we subsequently investigated the electrochemical reduction and oxidation of these heterobimetallic complexes under CO_2 atmosphere. The results will be discussed in the following section.

6.1.4 Electrochemical behaviour of the heterobinuclear complexes $[Wp(CH_2)_4PtIMe_2(Me_2\text{-bipy})]$ and $[Wp^*(CH_2)_4PtIMe_2(Me_2\text{-bipy})]$

It is of interest to study the electrochemical properties of the new heterobinuclear complexes and to compare their behaviour with that of the related mononuclear alkyl complexes, since electrochemical studies could provide information on the intramolecular interation of one metal centre with the other [44]. We have selected two heterobinuclear complexes, $[Wp(CH_2)_4PtIMe_2(Me_2\text{-bipy})]$, **5**, and $[Wp^*(CH_2)_4PtIMe_2(Me_2\text{-bipy})]$, **10**, and studied their electrochemical behaviour by cyclic voltammetry under both argon and CO_2 atmospheres. The CVs of these complexes were measured in acetonitrile solution at room temperature using a Pt microelectrode and a voltage sweep rate of 200 mV/s or 100 mV/s. The cyclic

voltammograms of **10** are shown in Figure 6.5. The data for these two complexes are summarized in Table 6.9, together with those for related mononuclear complexes.

Table 6.9 Reduction and oxidation potentials for the complexes **5** and **10** under argon or CO_2, measured in 1.0 mM acetonitrile solution containing 0.1 M $[NBu^n_4]ClO_4$ at room temperature, at a Pt microelectrode.

Compound	Atmo-sphere	Scan rate (mV/s)	Reduction V *vs.* Fc/Fc^+		Oxidation V *vs.* Fc/Fc^+		
			E_{c1}[a]	E_{c2}[b]	E_{a1}[c]	E_{a2}[d]	E_{a3}[e]
$[Wp(CH_2)_4PtIMe_2(Me_2\text{-bipy})]$	Argon	100	-1.92	-2.19	-0.04	0.30	n/o[h]
	CO_2	100	-1.93	-2.18	0.00	0.34	n/o
$[Wp^*(CH_2)_4PtIMe_2(Me_2\text{-bipy})]$	Argon	200	-1.97	-2.14	0.03	0.24	n/o
	CO_2	200	-1.93	-2.17	0.03	0.23	n/o
$[PtIMe_2(C_5H_{13})(Me_2\text{-bipy})]$[f]	Argon	200	-1.94	-2.13	-0.01	0.26	n/o
	CO_2	200	-1.89	-2.13	-0.03	0.27	0.18
$[Wp\{(CH_2)_6CH_3\}]$[g]	Argon	200	n/o	n/o	0.56	n/o	n/o
	CO_2	200	n/o	n/o	0.55	n/o	n/o

[a]: irreversible; [b]: irreversible or quasi-reversible; [c]: irreversible; [d]: irreversible; [e]: irreversible; [f]: results from Chapter 4; [g]: results from Chapter 3; [h]: not observed.

It can be seen from Table 6.9 that the CVs of **5** and **10** are very similar to each other under both argon and CO_2. The reduction and oxidation peaks for these heterobimetallic complexes resemble those of the mononuclear Pt(IV) $[PtIMe_2(C_5H_{11})(Me_2\text{-bipy})]$ complex [33], *i.e.* the redox activity is centred on the $[PtIMe_2(Me_2\text{-bipy})]$ moiety. On the other hand, the tungsten centre in these heterobimetallic complexes does not show oxidation waves at potentials similar to those observed for the mononuclear complexes $[Wp\{(CH_2)_6CH_3\}]$ [45] and $[Wp^*\{(CH_2)_4I\}]$ [32]. There could be two reasons for this: (1) the oxidation wave for the tungsten centre might be affected by the platinum metal centre and hence could appear at a similar potential to those observed for the platinum centre; or (2) the first two oxidation waves might have generated a reactive species which

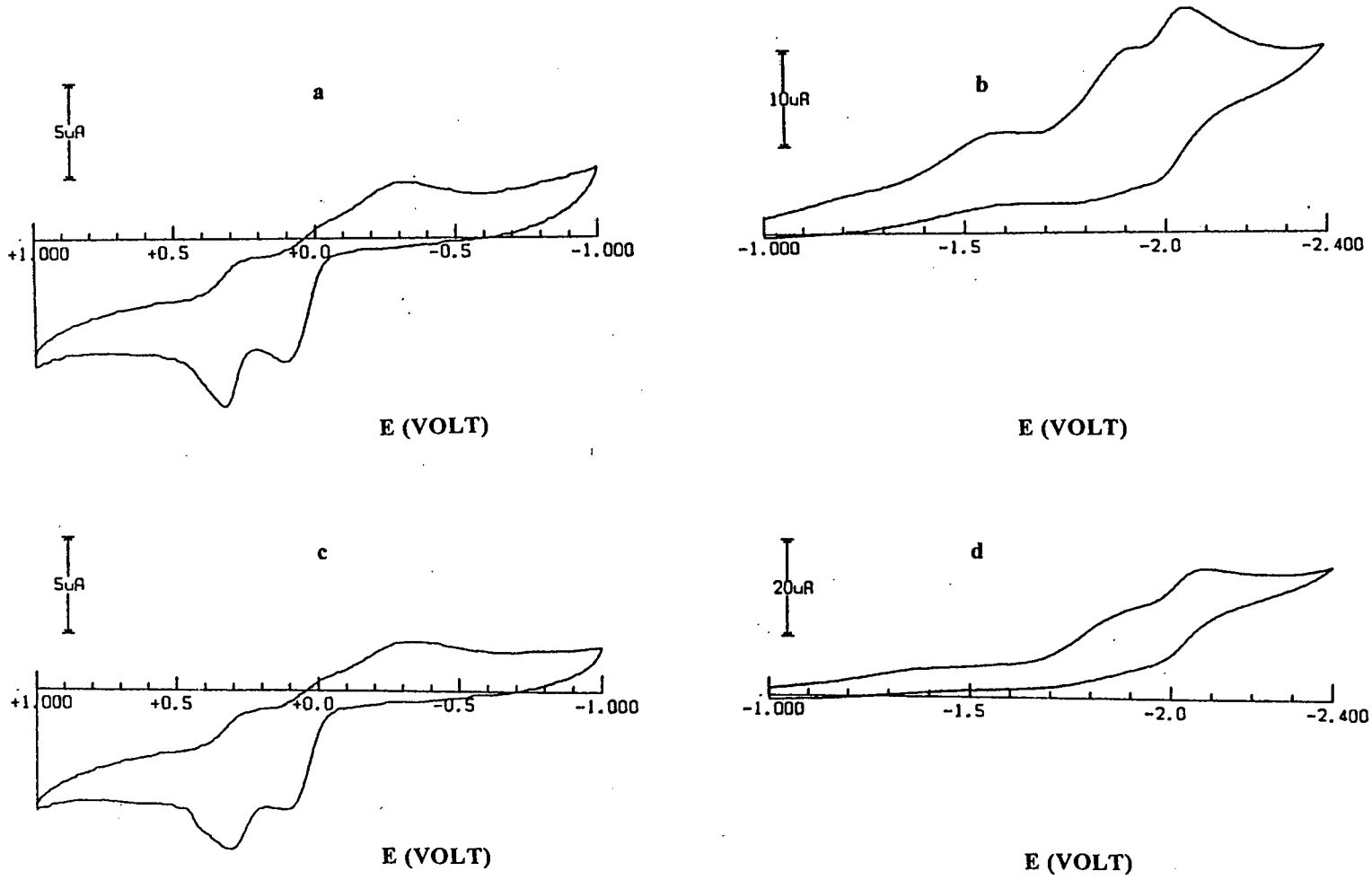

Figure 6.5 Cyclic voltammograms of 1.0 mM [$Wp^*(CH_2)_4PtIMe_2(Me_2$-bipy] in acetonitrile containing 0.1 M [NBu^n_4]ClO_4 at a Pt microelectrode with a scan rate of 200 mV/s, a and b: under argon; c and d: under CO_2.

has reacted with the tungsten centre to form a non-reducible or decomposition product. Evidence for the second possibility is also provided by the observation that, when the oxidation of the heterobinuclear complexes was performed under a CO_2 atmosphere, we observed the same CV as under argon. This differs from the oxidation of the Pt(IV) alkyl complex [$PtIMe_2(C_5H_{11})(Me_2$-bipy)] under CO_2, where we observed an additional peak which might be due to a CO_2-containing species.

Thus, an intramolecular reaction between the tungsten centre and the anodically generated platinum species appears to take place under both argon and CO_2 atmospheres.

Our present results suggest that the heterobimetallic complexes display different electrochemical properties to the corresponding mononuclear complexes, and by varying the metal combination the properties of the heterobinuclear complexes could be modified.

6.2 Synthesis and characterization of binuclear and dendritic polynuclear Pt(II) alkyl complexes

6.2.1 Introduction

We have shown in Chapter 4 that the reactions of the complexes $[PtMe_2(R_2\text{-bipy})]$ (R = H, CH_3) with CO_2/R'OH give the corresponding monoalkyl carbonate complexes $[PtMe\{OC(O)OR'\}(R_2\text{-bipy})]$. We have also shown, in the previous section of this chapter, that the reactions of the complexes $[PtMe_2(R_2\text{-bipy})]$ (R = H, CH_3) with haloalkyl complexes $[LM\{(CH_2)_nI\}]$ give the polymethylene bridged heterobinuclear complexes $[LM(CH_2)_nPtIMe_2(R_2\text{-bipy})]$. These successful results have prompted us to investigate the chemistry of structurally similar binuclear and polynuclear Pt(II) alkyl complexes containing polypyridyl ligands. We chose 1,5-bis(4'-methyl-2,2'-bipyridyl-4-yl)pentane [46,47], **20** (see below) as the ligand for the preparation of a binuclear Pt(II) alkyl complex.

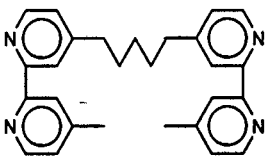

20

This ligand has been previously used for the preparation of binuclear ruthenium [46] and heterobinuclear ruthenium/osmium [47] complexes. We have in addition synthesized some new dendrimers containing polypyridyl groups, and investigated the use of these dendrimers for the preparation of new dendritic Pt(II) alkyl complexes.

Dendritic polymers [48-62] are currently receiving much attention due to their unique structural properties and potential utility. Dendrimers could find use in catalysis [56], molecular biology [55] and material science [57-59], as well as electrochemical reduction of CO_2 [60]. Through judicious choice of branched building blocks and functional group chemistry, one can precisely control their shape, dimensions, density, polarity, flexibility and solubility [63,64].

Dendrimers with functional components located on the exterior surface are of particular interest since they exploit dendritic topology to modify the physical and chemical behaviours of these components, giving rise to new materials with desirable properties [48-62,65].

Dendrimers can be synthesized in a carefully controlled stepwise manner by two routes: the convergent approach, first reported in 1990 by Hawker and Frechet [66], and the divergent approach, first reported by Tomalia and co-workers [67] in 1986. In the convergent approach, as shown in Scheme 6.8, the construction of the dendrimer initiates from what will eventually become the periphery of the dendritic molecule. Each successive generation is then synthesized in stepwise fashion producing a new dendritic molecule in which a single reactive group located at the focal point. The dendritic wedge can then be reacted with a core molecule to give the final dendrimer. In the divergent approach, as shown in Scheme 6.9, the synthesis starts from a polyfunctional core molecule and chain propagation initiates from the core outwards.

Organoplatinum dendrimers containing diimine ligands [68] or diphosphino ligands [69] have been reported. Puddephatt and co-workers have synthesized some large platinum dendrimers using the convergent strategy [68]. This strategy involved the oxidative addition of the C-Br bonds of 4,4′-bis(bromomethyl)-2,2′-bipyridine to $[PtMe_2(^tBu_2\text{-bipy})]$ to give $[4,4'\text{-}\{BrPtMe_2(^tBu_2\text{-bipy})CH_2\}_2\text{-}2,2'\text{-}C_5H_3N]$, followed by regeneration of a $[PtMe_2(NN)]$ functionality by reaction of the free diimine group with $[Pt_2Me_4(SMe_2)_2]$ to give **C**, as shown in Scheme 6.10. Repetition of this cycle several times gave the dendrimer **D** containing 14 platinum atoms.

Very recently, Liu and Puddephatt, independent of our work, have also reported platinum and palladium dendrimers prepared by the divergent approach [70]. This method is based on the ligands **E** and **F**, as shown in Scheme 6.11. The ligand **E** acts as a core molecule for dendrimer growth. Reaction of **E** with $[Pt_2Me_4(SMe_2)_2]$ gave the triplatinum(II) complex **G**, while reaction with $[Pd_2Me_4(pyridazine)_2]$, **H** gave the corresponding tripalladium complex **I**.

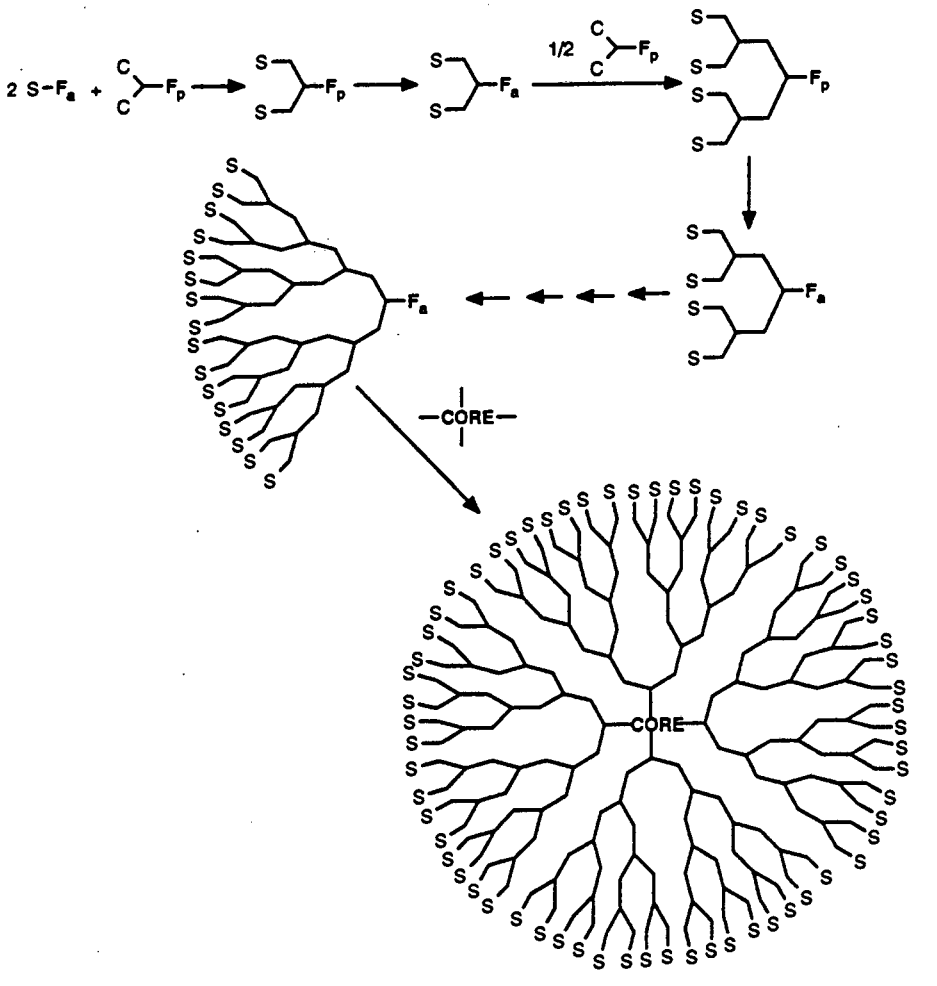

Scheme 6.8

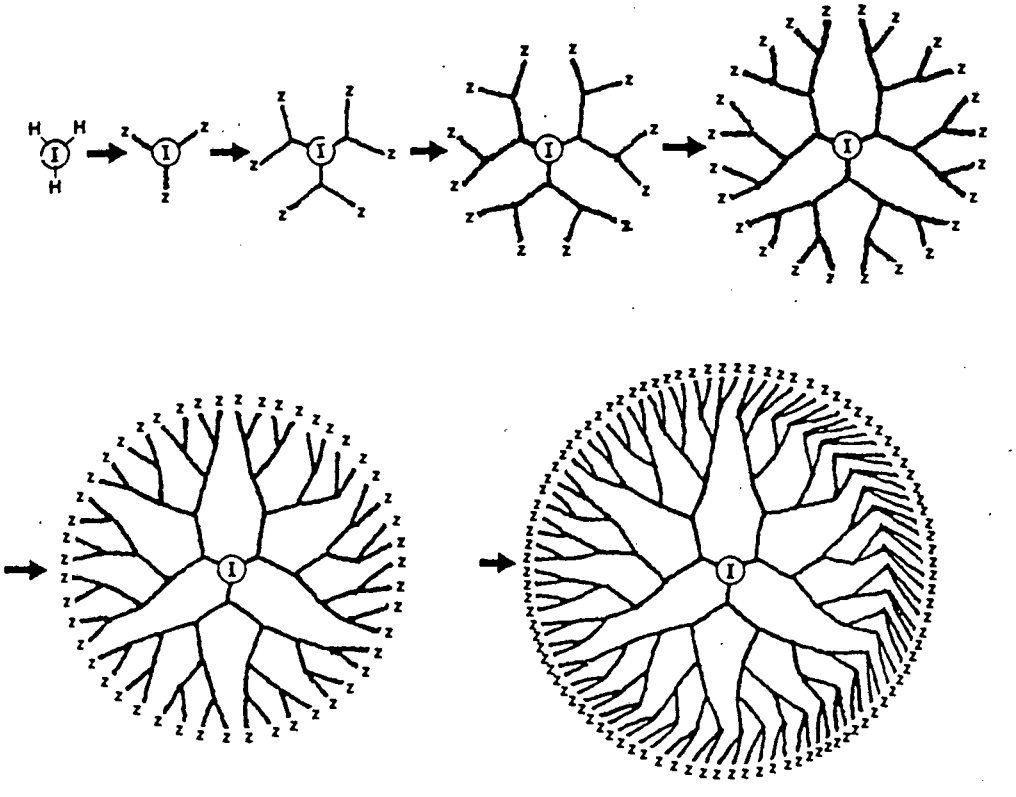

Scheme 6.9

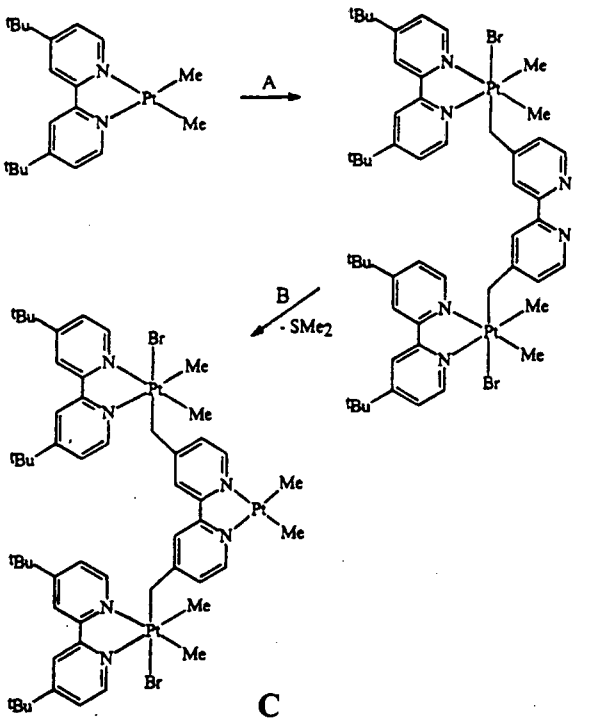

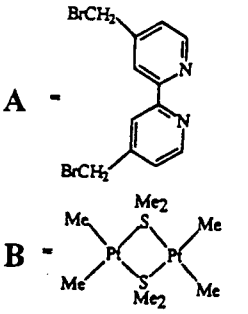

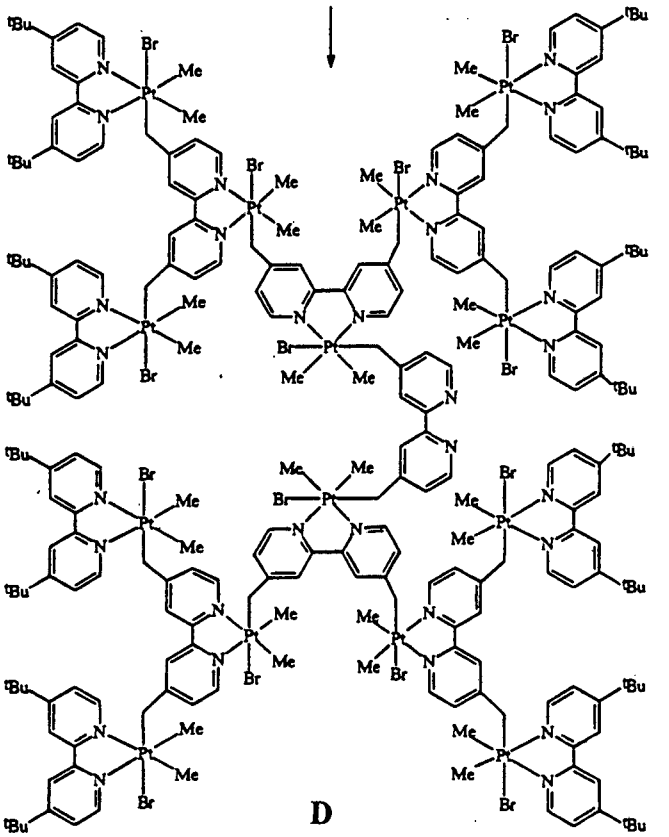

Scheme 6.10

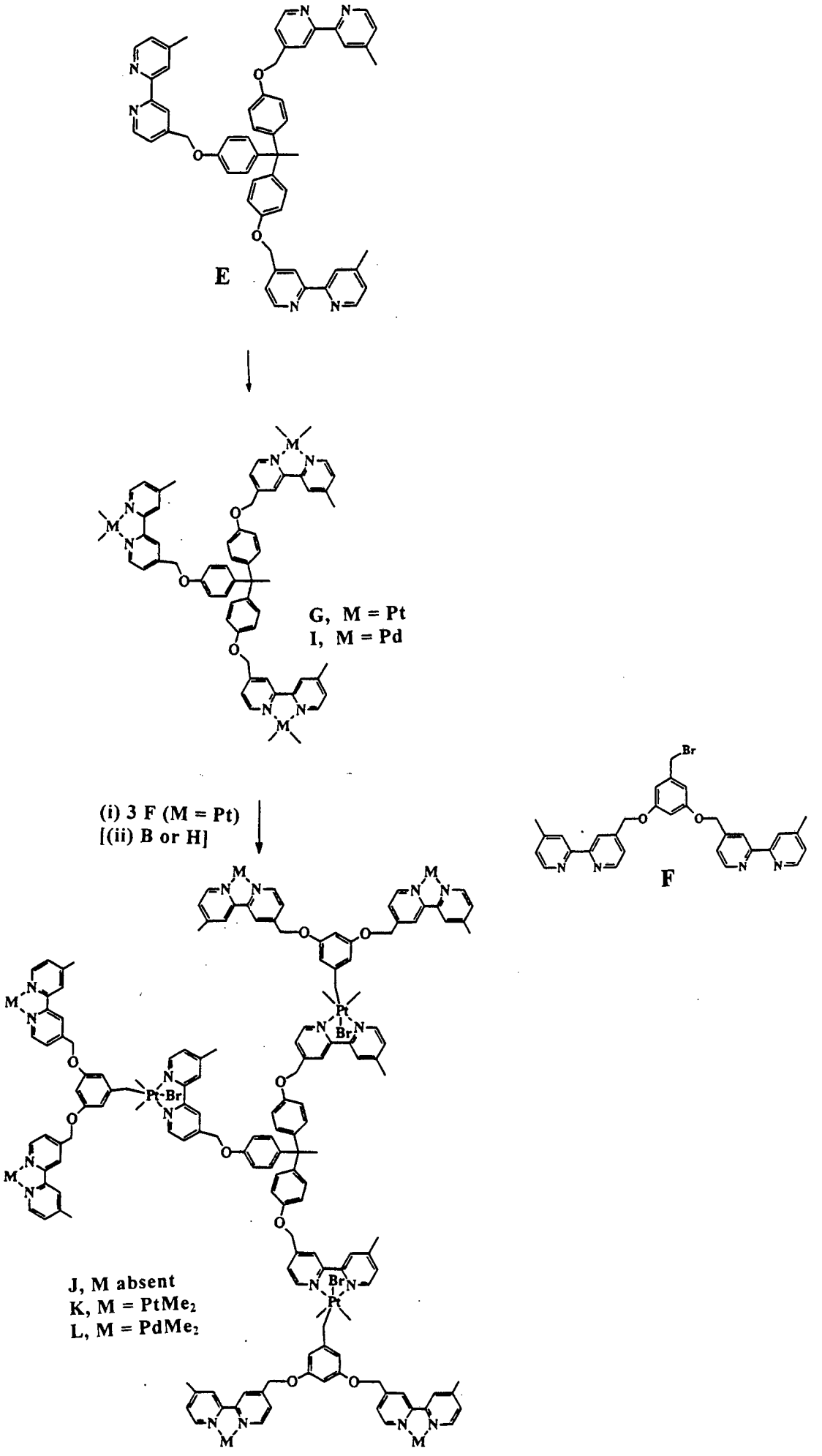

Scheme 6.11

Each of the Pt(II) centres in **G** reacted with **F** to give the $Pt(IV)_3$ complex **J**, which contains six free bipyridine donors. Finally, complex **J** reacted with $[Pt_2Me_4(SMe_2)_2]$ or $[Pd_2Me_4(pyridazine)_2]$ to give the $Pt(IV)_3Pt(II)_6$ (**K**) or $Pt(IV)_3Pd(II)_6$ complex (**L**), respectively. The complexes **K** and **L** were found to be sparingly soluble, which makes the further growth of larger dendrimers difficult [70].

Here, we wish to report (1) the synthesis of the binuclear Pt(II) alkyl complex $[Me_2Pt\{(Me\text{-}bipy)\text{-}(CH_2)_5\text{-}(Me\text{-}bipy)\}PtMe_2]$ and its reactions with CO_2 and $[CpW(CO)_3\{(CH_2)_4I\}]$; (2) the synthesis of the zero and first generation 4-methyl-2,2′-bipyridine (Me-bipy) containing dendrimers; and (3) the use of these dendrimers for the preparation of the zero and first generation dendritic Pt(II) alkyl complexes.

6.2.2 Synthesis and reactivity of the binuclear Pt(II) alkyl complex $[Me_2Pt\{(Me\text{-}bipy)\text{-}(CH_2)_5\text{-}(Me\text{-}bipy)\}PtMe_2]$

Synthesis and characterization

The compound 1,5-bis(4′-methyl-2,2′-bipyridyl-4-yl)pentane, **20** was synthesized by the reaction of 4,4′-dimethyl-2,2′-bipyridine with diisopropylamine and ^{n}BuLi, followed by excess 1,3-dibromopropane, as shown in Scheme 6.12. This method has been reported by Schmehl and co-workers [46] for the preparation of **20**. This compound was previously characterized by elemental analysis and ^{1}H NMR [46,47]. We have also characterized this compound by ^{1}H NMR and our results are in good agreement with the literature [46,47]. In addition, we have characterized this compound by IR, UV-vis and ^{13}C NMR spectroscopy and the data are given in the experimental section 7.6.2.

Compound **20** reacted with $[Pt_2Me_4(SMe_2)_2]$ in acetone/benzene to give the binuclear Pt(II) alkyl complex $[Me_2Pt\{(Me\text{-}bipy)\text{-}(CH_2)_5\text{-}(Me\text{-}bipy)\}PtMe_2]$, **21** in

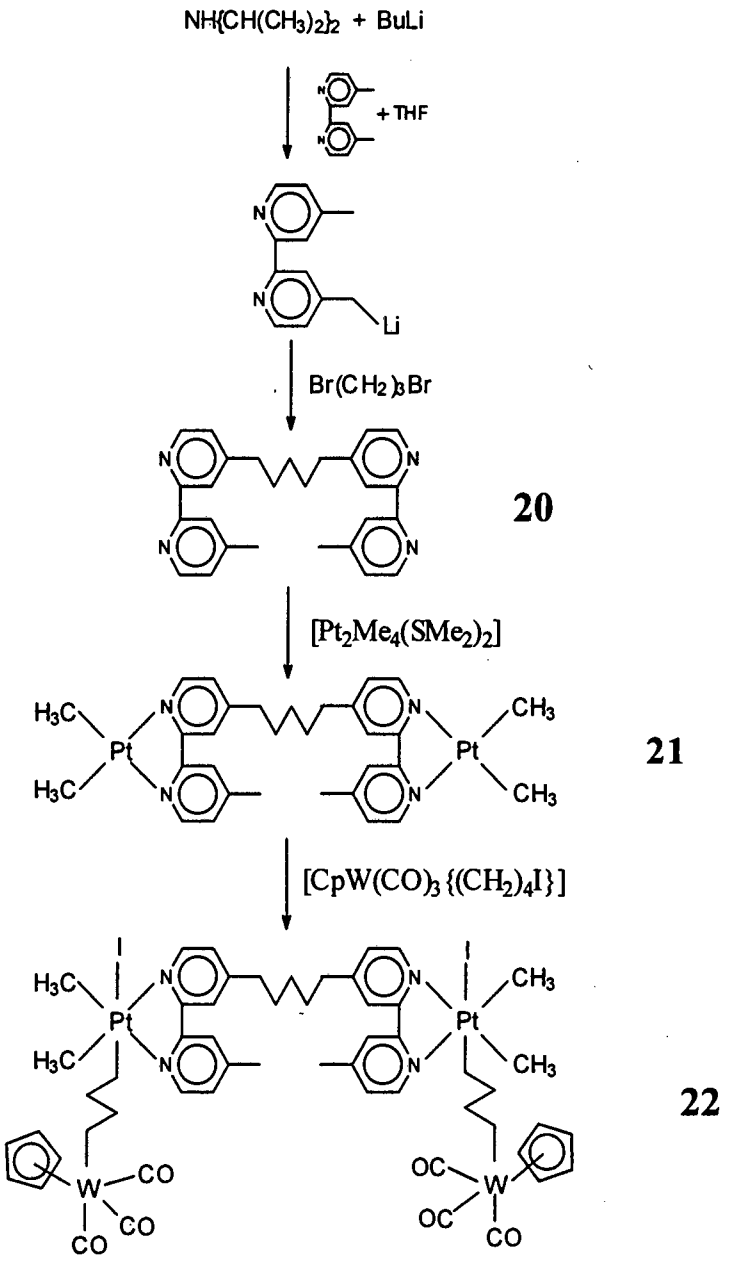

Scheme 6.12

high yield (87%). This complex has been characterized by elemental analysis, melting point, UV-Vis, IR, and ^{1}H NMR spectroscopy as well as ES mass spectroscopy. The data are given in the experimental section 7.6.2.

Notable characteristics of the complex **21** includes that the UV-Vis spectrum of **21** shows an absorption band at λ_{max} = 448 nm (ε 598, in CH_2Cl_2) due to the Pt(II)

5d-diimine π^* MLCT, which is similar to that found in the mononuclear Pt(II) alkyl complexes [$PtMe_2(R_2$-bipy)] [33]. The IR spectrum shows a peak at 2786 cm^{-1}, which may be due to the C-H stretching vibration of the Pt-CH_3 groups. The IR spectrum shows the shift of a peak seen in the free diimine ligand **20** at 1595 to 1611 cm^{-1} for **21**. This peak is probably due to the bipy ring [71]. The shift of this band indicates the coordination of the platinum. The proton resonances of the bipy rings for **21** are found at lower field than those for the ligand **20,** which is due to the deshielding effect of the platinum. The peak observed at δ 0.93 ppm with platinum satellites ^2J(PtH) 86 Hz in the ^1H NMR spectrum is similar to that observed for the mononuclear complexes [$PtMe_2(R_2$-bipy)] [33]. In the ES-MS spectrum of **21**, a peak due to $[M - CH_3 + CH_3CN]^+$ is observed at *m/z* 883.9 with the expected isotope pattern. These characterization confirm the postulated structure for **21**.

Reactivity studies

a) Reaction of $[Me_2Pt\{(Me\text{-}bipy)\text{-}(CH_2)_5\text{-}(Me\text{-}bipy)\}PtMe_2]$, 21 with $[CpW(CO)_3\{(CH_2)_4I\}]$

Complex **21** reacted with $[CpW(CO)_3\{(CH_2)_4I\}]$ at room temperature in CH_2Cl_2 to give the heterobimetallictetranuclear complex **22** in good yield, by double oxidative addtion of 2 equivalents of the iodoalkyl complex at the Pt(II) centres, as shown in Scheme 6.12. This reaction is similar to the reactions of mononuclear Pt(II) alkyl complexes [$PtMe_2(R_2$-bipy)] with iodoalkyl complexes as shown in section 6.1 of this chapter. The tetranuclear complex **22** has been characterized by satisfactory elemental analysis, IR and UV-Vis spectroscopy. The IR spectrum of **22** shows two ν(CO) peaks at 2007 and 1907 cm^{-1}, similar to those observed in the heterobinuclear complexes [$CpW(CO)_3(CH_2)_nPtIMe_2(R_2$-bipy)]. The UV-vis spectrum shows two bands at λ_{max} 312 and 350 nm in CH_2Cl_2, which indicates the change from Pt(II) to Pt(IV). Similar trends have been observed for the

heterobinuclear complexes discussed in section 6.1 of this chapter. Because of the poor solubility of **22**, no further chacterization data were obtained.

b) Reaction of $[Me_2Pt\{(Me\text{-}bipy)\text{-}(CH_2)_5\text{-}(Me\text{-}bipy)\}PtMe_2]$, 21 with CO_2/EtOH

The reaction of **21** with 40 bar of CO_2 in EtOH/NEt_3 was carried out at 40 °C for 22 hours. The reaction gave probably the platinum carbonate complex **23** as postulated in Scheme 6.13. The IR spectrum (neat) of the reaction solution

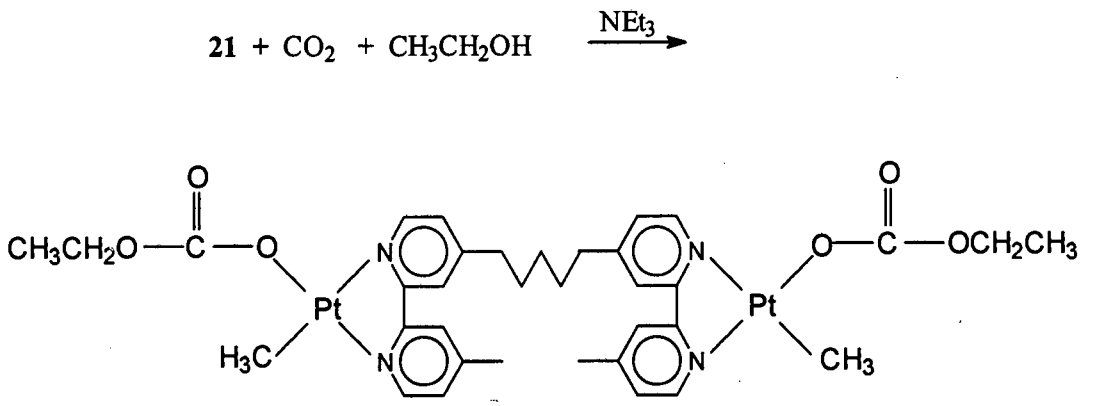

23

Scheme 6.13

shows a peak at 1644 cm^{-1}, which may be due to the ν(CO) of the carbonate group. A similar ν(CO) band has been observed for the mononuclear carbonate complexes [PtMe{OC(O)OR'}(R_2-bipy)] [33]. The UV spectrum of the product in acetone shows a band at λ_{max} = 416 nm, which is similar to that observed for [PtMe{OC(O)OR'}(R_2-bipy)] [33]. Unfortunately, due to the instability of this compound, further characterization data were not obtained.

6.2.3 Synthesis and characterization of the zero and first generation dendrimers containing 4-methyl-2,2′-bipyridine pendant groups

Synthesis

A series of dendrimers containing 4-methyl-2,2′-bipyridine (Me-bipy) pendant groups located at the periphery of their dendritic structures have been prepared using the convergent approach. This approach was first developed by Hawker and Frechet [66] for the preparation of organic dendrimers. Recently, Liao and Moss [72] have applied this methodology for the preparation of organoruthenium dendrimers containing up to 48 ruthenium atoms.

The precursor 4-(4-bromobutyl)-4′-methyl-2,2′-bipyridine (denoted as Me-bipyC4G0Br) **24** was prepared by the reaction of lithiated Me_2-bipy with excess 1,3-dibromopropane as illustrated in Scheme 6.14. This method is more straightforward than the method reported by Furue and co-workers for the preparation of the same compound [47]. This product was purified by chromatography on silica gel eluting with acetone/CH_2Cl_2 and recrystallized from ethyl acetate. We have characterized **24** by ^1H and ^{13}C NMR. The ^1H NMR data has been previously reported and our results are in agreement with the literature [47]. This compound has good solubility in polar organic solvents which is important for the preparation and characterization of larger dendrimers.

The preparation of new dendrimers starts from Me-bipyC4G0Br, **24** which will eventually become the chain-end functional groups. Compound **24** reacted with the building block 3,5-dihydroxybenzyl alcohol, in the presence of K_2CO_3 and 18-crown-6 in refluxing acetone for 48 hours, to give the first generation benzyl alcohol Me-bipyC4G1OH, **25** in 96% yield.

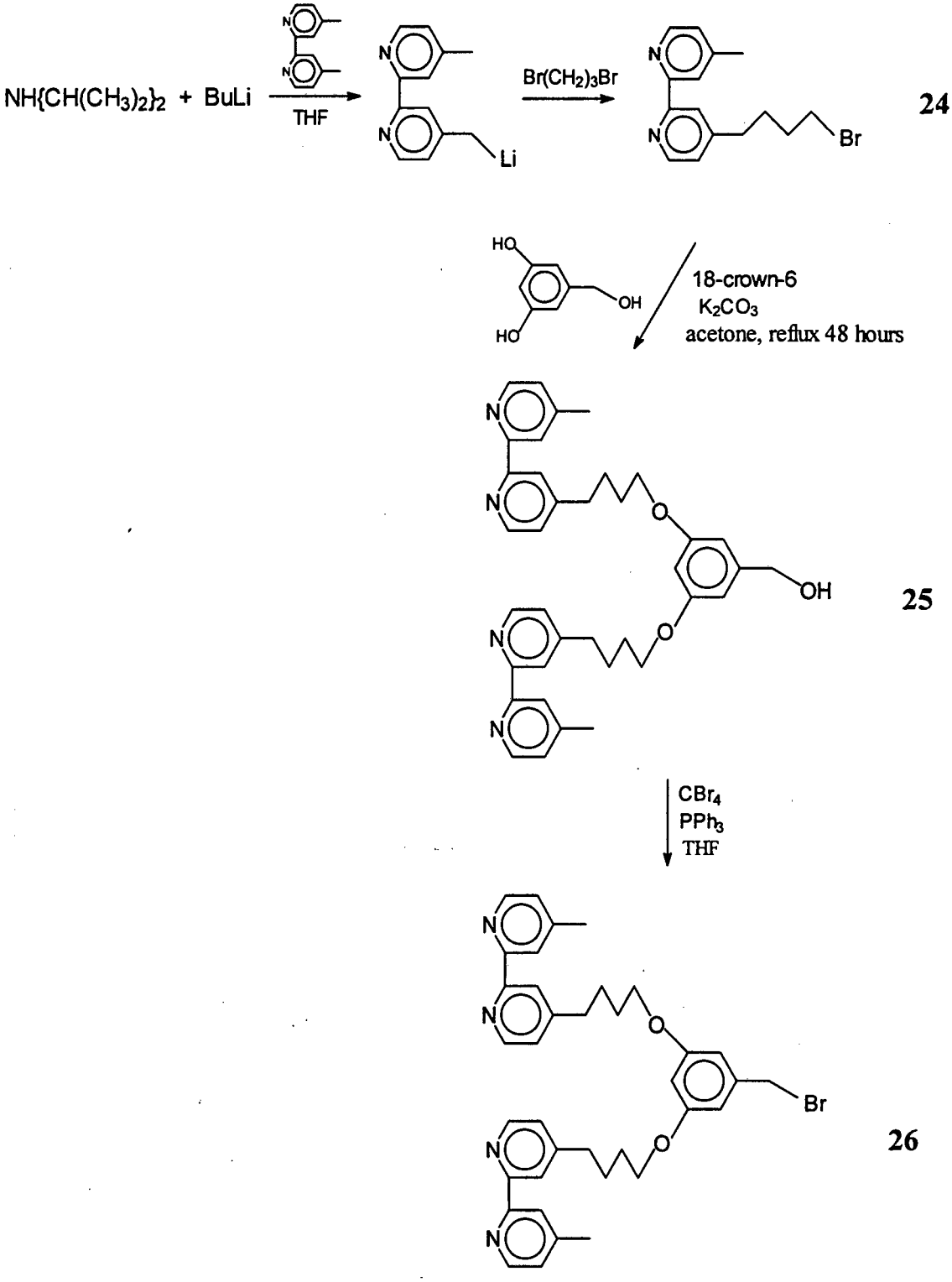

Scheme 6.14

Compound **25** was purified by chromatography and recrystallized from ethyl acetate to give a white solid. Bromination of the first generation benzyl alcohol Me-bipyC4G1OH (**25**) with PPh_3 and CBr_4 in a minumum volume of THF at room temperature restored the reactive bromomethyl functionality at the focal point of

the dendritic wedge to give the corresponding benzyl bromide Me-bipyC4G1Br (**26**). This was also purified by chromatography and recrystallized from CH_2Cl_2/hexane.

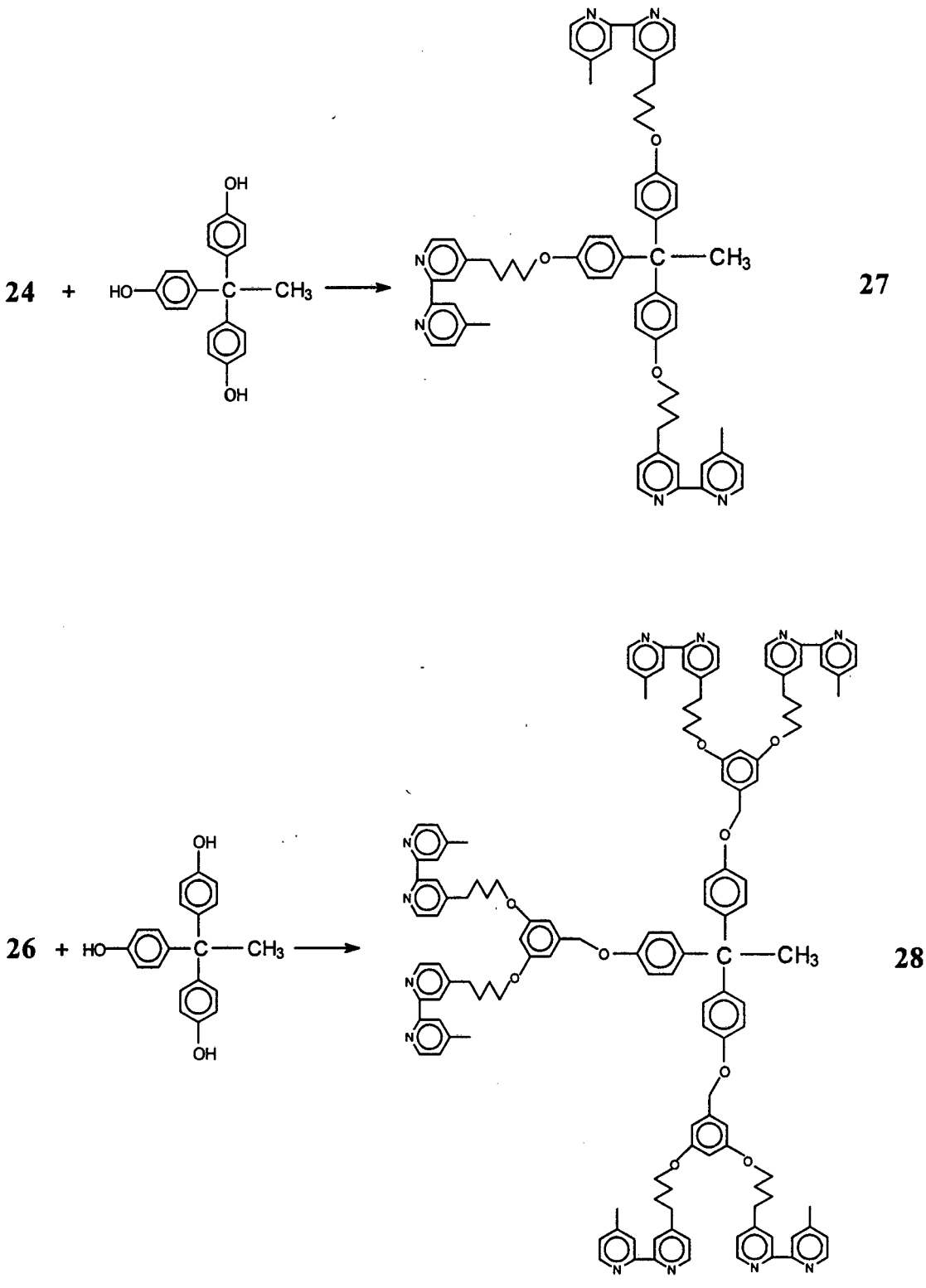

Scheme 6.15

In the convergent approach, the dendritic wedges obtained are attached to a polyfunctional core. The polyfunctional core we chose was 1,1,1-tris(4'-hydroxyphenyl)ethane. This molecule was first used by Hawker and Frechet [66]. Coupling reactions of the phenolic groups of the core molecule with the bromide compounds, Me-bipyC4G0Br and Me-bipyC4G1Br, were carried out respectively, as shown in Scheme 6.15. Thus the zero and first generation dendrimers Me-bipyC4G0C (**27**) and Me-bipyC4G1C (**28**) were obtained. These compounds were purified by chromatography and recrystallization to give oils but turned into solids upon drying under high vacuum.

It is found that the compounds **25** - **28** tend to contain solvents of recrystallization which could not be removed even after drying under high vacuum at room temperature for *ca.* 10 hours. It has been reported that dendrimers can hold or trap smaller molecules inside the dendrimer's flexible cavities [73].

Characterization

The new compounds **25** - **28** have been characterized by melting point, elemental analysis, IR, ^{1}H and ^{13}C NMR as well as ES mass spectroscopy. The data are given in the experimental section 7.6.2. The results are discussed in the following context.

IR spectroscopy

The IR spectra of **25** - **28** were recorded in KBr discs in the range 4000 to 750 cm^{-1}. The IR spectra of these compounds show the characteristic band at *ca.* 1595 cm^{-1} due to the bipy rings, among others. This is found at the same position as that found in the monomer Me_2-bipy measured at identical conditions. This is good evidence that the Me-bipy groups of these dendritic molecules are not affected by the dendrimer growth.

^{1}H and ^{13}C NMR spectroscopy

^{1}H and ^{13}C NMR spectroscopy have proved to be invaluable in characterization of the new dendritic compounds. All the dendrimers prepared in this study have been characterized. The ^{1}H NMR spectrum of the first generation dendrimer **28** is shown in Figure 6.6. In all cases, the Me-bipy groups of the molecules give seven sets of resonances at positions δ 8.53 (H^{6}, $H^{6'}$), 8.24 (H^{3}, $H^{3'}$), 7.10 (H^{5}, $H^{5'}$), 3.96 (CH_2O), 2.76 (bipy-CH_2), 2.43 (bipy-CH_3) and 1.85 ppm ($CH_2CH_2CH_2O$) (see the experimental section 7.6.2 for numbering schemes). These results are consistent with the expected symmetrical structures of the dendrimers. The triplet observed at δ 3.96 ppm is particularly important since this indicates the formation of the CH_2O group of **25,** at the first stage of construction of the dendrimers. The other resonances indicate that the Me-bipy groups remain in the dendritic structure during the course of the reactions required for their synthesis.

The resonances for the aromatic protons of the benzyl group occur in the region δ 6.3 - 6.6 ppm, as shown in Figure 6.7. Perhaps the most important feature in Figure 6.7 is the resonances of benzyl protons at the focal point at which CH_2OH appears at δ 4.60 ppm and CH_2Br at 4.38 ppm, which confirms the conversion of the dendritic alcohol, **25** to the corresponding bromide, **26**. On attachment of the bromide to the polyfunctional core, a shift from δ 4.38 to 4.92 ppm of the same CH_2 resonance is observed. This is accompanied by a new resonance at δ 2.16 ppm, corresponding to methyl protons of the core molecule, while the aromatic protons of the core molecule give two distinguishable doublets at δ 6.98 and 6.84 ppm, as shown in Figure 6.7.

In all cases, the integration of resonances was employed to confirm the structures of the dendrimers.

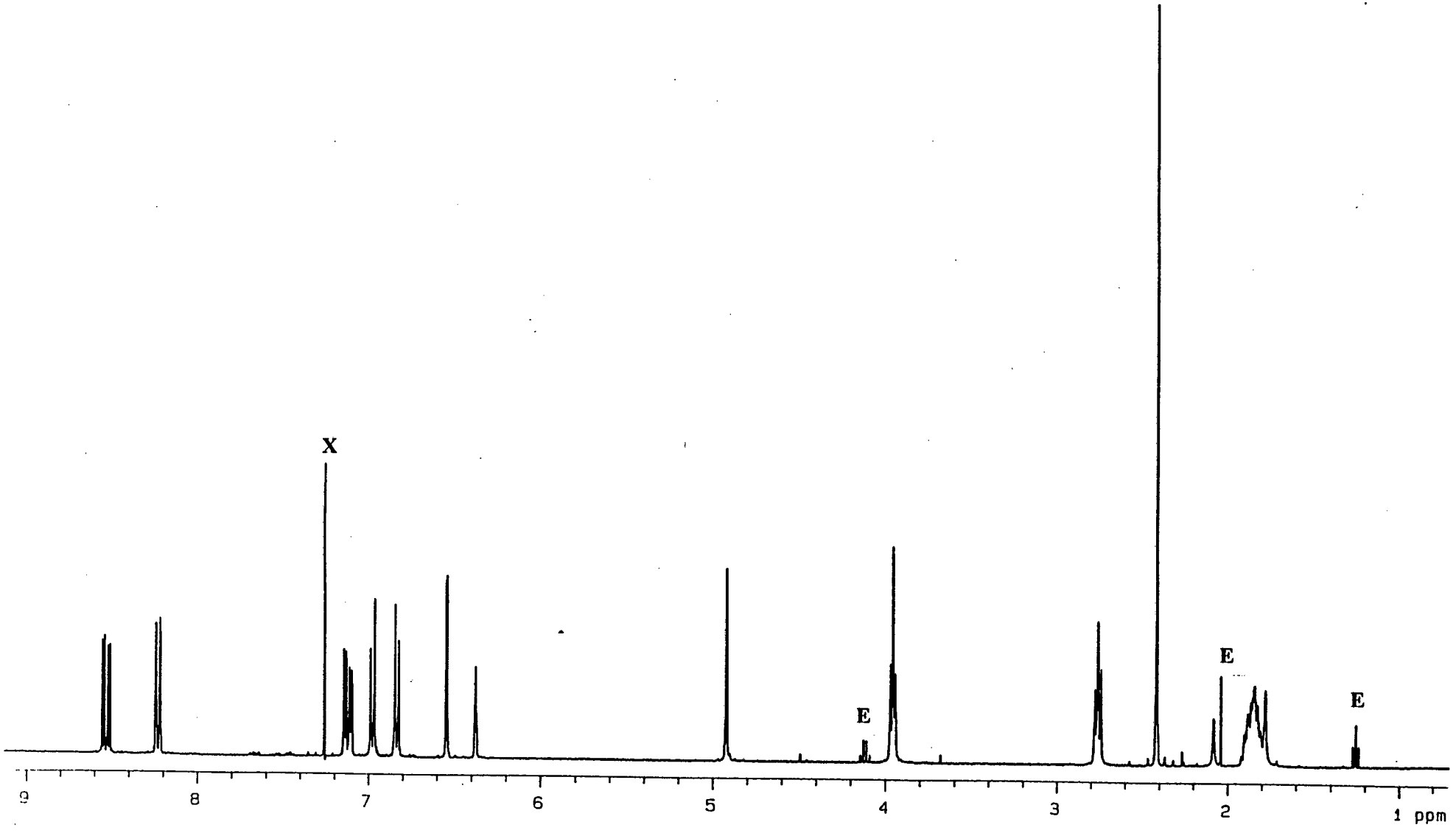

Figure 6.6 ^{1}**H NMR spectrum of the first generation dendrimer, 28 (400 MHz, X = $CDCl_3$, E = ethyl acetate).**

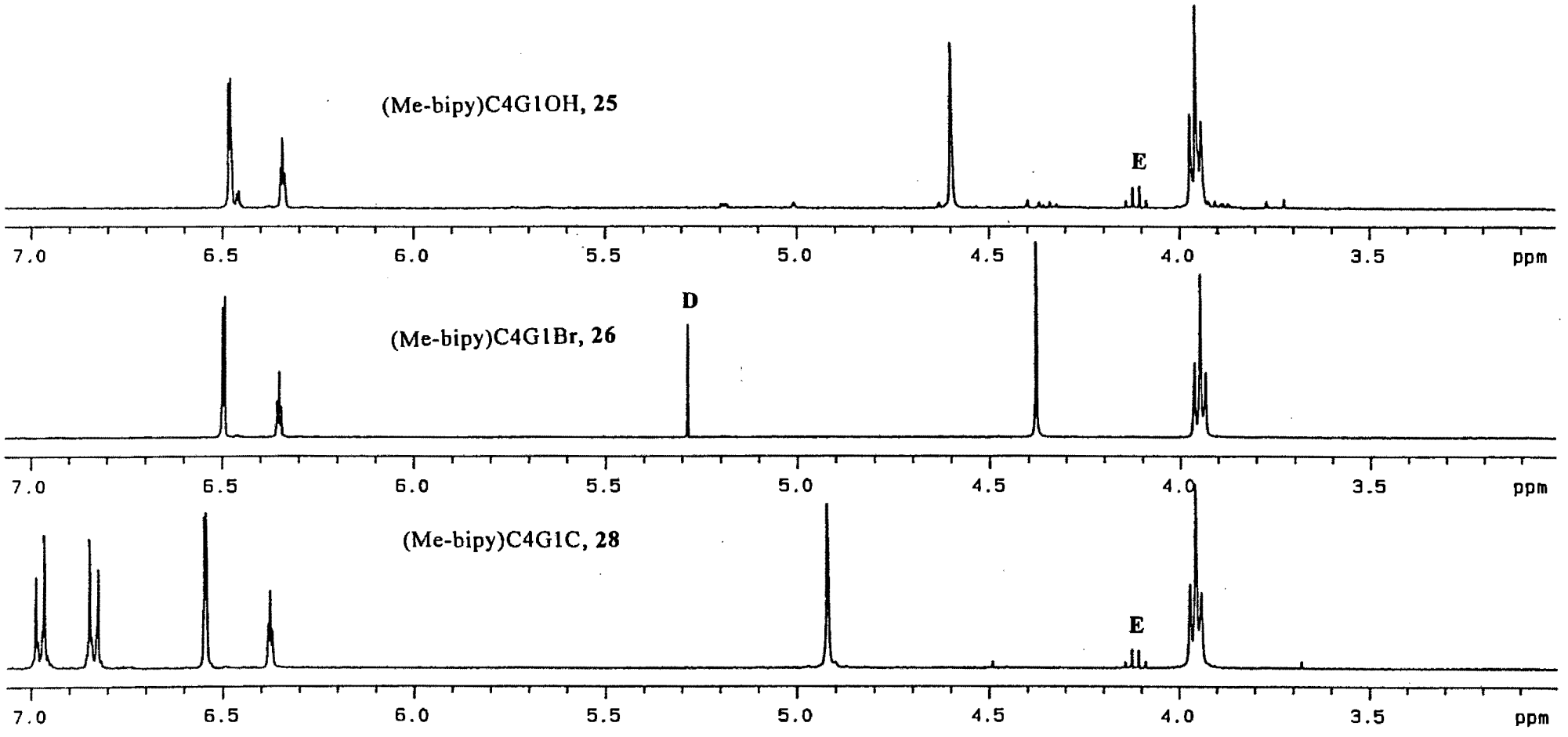

Figure 6.7 ^{1}H NMR spectrum of the first generation dendrimers in the region 3.0 - 7.0 ppm (400 MHz, X = $CDCl_3$, D = CH_2Cl_2, E = ethyl acetate).

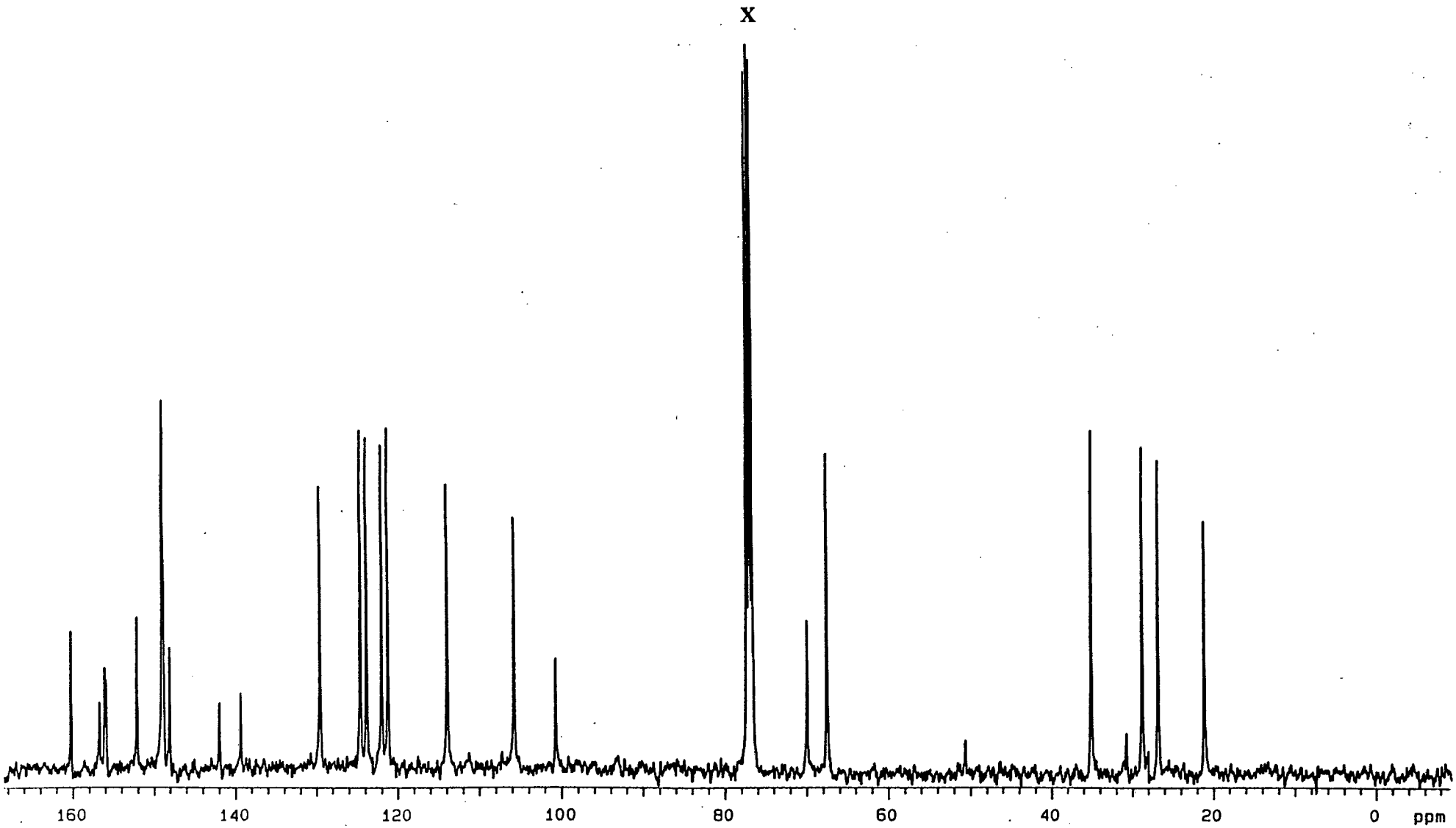

Figure 6.8 ^{13}C NMR spectrum of the first generation dendrimer, 28 (100 MHz, X = $CDCl_3$).

^{13}C NMR spectroscopy added further support to the structural assignments made by the ^{1}H NMR. Effort was made to completely assign the resonances in the ^{13}C NMR spectra of these dendrimers, which are given in the experimental section 7.6.2. Figure 6.8 shows the ^{13}C NMR spectrum of the first generation dendrimer Me-bipyC4G1C (**28**).

All the Me-bipy groups give the same set of signals for compounds **25** - **28** due to their symmetrical structures. However, the carbon atoms of the bipy rings give rise to 10 distinguishable signals in the range δ 121 to 156 ppm, which is due to the effect of different R groups at the 4 and 4′ positions. The resonances of the aromatic carbons are observed in the region δ 100 - 160 ppm and these have been assigned (see experimental section 7.6.2). The change of the resonances due to the focal CH_2 groups are clearly discernible for various functional groups, such as $-CH_2OH$ (65.3), $-CH_2Br$ (33.6) and $-CH_2O(C_6H_4)$ (69.9 ppm).

Electrospray mass spectroscopy

The new compounds **25** - **28** have been characterized by ES mass spectroscopy. Single-charged molecular ions $[M]^+$ are observed in the spectra of **25** - **28**, which unambiguously confirm the formulae of these compounds. In addition, multi-charged ions due to $[M + nH]^{n+1}$ (n = number of bipy rings - 1) are also observed. For each compound, the molecular mass calculated by the multi-charged ions is in accordance with that obtained by the single-charged species.

Elemental analysis

Satisfactory elemental analysis results were obtained for the new compounds **25** - **28**. It was found that these molecules contained certain amounts of solvents of recrystallization, as were found in the ^{1}H NMR experiments. The results determined by the ^{1}H NMR experiments and those obtained from the elemental analysis are in consistant with each other. For example, the ^{1}H NMR spectrum of **28** shows that the compound contains 0.2 mole of ethyl acetate. The elemental

analysis found C, 77.30; H, 6.68; N, 8.15 %; which are in agreement with the data calculated for (**28** + 0.2 x $C_4H_8O_2$): C, 77.75; H, 6.61; N, 8.25 %.

We have successfully prepared and characterized new dendrimers containing Me-bipy pendant groups at the periphery of these dendrimers. We subsequently investigated the use of these dendrimers for the preparation of dendritic Pt(II) alkyl complexes and the results are reported in the following section.

6.2.4 Synthesis and characterization of the zero and first generation Pt(II) alkyl dendrimers

Synthesis

We have demonstrated, in chapter 4 and in an earlier section of this chapter, that the reactions of Me_2-bipy and **20** with $[Pt_2Me_4(SMe_2)_2]$ gave the mono- and bi-nuclear Pt(II) alkyl complexes respectively. Similarly, reacting **27** with $[Pt_2Me_4(SMe_2)_2]$ in acetone/benzene at room temperature for 9 hours gave the zero generation Pt(II) alkyl complex **29** as an orange-red solid in high yield (90%), as shown in Scheme 6.16. The reaction of **28** and $[Pt_2Me_4(SMe_2)_2]$ was similarly carried out for 9 hours. The ^1H NMR spectrum of the reaction product shows the existence of the free ligand, suggesting that the reaction did not go to completion. Thus, the reaction product reacted further with excess $[Pt_2Me_4(SMe_2)_2]$ in acetone for 16 hours, which gave the first generation Pt(II) alkyl dendrimer **30** as an orange-red solid.

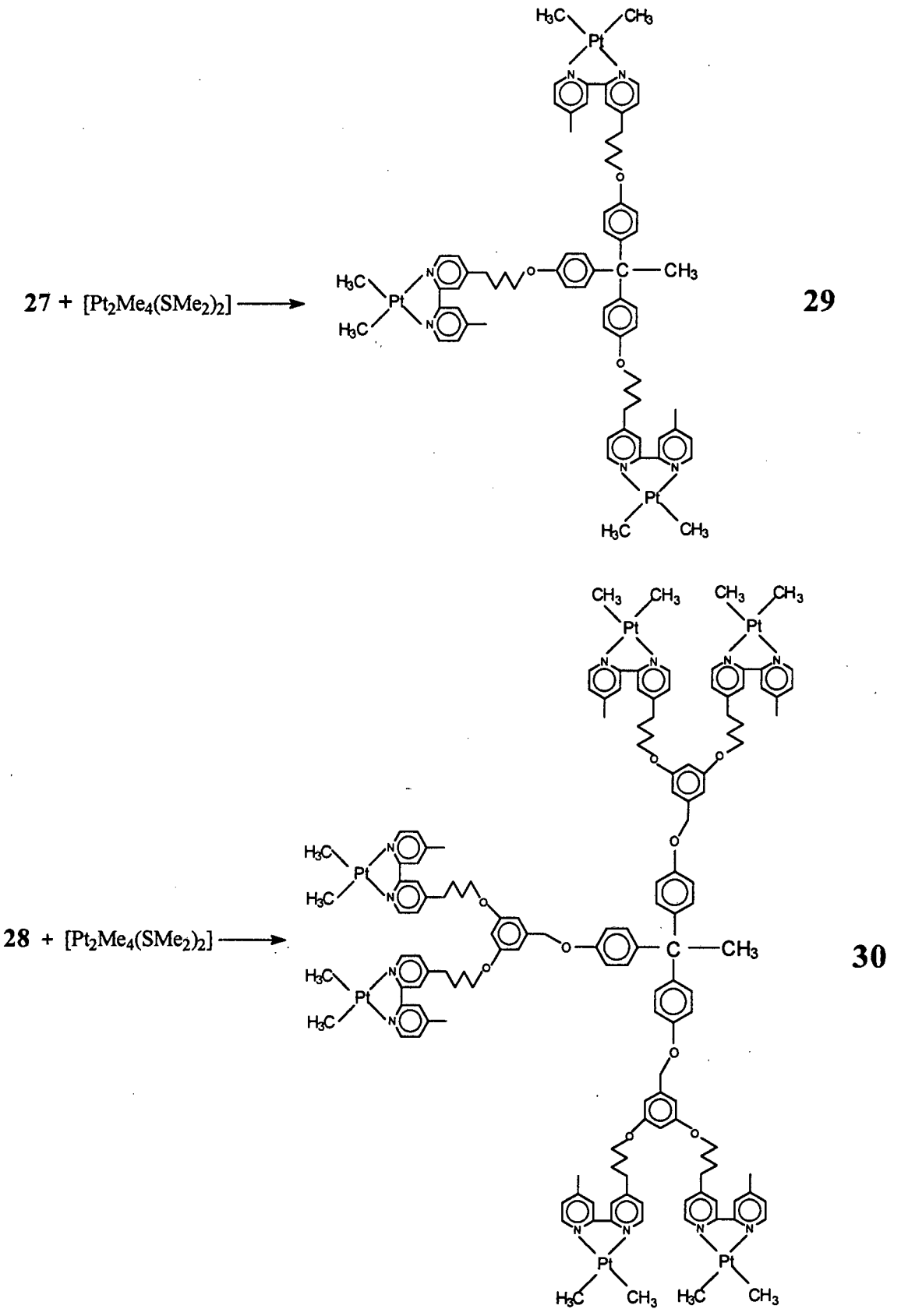

Scheme 6.16

Characterization

The dendrimers **29** and **30** have been characterized by UV-Vis, IR, ^{1}H NMR, elemental analysis and melting points, and in the case of **29** also ^{13}C NMR and ES mass spectroscopy. The data are given in the experimental section 7.6.2. The results are briefly discussed below.

We find that these dendritic complexes show similar spectroscopic properties as those found for the mononuclear complexes [$PtMe_2(R_2$-bipy)] and the binuclear complex [$Me_2Pt\{$(Me-bipy)-$(CH_2)_5$-(Me-bipy)$\}PtMe_2$], **21** as we anticipated. For example, the UV-Vis spectra of these dendrimers show an absorption band at λ_{max} = 454 nm which is due to the Pt(II)-diimine π^* metal to ligand charge transfer. Similar results have been obtained for the mononuclear and binuclear Pt(II) alkyl complexes [33]. The IR spectra show a band at 1611 cm^{-1} due to the bipy rings coordinated to platinum, as has been seen for **21**. The ^{1}H NMR spectra show the characteristic resonances of the Pt-CH_3 groups at 1.04 ppm with platinum satellites ^{2}J(Pt-H) 86 Hz for each compound (as shown in Figure 6.9 for the ^{1}H NMR spectrum of **29**). These data are similar to those observed for the complexes [$PtMe_2(R_2$-bipy)] [33] and **21**. The integration also confirms the formation of these dendrimers.

In addition, the solubility of the zero generation Pt(II) alkyl dendrimer **29** allowed us to further characterize this compound by ^{13}C NMR. The spectrum is shown in Figure 6.10 and the assignments are reported in the experimental section 7.6.2. The charateristic peak due to the Pt-CH_3 groups is found at δ -17.4 ppm with platinum satellites ^{2}J(Pt-C) 805 Hz which is similar to that found for [$PtMe_2(Me_2$-bipy)] [33]. The poor solubility of **30** precluded its characterization by ^{13}C NMR.

The complex **29** has also been characterized by ES mass spectroscopy. The experiment was carried out in $CH_3CN/CHCl_3$ with added NH_4OH, at source temperature 30 °C. A very weak peak at *m/z* 1654.77, $[M]^+$ is observed, which

corresponds to the calculated molecular mass (1654.74), at a cone voltage of 50V. Much stronger peaks corresponding to $[M + NH_3]^+$ and $[M + 2NH_3]^+$ are observed at *m/z* 1670.23 and 1687.54, respectively, with expected isotope patterns. This evidence further confirms the postulated structure of **29**.

6.3 Conclusion

A new, general method has been developed for the synthesis of polymethylene bridged heterobinuclear complexes of the type $[LM(CH_2)_nPtIMe_2(R_2\text{-bipy})]$, by the oxidative addition of the iodoalkyl complexes $[LM\{(CH_2)_nI\}]$ to $[PtMe_2(R_2\text{-bipy})]$ (R = H, CH_3). This gives a series of novel polymethylene bridged heterobinuclear complexes $[LM(CH_2)_nPtIMe_2(R_2\text{-bipy})]$ (where LM = $CpW(CO)_3$, R = H and CH_3, n = 3-5; LM = $Cp^*W(CO)_3$, R = H and CH_3, n = 3 and 4; LM = $CpFe(CO)_2$, R = H and CH_3, n = 4; LM = $CpRu(CO)_2$, R = H and CH_3, n = 4; LM = $Cp^*Fe(CO)_2$, R = H and CH_3, n = 3 and 4; and LM = $Re(CO)_5$, R = CH_3, n = 4). These complexes have been prepared in high yields and fully characterized by elemental analysis, IR, UV-vis, ^1H and ^{13}C NMR as well as FAB and ES mass spectroscopy.

The electrochemical behaviour of the heterobinuclear W/Pt complexes $[Wp(CH_2)_4PtIMe_2(Me_2\text{-bipy})]$ and $[Wp^*(CH_2)_4PtIMe_2(Me_2\text{-bipy})]$ has been investigated by cyclic voltammetry under both argon and carbon dioxide atmospheres. An intramolecular interaction may take place between the tungsten and platinum after oxidizing these complexes. These heterobinuclear complexes display different electrochemical properties to those of the mononuclear tungsten and platinum complexes.

The binuclear Pt(II) alkyl complex [$PtMe_2${(Me-bipy)-$(CH_2)_5$-(Me-bipy)}$PtMe_2$] has been prepared and its reactivity investigated. This binuclear complex shows similar spectroscopic and chemical properties to that of [$PtMe_2(Me_2$-bipy)].

New dendrimers containing Me-bipy pendant groups have been successfully synthesized using the stepwise convergent approach. The zero and first generation dendrimer {Me-bipy-$(CH_2)_4$-OC_6H_4}$_3CCH_3$ and {[Me-bipy-$(CH_2)_4$-O]$_2C_6H_3$-CH_2O-C_6H_4}$_3CCH_3$ contain 3 and 6 diimine functionalities respectively at the periphery of these molecules. These dendrimers have been fully characterized. We have also shown that the dendritic polynuclear Pt(II) alkyl complexes [{$PtMe_2$(Me-bipy)-$(CH_2)_4$-OC_6H_4}$_3CCH_3$] and {[$PtMe_2$(Me-bipy)-$(CH_2)_4$-O]$_2C_6H_3$-CH_2O-C_6H_4}$_3CCH_3$ can be obtained by the reactions of these Me-bipy containing dendrimers with [$Pt_2Me_4(SMe_2)_2$]. These new complexes have also been characterized. Since the new Me-bipy-containing dendrimers behave similarly to the monomer bipy and Me_2-bipy, we expect that these Me-bipy containing dendrimers may also be used to prepare other transition metal complexes.

References

1. W. Beck, B. Niemer and M. Wieser, Angew. Chem. Int. Ed. Engl., 1993, **32**, 923, and references therein.
2. For recent reviews of heterobinuclear complexes with metal-metal bonds, see (a): R. D. Adams, in *Comprehensive Organometallic Chemistry II,* Eds: E.W. Abel, F. G. A. Stone and G. Wilkinson, Pergamon: New York, 1995, vol 10, chapter 1, p1, (b): M. J. Chetcuti, *ibid.*, chapter 2, p 23.
3. R. J. Puddephatt, Polyhedron, 1988, **7**, 767.
4. S. Lotz, P. H. van Rooyen and R. Meyer, Adv. Organomet. Chem., 1995, **37**, 219.
5. S. Doherty, J. F. Corrigan, A. J. Carty and E. Sappa, Adv. Organomet. Chem., 1995, **37**, 39.
6. J. R. Moss and L. G. Scott, Coord. Chem. Rev., 1984, **60**, 171.
7. C. P. Casey and J. D. Audett, Chem. Rev., 1986, **86**, 339.
8. J. Holton, M. F. Lappert, R. Pearce and P. I. W. Yarrow, Chem. Rev. 1983, **83**, 135.
9. C. Masters, Adv. Organomet. Chem., 1979, **17**, 61.
10. J. Xiao and R. J. Puddephatt, Coord. Chem. Rev. 1995, **143**, 457.
11. J. R. Moss, Trends in Organomet. Chem., 1994, **1**, 211.
12. H. B. Friedrich, P.A. Makhesha, J. R. Moss and B. K. Williamson, J. Organomet. Chem., 1990, **384**, 325.
13. J. R. Moss and L. G. Scott, J. Organomet. Chem., 1989, **363**, 351.
14. R. B. King, Inorg. Chem., 1963, **2**, 531.
15. H. B. Friedrich and J. R. Moss, Adv. Organomet. Chem., 1991, **33**, 235.
16. H. B. Friedrich, P. A. Makhesha and J. R. Moss, J. Organomet. Chem., 1990, **384**, 325.
17. J. P. Collman and M. R. Maclaury, J. Am. Chem. Soc., 1974, **96**, 5247.
18. G. N, Schrauzer and R. J. Windgassen, J. Am. Chem. Soc., 1966, **88**, 3738.
19. K. P. Finch and J. R. Moss, J. Organomet. Chem., 1988, **346**, 253.
20. P. K. Monaghan and R. J. Puddephatt, Organometallics, 1985, **4**, 1406.

21. P. K. Monaghan and R. J. Puddephatt, J. Chem. Soc. Dalton Trans., 1988, 595.

22. P. K. Monaghan and R. J. Puddephatt, Inorg. Chim. Acta., 1983, **76,** L237.

23. P. K. Byers, A. J. Canty, B. W. Skelton, P. R. Traill, A. K. Watson and A.H. White, Organometallics, 1990, **9**, 3080.

24. J. D. Scott and R. J. Puddephatt, Inorg. Chim. Acta, 1984, **89**, L27.

25. G. J. Arsenault, M. Crespo and R. J. Puddephatt, Organometallics, 1987, **6**, 2255.

26. Review on heterobinuclear complexes, D. W. Stephan, Coord. Chem. Rev., 1989, **95**, 41.

27. J. C. Jeffery and M. J. Went, Polyhedron, 1988, **7**, 775.

28. F. R. Lemke and R. M. Bullock, Organometallics, 1992, **11,** 4261.

29. T. A. Hanna, A. M. Baranger and R. G. Bergman, J. Am. Chem. Soc., 1995, **117**, 11363.

30. J. R. Pinkes, B. D. Steffey, J. C. Vites and A. R. Cutler, Organometallics, 1994, **13**, 21.

31. (a): J. R. Moss, M. L. Niven and E. E. Sutton, Inorg. Chim. Acta, 1989, **165**, 165. (b): S-G. Shyu, J-S Wu, S-H Chuang, K-M. Chi and Y-S. Sung, J. Chem. Soc. Chem. Commun., 1996, 2239.
(c): B. C. Gates, *Catalytic Chemistry*, John Wiley & Sons, New York, 1992, p396.

32. see Chapter 5 of this thesis.

33. see Chapter 4 of this thesis.

34. N. Chaudhury and R. J. Puddephatt, J. Organomet. Chem., 1975, **84**, 105.

35. Y-H. Liao, Ph D. Thesis, University of Cape Town, 1994.

36. V. F. Sutcliffe and G. B. Young, Polyhedron, 1984, **3**, 87.

37. K. A. N. Verkerk, C. G. de Koster, B. A. Markies, J. Boersma, G. van Koten, W. Heerma and J. Haverkamp, Organometallics, 1995, **14**, 2081.

38. W. T. S. Huck, F. C. J. M. van Veggel and D. N. Reinhoudt, Angew. Chem. Int. Ed. Engl., 1996, **35**, 1213.

39. P. J. Dandliker, F. Diederich, J-P. Gisselbrecht, A. Louati and M. Gross, Angew. Chem. Int. Ed. Engl., 1995, **34**, 2725.

40. C. J. Levy, J. J. Vittal and R. J. Puddephatt, Organometallics, 1996, **15**, 2108.

41. S. S. M. Ling, I. R. Jobe, L. Manojlovic-Muir, K. W. Muir and R. J. Puddephatt, Organometallics, 1985, **4**, 1198.

42. R. J. Haines and A. L. du Preez, J. Chem. Soc. (A), 1970, 2341.

43. W. J. Geary, Coord. Chem. Rev., 1971, **7**, 81.

44. For a brief introduction of cyclic voltammetry, (a): P. T. Kissinger and W. R. Heineman, J. Chem. Educ., 1983, **60**, 702; (b): G. A. Mabbott, *ibid*, 1983, **60**, 697; (c): U. Loffler, Sensorik, 1994, **4** (Chemische Sensoren Heute und Morgen), 100-22, 174; Chem. Abstr., 1995, **123**:101385.

45. see Chapter 3 of this thesis.

46. R.H. Schmehl, R.A. Auerbach, W.F. Wacholtz, C.M. Elliott, R.A. Freitag and J.W. Merkert, Inorg. Chem., 1986, **25**, 2440.

47. M. Furue, T. Yoshidzumi, S. Kinoshita, T. Kushida, S. Nozakura and M. Kamachi, Bull. Chem. Soc. Jpn., 1991, **64**, 1632.

48. (a): G.R. Newkome, C.N. Moorefield and F. Vögtle, *Dendritic Molecules, Concepts, Syntheses, Perspectives*, VCH: Weinheim, 1996.
(b): G.R. Newkome (ed.) *Advances in Dendritic Macromolecules*, vol 1, JAI Press Inc.: Connecticut, 1994; vol 2, 1995.

49. R.F. Service, Science, 1995, **267**, 458.

50. R. Dagani, Chem. Eng. News, June 3, 1996, p 30.

51. N. Ardoin and D. Astruc, Bull. Soc. Chim. Fr., 1995, **132**, 875.

52. P.R. Dvornic and D.A. Tomalia, Curr. Opin. Colloid. Interface - Sci., 1996, **1**, 221.

53. D.A. Tomalia, Aldrichimica Acta, 1993, **26**, 91.

54. J.R. Moss, Platinum Metals Rev., 1995, **39**, 33.

55. N.J. Turro, J.K. Barton and D.A. Tomalia, Acc. Chem. Res., 1991, **24**, 332.

56. J.W.J. Knapen, A.W. van der Made, J. C. de Wilde, P.W.N.M. van Leeuwen, P. Wijkens, D. M. Grove and G. van Koten, Nature, **372**, 659.

57 J.H. Cameron, A. Facher, G. Lattermann and S. Diele, Adv. Mater., 1997, **9**, 398.

58. D.M. Junge and D.V. McGrath, J. Chem. Soc. Chem. Commun., 1997, 857.

59. S. Serroni, G. Denti, S. Campagna, A. Juris, M. Ciano and V. Balzani, Angew. Chem. Int. Ed. Engl., 1992, **31**, 1493.

60. A. Miedaner, C.J. Curtis, R. M. Barkley and D.L. DuBois, Inorg. Chem., 1994, **33**, 5482.

61. Some recent papers of dendrimers containing transition metals, see
(a): V.J. Catalano and N. Parodi, Inorg. Chem., 1997, **36**, 537.
(b): G.R. Newkome, J. Groß, C.N. Moorefield and B.D. Woosley, J. Chem. Soc. Chem. Commun., 1997, 515.
(c): P. Jutzi, C. Batz, B. Neumann and H-G. Stammler, Angew. Chem. Int. Ed. Engl., 1996, **35**, 2118.
(d): C. Valério, J-L. Fillaut, J. Ruiz, J. Guittard, J-C. Blais and D. Astruc, J. Am. Chem. Soc., 1997, **119**, 2588.
(e): F. Moulines, L. Djakovitch, R. Boese, B. Gloaguen, W. Thiel, J-L. Fillaut, M-H. Delville and D. Astruc, Angew. Chem. Int. Ed. Engl., 1993, **32**, 1075.
(f): G.R. Newkome, F. Cardullo, E.C. Constable, C.N. Moorefield and A.M.W.C. Thompson, J. Chem. Soc., Chem. Commun., 1993, 925.
(g): C-F. Shu and H-M. Shen, J. Mater. Chem., 1997, **7**, 47.
(h): F. Lobete, I. Cuadrado, C.M. Casado, B. Alonso, M. Morán and J. Losada, J. Organomet. Chem., 1996, **509**, 109.
(i): I. Cuadrado, M. Morán, C.M. Casado, B. Alonso, F. Lobete, B. García, M. Ibisate and J. Losada, Organometallics, 1996, **15**, 5278.
(j): M. Slany, M. Bardají, M-J. Casanove, A-M. Caminade, J-P. Majoral and B. Chaudret, J. Am. Chem. Soc., 1995, **117**, 9764.

62. Some recent papers of organic dendrimers, see
(a): K.L. Wooley, C.J. Hawker and J.M.J. Fréchet, J. Chem. Soc. Perkin Trans. 1, 1991, 1059.
(b): C.J. Hawker, K.L. Wooley and J.M.J. Fréchet, J. Chem. Soc. Perkin Trans.1, 1993, 1287.
(c): N. Launay, A-M. Caminade, R. Lagana and J-P Majoral, Angew. Chem. Int. Ed. Engl., 1994, **33**, 1589.

(d): A.B. Padias, H.K. Hall, D.A. Tomalia and J.R. McConnell, J. Org. Chem., 1987, **52**, 5305.

(e): H-B. Mekelburger and F. Vögtle, Supramolecular Chem., 1993, **1**, 187.

(f): V.S.K. Balagurusamy, G. Ungar, V. Percec and G. Johansson, J. Am. Chem. Soc., 1997, **119**, 1539.

(g): P. Bharathi and J.S. Moore, J. Am. Chem. Soc., 1997, **119**, 3391.

(h): B. Karakaya, W. Claussen, K. Gessler, W. Saenger and A-D. Schlüter, J. Am. Chem. Soc., 1997, **119**, 3296.

(i): E. Cloutet, J-L. Fillaut, Y. Gnanou and D. Astruc, J. Chem. Soc. Chem. Commun., 1996, 2047.

(j): F. Morgenroth, E. Reuther and K. Müllen, Angew. Chem. Int. Ed. Engl., 1997, **36**, 631.

(k): N. Launay, A-M. Caminade and J.P. Majoral, J. Organomet. Chem., 1997, **529**, 51.

63. D.A. Tomalia, A.M. Naylor and W.A. Goggard III, Angew. Chem. Int. Ed. Engl., 1990, **29**, 138.

64. D.A. Tomalia and H.D. Durst, Top. Curr. Chem., 1993, **165**, 193.

65. J. Issberner, R. Moors and F. Vogtle, Angew. Chem. Int. Ed. Engl., 1994, **33**, 2413.

66. C. Hawker and J.M.J. Fréchet, J. Chem. Soc., Chem. Commun., 1990, 1010.

67. D.A. Tomalia, H. Baker, J. Dewald, M. Hall, G. Kallos, S. Martin, J. Roeck, J. Ryder and P. Smith, Macromolecules, 1986, **19**, 2466.

68. (a): S. Achar, J.J. Vittal and R.J. Puddephatt, Organometallics, 1996, **15**, 43.

(b): S. Achar and R.J. Puddephatt, Angew. Chem. Int. Ed. Engl., 1994, **33**, 847.

(c): S. Achar and R.J. Puddephatt, J. Chem. Soc. Chem. Commun., 1994, 1895.

(d): S. Achar, R.J. Puddephatt and J.D. Scott, Polyhedron, 1996, **15**, 2363.

(e): S. Achar and R.J. Puddephatt, Organometallics, 1995, **14**, 1681.

(f): G-X. Liu and R.J. Puddephatt, Inorg. Chim. Acta, 1996, **251**, 319.

69. M. Bardaji, M. Kustos, A-M. Caminade, J-P. Majoral and B. Chaudret, Organometallics, 1997, **16**, 403.

70. G-X. Liu and R.J. Puddephatt, Organometallics, 1996, **15**, 5257.

71. N.B. Colthup, *Introduction to Infrared and Raman Spectroscopy*, Academic Press: New York, 1990.

72 (a): Y-H. Liao and J.R. Moss, Organometallics, 1996, **15**, 4307.
(b): Y-H. Liao and J.R. Moss, Organometallics, 1995, **14**, 2130.
(c): Y-H. Liao and J.R. Moss, J. Chem. Soc. Chem. Commun., 1993, 1774.

73. J.F.G.A. Jansen, E.M.M. de Brabander-van den Berg, E.W. Meijer, Science, 1994, **266**, 1226.

Chapter 7
Experimental

7.1 General

All reactions were carried out under an atmosphere of high purity nitrogen using standard Schlenk tube techniques, unless stated otherwise.

The solvents used were generally analytical grade and were purified by distillation under a nitrogen atmosphere as described in the following text. Tetrahydrofuran (THF), diethyl ether (ether) and petroleum ether were dried by distilling over sodium/benezophonone. Hexane, heptane, benzene and toluene were distilled over sodium wire. Dichloromethane (CH_2Cl_2) was distilled over anhydrous $CaCl_2$. Acetone was distilled over anhydrous $CaCl_2$ or K_2CO_3. Acetonitrile was distilled over P_2O_5. Pyridine and dimethylformamide (DMF) were dried over sodium hydroxide pellets. Methanol (MeOH), ethanol (EtOH) and triethylamine (NEt_3) were distilled over molecular sieve (3A or 4A).

$[Mn_2(CO)_{10}]$, $[Re_2(CO)_{10}]$, $[W(CO)_6]$, $[CpFe(CO)_2]_2$, $[Cp^*Fe(CO)_2]_2$ and $[CpW(CO)_3]_2$ were obtained from Strem Chemical Inc., USA and were used without further purification. The complexes $[Cp^*W(CO)_3]_2$ [1], $[Mn(CO)_5(CH_3)]$ [2], $[Re(CO)_5(C_{16}H_{33})]$ [3], $[CpFe(CO)_2(CH_3)]$ [4] and $[CpFe(CO)_2(C_{11}H_{23})]$ [5] were prepared by literature methods. Alumina (BDH, active neutral, Brockman grade I) was deactivated before use. Silica gel 60 (35 - 70 mesh) and Florisil (60 - 100 mesh) were purchased from Merck, while silica gel (60 - 100 mesh) was obtained from BDH. All other reagents were obtained commercially and were used without purification, unless otherwise stated. The carbon dioxide gas used was high purity grade (99.995 %) obtained from Messer Griesheim, Germany.

Melting points were recorded on a Kofler hot stage microscope (Reichert Thermovar) and are uncorrected. Differential scanning calorimetry (DSC) and thermal gravimetry analysis (TGA) were performed on a Perkin-Elmer PC Series

7 instrument under a nitrogen atmosphere with a heating rate of 10 or 20 °C per minute.

Microanalyses were performed by the University of Cape Town Microanalytical Laboratory.

Infrared spectra were recorded either on a Perkin-Elmer 983 or a Paragon 1000 FT-IR spectrophotometer in solution cells with NaCl windows, between NaCl or CsI plates as neat films or Nujol mulls, or as KBr, KI or CsI discs. The following abbreviations are used in the description of infrared spectra: w = weak, m = medium, s = strong, sh = shoulder and br = broad.

Ultraviolet and visible (UV-vis) spectra were recorded on a Hewlett-Packard 8452A Diode Array Spectrophotometer in a 1 cm quartz cell at room temperature.

^{1}H NMR spectra were recorded on a Varian XR 200 (200 MHz) spectrometer or a Varian Unity 400 (400 MHz) spectrometer. ^{13}C NMR spectra were recorded on the Varian XR 200 (50 MHz) spectrometer or the Varian Unity 400 (100 MHz) spectrometer. The chemical shifts are relative to TMS (0 ppm) in the ^{1}H and ^{13}C NMR spectra whereas the deuterated solvent signals were used as references and the chemical shifts adjusted accordingly. ^{31}P NMR spectra were recorded on the Varian Unity 400 (161.9 MHz) spectrometer. The chemical shifts are relative to external H_3PO_4. ^{195}Pt NMR spectra were also recorded on the Varian Unity 400 (85.6 MHz) spectrometer. The chemical shifts are relative to external H_2PtCl_6 (500 mg in 1 ml 30% (vol/vol) D_2O/1 M HCl). The following abbreviations are used in the description of NMR spectra: s = singlet, d = doublet, t = triplet, q = quartet, qn = quintet, m = multiplet and br = broad.

Low resolution mass spectra were recorded with a VG Micromass 16F spectrometer operated at 70eV ionizing voltage and using an accelerating voltage of 4 kV. Fast atom bombardment (FAB) mass spectra were obtained from the University of California, Riverside, Colorado State University, USA and the Cape

Technikon of South Africa. Electrospray mass spectra were obtained from the University of Stellenbosch on a VG Quattro mass spectrometer.

Cyclic voltammetry (CV) was carried out on a BAS-100B electrochemical analyser in a one-compartment three-electrode system, consisting of Ag/Ag^{+} (0.01 M) as the reference electrode, platinum wire as the auxiliary electrode and a platinum disk electrode as the working electrode. The supporting electrolyte was a solution of 0.1 M $[NBu^{n}_{4}][ClO_4]$ in dry acetonitrile. The potentials E were recorded without IR compensation. All potentials reported are relative to the half-wave potential E1/2 of the ferrocene/ferrocenium couple run under the same conditions. The experiments were performed on 1.0 mM solutions under an argon or a carbon dioxide atmosphere at room temperature. The solutions were saturated with argon or carbon dioxide by bubbling the gas for 10 - 25 minutes at room temperature and atmospheric pressure. The platinum disk electrode was polished after every three runs.

The conductivity measurements were performed on a Metrohm 660 conductometer in 1.0 mM nitrobenzene solutions at room temperature.

All high pressure reactions were carried out in a 250 ml Berghoff autoclave.

Solvents were removed under reduced pressure and the resultant samples were dried under high vacuum (0.01 - 0.1 mmHg), unless otherwise stated.

7.2 Experimental details pertaining to Chapter 2

7.2.1 Synthesis of acyl complexes $[Mn(CO)_5\{C(O)R'\}]$ and alkoxycarbonyl $[Mn(CO)_5\{C(O)OR\}]$ complexes

Preparation of the acyl complexes $[Mn(CO)_5\{C(O)R'\}]$

The acyl complexes $[Mn(CO)_5\{C(O)R'\}]$ (R' = *n*-C_6H_{13} to *n*-C_9H_{19}, *n*-$C_{11}H_{23}$, and *n*-$C_{15}H_{31}$) were prepared according to the literature method [6]. A modified procedure was used to prepare $[Mn(CO)_5\{C(O)C_{11}H_{23}\}]$ in better yield. The procedure is described below:

A solution of $Na[Mn(CO)_5]$ (11.3 mmol) was prepared by the reaction of $[Mn_2(CO)_{10}]$ (2.20 g, 5.65 mmol) with a sodium amalgam (0.60 g Na/6 ml Hg) in THF (40 ml) for 4.5 hours at room temperature. This solution was added dropwise with stirring during 5 minutes to lauroyl chloride (2.50 g, 11.3 mmol) in THF (5 ml) at room temperature. The solution was stirred for 5 hours and then the solvent was removed under reduced pressure, leaving a yellow residue. This was extracted with CH_2Cl_2 (3 x 50 ml) and the combined extracts were filtered through a short alumina column. The solvent was removed from the filtrate to give a pale yellow solid. This was dissolved in a minimum amount of hexane and chromatography on an alumina column (15 cm x 1.3 cm) with hexane as eluant. This gave a yellow band $[Mn_2(CO)_{10}]$ followed immediately by a second, virtually colourless band. The solvent was removed from the second band under reduced pressure to give a pale yellow solid. Recrystallization from hexane at -78 °C gave $[Mn(CO)_5\{C(O)C_{11}H_{23}\}]$ (2.50 g, 59%) as an off-white crystalline solid, m.p., 27 - 30 °C; IR ν(CO) (hexane): 2114w, 2050w, 2007s, 1969w, 1658w cm^{-1}. The m.p. and IR data are in agreement with the literature data for $[Mn(CO)_5\{C(O)C_{11}H_{23}\}]$ [6]. The DSC and TGA analyses were performed and the results are given in the section 2.2.1 of this thesis.

Synthesis of new long-chain alkoxycarbonyl manganese pentacarbonyl complexes [$Mn(CO)_5${C(O)OR}] (R = CH_2R') - Reaction of the acyl complexes [$Mn(CO)_5${C(O)R'}] with syngas in hexane

The complexes [$Mn(CO)_5${C(O)OR}] (R= *n*-C_7H_{15}, *n*-C_8H_{17}, *n*-C_9H_{19}, *n*-$C_{10}H_{21}$, and *n*-$C_{16}H_{33}$) were synthesized by the reaction of the acyl complexes [$Mn(CO)_5${C(O)R'}] (R' = *n*-C_6H_{13} to *n*-C_9H_{19}, and *n*-$C_{15}H_{31}$) with syngas (CO/H_2) in hexane according to the following general procedure.

In a typical reaction, the autoclave was charged with the acyl complex [$Mn(CO)_5${C(O)R'}] (*ca.* 200 mg) in hexane (10 ml) with a stirrer bar in a flask and sealed. The autoclave was filled with CO/H_2 (20 bar) and the gas vented. This procedure was repeated two more times and then the autoclave was pressurized with CO/H_2 until a total pressure of 40 bar was reached. The reaction mixture was heated to *ca* 60 °C for 3 hours. During this time the pressure was maintained at *ca* 46 bar. At the end of 3 hours, the autoclave was cooled to room temperature and the gas vented. A dark yellow solution was obtained, which gave a yellow filtrate. The solvent was removed from this filtrate, leaving a yellow residue. This was then dissolved in a minimum amount of petroleum ether (b.p. 40 - 60 °C) and the solution cooled to -78 °C to crystallize the product. The product was recrystallized again to give the alkoxycarbonyl complex [$Mn(CO)_5${C(O)OR}] (R = CH_2R') as an off-white microcrystalline solid. This is a general procedure.

The complex [$Mn(CO)_5${C(O)$OC_{12}H_{25}$}] was similarly prepared by the reaction of [$Mn(CO)_5${C(O)$C_{11}H_{23}$}] (2.50 g, 6.3 mmol) with CO/H_2 (45 bar) in hexane (20 ml) at 60 °C, with a longer reaction time (15 hours). Recrystallization from pentane twice at -78 °C gave the complex [$Mn(CO)_5${C(O)$OC_{12}H_{25}$}] (2.35 g, 87%) as a white microcrystalline solid.

All the new alkoxycarbonyl complexes were fully characterized by elemental analysis, IR, ^1H NMR, ^{13}C NMR, mass spectra, melting point and DSC/TGA. The characterization data are given in the section 2.2.3 of this thesis.

7.2.2 Reactivity of acyl complexes [$Mn(CO)_5\{C(O)R'\}$] and alkoxycarbonyl complexes [$Mn(CO)_5\{C(O)OR\}$]

Reaction of the acyl complex [$Mn(CO)_5\{C(O)C_{11}H_{23}\}$] with syngas in THF: Synthesis of alcohol

The reaction was carried out in an autoclave which was charged with [$Mn(CO)_5\{C(O)C_{11}H_{23}\}$] (0.20 g, 0.53 mmol) and THF (15 ml). The autoclave was sealed and filled with syngas to 20 bar and the gas vented. This procedure was repeated two more times. The autoclave was then pressurized with syngas to 48 bar. The solution was then heated at 60 °C for 4 hours with stirring. The autoclave was allowed to cool to room temperature and the gas vented. IR analysis of the solution revealed that *ca.* 1/2 of the starting complex was converted. Thus, the reaction was continued at the abovementioned conditions for additional 4 hours. The autoclave was again allowed to cool to room temperature and the gas vented. A yellow solution was obtained. After removing the solvent under vacuum, a yellow solid was obtained. The IR spectrum of the removing solution showed two ν(CO) bands at 2020s, 1995s cm^{-1}, suggesting that the solution contained a small amount (< 5%) of [$HMn(CO)_5$] [7]. The yellow solid was dissolved in a minimum amount of CH_2Cl_2/pentane (1/4) and chromatographed on a short silica gel column (7 cm x 2 cm). Elution with 5% CH_2Cl_2/pentane separated a yellow band, which, on evaporation of the solvent and drying under vacuum, yielded a yellow solid identified as [$Mn_2(CO)_{10}$] (0.097 g, 95%), on the basis of its IR spectrum {ν(CO) in Nujol mull, 2045s, 2013vs, 1983m cm^{-1}, these data are the same as the IR spectrum of authentic [$Mn_2(CO)_{10}$] [8]}. Elution with CH_2Cl_2 separated a second band which was colurless. After removing the solvent and drying under vacuum, this gave an off-white solid which was identified as *n*-$C_{12}H_{25}OH$ (0.090 g, 92%), on the basis of its melting point, IR, MS, ^1H NMR and ^{13}C NMR data; m.p. 24-27 °C (literature [9] 26 °C), IR ν/cm^{-1} (neat): 3343m, br (νOH), 2925s, 2854s [$\nu(CH_2 + CH_3)$], 1466m, 1378w, 1056m, 720w; ^1H NMR ($CDCl_3$) δ (ppm): 3.88 (2H, br, CH_2O), 2.46 (1H, br, OH), 1.53 (2H, m, CH_2CH_2O), 1.25 (18H, br, 9xCH_2), 0.86(3H, br, CH_3); ^{13}C

NMR ($CDCl_3$) δ (ppm): 63.44 (CH_2OH), 32.94, 31.92, 29.62, 29.46, 29.35, 25.80, 22.68, 14.09 (CH_3). These data are in good agreement with the reported melting point [9], IR [10], ^1H NMR [11] and ^{13}C NMR [12] data.

Reaction of $[Mn(CO)_5\{C(O)OC_{12}H_{25}\}]$ with syngas in hexane at 85 °C

A solution of $[Mn(CO)_5\{C(O)OC_{12}H_{25}\}]$ (0.13 g, 0.32 mmol) in hexane (10 ml) in a flask was placed in an autoclave. The autoclave was sealed and filled with syngas to 20 bar and the gas vented. This procedure was repeated two more times. The autoclave was then pressurized with syngas to 48 bar. The solution was then heated at 85 °C for 4.5 hours with stirring. The autoclave was allowed to cool to room temperature and the gas vented. An IR spectrum of the reaction mixture showed that there was still unreacted starting material. The reaction was continued using the same conditions as above for additional 6.5 hours. The autoclave was again allowed to cool to room temperature and the gas vented. A yellow solution was obtained. After removing the solvent under reduced pressure, a mixture of white and yellow solids was obtained, which was dissolved in a minimum amount of 5% CH_2Cl_2/hexane and chromatographed on a short silica gel column (7 cm x 2 cm). Three fractions were obtained. Elution with 5% CH_2Cl_2/hexane separated a yellow band. A yellow solid was obtained by evaporation of the solvent and drying under vacuum. The yellow solid was identified as $[Mn_2(CO)_{10}]$ (0.060g, 96%) on the basis of its IR spectrum (in Nujol mull, 2045s, 2013vs, 1983m cm^{-1}) [8]. The second band was colourless and gave an off-white solid *n*-$C_{12}H_{25}O_2CH$ (0.024g, 33%), mass spectrum M^+ = 169 (M-HCO_2); IR (neat) ν/cm^{-1}: 2925s, 2856s, 1725vs, 1467m, 1380w, 1178s, 1022m; ^1H NMR ($CDCl_3$) δ (ppm): 8.04 (1H, s, HCO_2), 4.14 (2H, br, CO_2CH_2), 1.64 (2H, br), 1.24 (18H, br), 0.83 (3H, br); ^{13}C NMR ($CDCl_3$) δ (ppm): 161.28 (CO_2), 64.16, 31.93, 29.63, 29.56, 29.51, 29.35, 29.20, 28.53, 25.84, 22.70, 14.12. These data are in agreement with the reported IR [10], ^1H [11] and ^{13}C [12] NMR data. The third fraction gave a white solid *n*-$C_{12}H_{25}OH$ (0.39g, 66%), mass spectrum M^+ = 169 (M-OH); IR (neat) ν/cm^{-1}: 3339m, br (νOH), 2925s, 2854s [ν(CH_2 + CH_3)], 1466m, 1378w, 1123w, 1056m, 892w, 720w; ^1H NMR ($CDCl_3$) δ (ppm):

3.61 [2H, t, J(HH) 6.4 Hz, CH_2O], 1.55 [2H, t, J(HH) 6.4 Hz, CH_2CH_2O], 1.39 - 1.24 (18H, br), 0.86 [3H, t, J(HH) 6.4 Hz, CH_3]. These data are in agreement with the reported IR [10] and ^1H NMR [11] data.

Reaction of $[Mn(CO)_5\{C(O)OC_{12}H_{25}\}]$ with syngas in THF

The reaction was carried out in a similar way to that described previously for the reaction of $[Mn(CO)_5\{C(O)OC_{12}H_{25}\}]$ with syngas in hexane.

A solution of $[Mn(CO)_5\{C(O)OC_{12}H_{25}\}]$ (0.20 g, 0.49 mmol) in THF (10 ml) in a flask was placed in an autoclave. The autoclave was sealed and filled with syngas to 20 bar and the gas vented. This procedure was repeated two more times. The autoclave was then pressurized with syngas to 48 bar. The solution was then heated at 60 °C for 8 hours with stirring. The autoclave was allowed to cool to room temperature and the gas vented. An IR spectrum of the reaction mixture showed that there was still unreacted starting material. The reaction was continued using the same conditions as above for additional 15 hours. The autoclave was again allowed to cool to room temperature and the gas vented. A yellow solution was obtained. After removing the solvent under vacuum, a mixture of white and yellow solids was obtained. The IR spectrum of the removing solution showed two ν(CO) bands at 2019s, 1993s cm^{-1}, suggesting that the solution contained $[HMn(CO)_5]$ [7]. The solid mixture was dissolved in a minimum amount of 5% CH_2Cl_2/pentane and chromatographed on a short silica gel column (7 cm x 2 cm). Four fractions were obtained. The first fraction, eluted with 5% CH_2Cl_2/pentane, was a yellow band. Evaporation of the solvent and drying under vacuum gave a yellow solid, which was identified as $[Mn_2(CO)_{10}]$ (0.06g, 63%), on the basis of its IR spectrum [8]. The other fractions were eluted with CH_2Cl_2. The second band gave a white solid product and was identified as *n*-$C_{12}H_{25}OH$ (0.04 g, 46%), IR (neat) ν/cm^{-1}: 3346m, br (νOH), 2926s, 2855s [$\nu(CH_2+CH_3)$], 1466m, 1378w, 1123w, 1058m, 907w (the IR spectrum also shown very week peak at 2046w, 2032w, 2012w cm^{-1} presumably due to a trace amount of $[Mn_2(CO)_{10}]$; ^1H NMR ($CDCl_3$) δ (ppm): 3.65 (2H, br, CH_2O), 1.55

(2H, br, CH_2CH_2O), 1.26 (18H, br), 0.86 (3H, br, CH_3). These data are in agreement with the reported IR [10] and ^1H NMR [11] data. The next product was identified as an ester $CH_3(CH_2)_3CO_2(CH_2)_{11}CH_3$ (0.06 g, 43%), mass spectrum M^+ = 271 (calculated for $C_{17}H_{34}O_2$ M = 270.5); IR (neat) ν/cm^{-1}: 2925s, 2854s, 1768s, 1461m, 1377w, 1168m, 1037m, 993w, 931w, 869w; ^1H NMR ($CDCl_3$) δ (ppm): 4.29, 3.58, 2.43, 2.21, 1.50, 1.20, 0.82 (These showed that the sample contained some impurity *n*-$C_{12}H_{25}OH$, but the peak at 4.29 ppm is a characteristic peak for CO_2CH_2); ^{13}C NMR ($CDCl_3$) δ (ppm): 177.82 (CO_2), 68.54 (CO_2CH_2) , 32.85, 31.88, 29.60, 29.43, 29.32, 27.78, 25.77, 22.66, 22.16, 14.08. These data are in agreement with the reported IR [10], ^1H NMR [11] and ^{13}C NMR [12] data. The last product was identified as *n*-$C_{12}H_{25}O_2CH$ (*ca.* 0.015 g, 12%) by its characteristic IR ν(C=O) peak at 1723 cm^{-1} and ^1H NMR peak at 8.01 ppm (HCO_2). Some overlapping of these fractions were observed, however, these products can be distinguished by ^1H NMR spectroscopy.

Reaction of $[Mn(CO)_5\{C(O)OC_{12}H_{25}\}]$ with tetrafluoroboric acid HBF_4 and boron trifluoride etherate $BF_3(OEt_2)$

Reaction of $[Mn(CO)_5\{C(O)OC_{12}H_{25}\}]$ with HBF_4 in $CDCl_3$

To a solution of $[Mn(CO)_5\{C(O)OC_{12}H_{25}\}]$ (0.020 g, 0.049 mmol) in $CDCl_3$ (0.8 ml) in a NMR tube was added HBF_4 (40% aqueous solution, 4 drops) at room temperature. The NMR tube was shaken to mix the components. A white precipitate was formed immediately. After *ca.* 5 minutes, ^1H NMR spectrum of the resulting solution was run. It showed the complete conversion of the starting material to *n*-$C_{12}H_{25}OH$; ^1H NMR δ (ppm): 3.63 (2H, br, CH_2OH), 1.56 (2H, br, CH_2CH_2OH), 1.25 (18H, br), 0.87 (3H, br, CH_3) [11]. No peak which could be assigned to formate was observed. The white precipitate was analyzed by IR spectroscopy, which showed a ν(CO) peak at 2094 cm^{-1} (Nujol mull) due to $[Mn(CO)_6][BF_4]$ (literature [13] $[Mn(CO)_6][BF_4]$ in THF, 2090 cm^{-1}). The formation of $[Mn_2(CO)_{10}]$ was also observed by IR spectroscopy [ν(CO) in THF: 2045s, 2009vs, 1980m cm^{-1}]. These data are identical to the data obtained using the authentic $[Mn_2(CO)_{10}]$.

Reaction of [Mn(CO)$_5${C(O)OC$_{12}$H$_{25}$}] with BF$_3$(OEt$_2$) in hexane

To a solution of [Mn(CO)$_5${C(O)OC$_{12}$H$_{25}$}] (*ca.*0.011 g, 0.03 mmol) in hexane (2 ml) was added BF$_3$(OEt$_2$) (48 % solution in diethyl ether, 3 drops) at room temperature. A white precipitate was formed immediately. The mixture was shaken for 5 minutes. The solvent was removed from the reaction mixture and the white precipitate was then washed once with hexane (1 ml). The IR spectrum of the white precipitate (in Nujol mull) showed a strong ν(CO) bands at 2096 cm^{-1} due to [Mn(CO)$_6$][BF$_4$] [13]. The IR spectrum of the hexane solution showed the presence of [Mn$_2$(CO)$_{10}$] (ν(CO) 2046s, 2014s and 1984m cm^{-1}) [8].

Reaction of [Mn(CO)$_5${C(O)OC$_{12}$H$_{25}$}] with HCl

To a solution of [Mn(CO)$_5${C(O)OC$_{12}$H$_{25}$}] (0.020 g, 0.05 mmol) in CDCl$_3$ (0.8 ml) in a NMR tube was added HCl (36% aqueous solution, 4 drops) at room temperature. The NMR tube was shaken to mix the components. After *ca.* 5 minutes, ^{1}H NMR spectrum of the resulting solution was run. It showed the complete conversion of the starting materials to *n*-C$_{12}$H$_{25}$OH; ^{1}H NMR δ (ppm): 3.65 (2H, br, CH$_2$OH), 1.57 (2H, br, C*H*$_2$CH$_2$OH), 1.27 (18H, br), 0.89 (3H, br, CH$_3$) [11]. Other new weak peaks at 7.43 and 10.49 ppm were observed, which could be assigned to formic acid HCOOH [11] in a trace amount. The solvent was removed from the reaction mixture, leaving a yellow residue. IR analysis of this residue (in hexane) revealed the existence of [Mn$_2$(CO)$_{10}$] [ν(CO) 2046s, 2014s and 1984m cm^{-1}] and an alcohol [3343m, br ν(OH), 1055m, ν(C-O)] [10].

Reaction of [Mn(CO)$_5${C(O)OC$_{12}$H$_{25}$}] with Br$_2$ in C$_6$D$_6$

To a solution of [Mn(CO)$_5${C(O)OC$_{12}$H$_{25}$}] (*ca.* 0.020 g, 0.05 mmol) in C$_6$D$_6$ (*ca.* 0.8 ml) in a NMR tube was added Br$_2$ (4 drops) at room temperature. The NMR tube was shaken to mix the components. The reaction was monitored by ^{1}H NMR. After 2 days, ^{1}H NMR spectrum of the reaction mixture showed the complete disappearance of the starting complex and the formation of presumably *n*-C$_{12}$H$_{25}$Br or *n*-C$_{12}$H$_{25}$OBr; ^{1}H NMR (in C$_6$D$_6$) δ (ppm): 3.41, 1.59, 1.31, 0.95 (The

integration for these peaks could not be certain as these peaks were broad and were not completely resolved). A white precipitate (presumably $[Mn(CO)_6]^+$) was formed in the NMR tube.

Reaction of $[Mn(CO)_5\{C(O)OC_{12}H_{25}\}]$ with Br_2 in hexane

To a solution of $[Mn(CO)_5\{C(O)OC_{12}H_{25}\}]$ (*ca.* 0.020 g, 0.05 mmol) in hexane (*ca.* 2 ml) was added Br_2 (4 drops) at room temperature. The reaction was monitored by IR spectroscopy. It was found that the reaction went slowly. After 17 hours, IR monitoring of the reaction mixture revealed that the ν(CO) peaks due to the starting complex had disappeared. A white precipitate was formed and identified as $[Mn(CO)_6]^+$ by its IR spectrum [Nujol mull ν(CO) at 2094 cm^{-1}] [13].

Attempted reaction of $[Mn(CO)_5\{C(O)OC_{12}H_{25}\}]$ with CH_3I

To a solution of $[Mn(CO)_5\{C(O)OC_{12}H_{25}\}]$ (0.015 g, 0.04 mmol) in $CHCl_3$ (2 ml) was added CH_3I (3 drops) at room temperature. The mixture was shaken for 8 hours. IR spectrum of the resulting solution showed the same peaks with similar intensity as those in the IR spectrum of the starting solution, suggested that no reaction occurred.

Attempted reaction of $[Mn(CO)_5\{C(O)OC_{12}H_{25}\}]$ with water

To a solution of $[Mn(CO)_5\{C(O)OC_{12}H_{25}\}]$ (0.015 g, 0.04 mmol) in $CHCl_3$ (2 ml) was added H_2O (1 ml) at room temperature. The mixture was shaken for 8 hours. H_2O was removed from the mixture and the $CHCl_3$ phase was analyzed by IR spectroscopy. The same peaks with similar intensity of peaks as those of the starting solution were observed, suggested that no reaction occurred.

Thermal decomposition of $[Mn(CO)_5\{C(O)OC_9H_{19}\}]$

A solution of $[Mn(CO)_5\{C(O)OC_9H_{19}\}]$ (0.047 g, 0.12 mmol) in C_6D_6 (0.5 g) was placed in a NMR tube. The NMR tube was connected to a vacuum pump and evacuated at 0.01 mmHg. Two freeze-pump-thaw circles were performed and then the NMR tube was sealed with the lower part of the NMR tube still remaining in liquid nitrogen. The sealed NMR tube was then heated in an oil bath at 70 ± 3 °C. ^1H NMR were run periodically to monitor the decomposition of the complex, by monitoring the decrease of the characteristic CO_2CH_2 peak at δ 4.04 ppm due to the starting complex. The decomposition was complete in about 55 hours. The solution was then analyzed by GC-MS. One major peak (other than the solvent C_6D_6) was separated by chromatography and the mass spectrum of the major peak showed $M^+ = 390$ ($[Mn_2(CO)_{10}]$).

General procedure for the reactions of alkyl complexes $[Mn(CO)_5(CH_3)]$ and $[Re(CO)_5(C_{16}H_{33})]$ with CO_2

A solution of the appropriate alkyl complex $[Mn(CO)_5(CH_3)]$ or $[Re(CO)_5(C_{16}H_{33})]$ (*ca* 0.4 mmol) in a solvent (hexane, heptane or THF, *ca* 10 ml) in a small flask was sealed in an autoclave. The autoclave was flushed with CO_2 three times and then filled with the same gas to certain pressure (7 or 48 bar). The autoclave was heated to higher temperature (60 - 75) for 8 to 24 hours. Then the autoclave was allowed to cool to room temperature and the gas vented. The resulting solution was analyzed by IR spectroscopy. The solvent was removed and the residue dried. The dried product was further analyzed by IR spectroscopy and ^1H NMR. The reaction led either decomposition of the starting complexes or recovery the starting complexes in high yield (80-90%). No reaction of these alkyl complexes with CO_2 was observed.

7.3 Experimental details pertaining to Chapter 3

7.3.1 Synthesis and reactivity of long chain acyl complexes

General procedure for the synthesis of long chain acyl complexes [CpFe(CO)$_2${C(O)R}] (R = *n*-C_5H_{11}, *n*-C_8H_{17}, *n*-$C_{11}H_{23}$ and *n*-$C_{17}H_{35}$).

A solution of Na[CpFe(CO)$_2$] (5.9 mmol) [prepared by reductive cleavage of [CpFe(CO)$_2$]$_2$ over Na/Hg at room temperature for 3 hours in THF (35 ml)], was added dropwise over 10 minutes to the acyl chloride (6.0 mmol) at 0 °C with rapid stirring. The reaction mixture was allowed to warm to room temperature and then stirred for 3 hours. The solvent was removed under reduced pressure, leaving a green residue. This was extracted with CH_2Cl_2 (3 x 50 ml) and filtered. The solvent was removed, leaving a red oil. This was dissolved in hexane, filtered and recrystallized from hexane at -25 °C for 2-3 times to give the product as a red oil [CpFe(CO)$_2${C(O)R}] (R = *n*-C_5H_{11}, *n*-C_8H_{17}) or as a yellow crystalline solid [CpFe(CO)$_2${C(O)R}] (R = *n*-$C_{11}H_{23}$, *n*-$C_{17}H_{35}$). The yields, m.p.s and characterization data are given in the section 3.2.2 of this thesis.

Preparation of [Cp*Fe(CO)$_2${C(O)$C_{11}H_{23}$}]

A solution of Na[Cp*Fe(CO)$_2$] (2.2 mmol) [prepared by reductive cleavage of [Cp*Fe(CO)$_2$]$_2$ (0.55g, 1.1 mmol) over Na/Hg (0.39 g Na, 6 ml Hg) at room temperature for 20 hours in THF (20 ml)], was added dropwise over 10 minutes to lauroyl chloride (0.51 g, 2.3 mmol) at 0 °C with rapid stirring. The reaction mixture was allowed to warm to room temperature and then stirred for 4 hours. The solvent was removed under reduced pressure, leaving a green residue. This was extracted with CH_2Cl_2 (3 x 30 ml) and filtered. The solvent was removed, leaving a red oil. This was dissolved in 5% CH_2Cl_2/pentane and chromatographed on a silica gel column (2 x 7 cm). Elution with 5% CH_2Cl_2/pentane gave a red band of [Cp*Fe(CO)$_2$]$_2$. Then elution with CH_2Cl_2 gave an orange-yellow band, from which the product [Cp*Fe(CO)$_2${C(O)$C_{11}H_{23}$}] was obtained, after recrystallization from

pentane at -78 °C, as a yellow crystalline solid (0.64 g). The yield, m.p. and characterization data are given in the section 3.2.2 of this thesis.

Preparation of $[CpW(CO)_3\{C(O)C_{11}H_{23}\}]$

A solution of $Na[CpW(CO)_3]$ (1.0 mmol) [prepared by reductive cleavage of $[CpW(CO)_3]_2$ (0.33 g, 0.5 mmol) over Na/Hg (0.19 g Na, 3 ml Hg) at room temperature for 2 hours in THF (22 ml)], was added dropwise over 5 minutes to lauroyl chloride (0.25 g, 1.1 mmol) at 0 °C with rapid stirring. The reaction mixture was allowed to warm to room temperature and then stirred for 10 hours. The solvent was removed under reduced pressure, leaving a green residue. This was extracted with hexane, filtered and concentrated. This was then chromatographed on an alumina column (2 x 9 cm). Elution with hexane and gradually increasing the polarity by adding CH_2Cl_2 gave first a yellow band, from which the product $[CpW(CO)_3\{C(O)C_{11}H_{23}\}]$ was obtained, after recrystallized from pentane at -78 °C, as a yellow crystalline solid (0.27 g). The second band was orange-red in colour, which was identified as $[CpW(CO)_3]_2$ by IR spectroscopy. The yield, m.p. and characterization data for $[CpW(CO)_3\{C(O)C_{11}H_{23}\}]$ are given in the section 3.2.2 of this thesis.

Reaction of the acyl complex $[CpFe(CO)_2\{C(O)C_{11}H_{23}\}]$ with syngas in hexane

A solution of $[CpFe(CO)_2\{C(O)C_{11}H_{23}\}]$ (0.42 g, 1.2 mmol) in hexane (ca. 15 ml) in a small flask was sealed in an autoclave. The autoclave was filled with syngas (20 bar) and the gas vented. This procedure was repeated two more times.The autoclave was then filled with syngas (45 bar). After heating at 62 °C for 20 hours, the autoclave was cooled to room temperature and the gas vented. The IR spectrum of the yellow solution outside of the reaction flask showed two ν(CO) bands at 2023s and 2000s cm^{-1} in hexane, which suggested that the solution contained $[Fe(CO)_5]$ (literature [14] data for $[Fe(CO)_5]$ in cyclohexane ν(CO): 2023s and 2000s cm^{-1}). The solvent was removed from thesolution, leaving a yellow solid, the IR spectrum of which showed three ν(CO) bands at 2017s, 1960vs and 1658m cm^{-1},

which is identical to the IR spectrum of the starting complex. The recovery of the starting complex is 0.38 g, 91%.

Reaction of the acyl complex [$CpFe(CO)_2\{C(O)C_{11}H_{23}\}$] with syngas in THF

A solution of [$CpFe(CO)_2\{C(O)C_{11}H_{23}\}$] (0.10 g, 0.27 mmol) in THF (10 ml) in a small flask was sealed in an autoclave. The autoclave was filled with syngas (20 bar) and the gas vented. This procedure was repeated two more times.The autoclave was then filled with syngas 48 bar. After heating at 60 °C for 20 hours, the autoclave was cooled to room temperature and the gas vented. The IR spectrum of the yellow solution outside of the reaction flask showed two ν(CO) bands at 2020s and 1995s cm^{-1} in THF, which suggested that the solution contained [$Fe(CO)_5$] [14]. The solvent was removed from the reaction solution, leaving a yellow residue (0.088 g). The IR spectrum of the yellow residue in THF showed ν(CO) bands at 2017s, 1960vs, 1779s, 1726s and 1658m cm^{-1}. A portion of the yellow residue was separated on a preparative silica gel plate, eluting with 20% CH_2Cl_2/pentane. Three bands were developed, which were separated and extracted with CH_2Cl_2 respectively. The IR spectra of the extracts were recorded between 2200 and 1600 cm^{-1} in CH_2Cl_2. The IR spectrum of the fisrt yellow band showed three ν(CO) bands at 2015s, 1956vs and 1642m cm^{-1}, which was identified as the starting complex. The IR spectrum of the second band showed ν(CO) bands at 1771s and 1724w cm^{-1}, suggesting that this may be an ester. The IR spectrum of the third band showed a ν(CO) band at 1723s cm^{-1}, suggesting that this may be a formate. A portion of the yellow residue was analyzed by ^1H and ^{13}C NMR in $CDCl_3$, ^1H NMR δ (ppm): 7.99, 4.79, 4.28, 4.14, 2.81, 2.43, 2.20, 1.94, 1.38, 1.17, 0.80 (all broad signals); ^{13}C NMR δ (ppm): 258.13, 214.38, 178.11, 161.19, 99.01, 86.32, 68.89, 68.60, 66.71, 62.83, 31.99, 31.84, 30.80, 29.55, 29.44, 29.41, 29.26, 29.01, 27.81, 25.18, 23.68, 22.81, 22.62, 22.12, 14.05. From these data, the starting complexes could be identified by its characteristic peak at δ 4.79 ppm in the ^1H NMR spectrum and the peaks at δ 258.13, 214.38, 86.32 and 66.71 ppm in the ^{13}C NMR spectrum. The formate was identified by characteristic peaks at δ 7.99 and 4.28 ppm in the ^1H NMR spectrum and a peak at δ 161.19 ppm in the ^{13}C NMR spectrum as well as a

strong ν(CO) band at 1723 cm^{-1} in the IR spectrum. The ester was identified by a peak at δ 178.11 ppm in the ^{13}C NMR spectrum and a strong ν(CO) band at 1771 cm^{-1} in the IR spectrum. The ratio of the formate, the ester and the starting complex is 51:28:21, estimated by the integrations of the characteristic peaks of these compounds in the ^{1}H NMR spectrum.

Reaction of the acyl complex [Cp*Fe(CO)$_2${C(O)C$_{11}$H$_{23}$}] with syngas in hexane

A solution of [Cp*Fe(CO)$_2${C(O)C$_{11}$H$_{23}$}] (0.12 g, 0.30 mmol) in hexane (ca. 12 ml) in a small flask was sealed in an autoclave. The autoclave was filled with syngas (20 bar) and the gas vented. This procedure was repeated two more times.The autoclave was then filled with syngas 48 bar. After heating at 75 °C for 22 hours, the autoclave was cooled to room temperature and the gas vented. The IR spectrum of the yellow solution outside of the reaction flask showed two ν(CO) bands at 2024s and 2001s cm^{-1} in hexane, which suggested that the solution contained [Fe(CO)$_5$] [14]. The solvent was removed from the reaction solution, leaving a yellow solid, the IR spectrum of which showed three ν(CO) bands at 2001s, 1942vs and 1647m cm^{-1}, which is identical to the starting complex. The recovery of the starting complex is 0.11 g, 93%.

Reaction of the acyl complex [CpW(CO)$_3${C(O)C$_{11}$H$_{23}$}] with syngas in hexane

A solution of [CpW(CO)$_3${C(O)C$_{11}$H$_{23}$}] (0.043 g, 0.083 mmol) in hexane (ca. 10 ml) in a small flask was sealed in an autoclave. The autoclave was filled with syngas (20 bar) and the gas vented. This procedure was repeated two more times.The autoclave was then filled with syngas 42 bar. After heating at 75 °C for 22 hours, the autoclave was cooled and the gas vented. The solvent was removed from the reaction solution, leaving a yellow solid, the IR spectrum of which showed four ν(CO) bands at 2017s, 1937s, 1922s and 1650m cm^{-1}, which is identical to the IR spectrum of the starting complex. The recovery of the starting complex was quantitative.

7.3.2 Synthesis and reactivity of long chain alkyl complexes [$CpW(CO)_3R$]

General procedure for the preparation of [$CpW(CO)_3R$] (R = *n*-C_6H_{13} - *n*-C_8H_{17}, and *n*-$C_{10}H_{23}$)

A solution of $Na[CpW(CO)_3]$ (2.1 mmol) in THF (21 ml) was added dropwise over 5 minutes to the alkyl iodide RI (R = *n*-C_6H_{13}, *n*-C_7H_{15}, or *n*-$C_{10}H_{23}$; or *n*-$C_8H_{17}Br$) (3.5 mmol) at 0 °C with rapid stirring. The reaction mixture was allowed to warm to room temperature and then stirred for 45 hours at room temperature. The solvent was removed under reduced pressure, leaving a green residue. This was extracted with hexane, filtered and concentrated. This was then chromatographed on a silica gel column. Elution with hexane gave a yellow band, which was collected, concentrated and recrystallized from hexane at -78 °C, to give the alkyl complex [$CpW(CO)_3R$] as a yellow crystalline solid. The second band was orange-red in colour and was identified as $[CpW(CO)_3]_2$ by IR spectroscopy. The yields, m.p.s and characterization data are given in the section 3.3.2 of this thesis.

General procedure for the attempted reactions of alkyl complexes with CO_2

A solution of the appropriate alkyl complex [$CpFe(CO)_2R$] (R = CH_3, or *n*-$C_{11}H_{23}$) or [$CpW(CO)_3R$] (R = *n*-C_8H_{17}) (0.2 mmol) in THF (6 - 10 ml) in a small flask was sealed in an autoclave. The autoclave was filled with CO_2 (20 bar) and the gas vented. This procedure was repeated two more times. The autoclave was then filled with CO_2 (48-50 bar). After heating at 50 °C for 48 hours, the autoclave was cooled and the gas vented. The solution was analyzed by IR spectroscopy. The solvent was removed and the residue dried. The dried product was further analyzed by ^1H and ^{13}C NMR. Only the starting complex was recovered (recovery 50 - 100%).

7.3.3 Synthesis and reactivity of the carbyne complexes [CpW(CO)$_2$(≡CR)]

Preparation of the carbyne complexes [CpW(CO)$_2$(≡CR)] (R = C$_6$H$_5$ and C$_6$H$_4$-OMe-(4))

The complexes [CpW(CO)$_2$(≡CR)] (R = C$_6$H$_5$ and C$_6$H$_4$-OMe-(4)) were prepared according to the procedure reported by Stone and co-workers in the literature [15]. These carbyne complexes have been characterized by IR, ^{1}H and ^{13}C NMR and our results are in good agreement with the data reported by Fischer and co-workers [16]. The DSC and TGA analysis results for the complex [CpW(CO)$_2$(≡CR)] (R = C$_6$H$_4$-OMe-(4)) are new and are given in the section 3.3.5 of this thesis.

[CpW(CO)$_2$(≡CR)] (R = C$_6$H$_5$): IR ν(CO) (CH$_2$Cl$_2$) 1977s, 1909s cm^{-1}; ^{1}H NMR (CD$_2$Cl$_2$) δ (ppm): 7.36 (3H, m), 7.23 (2H, m), 5.78 (5H, s); ^{13}C NMR (CD$_2$Cl$_2$) δ (ppm): 299.35, 220.95, 151.21, 128.77, 128.70, 128.21, 91.90.

[CpW(CO)$_2$(≡CR)] (R = C$_6$H$_4$-OMe-(4)): IR ν(CO) (CH$_2$Cl$_2$) 1981s, 1903s cm^{-1}; ^{1}H NMR (CD$_2$Cl$_2$) δ (ppm): 7.38 (2H, m), 6.77 (2H, m), 5.71 (5H, s); ^{13}C NMR (CD$_2$Cl$_2$) δ (ppm): 299.98, 221.36, 160.35, 144.79, 130.97, 113.51, 91.72, 55.68.

Reactions of the carbyne complexes [CpW(CO)$_2$(≡CR)] (R = C$_6$H$_5$, and C$_6$H$_4$-OMe-(4)) with CO$_2$

(A) in CH$_2$Cl$_2$

A solution of [CpW(CO)$_2$(≡CR)] (R = C$_6$H$_5$) (0.060 g, 0.15 mmol) in CH$_2$Cl$_2$ (20 ml) in a small flask was sealed in an autoclave. The autoclave was filled with CO$_2$ (20 bar) and the gas vented. This procedure was repeated two more times. The autoclave was then filled with CO$_2$ 50 bar. The autoclave was stirred at room temperature for *ca.* 22 hours and the gas vented. The solution was analyzed by IR spectroscopy. The IR spectrum of the solution showed peaks at 2020s, 1987s, 1977sh and 1908s cm^{-1}. The later two peaks indicated the presence of the starting complex. Thus, the reaction was continued at the same conditions and was complete in about 10 days. The IR spectrum of the resulting solution showed peaks at 2020s, 1993sh, 1976s, 1770w, 1713w cm^{-1}. The solution was filtered to remove insoluble

precipitate. The filtrate was concentrated and pentane was added to precipitate the product(s). A mixture of yellow and black solids were obtained (*ca.* 0.020g). ^{13}C NMR of the mixture in DMF-d_7, δ (ppm): 192.00, 172.99, 135.76, 133.11, 129.72, 129.57, 128.85, 128.57, 128.31, 126.91, 111.25, 78.88, 41.08. Attempts to isolate pure products were unsuccessful.

(B) in benzene

A solution of $[CpW(CO)_2(\equiv CR)]$ (R = C_6H_5) (0.040 g, 0.10 mmol) in benzene (6 ml) in a small flask was sealed in an autoclave. The autoclave was filled with CO_2 (20 bar) and the gas vented. This procedure was repeated two more times. The autoclave was then filled with CO_2 50 bar. The autoclave was stirred at 50 °C for 26 hours. Then the autoclave was cooled and the gas vented. The IR spectrum of the solution showed peaks at 2016m, 1975m, 1915m,br and 1712s cm^{-1}, indicated that the complete conversion of the starting complex had occurred. Attempted isolation of the product by preparative TLC or by recrystallization was unsuccessful.

7. 4 Experimental details pertaining to Chapter 4.

7.4.1. Synthesis and reactivity of alkylplatinum(II) complexes containing tertiary phosphine ligands.

The complexes *cis*-$[PtCl_2(PPh_3)_2]$ [17], *cis*-$[PtCl_2(PBu_3)_2]$ [18], and *trans*-$[PtCl_2(PCy_3)_2]$ [19] were prepared by the literature methods with slight modification.

Synthesis of *cis*-di-*n*-butylbis(tributylphosphine)platinum(II), *cis*-$[PtBu_2(PBu_3)_2]$

To a suspension of *cis*-$[PtCl_2(PBu_3)_2]$ (0.46 g, 0.65 mmol) in ether (8 ml) at -78 °C was added *n*-butyllithium in hexane (1.5 ml of a 1.6 M solution, 2.4 mmol). The reaction mixture was allowed to warm to 0 °C. After stirring at this temperature for 0.5 hour, the reaction mixture was cooled again to -78 °C and a mixture of water (0.9 ml) and methanol (0.1 ml) was added. Evaporation of the organic layer gave a

pale-yellow oil that turned into a white solid after recrystallization from ether/methanol (1.5/3.0 ml) by cooling to *ca.* -30 °C for 10 hours. After drying *in vacuo*, the product *cis*-[$PtBu_2(PBu_3)_2$] (0.41 g, 80 %) was obtained as a white crystalline solid, m.p. 24-25 °C (Found: C, 53.84; H, 10.29 %, $C_{32}H_{72}P_2Pt$ requires: C, 53.83; H, 10.16 %); IR (Nujol mull between CsI discs): ν(Pt-P) 454w, 393w cm^{-1}; ^1H NMR (C_6D_6) δ (ppm): 1.88 - 1.30 (48 H, m, CH_2), 1.22 [6 H, t, ^3J(HH) 7 Hz, CH_3], 0.93 [18 H, t, ^3J(HH) 7 Hz, CH_3]; ^{13}C NMR (C_6D_6) δ (ppm): 36.26, 30.29, 27.84, 25.64, 25.58, 25.51, 15.51, 14.74; ^{31}P NMR (C_6D_6) δ (ppm): 1.95, s, $^1J(^{195}Pt\text{-}^{31}P)$ 1704 Hz; DSC: T_{max} (endo) = 32.2 °C (sharp peak), 132.5 °C (broad peak); TGA: from 80.6 °C to 161.0 °C, mass loss 20.7%; from 161.0 °C - 227.8 °C, mass loss 28.0%.

Synthesis of *cis*-di-*n*-butylbis(triphenylphosphine)platinum(II) *cis*-[$PtBu_2(PPh_3)_2$]

The complex *cis*-[$PtBu_2(PPh_3)_2$] was prepared by the literature method reported by Whitesides et. al. [20]. This complex had been characterized previously by elemental analysis, melting point, IR and ^1H NMR spectroscopy [20]. Our results are in good agreement with the reported data. Additional characterization data are follows: ^{13}C NMR ($CDCl_3$) δ (ppm): 134.52 (m, *ortho*), 133.81 [d, $^1J(^{31}P\text{-}^{13}C)$ 41 Hz, $^2J(^{195}Pt\text{-}^{13}C)$ 15 Hz, *ipso*], 128.94 (*para*), 127.36 (m, *meta*), 33.78 [s, $^3J(^{195}Pt\text{-}^{13}C)$ 22 Hz, CH_2CH_3], 28.32 [m, ^2J(PtC) 116 Hz, $PtCH_2CH_2$], 26.46 [d.d, ^1J(PtC) 666 Hz, $^2J(^{31}P\text{-}^{13}C$, *trans*) 94 Hz, $^2J(^{31}P\text{-}^{13}C$, *cis*) 6.9 Hz, $PtCH_2$], 13.94 (CH_3); ^{31}P NMR ($CDCl_3$) δ (ppm): 27.36, s, $^1J(^{195}Pt\text{-}^{31}P)$ 1719 Hz.

Preparation of *trans*-chlorobutylbis(tributylphosphine)platinum(II), *trans*-[$PtBu(Cl)(PBu_3)_2$]

To a solution of *cis*-[$PtBu_2(PBu_3)_2$] (0.85 g, 1.2 mmol) in dry ether (12 ml) was added dry HCl in ether (1.12 ml, 1.2 mmol) at room temperature under nitrogen. The reaction mixture was stirred at room temperature for 0.5 hour. The solvent was removed to give a yellow oil. Attempted recrystallization of the oil from petroleum ether and from $MeOH/H_2O$ was unsuccessful. The product was obtained after

removal of the solvent under high vacuum to give *trans*-[PtBu(Cl)(PBu_3)$_2$] (0.65 g, 77%) as a pale-yellow oil. Found: C, 48.89; H, 9.32 %, $C_{28}H_{63}ClP_2Pt$ requires: C, 48.63; H, 9.18 %; IR (neat film between CsI discs) ν(Pt-P) 447w, 392w cm^{-1}; ν(Pt-Cl) 264w cm^{-1}; ^{1}H NMR (C_6D_6) δ (ppm): 1.95 - 1.30 (42 H, m, CH_2), 1.12 [3 H, t, ^{3}J(HH) 7 Hz, CH_3], 0.94 [18 H, t, ^{3}J(HH) 7 Hz, CH_3]; ^{13}C NMR (C_6D_6) δ (ppm): 37.20, 28.69, 27.22 (t, J 11 Hz), 25.33 (t, J 6 Hz), 21.95 (qn, J 16 Hz), 14.99, 14.68, -1.37; ^{31}P NMR (C_6D_6) δ (ppm): 8.00, s, ^{1}J(^{195}Pt-^{31}P) 2942 Hz.

Reaction of *cis*-[$PtBu_2(PPh_3)_2$] with CO_2 to give [$Pt(CO_3)(PPh_3)_2$]

The complex *cis*-[$PtBu_2(PPh_3)_2$] (0.18 g, 0.22 mmol) in triethylamine (3 ml) was transferred to a small flask and sealed in an autoclave. The autoclave was filled with CO_2 and the gas vented. This procedure was repeated three times, then the autoclave was filled with the same gas to 50 bar. After heating at 60 °C for 14 hours, the autoclave was cooled and the gas vented. A red-orange solid separated out from the solution. The colour of the solid could be due to the presence of $[Pt(PPh_3)_2]_n$. The solid was washed with pentane to give an orange-yellow solid (0.14 g, 82 %) which was further washed with a small amount of toluene and hexane to give a white solid [$Pt(CO_3)(PPh_3)_2$], IR ν(CO) (Nujol mull) 1676s, 1625w cm^{-1}; ^{31}P NMR ($CDCl_3$) δ (ppm): 6.61, s, ^{1}J(^{195}Pt-^{31}P) 3711 Hz. An authentic sample of [$Pt(CO_3)(PPh_3)_2$] [21], made from *cis*-[$PtCl_2(PPh_3)_2$] and Ag_2CO_3, had IR ν(C=O) (Nujol mull) 1674s, 1630w cm^{-1}; ^{31}P NMR ($CDCl_3$) δ (ppm): 6.59, s, ^{1}J(^{195}Pt-^{31}P) 3706 Hz.

Reaction of *cis*-[$PtBu_2(PBu_3)_2$] with CO_2 to give [$Pt(CO_3)(PBu_3)_2$]

A solution of *cis*-[$PtBu_2(PBu_3)_2$] (0.20 g, 0.28 mmol) in triethylamine (3 ml) was transferred to a small flask and sealed in an autoclave. The autoclave was filled with CO_2 and the gas vented. This procedure was repeated three times, then the autoclave was filled with the same gas to 50 bar. After heating at 58 °C for 24 hours, the autoclave was cooled and the gas vented. A red-orange solution was obtained. The solvent was removed to give a red oily product (0.13 g, 70%) after

drying under high vacuum. The product was identified as mainly (75%) $[Pt(CO_3)(PBu_3)_2]$ IR ν(CO) (CsI disc) 1659s, 1632w cm^{-1}; ^{31}P NMR (C_6D_6) δ (ppm): -4.84, s, $^1J(^{195}Pt-^{31}P)$ 3417 Hz. The minor product, presumably $[Pt(PBu_3)_2]_n$, (*ca.* 25%) had ^{31}P NMR (C_6D_6) δ (ppm): 15.18, s, $^1J(^{195}Pt-^{31}P)$ 2714 Hz. An authentic sample of $[Pt(CO_3)(PBu_3)_2]$, made from *cis*-$[PtCl_2(PBu_3)_2]$ and Ag_2CO_3, had ^{31}P NMR (C_6D_6) δ (ppm): -4.74, s, $^1J(^{195}Pt-^{31}P)$ 3473 Hz.

Preparation of (η^2-methyl acrylate)-bis(triphenylphosphine)platinum(0) $[Pt(CH_2=CH_2CO_2Me)(PPh_3)_2]$ [22]

Although the complex $[Pt(CH_2=CH_2CO_2Me)(PPh_3)_2]$ has been reported before [22], the following method is a new and simple method.

To a white heterogeneous mixture of *cis*-$[PtBu_2(PPh_3)_2]$ (0.18 g, 0.22 mmol) in benzene (2 ml) was added methyl acrylate (40 μl, 0.44 mmol) by a syringe. The mixture was stirred at 60 °C in a carefully controlled oil bath for 12 hours, to give a homogeneous pale yellow solution. After cooling, the solvent was removed from the reaction mixture *in vacuo* to leave a yellow oil. The yellow oil was dissolved in acetone (2 ml) and the solution was quickly filtered and pentane (10 ml) added. After standing overnight at -15 °C, cream crystals separated out, which were washed with pentane (2 x 4 ml) and dried *in vacuo* for *ca.* 1 hour to produce $[Pt(CH_2=CH_2CO_2Me)(PPh_3)_2]$ (0.14 g, 81 %), m.p. 127 - 132 °C dec. (lit. [22] m.p. 86 - 91 °C); anal calcd. for $C_{40}H_{36}O_2P_2Pt$: C, 59.62; H, 4.50 %; found: C, 59.67; H, 4.53 %; IR ν(CO) (KI disc): 1688s cm^{-1}; ^{31}P NMR (C_6D_6) δ (ppm): 32.11 [d, $^1J(^{195}Pt-^{31}P)$ 3618 Hz, $^2J(PP)$ 43 Hz], 30.62 [d, $^1J(^{195}Pt-^{31}P)$ 4057 Hz, $^2J(PP)$ 43 Hz]. These data are in good agreement with the literature data except the melting point [22].

7.4.2 Synthesis of platinum(II) alkoxycarbonyl and carboxylate complexes

Some model complexes which could be considered as formal derivatives of CO_2 and dialkyl-bis(trialkylphosphine)platinum(II) complexes, such as the

alkoxycarbonyl complexes *trans*-$[Pt(CO_2CH_3)_2(PPh_3)_2]$ [23], *trans*-$[Pt(CO_2CH_2CH_3)_2(PPh_3)_2]$ [24,25], the carbonyl complexes $[Pt(CO)_2(PPh_3)_2]$ [26], $[Pt(CO)_2(PBu_3)_2]$ [26], the carboxylate complex *cis*-$[Pt(O_2CCH_3)_2(PPh_3)_2]$ [27,28], and the oxalate complex $[Pt(C_2O_4)(PBu_3)_2]$ [29] have been prepared by simple routes starting from *cis*-$[PtCl_2(PR_3)_2]$ complexes. Although these complexes have been reported in the literature, the syntheses reported in this thesis are either new, or simple and usually give better yields.

Synthesis of the alkoxycarbonyl complex *trans*-$[Pt(CO_2CH_3)_2(PPh_3)_2]$ [23]

The preparation of *trans*-$[Pt(CO_2CH_3)_2(PPh_3)_2]$ has been reported in the literature [23], but the following method provided a novel and simple way to synthesize analytical pure *trans*-$[Pt(CO_2CH_3)_2(PPh_3)_2]$. Additional characterization data have also been obtained. More detailed discussion can be found in the section 4.2.3 of Chapter 4 of this thesis.

A suspension of *cis*-$[PtCl_2(PPh_3)_2]$ (0.28 g, 0.35 mmol) in methanol (5 ml) and NEt_3 (5 ml) was transferred to a flask and sealed in an autoclave. The autoclave was filled with CO (10 bar) and the gas vented. This procedure was repeated three times then the autoclave was filled with CO (7 bar) and stirred at room temperature for 5 hours. After the gas was vented, the solid product *trans*-$[Pt(CO_2CH_3)_2(PPh_3)_2]$ (0.22 g, 81 %) was obtained by filtration, and washed with methanol and dried *in vacuo*, m.p. 186 - 188 °C (literature [23] m.p. 178 - 183 °C); anal. calcd. for $C_{40}H_{36}O_4P_2Pt$: C, 57.20; H, 4.32 %; found: C, 57.43; H, 4.25 %; IR ν(CO) ($CHCl_3$): 1624s cm^{-1}; ^{31}P NMR ($CDCl_3$) δ (ppm): 16.49, s, $^1J(^{195}Pt\text{-}^{31}P)$ 3089 Hz. Additional characterization data are follows: ^{195}Pt NMR ($CDCl_3$ at 30 °C) δ (ppm): -4531.80, s, $^1J(^{195}Pt\text{-}^{31}P)$ 3091 Hz. When the solution of 7 in $CDCl_3$ was kept at room temperature for 48 hours, an additional new species was observed by ^{195}Pt NMR in 7 % yield. ^{195}Pt NMR of the new species ($CDCl_3$ at 30 °C) δ (ppm): -4269.23, s, $^1J(^{195}Pt\text{-}^{31}P)$ 3047 Hz. This new species could be a result of the isomerization of the *trans* compound to its *cis* derivative; DSC: one sharp endothermic peak at 242 °C (onset), peak maximum at 244 °C; TGA: *ca.* 30 % mass loss from 235 °C to 255°C.

Preparation of *trans*-[$Pt(CO_2CH_2CH_3)_2(PPh_3)_2$] [23]

The complex *trans*-[$Pt(CO_2CH_2CH_3)_2(PPh_3)_2$] was obtained using a similar method to that described above for *trans*-[$Pt(CO_2CH_3)_2(PPh_3)_2$], from *cis*-[$PtCl_2(PPh_3)_2$] (0.13 g, 0.16 mmol), CO (10 bar), ethanol (3 ml) and NEt_3 (3 ml). The mixture was stirred under CO (10 bar) at room temperature for 12 hours. The complex *trans*-[$Pt(CO_2CH_2CH_3)_2(PPh_3)_2$] (0.11 g, 77 %) was obtained as a white solid, m.p. 108-110 °C dec.; anal. calcd. for $C_{42}H_{40}O_4P_2Pt$: C, 58.12; H, 4.65 %; found: C, 58.28; H, 4.55 %; IR ν(CO) (Nujol mull): 1628s cm^{-1}; ^1H NMR ($CDCl_3$) δ (ppm): 7.72 - 7.25 (30 H, m, aromatic), 2.86 [4 H, q, $^3J(HH)$ 7 Hz, CH_2], 0.41 (6 H, t, $^3J(HH)$ 7 Hz, CH_3); ^{13}C NMR ($CDCl_3$) δ (ppm): 197.88 (weak, CO_2), 134.59 (m), 131.66 (m), 130.21, 127.81 (m), (aromatic), 56.91 (OCH_2), 14.02 (CH_3); ^{31}P NMR ($CDCl_3$) δ (ppm): 16.37, s, $^1J(^{195}Pt-^{31}P)$ 3119 Hz; DSC: one sharp endothermic peak at 227 °C (onset), peak maximum at 230 °C.

Attempted preparation of *trans*-[$Pt\{(CO_2CH(CH_3)_2\}_2(PPh_3)_2$] and *trans*-[$Pt(CO_2CH_2CH_2CH_3)_2(PPh_3)_2$]

The procedure described above for *trans*-[$Pt(CO_2CH_3)_2(PPh_3)_2$] was used in an attempt to prepare new complexes *trans*-[$Pt\{(CO_2CH(CH_3)_2\}_2(PPh_3)_2$] and *trans*-[$Pt(CO_2CH_2CH_2CH_3)_2(PPh_3)_2$], starting from *cis*-[$PtCl_2(PPh_3)_2$], CO, NEt_3 and 2-propanol or 1-propanol. These reactions, however, were unsucessful. A mixture of [$Pt(CO)_2(PPh_3)_2$] and *trans*-[$Pt\{(CO_2CH(CH_3)_2\}_2(PPh_3)_2$], or *trans*-[$Pt(CO_2CH_2CH_2CH_3)_2(PPh_3)_2$], was obtained and identified by IR; ν(CO) (neat reaction solution), 1982s, 1946s, 1636s, 1612s cm^{-1}.

Preparation of [$Pt(CO)_2(PPh_3)_2$] [26].

Although the complex [$Pt(CO)_2(PPh_3)_2$] has been prepared before [26], the new procedure described below makes it possible to obtain analytical pure [$Pt(CO)_2(PPh_3)_2$] more conveniently.

A mixture of *cis*-$[PtCl_2(PPh_3)_2]$ (0.23 g, 0.29 mmol), NEt_3 (1 ml) and 1-butanol (6 ml), in a flask, was heated in an autoclave under CO (42 bar) at 70 °C for 6 hours. After cooling, the gas was vented and the autoclave opened. The white microcrystalline product $[Pt(CO)_2(PPh_3)_2]$ (0.18 g, 79 %) was separated by filtration, washed with methanol (10 ml) and dried *in vacuo*; m.p. 102 - 105 °C; anal. calcd. for $C_{38}H_{30}O_2P_2Pt$: C, 58.83; H, 3.87 %; found: C, 58.96; H, 3.81 %; IR ν(CO) (Nujol mull) 1983s, 1948s, 1912 m; ^{31}P NMR ($CDCl_3$) δ (ppm): 9.05, s, ^1J(Pt-P) 3295 Hz. These characterization data are in good agreement with the literature [26].

The complex $[Pt(CO)_2(PPh_3)_2]$ was also obtained when the reaction was carried out at room temperature. When 1-butanol was replaced by Ph-CH_2OH, 1,3-propandiol or 1-heptanol, $[Pt(CO)_2(PPh_3)_2]$ was also obtained.

Preparation of $[Pt(CO)_2(PBu_3)_2]$ [26]

A mixture of *cis*-$[PtCl_2(PBu_3)_2]$ (0.20 g, 0.25 mmol) and NEt_3 (2 ml) in methanol (3 ml) in a flask, was stirred in an autoclave under CO (5 bar) at room temperature for 24 hours. After cooling, the gas was vented and the autoclave opened. The IR spectrum of the resulting solution shown ν(CO) bands at 1977s and 1936s cm^{-1}, which are quite similar to the data reported for $[Pt(CO)_2(PBu_3)_2]$ (literature [26]: 1970s, 1923s cm^{-1} in THF). The product was not isolated due to the instability of the complex.

Preparation of the carboxylate complex *cis*-$[Pt(O_2CCH_3)_2(PPh_3)_2]$ [27,28]

The complex *cis*-$[Pt(O_2CCH_3)_2(PPh_3)_2]$ has been prepared from $[Pt(PPh_3)_n]$ (n = 3 or 4) and CH_3COOH [28]. The following method starting from *cis*-$[PtCl_2(PPh_3)_2]$ and $Ag(O_2CCH_3)$ gave *cis*-$[Pt(O_2CCH_3)_2(PPh_3)_2]$ in high yield. In a recent literature report [27] this method has also been reported independently.

A solution of *cis*-$[PtCl_2(PPh_3)_2]$ (0.70 g, 0.89 mmol) and $Ag(O_2CCH_3)$ (0.51 g, 3.1 mmol) in CH_2Cl_2 (25 ml) was stirred under N_2 at room temperature for 3 days, shielded from direct light. The mixture was filtered, and the solid washed with CH_2Cl_2 (3 x 10 ml). The filtrate and combined washings were concentrated, ether was added to precipitate the product. The white product was washed with ether and dried under high vacuum to yield *cis*-$[Pt(O_2CCH_3)_2(PPh_3)_2]$ (0.60 g, 82 %); IR ν(CO) (Nujol mull) 1625s, 1598sh cm^{-1}; [ν(CO) (in $CHCl_3$) 1619s, 1599sh cm^{-1}]; ^{31}P NMR ($CDCl_3$) δ (ppm): 5.52, s, ^1J(Pt-P) 3824 Hz. A solution of *cis*-$[Pt(O_2CCH_3)_2(PPh_3)_2]$ in $CHCl_3$ showed no change in its IR spectrum after keeping under a CO_2 atmosphere for 48 hours: ν(CO) (in $CHCl_3$) 1619s, 1600sh cm^{-1}.

Preparation of the oxalate complex $[Pt(C_2O_4)(PBu_3)_2]$ [29]

This complex was prepared by a similar method to that reported for the synthesis of $[Pt(C_2O_4)(PPh_3)_2]$ in the literature [29]. Thus, the reaction of *cis*-$[PtCl_2(PBu_3)_2]$ (0.40 g, 0.6 mmol) with $K_2C_2O_4$ (0.33 g, 1.8 mmol) gave $[Pt(C_2O_4)(PPh_3)_2]$ (0.35 g, 85 %), m.p. 183 - 184 °C; anal. calcd. for $C_{26}H_{54}O_4P_2Pt$: C, 45.41; H, 7.91 %; found: C, 45.66; H, 8.04 %; IR ν(CO) (in CH_2Cl_2) 1702s, 1679s cm^{-1}; ^{31}P NMR ($CDCl_3$) δ (ppm): -2.47, s, ^1J(Pt-P) 3530 Hz. These characterization data are in good agreement with the literature [29].

7.4.3. Synthesis and reactivity of alkylplatinum(II) complexes containing nitrogen donor ligands

The complexes *cis*- and *trans*-$[PtCl_2(SMe_2)_2]$ [30], $[Pt_2Me_4(SMe_2)_2]$ [31,32], $[PtMe_2(bipy)]$ [33], 1-(diphenylphosphino)-2-(2-pyridyl)ethane (NP) [34] and $[Pt(COD)Cl_2]$ [35] were prepared according to the literature methods.

Preparation of $[PtMe_2(Me_2\text{-bipy})]$

To a solution of $[Pt_2Me_4(SMe_2)_2]$ (0.48 g, 0.84 mmol) in benzene (20 ml) was added 4,4′-dimethyl-2,2′-bipyridine (0.78 g, 4.24 mmol) in ether (20 ml). An

immediate red coloration was observed. The reaction mixture was stirred at room temperature for 1 hour and then kept at 0 °C overnight. The cold mixture was filtered and the resulting orange solid was washed with ether (2 x 10 ml) and dried under high vacuum to give [$PtMe_2(Me_2$-bipy)]. The yield, melting point, elemental analysis and physical characterization data are given in the section 4.3.1 of Chapter 4 of this thesis.

General procedure for the preparation of [$PtIMe_2(R')(Me_2$-bipy)] (R′ = Me, Et, *n*-Pr, *n*-Bu and *n*-Pentyl)

To a solution of [$PtMe_2(Me_2$-bipy)] (0.048 g, 0.12 mmol) in acetone (15 ml) was added excess MeI (0.4 ml) at room temperature and the reaction mixture was stirred for 15 minutes. The solvent was removed under reduced pressure, leaving a yellow solid. Recrystallization of this solid from CH_2Cl_2/hexane gave [$PtIMe_2(Me)(Me_2$-bipy)] as a yellow crystalline solid, which was dried under high vacuum.

The complexes [$PtIMe_2(R')(Me_2$-bipy)] (R′ = Et, *n*-Pr, *n*-Bu and *n*-Pentyl) were prepared similarly but with longer reaction times. The complex with ethyl group was prepared using a molar ratio of [$PtMe_2(Me_2$-bipy)] (1 mmol) to EtI (2 mmol) and the reaction time was 16 hours.

The yields, melting points, elemental analyses and physical charaterization data for these complexes are given in the section 4.3.1 of Chapter 4 of this thesis.

Reactions of [$PtMe_2$(bipy)] and [$PtMe_2(Me_2$-bipy)] with (i) CO_2 and (ii) R′OH in NEt_3: Preparation of monoalkyl carbonate complexes [PtMe{OC(O)OR′}(R_2-bipy)] (R = H, R′ =Et; R = Me, R′ = Me; R = Me, R′ = Et)

All the preparations of these monoalkyl carbonate complexes were carried out similarly. An example, for the preparation of [PtMe{OC(O)OEt}(Me_2-bipy)], is given below.

A suspension of [$PtMe_2(Me_2$-bipy)] (0.070 g, 0.17 mmol) in EtOH (10 ml) and NEt_3 (6 ml) was transferred to a small flask and sealed in an autoclave. The autoclave was filled with CO_2 (20 bar) and the gas vented. This procedure was repeated three times and then the autoclave was filled with CO_2 (40 bar). The autoclave was then heated at 40 °C for 22 hours. After cooling the autoclave to room temperature, the gas was vented and the autoclave opened. A clear yellow solution was obtained from which the solvent was removed in a stream of CO_2 to give a yellow solid, [PtMe{OC(O)OEt}(Me_2-bipy)]. (Alternatively, the yellow solution could be kept at -15 °C for two days to crystallize the product [PtMe{OC(O)OEt}(Me_2-bipy)]). When the yellow product was dried under high vacuum, it turned to an orange solid. This turned yellow again when the flask was refilled with CO_2. The reaction gave exclusively [PtMe{OC(O)OEt}(Me_2-bipy)] (isolated yield 0.06 g, 73%); the yellow solid decomposed at 165 - 167 °C without melting (Found: C, 40.07; H, 4.28; N, 6.17 %; $C_{16}H_{20}N_2O_3Pt$ requires: C, 39.75; H, 4.17; N, 5.79 %); IR ($CHCl_3$) ν(C=O): 1663s cm^{-1}, ν(bipy): 1614s cm^{-1}; UV-visible (acetone) λ_{max}/nm: 422 (ε 125); ^1H NMR (C_6D_6) δ (ppm): 8.26 [1 H, d, ^3J(HH) 5 Hz], 8.17 (1 H, m), 8.14 (1 H, m), 8.11 [1 H, d, ^3J(HH) 6 Hz], 5.96 [1 H, d, ^3J(HH) 5 Hz], 5.89 [1 H, d, ^3J(HH) 6 Hz] (bipy ring protons), 4.39 [2 H, q, ^3J(HH) 7 Hz, OCH_2], 1.91 (3 H, s, ring-Me), 1.81 (3 H, s, ring-Me), 1.46 (3 H, s, PtMe), 1.32 [3 H, t, ^3J(HH) 7 Hz, OCH_2CH_3]; ^{13}C NMR (CD_2Cl_2 under a CO_2 atmosphere) δ (ppm): 159.39 (CO_3), 158.09, 153.43, 150.51, 150.28, 149.22, 145.99, 127.63, 127.57, 124.95 (t, J 29 Hz), 123.87 (bipy ring carbons), 62.05 (OCH_2), 21.84, 21.68 (ring-Me carbons), 15.15, (OCH_2CH_3), -13.80 (PtMe); ^{13}C NMR DEPT (CD_2Cl_2) δ (ppm): 149.24, 146.01, 127.64, 127.58, 124.95, 123.88 (bipy ring carbons), 62.05 (OCH_2), 21.84, 21.69 (ring-Me carbons), 15.15, (OCH_2CH_3), -13.80 (PtMe), (weak peaks were also seen at 58.22 and 18.57 ppm, which might be resulted from the decomposition of the product in solution).

The complexes [PtMe{OC(O)OMe}(Me_2-bipy)] and [PtMe{OC(O)OEt}(bipy)] were prepared using a similar method to that described above for [PtMe{OC(O)OEt}(Me_2-bipy)], however these two complexes could not be isolated in a pure form due to decomposition, and they were only characterized by IR and

UV-visible spectra. The data can be found in the section 4.3.2 of Chapter 4 of this thesis.

Preparation of $[Pt(NP)_2Cl_2]$

A mixture of 1-(diphenylphosphino)-2-(2-pyridyl)ethane (NP) [34] (0.35 g, 1.2 mmol) and $[Pt(COD)Cl_2]$ [35] (0.21 g, 0.8 mmol) in benzene (15 ml) was heated at 50 °C for 24 hours under nitrogen. The reaction mixture was cooled to room temperature. The reaction mixture was filtered to give a white solid which was washed with ethanol and dried under high vacuum to give the new compound $[Pt(NP)_2Cl_2]$ (0.27 g, 32 %), m.p. 214 - 216 °C (Found: C, 53.30; H, 4.66; N, 3.16 %; $C_{38}H_{36}N_2P_2Cl_2Pt$ requires: C, 53.78; H, 4.28; N, 3.30 %); IR (CsI disc): 1630s, 1614s cm^{-1}; conductivity (in nitrobenzene in 2.5 x 10^{-4} mol/L solution) Λ = 20.5 Ω^{-1} cm^2 mol^{-1}.

7.5 Experimental details pertaining to Chapter 5

7.5.1 Synthesis and reactivity of haloalkyl complexes $[(\eta^5\text{-}C_5R_5)W(CO)_3\{(CH_2)_nX\}]$

The preparation of complexes $[CpW(CO)_3\{(CH_2)_3Br\}]$ [36], $[CpW(CO)_3\{(CH_2)_4Br\}]$ [36], $[CpW(CO)_3\{(CH_2)_4I\}]$ [37], $[CpW(CO)_3\{(CH_2)_5I\}]$ [37], $[Cp^*W(CO)_3\{(CH_2)_3Br\}]$ [38], and $[Re(CO)_5\{(CH_2)_4I\}]$ [39] have been reported in the literature, however, the procedures given in this thesis lead to better yields for these complexes. All other complexes synthesized in this work are new complexes. 3,5-dihydroxybenzyl alcohol [40], $[RhCl_2(DH_2)(DH)]$ [41] and $[Cp^*Re(NO)(CO)_2]^+BF^-_4$ [42] were prepared by literature methods.

Synthesis of bromopropylcyclopentadienyltricarbonyltungesten complex $[CpW(CO)_3\{(CH_2)_3Br\}]$ [36]

A solution of $Na[CpW(CO)_3]$ (3.0 mmol), generated from $[CpW(CO)_3]_2$ (1.00 g, 1.5 mmol) over Na/Hg (0.40 g Na, 4 ml Hg) in THF (20 ml) at room temperature,

was added dropwise over 5 minutes to 1,3-dibromopropane (1.20 g, 6.0 mmol) in THF (2 ml) with stirring at room temperature. The reaction mixture was stirred for 44 hours at room temperature to effect completion. The reaction was monitored by IR spectroscopy, based on the decrease of the ν(CO) bands of the anion $[CpW(CO)_3]^-$ at 1894, 1790 and 1744 cm^{-1}. The solvent was removed under reduced pressure and the residue was extracted with CH_2Cl_2 (3 x 30 ml), filtered and the solvent removed. The residue was dissolved in a minimum amount of 10% CH_2Cl_2/hexane, then separated on an alumina column. Elution with hexane gave a yellow band which was concentrated, and cooled to -78 °C to yield yellow crystals of the pure product $[CpW(CO)_3\{(CH_2)_3Br\}]$ (0.90 g, 66%). The melting point, elemental analysis and physical characterization data are given in the section 5.1.3 of Chapter 5 of this thesis.

Preparation of $[CpW(CO)_3\{(CH_2)_4Br\}]$ [36]

This was prepared by the method described above for $[CpW(CO)_3\{(CH_2)_3Br\}]$ with the following quantities of reagents: $[CpW(CO)_3]_2$, (0.57 g, 0.85 mmol), 1,4-dibromobutane (1.10 g, 4.9 mmol), and a reaction time of 114 hours at room temperature. Work-up as described above for $[CpW(CO)_3\{(CH_2)_3Br\}]$, gave $[CpW(CO)_3\{(CH_2)_4Br\}]$ as yellow crystals (0.36 g, 45 %).

Preparation of $[CpW(CO)_3\{(CH_2)_5Br\}]$

This was prepared by the method described above for $[CpW(CO)_3\{(CH_2)_3Br\}]$ with the following quantities of reagents: $[CpW(CO)_3]_2$, (0.80 g, 1.2 mmol), 1,5-dibromopentane (1.04 g, 4.5 mmol), and a reaction time of 10 days at room temperature. Work-up as described above for $[CpW(CO)_3\{(CH_2)_3Br\}]$, gave $[CpW(CO)_3\{(CH_2)_5Br\}]$ as yellow crystals (0.60 g, 50 %).

Preparation of [$CpW(CO)_3\{(CH_2)_6Br\}$]

This was prepared by the method described above for [$CpW(CO)_3\{(CH_2)_3Br\}$] with the following quantities of reagents: $[CpW(CO)_3]_2$, (0.45 g, 0.68 mmol), 1,6-dibromohexane (0.38 g, 1.56 mmol), and a reaction time of 16 hours under refluxing condition. Work-up as described above for [$CpW(CO)_3\{(CH_2)_3Br\}$], elution with hexane and gradually increasing the polarity by addition of diether ether, and recrystallization from hexane at -20 °C, gave [$CpW(CO)_3\{(CH_2)_6Br\}$] as yellow crystals (0.33 g, 49 %).

Preparation of [$CpW(CO)_3\{(CH_2)_7Br\}$]

This was prepared by the method described above for [$CpW(CO)_3\{(CH_2)_6Br\}$] with the following quantities of reagents: $[CpW(CO)_3]_2$, (0.50 g, 0.75 mmol), 1,7-dibromoheptane (0.46 g, 1.78 mmol), and a reaction time of 16 hours under refluxing condition. Work-up as described above for [$CpW(CO)_3\{(CH_2)_6Br\}$], and recrystallization from hexane at -78 °C, gave [$CpW(CO)_3\{(CH_2)_7Br\}$] as yellow crystals (0.28 g, 37 %).

Preparation of [$CpW(CO)_3\{(CH_2)_3I\}$]

Sodium iodide (0.10 g, 0.68 mmol) was added to a solution of [$CpW(CO)_3\{(CH_2)_3Br\}$] (0.16 g, 0.34 mmol) in acetone (10 ml). The mixture was stirred at room temperature for 27 hours. The solvent was removed under reduced pressure and the residue extracted with hexane. The combined extracts were filtered, concentrated and transferred to an alumina column. Elution with hexane gave a yellow band, which was concentrated, filtered and recrystallized from hexane at -20 °C. The product [$CpW(CO)_3\{(CH_2)_3I\}$] (0.12 g, 70 %) was obtained as yellow crystals.

Preparation of $[CpW(CO)_3\{(CH_2)_4I\}]$ [37]

This was prepared by the method described above for $[CpW(CO)_3\{(CH_2)_3Br\}]$ with the following quantities of reagents: $[CpW(CO)_3]_2$, (1.00 g, 1.5 mmol), 1,4-diiodobutane (1.10 g, 3.5 mmol), and a reaction time of 6 hours at room temperature. Work-up as described above for $[CpW(CO)_3\{(CH_2)_3Br\}]$, and recrystallization from hexane at -20 °C gave $[CpW(CO)_3\{(CH_2)_4I\}]$ as yellow crystals (0.87 g, 56 %).

Preparation of $[CpW(CO)_3\{(CH_2)_5I\}]$ [37]

This was prepared by the method described above for $[CpW(CO)_3\{(CH_2)_3I\}]$ with the following quantities of reagents: $[CpW(CO)_3\{(CH_2)_5Br\}]$ (0.30 g, 0.62 mmol), NaI (0.30 g, 1.8 mmol), and a reaction time of 30 hours. Work-up as described above for $[CpW(CO)_3\{(CH_2)_3I\}]$, and recrystallization from acetone/hexane at -20 °C for 4 days gave $[CpW(CO)_3\{(CH_2)_5I\}]$ as yellow crystals (0.21 g, 63 %).

Preparation of $[CpW(CO)_3\{(CH_2)_6I\}]$

This was prepared by the method described above for $[CpW(CO)_3\{(CH_2)_3I\}]$, with the following quantities of reagents: $[CpW(CO)_3\{(CH_2)_6Br\}]$ (0.17 g, 0.35 mmol), NaI (0.12 g, 0.8 mmol), and a reaction time of 36 hours. Work-up as described above for $[CpW(CO)_3\{(CH_2)_3I\}]$, and recrystallization from hexane at -20 °C gave $[CpW(CO)_3\{(CH_2)_6I\}]$ as yellow crystals (0.12 g, 62 %).

Preparation of $[CpW(CO)_3\{(CH_2)_7I\}]$

This was prepared by the method described above for $[CpW(CO)_3\{(CH_2)_3I\}]$ with the following quantities of reagents: $[CpW(CO)_3\{(CH_2)_7Br\}]$ (0.15 g, 0.30 mmol), NaI (0.11 g, 0.7 mmol), and a reaction time of 36 hours. Work-up as

described above for [$CpW(CO)_3\{(CH_2)_3I\}$], and recrystallization from hexane at -78 °C gave [$CpW(CO)_3\{(CH_2)_7I\}$] as yellow crystals (0.09 g, 57 %).

Preparation of [$Cp^*W(CO)_3\{(CH_2)_3Br\}$] [38]

A solution of $Na[Cp^*W(CO)_3]$ (0.64 mmol, generated from $[Cp^*W(CO)_3]_2$ (0.26 g, 0.32 mmol) over Na/Hg (0.16 g Na, 2 ml Hg) in THF (15 ml) at room temperature for 1 hour, was added dropwise to a solution of 1,3-dibromopropane (0.26 g, 1.28 mmol) in THF (2 ml) at 0 °C with rapid stirring. The reaction mixture was allowed to be stirred for 18 hours at room temperature. After completion, the solvent was removed under reduced pressure, leaving a yellow residue. This was extracted with diether ether, concentrated and chromatographed on an alumina column. Elution with hexane gave a fast moving yellow band, which was collected. The solvent was removed to give a yellow oily product. Recrystallization from pentane at -78 °C gave [$Cp^*W(CO)_3\{(CH_2)_3Br\}$] as a yellow crystalline solid (0.23 g, 68 %).

Preparation of [$Cp^*W(CO)_3\{(CH_2)_4Br\}$]

This was prepared similarly as above from $[Cp^*W(CO)_3]_2$ (0.48 g, 0.60 mmol) and 1,4-dibromobutane (0.39 g, 1.8 mmol), and a reaction time of 18 hours. Recrystallization from hexane at -78 °C gave [$Cp^*W(CO)_3\{(CH_2)_4Br\}$] as a yellow crystalline solid (0.40 g, 62 %).

Preparation of [$Cp^*W(CO)_3\{(CH_2)_3I\}$]

This was prepared by the method described previously for the preparation of [$CpW(CO)_3\{(CH_2)_3I\}$] with the following quantities of reagents: [$Cp^*W(CO)_3\{(CH_2)_3Br\}$] (0.17 g, 0.32 mmol), NaI (0.14 g, 0.93 mmol) and a reaction time of 45 hours. Recrystallization from hexane at -78 °C gave [$Cp^*W(CO)_3\{(CH_2)_3I\}$] as yellow crystals (0.15 g, 78%).

Preparation of $[Cp^*W(CO)_3\{(CH_2)_4I\}]$

This was prepared by the method described for the preparation of $[Cp^*W(CO)_3\{(CH_2)_3I\}]$ with the following quantities of reagents: $[Cp^*W(CO)_3\{(CH_2)_4Br\}]$ (0.25 g, 0.46 mmol), NaI (0.26 g, 1.7 mmol) and a reaction time of 42 hours. Recrystallization from hexane at -78 °C gave $[Cp^*W(CO)_3\{(CH_2)_4I\}]$ as yellow crystals (0.19 g, 71 %).

The melting points, elemental analyses and characterization data for abovementioned complexes are given in the section 5.1.3 of Chapter 5 of this thesis.

Reaction of $[CpW(CO)_3\{(CH_2)_3Br\}]$ with 3,5-dihydroxybenzyl alcohol to give the benzyl alcohol complexes $[\{CpW(CO)_3(CH_2)_3O-\}_2(C_6H_3)-CH_2OH]$ and $[\{CpW(CO)_3(CH_2)_3O-\}(C_6H_4)-CH_2OH]$

A mixture of $[CpW(CO)_3\{(CH_2)_3Br\}]$ (2.05 g, 4.52 mmol), 3,5-dihydroxybenzyl alcohol (0.31 g, 2.2 mmol), 18-crown-6 (0.116 g, 0.45 mmol) and K_2CO_3 (0.91 g, 6.6 mmol) in acetone (70 ml) was heated to reflux and stirred vigorously for 67 hours. The reaction was protected from light by aluminium foil and monitored by TLC (Alumina, 30% CH_2Cl_2/hexane). The reaction mixture was then allowed to cool and the solvent removed under reduced pressure, leaving a yellow-orange residue. The residue was extracted with CH_2Cl_2 three times. The combined extracts were filtered, concentrated and then transferred to an alumina column. The first yellow band was eluted with 70% CH_2Cl_2/hexane, which gave presumably unreacted starting material in very small amount. Eluting with CH_2Cl_2 and gradually increasing the polarity to 10% MeOH/CH_2Cl_2 gave additional two yellow bands. The major band was collected, and the solvent was removed, giving a yellow solid product. The yellow product was then recrystallized from CH_2Cl_2/hexane to give the yellow crystalline product $[\{CpW(CO)_3(CH_2)_3O-\}_2(C_6H_3)-CH_2OH]$ (1.02 g, 51% based on 3,5-dihydroxybenzyl alcohol); m.p. 155 -157 °C (Found: C, 38.97; H, 3.14%;

$C_{29}H_{28}O_9W_2$ requires: C, 39.21; H, 3.18%), IR ν(CO) (CH_2Cl_2): 2013s, 1913s cm^{-1}; ^1H NMR ($CDCl_3$) δ (ppm): 6.49 (2 H, d, ^4J(HH) 2.4 Hz, aromatic), 6.37 (1 H, t, ^4J(HH) 2.4 Hz, aromatic), 5.41 (10 H, s, Cp), 4.61 (2 H, s, C*H*$_2$OH), 3.86 (4 H, t, ^3J(HH) 6.4 Hz, CH_2OAr), 2.01 (4 H, m, $CH_2CH_2CH_2$), 1.56 (4 H, m, WCH_2); ^{13}C NMR ($CDCl_3$) δ (ppm): 228.57, 217.37 (CO), 160.52, 143.19, 105.10, 100.52 (Ar), 91.57 (Cp), 71.96 (CH_2OAr), 65.48 (CH_2OH), 36.22 ($CH_2CH_2CH_2$), -16.43 (WCH_2). The minor yellow band was also collected, which after removing solvent and recrystallization from CH_2Cl_2/hexane, gave another yellow product [{$CpW(CO)_3(CH_2)_3O$-}(C_6H_4)-CH_2OH] (0.071 g, 3%); m.p. 141 - 144 °C (Found: C, 41.75; H, 3.51%; $C_{18}H_{18}O_6W$ requires: C, 42.05; H, 3.53%), IR ν(CO) (CH_2Cl_2): 2013s, 1911s cm^{-1}; ^1H NMR ($CDCl_3$) δ (ppm): 6.49 (1 H, d, ^4J(HH) 2.4 Hz, aromatic), 6.42 (1 H, m, aromatic) 6.31 (1 H, t, ^4J(HH) 2.4 Hz, aromatic), 5.41 (5 H, s, Cp), 4.92 (1 H, s, ArO*H*), 4.60 (2 H, s, C*H*$_2$OH), 3.85 (2 H, t, ^3J(HH) 6.4 Hz, CH_2OAr), 2.01 (2 H, m, $CH_2CH_2CH_2$), 1.56 (2 H, m, WCH_2), 1.25 (1 H, s, CH_2OH).

Reaction of [$CpW(CO)_3\{(CH_2)_4I\}$] with 3,5-dihydroxybenzyl alcohol to give [{$CpW(CO)_3(CH_2)_4O$-}$_2$(C_6H_3)-CH_2OH]

A mixture of [$CpW(CO)_3\{(CH_2)_4I\}$] (0.13 g, 0.26 mmol), 3,5-dihydroxybenzyl alcohol (0.018 g, 0.13 mmol), 18-crown-6 (0.01 g, 0.04 mmol) and K_2CO_3 (0.09 g, 0.66 mmol) in acetone (20 ml) was heated to reflux and stirred vigorously for 48 hours. Work-up as described above for [{$CpW(CO)_3(CH_2)_3O$-}$_2$(C_6H_3)-CH_2OH], gave the complex [{$CpW(CO)_3(CH_2)_4O$-}$_2$(C_6H_3)-CH_2OH] (0.029 g, 24%) as a yellow solid; IR ν(CO) (CH_2Cl_2): 2011s, 1911s cm^{-1}; ^1H NMR ($CDCl_3$) δ (ppm): 6.51 (2 H, d, ^4J(HH) 2.4 Hz, aromatic), 6.38 (1 H, t, ^4J(HH) 2.4 Hz, aromatic), 5.38 (10 H, s, Cp), 4.62 (2 H, s, C*H*$_2$OH), 3.96 (4 H, t, ^3J(HH) 6.4 Hz, CH_2OAr), 1.76 (8 H, m, $CH_2CH_2CH_2CH_2$), 1.56 (4 H, m, WCH_2), 1.25 (1 H, s, CH_2OH); ^{13}C NMR ($CDCl_3$) δ (ppm): 228.79, 217.51 (CO), 160.52, 143.17, 105.15, 100.68 (Ar), 91.49 (Cp), 67.29 (CH_2OAr), 65.47 (CH_2OH), 35.03, 33.08 ($CH_2CH_2CH_2CH_2$), -11.24 (WCH_2). No satisfactory elemental analysis results were obtained.

Reaction of [CpW(CO)$_3${(CH$_2$)$_3$Br}] with 1,1,1-tris(4'-hydroxyphenyl)ethane to give the tritungsten complex [{CpW(CO)$_3$(CH$_2$)$_3$O-(C$_6$H$_4$)}$_3$-CCH$_3$]

A mixture of [CpW(CO)$_3${(CH$_2$)$_3$Br}] (0.26 g, 0.57 mmol), 1,1,1-tris(4'-hydroxyphenyl)ethane (0.052 g, 0.17 mmol), 18-crown-6 (0.012 g, 0.05 mmol) and K_2CO_3 (0.15 g, 1.1 mmol) in acetone (20 ml) was heated to reflux and stirred vigorously for 72 hours. Work-up as described above for [{CpW(CO)$_3$(CH$_2$)$_3$O-}$_2$(C$_6$H$_3$)-CH$_2$OH] gave [{CpW(CO)$_3$(CH$_2$)$_3$O-(C$_6$H$_4$)}$_3$-CCH$_3$] (0.050 g, 61%); m.p. 85 - 88 °C (Found: C, 44.86; H, 4.03 %; $C_{53}H_{48}O_{12}W_3$ requires: C, 44.56; H, 3.39 %), IR ν(CO) (CH_2Cl_2): 2012s, 1913s cm^{-1}; ^{1}H NMR ($CDCl_3$) δ (ppm): 6.96 (6 H, d, ^{3}J(HH) 8.8 Hz), 6.75 (6H, d, ^{3}J(HH) 8.8 Hz), 5.40 (15 H, s, Cp), 3.85 (6 H, t, ^{3}J(HH) 6.4 Hz), 2.09 (3 H, s, CH_3), 2.00 (6 H, m, $CH_2C\mathit{H}_2CH_2$), 1.57 (6 H, m, WCH_2); ^{13}C NMR ($CDCl_3$) δ (ppm): 228.49, 217.21 (CO), 157.02, 141.66, 129.54, 113.61 (Ar), 91.48 (Cp), 71.80 (CH_2O), 50.55 ($\mathit{C}CH_3$), 36.27 ($WCH_2\mathit{C}H_2$), 30.73 ($C\mathit{C}H_3$), -16.36 (WCH_2).

Conversion of the benzyl alcohol complex [{CpW(CO)$_3$(CH$_2$)$_3$O-}$_2$(C$_6$H$_3$)-CH$_2$OH] to the benzyl bromide complex [{CpW(CO)$_3$(CH$_2$)$_3$O-}$_2$(C$_6$H$_3$)-CH$_2$Br]

To a solution of [{CpW(CO)$_3$(CH$_2$)$_3$O-}$_2$(C$_6$H$_3$)-CH$_2$OH] (0.13 g 0.15 mmol) in THF (2 ml) was added PPh_3 (0.05g, 0.19 mmol) and CBr_4 (0.06 g, 0.19 mmol). The reaction mixture was stirred for 15 minutes at room temperature. Additional PPh_3 (0.05g, 0.19 mmol) and CBr_4 (0.06 g, 0.19 mmol) were added to the reaction mixture and the reaction continued for another 25 minutes. Monitoring the reaction by TLC showed that complete conversion of the starting complex had occurred. Distilled water (10 ml) was added to quench the reaction. The resulting mixture was extracted twice with CH_2Cl_2 and the combined extracts were dried (Mg_2SO_4), concentrated and transferred to an alumina column. The first yellow band, eluted with 30% CH_2Cl_2/hexane, was very unstable and turned black soon after it was eluted. The second yellow band gave an oily solid. Recrystallization

from CH_2Cl_2/hexane and drying under high vacuum gave [{$CpW(CO)_3(CH_2)_3O$-}$_2(C_6H_3)$-CH_2Br] (0.014 g, 10%) as a yellow-brown solid, m.p. 96 - 105 °C (Found: C, 37.48; H, 3.12%; $C_{29}H_{28}O_8BrW_2$ requires: C, 36.62; H, 2.86%), IR ν(CO) (CH_2Cl_2): 2013s, 1913s cm^{-1}; ^1H NMR ($CDCl_3$) δ (ppm): 6.49 (2 H, d, ^4J(HH) 2.4 Hz, aromatic), 6.35 (1 H, t, ^4J(HH) 2.4 Hz, aromatic), 5.40 (10 H, s, Cp), 4.39 (2 H, s, C*H*$_2$Br), 3.85 (4 H, t, ^3J(HH) 6.4 Hz, CH_2OAr), 2.00 (4 H, m, $CH_2CH_2CH_2$), 1.55 (4 H, m, WCH_2).

Attempted reaction of [$RhCl_2(DH_2)(DH)$] with [$CpW(CO)_3\{(CH_2)_4I\}$]: Isolation of [$CpW(CO)_3\{(CH_2)_4OCH_3\}$]

This procedure is similar to that reported for the synthesis of [$RhR(DH)_2(py)$] [41].

[$RhCl_2(DH_2)(DH)$] (0.12 g, 0.30 mmol) was suspended in MeOH (18 ml). The suspension was treated with 50% aqueous KOH solution (3 ml) at room temperature followed by a solution of $NaBH_4$ (0.012 g, 0.30 mmol) in MeOH (2 ml). An immediate colour change from yellow to black indicated that the reduction of Rh(III) to Rh(I) had occurred. After 30 minutes, [$CpW(CO)_3\{(CH_2)_4I\}$] (0.165 g, 0.32 mmol) was added to the Rh(I) solution at room temperature. The colour of the reaction mixture gradually turned to yellow. After 30 minutes, pyridine (0.03 g, 0.38 mmol) was added to the mixture and the solution stirred for further 40 minutes. The solvent was removed under reduced pressure, leaving a yellow oil. The oil was dissolved in CH_2Cl_2 and the solution washed with water and NH_4Cl solution. The organic layer was separated, the aqueous layer was washed once with CH_2Cl_2. The combined CH_2Cl_2 solution was dried (Mg_2SO_4), concentrated and dried, to give a yellow solid. This solid was further purified by chromatography on an alumina column, eluted with hexane then gradually increase the polarity by slow adding ether. The first yellow fraction was unreacted starting material [$CpW(CO)_3\{(CH_2)_4I\}$], based on its TLC and IR. The second yellow band, after recrystallization from hexane, gave [$CpW(CO)_3\{(CH_2)_4OCH_3\}$] (0.032 g, 25%), m.p. 59 - 60 °C (Found: C, 37.77; H, 3.91%; EI-Mass spectrum, *m/z* 420/422 (M^+), $C_{13}H_{16}O_4W$ requires: C, 37.17; H,

3.84%; M, 420), IR ν(CO) (hexane): 2016s, 1926vs cm^{-1}; ^1H NMR ($CDCl_3$) δ (ppm): 5.39 (5 H, s, Cp), 3.38 (2 H, t, $^3J(HH)$ 6.4, CH_2O), 3.34 (3 H, s, CH_3O), 1.58 (6 H, m, $WCH_2CH_2CH_2$). ^{13}C NMR ($CDCl_3$) δ (ppm): 228.91, 217.45 (CO), 91.47 (Cp), 72.27 (CH_2O), 58.49 (CH_3O), 35.60, 33.30 ($CH_2CH_2CH_2CH_2$), -10.69 (WCH_2).

7.5.2 Synthesis and reactivity of hydroxyalkyl complexes [$CpW(CO)_3\{(CH_2)_nOH\}$]

Preparation of [$CpW(CO)_3\{(CH_2)_3OH\}$]

A solution of $Na[CpW(CO)_3]$ (2.6 mmol) was added dropwise to 3-bromo-1-propanol (0.60 g, 4.3 mmol) at room temperature with stirring. The mixture was stirred for 51 hours at room temperature, then at refluxing THF for 17 hours. After cooling, the solvent was removed under reduced pressure and the residue extracted with diether ether. The combined extracts were concentrated, chromatographed on an alumina column. Elution with hexane and then ether gave a major yellow band, from which the solvent was removed and the residue dissolved in a minimum amount of ether. After filtration, hexane was added to precipitate the product. Recrystallization from CH_2Cl_2/hexane at -78 °C gave the product [$CpW(CO)_3\{(CH_2)_3OH\}$] as a yellow crystalline solid (0.28 g, 27 %).

Preparation of [$CpW(CO)_3\{(CH_2)_6OH\}$]

This was prepared by the method described above for [$CpW(CO)_3\{(CH_2)_3OH\}$] with the following quantities of reagents: $[CpW(CO)_3]_2$, (0.53 g, 0.8 mmol), 6-bromo-1-hexanol (0.52 g, 2.8 mmol), and a reaction time of 68 hours at *ca.* 50 °C. Work-up as described above for [$CpW(CO)_3\{(CH_2)_3OH\}$], elution with diether ether/CH_2Cl_2 gave a yellow band, from which a yellow solid was obtained. Recrystallization from CH_2Cl_2/hexane gave the product [$CpW(CO)_3\{(CH_2)_6OH\}$] as a yellow crystalline solid (0.20 g, 29 %).

Preparation of [$CpW(CO)_3\{(CH_2)_7OH\}$]

This was prepared by the method described above for [$CpW(CO)_3\{(CH_2)_6OH\}$] with the following quantities of reagents: $[CpW(CO)_3]_2$, (0.52 g, 0.78 mmol), 7-bromo-1-heptanol (0.30 g, 1.56 mmol) and a reaction time of 48 hours at refluxing THF. Excess 7-bromo-1-heptanol could not be used due to the difficulty in separation. Acetone/hexane were used as elution solvent. The final product [$CpW(CO)_3\{(CH_2)_7OH\}$] (0.32 g, 46 %) was isolated as a yellow oil.

Reaction of [$CpW(CO)_3\{(CH_2)_7OH\}$] with *p*-anisoyl chloride to give [$CpW(CO)_3\{(CH_2)_7OC(O)(C_6H_4)OMe\}$]

To a solution of [$CpW(CO)_3\{(CH_2)_7OH\}$] (0.30 g, 0.52 mmol) in ether (8 ml), cooled to -78 °C, was added ^nBuLi (0.65 ml, 1.6 mmol) in hexane dropwise. The mixture was stirred and allowed to warm to -30 °C in about 40 minutes, then cooled to -78 °C again. A solution of *p*-anisoyl chloride (0.17 g, 1.0 mmol) in ether (1 ml) was added dropwise at -78 °C. The reaction mixture was stirred and warmed to room temperature, and stirred for additional 10 minutes at room temperature. The solution was filtered, and the solid residue was washed with ether. The filtrate and combined washings were dried to give a yellow product. Recrystallization from ether/hexane at -20 °C for 3 days gave a yellow crystalline product, [$CpW(CO)_3\{(CH_2)_7OC(O)(C_6H_4)OMe\}$] (0.13 g, 33%), m.p. 71 - 74 °C (Found: C, 47.23, H, 4.61%; EI-Mass spectrum, *m/z* 580/581 (M^+), $C_{23}H_{22}O_6W$ requires: C, 47.44; H, 4.50%; M, 580), IR ν(CO) (CH_2Cl_2): 2009s, 1910s, ν(CO_2) 1706m, 1608m cm^{-1}; ^1H NMR ($CDCl_3$) δ (ppm): 8.00 (2 H, m, Ar), 6.92 (2 H, m, Ar), 5.36 (5 H, s, Cp), 4.28 (2 H, t, ^3J(HH) 6.8 Hz, CH_2O), 3.86 (3 H, s, CH_3O), 1.74 (2 H, qn, ^3J(HH) 6.8, CH_2CH_2O), 1.54 (4 H, m, $(CH_2)_n$), 1.38 (6 H, m, $(CH_2)_n$). ^{13}C NMR ($CDCl_3$) δ (ppm): 228.97, 217.52 (CO), 166.44 (CO_2), 163.22, 131.52, 123.00, 113.54 (Ar), 91.45 (Cp), 64.82 (CH_2O), 55.39 (CH_3O), 36.75, 35.74, 28.75, 26.08 $(CH_2)_n$, -10.13 (WCH_2).

Attempted reaction of $[CpW(CO)_3\{(CH_2)_3OH\}]$ with $[Cp^*Re(NO)(CO)_2]^+BF^-_4$

To a solution of $[CpW(CO)_3\{(CH_2)_3OH\}]$ (0.20 g, 0.51 mmol) in ether (8 ml), cooled to -78 °C, was added ^{n}BuLi (0.22 ml, 0.5 mmol) in hexane dropwise. The mixture was stirred and allowed to warm to -30 °C in about 1 hour, then cooled down to -78 °C again. Solid $[Cp^*Re(NO)(CO)_2]^+BF^-_4$ (0.25 g, 0.51 mmol) was added at -78 °C. The reaction mixture was allowed to warm to room temperature and stirred overnight. Work-up procedure was similarly carried out as described previously for the preparation of $[CpW(CO)_3\{(CH_2)_7OC(O)(C_6H_4)OMe\}]$. The crude product was obtained as a brown gum, expected to be $[Cp^*(NO)(CO)Re\{C(O)O(CH_2)_3\}WCp(CO)_3]$ (0.31 g, 76%), IR ν(CO) (CH_2Cl_2) 2010s, 1979s, 1913s, ν(CO_2) 1703m, 1616w. ^{1}H NMR spectrum of the product in $CDCl_3$ showed that this complex was not pure, however, multiplets in the region δ 3.8 - 4.3 ppm was observed which could be due to the CO_2CH_2 protons.

7.5.3 Synthesis of haloalkyl complexes $[Re(CO)_5\{(CH_2)_nX\}]$

General procedure for the preparation of $[Re(CO)_5\{(CH_2)_nBr\}]$ (n = 3, 4 and 5)

An orange solution of $Na[Re(CO)_5]$ (2 - 3 mmol), generated from $[Re_2(CO)_{10}]$ and Na/Hg in THF (*ca.* 20 ml) [43], was added dropwise to a solution of $Br(CH_2)_nBr$ (1 - 1.2 equiv.) in THF (10 ml) at -78 °C with stirring. The mixture was allowed to warm to room temperature and stirred for further 2 - 5 hours. The solvent was removed under reduced pressure. The residue was extracted with ether. The extracts were concentrated and transferred to an alumina column. Eluting with hexane separated a fast moving colourless band, which was collected, filtered and concentrated. A colourless solid was obtained which was further purified by recrystallization from hexane at -78°C. The yields, m.p.s, and characterization data for these complexes can be found in the section 5.3 of Chapter 5 of this thesis.

General procedure for the preparation of $[Re(CO)_5\{(CH_2)_nI\}]$ (n = 3, 4 and 5)

A mixture of $[Re(CO)_5\{(CH_2)_nBr\}]$ (0.8 mmol) and NaI (2.2 mmol) in acetone (10 ml) was stirred at room temperature for 44 - 45 hours. The reaction mixture was protected from light by aluminium foil. The solvent was removed under reduced pressure and the residue extracted with ether, concentrated and transferred to a short alumina column. Elution with hexane separated a fast moving colourless band, from which the solvent was removed. The residue was dissolved in hexane and the solution cooled down to -78 °C. The product $[Re(CO)_5\{(CH_2)_nI\}]$ separated out as a white solid at low temperature but turned to an oil at room temperature. The yields, m.p.s and characterization data can be found in the section 5.3 of Chapter 5 of this thesis. The complex $[Re(CO)_5\{(CH_2)_4I\}]$ has been prepared previously [39] by a different method to that reported here.

7.6 Experimental details pertaining to Chapter 6

7.6.1 Synthesis and reactivity of polymethylene bridged heterobimetallic complexes $[LM(CH_2)_nPtIMe_2(R_2\text{-bipy})]$

The complexes $[CpFe(CO)_2\{(CH_2)_4X\}]$ (X = Br [44], I [45]), $[Cp^*Fe(CO)_2\{(CH_2)_nI\}]$ (n = 3, 4) [45] and $[Cp^*Ru(CO)_2\{(CH_2)_4I\}]$ [46] were prepared according to the literature procedures.

General procedure for the synthesis of polymethylene bridged heterobimetallic complexes $[LM(CH_2)_nPtIMe_2(R_2\text{-bipy})]$

To a mixture of $[PtMe_2(R_2\text{-bipy})]$ (0.1 mmol) and $[LM\{(CH_2)_nI\}]$ (0.1 - 0.11 mmol) in a nitrogen flushed round-bottom flask wrapped in foil, was added benzene (or acetone, *ca.* 15 - 20 ml, see Scheme 6.4 and 6.5), to form an orange-red solution. The solution was stirred under nitrogen at room temperature for a desired time period (see Scheme 6.4 and 6.5). After this time, the solution

changed to yellow and yellow precipitate formed. The solution was concentrated to give a yellow solid product. Hexane was added to give more yellow product. The mother liquor was removed by syringe and the solid product washed twice with hexane to remove excess [LM{$(CH_2)_nI$}]. The pure product [LM$(CH_2)_n$PtIMe_2(R_2-bipy)] was obtained after recrystallization from CH_2Cl_2/ether and drying under high vacuum (0.02 - 0.1 mmHg), as a yellow crystalline solid. The yields, elemental analyses and characterization data are given in the section 6.1.3 of Chapter 6 of this thesis.

Attempted reactions of [Cp*W(CO)$_3$(CH$_2$)$_3$PtIMe_2(Me_2-bipy)] and [Cp*Fe(CO)$_2$(CH$_2$)$_4$PtIMe_2(Me_2-bipy)] with CO_2

(a): Reaction of [Cp*W(CO)$_3$(CH$_2$)$_3$PtIMe_2(Me_2-bipy)] with CO_2

A solution of [Cp*W(CO)$_3$(CH$_2$)$_3$PtIMe_2(Me_2-bipy)] (0.03 g, 0.03 mmol) in EtOH (4 ml) and NEt_3 (4 ml) in a small flask was saturated with CO_2. The flask was then placed in an autoclave. The autoclave was sealed, filled with CO_2 (20 bar) and the gas vented. This procedure was repeated three times and then the autoclave was pressurized with CO_2 (40 bar) at room temperature. The autoclave was stirred and heated to 25 °C for 24 hours. An IR spectrum of the reaction mixture showed that there was unreacted starting material. The reaction was then continued at 45° for 43 hours. The autoclave was then cooled to room temperature and the gas vented. The solvent was removed, leaving a yellow solid product. The product was dried and analyzed by IR, ^1H and ^{13}C NMR, and identified to be the starting complex [Cp*W(CO)$_3$(CH$_2$)$_3$PtIMe_2(Me_2-bipy)] (quantitative recovery).

(b): Reaction of [Cp*Fe(CO)$_2$(CH$_2$)$_4$PtIMe_2(Me_2-bipy)] with CO_2

A suspension of [Cp*Fe(CO)$_2$(CH$_2$)$_4$PtIMe_2(Me_2-bipy)] (0.04 g, 0.05 mmol) in toluene (8 ml) in a small flask was placed in an autoclave. The autoclave was sealed, filled with CO_2 (20 bar) and the gas vented. This procedure was repeated three times and then the autoclave was filled with CO_2 (43 bar) at room

temperature. The autoclave was stirred and heated to 80 °C for 42 hours. The autoclave was then cooled to room temperature and the gas vented. The solvent was removed, leaving a yellow solid product. The product was dried and analyzed by IR, ^{1}H and ^{13}C NMR, and identified to be the starting complex [Cp*Fe(CO)$_2$(CH$_2$)$_4$PtIMe$_2$(Me$_2$-bipy)] (quantitative recovery).

7.6.2 Synthesis and reactivity of the binuclear complex [Me$_2$Pt{(Me-bipy)-(CH$_2$)$_5$-(Me-bipy)}PtMe$_2$]

Preparation of 1,5-bis(4'-methyl-2,2'-bipyridyl-4-yl)pentane [47,48]

To a solution of diisopropylamine (1.20 g, 11 mmol) in dry THF (8 ml), ^{n}BuLi (5.4 ml of a 2.5 M solution in hexane, 13.5 mmol,) was added at -78 °C. The mixture was stirred for 20 minutes at -78 °C, then a solution of 4,4'-dimethyl-2,2'-bipyridine (2.00 g, 11 mmol) in THF (70 ml) was added by syringe at the same temperature. The reaction mixture was kept at this temperature for 3 hours, after that, 1,3-dibromopropane (1.10 g, 5.5 mmol) was added. The mixture was allowed to warm to room temperature and stirred overnight. Water (40 ml) was added to quench the solution. The mixture was extracted with CH_2Cl_2 (3 x 50 ml) and dried ($MgSO_4$). The solvent was removed, leaving a brown oily residue. The residue was dissolved in a minimum amount of CH_2Cl_2 and chromatographed on a silica gel column, eluted with 10% acetone in CH_2Cl_2. A colourless band was collected, which gave a white solid product. Recrystallization from ethyl acetate afforded 1,5-bis(4'-methyl-2,2'-bipyridyl-4-yl)pentane (1.00 g, 45%), m.p. 99 - 101°C; UV-vis λ_{max}/nm (CH_2Cl_2) 302 (ε/dm^3 mol^{-1}cm^{-1} 285); IR ν/cm^{-1} 3055w, 3006w, 2945m, 2917m, 2855w, 1945w,1595vs, 1548s, 1456s, 1444m, sh, 1424s, 1378m, 1359w, 1333m, 1284w, 1274w, 1238m, 1210s, 1193m, 1107s, 1072m, 1035w, 992s, 974w, 915w, 902m, 824vs, 770w 755w (KBr); ^{1}H NMR ($CDCl_3$) δ (ppm): 8.52 - 8.54 [4 H, m, (6,6')], 8.22 [4 H, m, (3, 3')], 7.10 - 7.13[4 H, m, (5, 5')], 2.69 [4 H, t, ^{3}J(HH) 7.6 Hz, (7, 7')], 2.43 [6 H, s, (CH_3)], 1.73 [4 H, m, (8, 8')], 1.43 [2 H, qn, ^{3}J(HH) 7.6 Hz, (9)]; ^{13}C NMR ($CDCl_3$) δ (ppm): 156.15, 156.05 (2, 2'), 152.49, 148.09 (4, 4'), 148.99, 148.90 (6, 6'), 124.60, 123.85 (5,

5'), 122.01, 121.23 (3, 3'), 35.33 (7, 7'), 30.15 (8, 8'), 28.88 (9), 21.16 (CH_3). The m.p. and ^1H NMR data have been reported [48] and our results are in agreement with the literature.

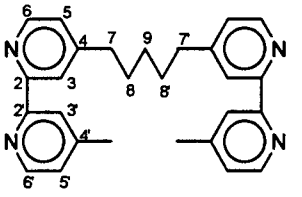

Atom numbering scheme for 1,5-bis(4'-methyl-2,2'-bipyridyl-4-yl)pentane

Preparation of the binuclear Pt(II) complex [Me_2Pt{(Me-bipy)-$(CH_2)_5$-(Me-bipy)}$PtMe_2$]

A solution of 1,5-bis(4'-methyl-2,2'-bipyridyl-4-yl)pentane (0.08 g, 0.2 mmol) in acetone (10 ml) was added to a stirred solution of [$Pt_2Me_4(SMe_2)_2$] (0.13 g, 0.23 mmol) in benzene (6 ml). The mixture was stirred for 3 hours at room temperature under nitrogen and then kept in fridge overnight. An orange-red solid product [Me_2Pt{(Me-bipy)-$(CH_2)_5$-(Me-bipy)}$PtMe_2$] (0.15 g, 87 %) was obtained after removal of the solvent, washing with diethyl ether and drying under high vacuum; m.p. 230 - 235 °C (decomposed without melting) (Found: C, 43.52; H, 4.68; N, 6.38%; ES-MS: 883.87 $[M+CH_3CN-CH_3]^+$, $C_{31}H_{40}N_4Pt_2$ requires C, 43.33; H, 4.70; N, 6.53 %; M 858.85); UV-vis λ_{max}/nm (CH_2Cl_2) 300 (ε/dm^3 mol^{-1} cm^{-1} 784), 448 (598); λ_{max}/nm (acetone) 466; IR ν_{max}/cm^{-1} 3065w, 2891m, 2853m, 2786m, 1611s, 1548w, 1478m, 1421s, 1376w, 1304w, 1280w, 1222w, 1025w, 929w, 893m, 853m, 828s, 806m, 766w (KBr); ^1H NMR (CD_2Cl_2) δ (ppm): 9.00 - 9.05 [4 H, m, (6,6')], 8.82 [4 H, m, (3, 3')], 7.33 [4 H, m, (5, 5')], 2.68 [4 H, t, ^3J(HH) 7.6 Hz, (7, 7')], 2.38 [6 H, s, (ring-CH_3)], 1.79 [4 H, qn, ^3J(HH) 7.6 Hz, (8, 8')], 1.48 [2 H, m, (9)], 0.93 [12 H, s, ^2J(PtH) 86 Hz, (Pt-CH_3)], (For numbering the protons, please refer to the scheme for the ligand).

Reaction of $[Me_2Pt\{(Me\text{-}bipy)\text{-}(CH_2)_5\text{-}(Me\text{-}bipy)\}PtMe_2]$ with $[CpW(CO)_3\{(CH_2)_4I\}]$: Preparation of the hetero-tetranuclear complex $[CpW(CO)_3(CH_2)_4PtIMe_2\{(Me\text{-}bipy)\text{-}(CH_2)_5\text{-}(Me\text{-}bipy)\}Me_2IPt(CH_2)_4WCp(CO)_3]$

To a solution of $[Me_2Pt\{(Me\text{-}bipy)\text{-}(CH_2)_5\text{-}(Me\text{-}bipy)\}PtMe_2]$ (0.03 g, 0.035 mmol) in CH_2Cl_2 (5 ml) was added $[CpW(CO)_3\{(CH_2)_4I\}]$ (0.043 g, 0.083 mmol). The mixture was stirred for 5 hours at room temperature under nitrogen. The solvent was removed under reduced pressure to give a yellow residue, which was recrystallized twice from CH_2Cl_2/diethyl ether to afford the title hetero-tetranuclear complex as a yellow solid (0.04 g, 60%), m.p. 190 - 200 °C (decomposed without melting) (Found: C, 34.82; H, 3.75; N, 2.84%; $C_{55}H_{66}N_4O_6I_2Pt_2W_2$ requires C, 34.94; H, 3.52; N, 2.96 %); UV-vis λ_{max}/nm (CH_2Cl_2) 312 (ε/dm^3 mol^{-1} cm^{-1} 2271), 350 (922); IR ν(CO) (CH_2Cl_2): 2007s, 1907s cm^{-1}.

Reaction of $[Me_2Pt\{(Me\text{-}bipy)\text{-}(CH_2)_5\text{-}(Me\text{-}bipy)\}PtMe_2]$ with CO_2

A solution of $[Me_2Pt\{(Me\text{-}bipy)\text{-}(CH_2)_5\text{-}(Me\text{-}bipy)\}PtMe_2]$ (0.036 g, 0.04 mmol) in EtOH (6 ml) and NEt_3 (4 ml) was transferred to a small flask. The flask was then placed in an autoclave. The autoclave was sealed, filled with CO_2 (20 bar) and the gas vented. This procedure was repeated three times and then the autoclave was pressurized with CO_2 (40 bar) at room temperature. The autoclave was heated at 40 °C for 22 hours, cooled to room temperature and the gas vented. The IR spectrum of the reaction solution showed ν(CO) 1643 cm^{-1}(neat reaction solution). The UV-vis spectrum showed λ_{max} (acetone) 416 nm. This suggested the formation of $[\{EtO(O)CO\}MePt\{(Me\text{-}bipy)\text{-}(CH_2)_5\text{-}(Me\text{-}bipy)\}PtMe\{OC(O)OEt\}]$, by comparison to the spectroscopic data of the complex $[PtMe\{OC(O)OEt\}(bipy)]$ [49]. This product was not isolated due to its decomposition.

7.6.3 Synthesis of dendrimers containing Me-bipy pendant groups

Synthesis of 4-(4-bromobutyl)-4'-methyl-2,2'-bipyridine [48]

To a solution of diisopropylamine (1.20 g, 11 mmol) in dry THF (8 ml), ^{n}BuLi (5.4 ml of a 2.5 M solution in hexane, 13.5 mmol) was added at -78 °C. The mixture was stirred for 20 minutes at -78 °C, then a solution of 4,4'-dimethyl-2,2'-bipyridine (2.00 g, 11 mmol) in THF (70 ml) was added by syringe at the same temperature. The reaction mixture was kept at this temperature for 3 hours, after that, 1,3-dibromopropane (3.30 g 16 mmol) was added. The mixture was allowed to warm to room temperature and stirred overnight. Water (40 ml) was added to quench the solution. The mixture was extracted with CH_2Cl_2 (3 x 50 ml) and the extracts were dried ($MgSO_4$). The solvent was removed, leaving a brown oily residue. The residue was dissolved in a mininium amount of CH_2Cl_2 and chromatographed on a silical gel column, eluted with 5 % acetone in CH_2Cl_2. A colourless band was collected, which gave a white solid product. Recrystallization from ethyl acetate afforded 4-(4-bromobutyl)-4'-methyl-2,2'-bipyridine [0.96 g, 29% (based on 4,4'-dimethyl-2,2'-bipyridine)], m.p. 45 - 46 °C; ^{1}H NMR ($CDCl_3$) δ (ppm): 8.52 - 8.57 [2 H, m, (6,6')], 8.22 [2 H, m, (3, 3')], 7.12 - 7.14 [2 H, m, (5, 5')], 3.42 [2 H, t, ^{3}J(HH) 6.4 Hz, (10)], 2.72 [2 H, t, ^{3}J(HH) 7.6 Hz, (7)], 2.43 [3 H, s, (CH_3)], 1.86 [4 H, m, (8 + 9)]. ^{13}C NMR ($CDCl_3$) δ (ppm): 156.26, 155.93 (2, 2'), 151.73, 148.14 (4, 4'), 149.10, 148.91 (6, 6'), 124.68, 123.77 (5, 5'), 122.03, 121.18 (3, 3'), 34.51, 33.22, 32.15, 28.76 (7 - 10), 21.17 (CH_3). The ^{1}H NMR data have been reported [48] and our results are in agreement with the literature.

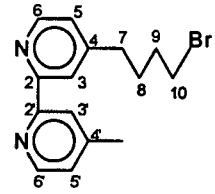

Atom numbering scheme for 4-(4-bromobutyl)-4'-methyl-2,2'-bipyridine

Synthesis of the first generation dendritic benzyl alcohol {(Me-bipy)-$(CH_2)_4O\}_2C_6H_3$-CH_2OH

A mixture of 4-(4-bromobutyl)-4'-methyl-2,2'-bipyridine (2.20 g, 7.2 mmol), 3,5-dihydroxybenzyl alcohol (0.45 g, 3.2 mmol), potassium carbonate (1.10 g, 8.0 mmol) and 18-crown-6 (0.17 g, 0.64 mmol) in acetone (45 ml) was heated to reflux and stirred vigorously under nitrogen for 48 hours. The mixture was allowed to cool and evaporated to dryness under reduced pressure. The residue was partitioned between water and CH_2Cl_2 and the aqueous layer was extracted with CH_2Cl_2 three times. The combined extracts were dried ($MgSO_4$) and evaporated. The crude product was purified by chromatography on a silica gel column, eluted with 20% acetone in CH_2Cl_2. A colourless band was collected which gave a white solid. Recrystallization from ethyl acetate and hexane yielded a white solid product {(Me-bipy)-$(CH_2)_4O\}_2C_6H_3$-CH_2OH (1.80 g, 96%), m.p. 124 - 126 °C [Found: C, 74.26; H, 7.18; N, 8.53%; ES-MS, *m/z* 588.70 ($[M]^+$, 35%), 294.88 ($[M+H]^{2+}$, 100%); $C_{37}H_{40}N_4O_3$ (+ 0.2 x ethyl acetate) requires C, 74.19; H, 6.72; N, 9.14%; M 588.76]; IR ν_{max}/cm^{-1} 3197w, 3055w, 2946m, 2927m, 2861m, 1593s, 1554m, 1457s, 1373m, 1320s, 1249w, 1205w, 1171s, 1108w, 1060m, 991m, 917w, 898w, 834s, 811m, 761m (KBr); ^1H NMR ($CDCl_3$) δ (ppm): 8.52 - 8.56 [4 H, m, (6,6')], 8.22 [4 H, m, (3, 3')], 7.12 - 7.14 [4 H, m, (5, 5')], 6.48 [2 H, d, ^4J(HH) 2 Hz, (12, 12')], 6.34 [1 H, t, ^4J(HH) 2 Hz (14)], 4.60 [2 H, s, (15)], 3.96 [4 H, t, ^3J(HH) 6 Hz, (10, 10')], 2.76 [4 H, t, ^3J(HH) 7.2 Hz, (7, 7')], 2.43 [6 H, s, (CH_3)], 1.86 [8 H, m, (8, 8' + 9, 9')]; [Peaks due to solvent ethyl acetate were observed at 4.13 (q), 2.04 (s) and 1.25 (tri)]; ^{13}C NMR ($CDCl_3$) δ (ppm): 160.29 (11, 11'), 156.15, 155.98 (2, 2'), 152.18, 148.14 (4, 4'), 149.02, 148.87 (6, 6'), 143.38 (13), 124.63, 123.87 (5, 5'), 122.04, 121.27 (3, 3'), 105.10 (12, 12'), 100.55 (14), 67.52 (10, 10'), 65.27 (15), 35.08 (7,7'), 28.79 (9, 9'), 26.84 (8, 8'), 21.15 (CH_3).

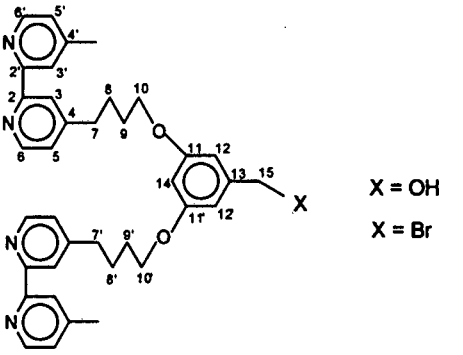

Atom numbering scheme for $\{(Me\text{-}bipy)\text{-}(CH_2)_4O\}_2C_6H_3\text{-}CH_2OH$ and $\{(Me\text{-}bipy)\text{-}(CH_2)_4O\}_2C_6H_3\text{-}CH_2Br$

Synthesis of the first generation dendritic benzyl bromide $\{(Me\text{-}bipy)\text{-}(CH_2)_4O\}_2C_6H_3\text{-}CH_2Br$

To a solution of $\{(Me\text{-}bipy)\text{-}(CH_2)_4O\}_2C_6H_3\text{-}CH_2OH$ (0.10 g, 0.16 mmol) in the minimum amount of THF (ca. 1 ml) was added PPh_3 (0.067 g, 0.26 mmol) and CBr_4 (0.085 g, 2.6 mmol). The reaction mixture was stirred at room temperature under nitrogen for 15 minutes. Monitoring the reaction by TLC (alumina plate, eluting with 10 % acetone in CH_2Cl_2) showed that complete conversion of the starting complex had occurred. Distilled water (*ca.* 1 ml) was added to quench the reaction mixture. The mixture was then extracted with CH_2Cl_2 (3 x 10 ml). The combined extracts were dried ($MgSO_4$) and evaporated to dryness. The crude product was purified by chromatography on a alumina column, eluted with first 20 % hexane in CH_2Cl_2 then gradually increasing the polarity to pure CH_2Cl_2 to give a colourless band. The pure product was obtained, after recrystallization from CH_2Cl_2/hexane, as a white solid product $\{(Me\text{-}bipy)\text{-}(CH_2)_4O\}_2C_6H_3\text{-}CH_2Br$ (0.09 g, 89%), m.p. 84 - 86 °C [Found: C, 67.30; H, 6.36; N, 8.04 %; ES-MS, *m/z* 652.59, 650.59, ($[M]^+$, 35%); 326.52, 325.90, ($[M+H]^{2+}$, 100%); $C_{37}H_{39}N_4O_2Br$ (+ 0.16 x CH_2Cl_2) requires C, 67.17; H, 6.01; N, 8.43 %; M 651.65]; IR ν_{max}/cm^{-1} 3053w, 3005w, 2949m, 2927m, 2861m, 1592s, 1554m, 1481w, 1457s, 1390m, 1372m, 1327s, 1265w, 1220w, 1203w, 1180s, 1072m, 1054m, 1035w, 990w, 936w, 898w, 853w, 833s, 812m, 759w (KBr); ^1H NMR ($CDCl_3$) δ (ppm): 8.52 -

8.56 [4 H, m, (6,6')], 8.23 [4 H, m, (3, 3')], 7.11 - 7.15 [4 H, m, (5, 5')], 6.50 [2 H, d, ^{4}J(HH) 2 Hz, (12, 12')], 6.35 [1 H, t, ^{4}J(HH) 2 Hz, (14)], 4.38 [2 H, s, (15)], 3.95 [4 H, t, ^{3}J(HH) 6 Hz, (10, 10')], 2.77 [4 H, t, ^{3}J(HH) 7.2 Hz, (7, 7')], 2.43 [6 H, s, (CH_3)], 1.86 [8 H, m, (8, 8' + 9, 9')]; [Peak due to the solvent CH_2Cl_2 was found at 5.29 (s)]; ^{13}C NMR ($CDCl_3$) δ (ppm): 160.21 (11, 11'), 156.19, 155.98 (2, 2'), 152.11, 148.11 (4, 4'), 149.04, 148.89 (6, 6'), 139.59 (13), 124.63, 123.85 (5, 5'), 122.01, 121.25 (3, 3'), 107.47 (12, 12'), 101.38 (14), 67.60 (10, 10'), 35.08 (7,7'), 33.62 (15), 28.77 (9, 9'), 26.84 (8, 8'), 21.15 (CH_3).

Preparation of the zero generation dendrimer {(Me-bipy)-$(CH_2)_4$-OC_6H_4}$_3$$CCH_3$

A mixture of 4-(4-bromobutyl)-4'-methyl-2,2'-bipyridine (0.46 g, 1.51 mmol), 1.1.1-tris(4'-hydroxyphenyl)ethane (0.14 g, 0.46 mmol), potassium carbonate (0.20 g, 1.5 mmol) and 18-crown-6 (0.04 g, 0.15 mmol) in acetone (25 ml) was heated to reflux and stirred vigorously under nitrogen for 48 hours. The mixture was allowed to cool to room temperature and evaporated to dryness under reduced pressure. The residue was partitioned between water and CH_2Cl_2 and the aqueous layer was extracted with CH_2Cl_2 three times. The combined extracts was dried ($MgSO_4$) and evaporated. The crude product was purified by chromatography on an alumina column, eluted with CH_2Cl_2 to give a colourless band. A colourless oil was obtained after removing the solvent. This oil was further recrystallized from ethyl acetate. After drying under high vacuum, the pure product was obtained as a white solid product {(Me-bipy)-$(CH_2)_4$-OC_6H_4}$_3$$CCH_3$ [0.16 g, 33% (based on 1.1.1-tris(4'-hydroxyphenyl)ethane], m.p. 59 - 64 °C (from glassy solid to oil), [Found: C, 78.74; H, 7.15; N, 8.35%; ES-MS: *m/z* 1000.94 ($[M-H+Na]^+$, 10%), 978.63 ($[M]^+$, 50%), 490.03 ($[M+H]^{2+}$, 94%), 326.97 ($[M+2H]^{3+}$, 100%); $C_{65}H_{66}N_6O_3$ (+ 0.2 x ethyl acetate) requires C, 79.12; H, 6.93; N, 8.42 %; M 979.28]; IR ν_{max}/cm^{-1} 3051w, 3004w, 2936m, 2863m, 1595s, 1551m, 1502s, 1456m, 1374m, 1290w, 1246s, 1180s, 1119w, 1053w, 1010w, 992m, 960w, 900w, 825s (KBr); ^{1}H NMR ($CDCl_3$) δ (ppm): 8.52 - 8.56 [6 H, m, (6,6')], 8.24 [6 H, m, (3, 3')], 7.12 - 7.15 [6 H, m, (5, 5')], 6.96 [6 H, d, ^{3}J(HH) 9 Hz, (12, 12')], 6.76 [6

H, d, ^{3}J(HH) 9 Hz, (13,13')], 3.95 [6 H, t, ^{3}J(HH) 6 Hz, (10)], 2.77 [6 H, t, ^{3}J(HH) 7.2 Hz, (7)], 2.43 [9 H, s, (ring-CH_3)], 2.09 [3 H, s, (16)], 1.85 [12 H, m, (8 + 9)]; [Peaks due to ethyl acetate were observed at 4.13 (q), 2.04 (s) and 1.25 (tr)]; ^{13}C NMR ($CDCl_3$) δ (ppm): 156.95 (11), 156.22, 156.05 (2, 2'), 152.24, 148.14 (4, 4'), 149.06, 148.84 (6, 6'), 141.80 (14), 129.61 (12, 12'), 124.66, 123.90 (5, 5'), 122.05, 121.29 (3, 3'), 113.58 (13, 13'), 67.42 (10), 50.59 (15), 35.16 (7), 30.79 (16), 28.96 (9), 26.95 (8), 21.20 (ring-CH_3).

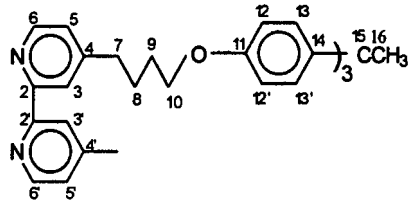

Atom numbering scheme for {(Me-bipy)-$(CH_2)_4$-OC_6H_4}$_3$$CCH_3$

Preparation of the first generation dendrimer {[(Me-bipy)-$(CH_2)_4$-O]$_2$$C_6H_3$-$CH_2O$-$C_6H_4$}$_3$$CCH_3$

This was prepared from the benzyl bromide {(Me-bipy)-$(CH_2)_4O$}$_2$$C_6H_3$-$CH_2Br$ (0.63 g, 0.97 mmol), 1.1.1-tris(4'-hydroxyphenyl)ethane (0.092 g, 0.30 mmol), potassium carbonate (0.14 g, 1.0 mmol) and 18-crown-6 (0.02 g, 0.07 mmol) in acetone, using the procedure described above for the preparation of the zero generation dendrimer {(Me-bipy)-$(CH_2)_4$-OC_6H_4}$_3$$CCH_3$. The product was purified by chromatography on an alumina column, eluted first with CH_2Cl_2 then with 20 % acetone/ CH_2Cl_2. A colourless band was collected to give a white solid product. This was further purified by recrystallization from ethyl acetate to give {[(Me-bipy)-$(CH_2)_4$-O]$_2$$C_6H_3$-$CH_2O$-$C_6H_4$}$_3$$CCH_3$ as a white solid [0.23 g, 38%, based on 1.1.1-tris(4'-hydroxyphenyl)ethane], m.p. 55 - 58 °C (from glassy solid to oil), [Found: C, 77.30; H, 6.68; N, 8.15%; ES-MS: *m/z* 2017.76, 2017.62 ($[M]^+$, 0.5%), 1009.42 ($[M+H]^{2+}$, 11%), 673.09 ($[M+2H]^{3+}$, 19%), 505.05 ($[M+3H]^{4+}$, 41%), 403.96 ($[M+4H]^{5+}$, 100%), 336.84 ($[M+5H]^{6+}$, 18%); [$C_{131}H_{132}N_{12}O_9$ (+ 0.2 x ethyl acetate) requires C, 77.75; H, 6.61; N, 8.25%; M 2018.58]; IR ν_{max}/cm^{-1} 3050w, 2937m, 2867m, 1595s, 1554m, 1502m, 1457m, 1375m, 1294w, 1244s, 1162s, 1064w, 1010w, 992w, 900w, 826m (KBr); ^{1}H NMR

($CDCl_3$) δ (ppm): 8.52 - 8.56 [12 H, m, (6,6')], 8.24 [12 H, m, (3, 3')], 7.10 - 7.15 [12 H, m, (5, 5')], 6.98 [6 H, d, ^{3}J(HH) 9 Hz, (17, 17')], 6.84 [6 H, d, ^{3}J(HH) 9 Hz, (18,18')], 6.54 [6 H, d, ^{4}J(HH) 2 Hz, (12,12')], 6.38 [3 H, t, ^{4}J(HH) 2 Hz, (14)], 4.92 [6 H, s, (15)], 3.96 [12 H, t, ^{3}J(HH) 6 Hz, (10)], 2.76 [12 H, t, ^{3}J(HH) 7.2 Hz, (7)], 2.42 [18 H, s, (ring-CH_3)], 2.08 [3 H, s, (21)], 1.85 [24 H, m, (8 + 9)]; ^{13}C NMR ($CDCl_3$) δ (ppm): 160.31 (11, 11'), 156.82 (16), 156.18, 155.99 (2, 2'), 152.18, 148.13 (4, 4'), 149.04, 148.90 (6, 6'), 142.02 (19), 139.41 (13) 129.61 (17, 17'), 124.65, 123.89 (5, 5'), 122.03, 121.28 (3, 3'), 113.96 (18, 18'), 105.81 (12, 12'), 100.76 (14), 69.99 (15), 67.57 (10), 50.64 (20), 35.11 (7), 30.78 (21), 28.83 (9), 26.87 (8), 21.16 (ring-CH_3).

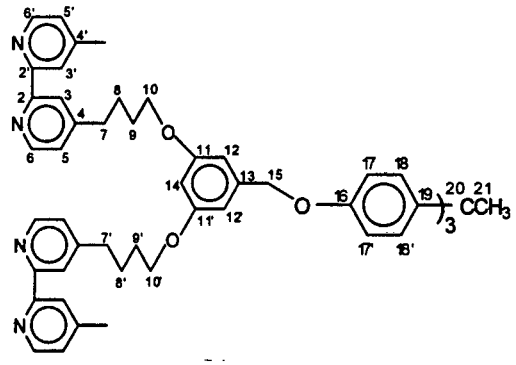

Atom numbering scheme for {[(Me-bipy)-$(CH_2)_4$-O]$_2$$C_6H_3$-$CH_2$O-$C_6H_4$}$_3$$CCH_3$

7.6.4 Synthesis of dendritic Pt(II) alkyl complexes

Preparation of the zero genaration Pt(II) alkyl complex [{$PtMe_2$(Me-bipy)-$(CH_2)_4$-OC_6H_4}$_3$$CCH_3$]

This was prepared from the zero generation dendrimer {(Me-bipy)-$(CH_2)_4$-OC_6H_4}$_3$$CCH_3$ (0.10 g, 0.10 mmol) in acetone (15 ml) and [$Pt_2Me_4(SMe_2)_2$] (0.10 g, 0.17 mmol) in benzene (6 ml) and a reaction time of 9 hours, using the procedure described previously for the preparation of the binuclear Pt(II) alkyl complex [Me_2Pt{(Me-bipy)-$(CH_2)_5$-(Me-bipy)}$PtMe_2$]. The product was obtained as an orange-red solid [{$PtMe_2$(Me-bipy)-$(CH_2)_4$-OC_6H_4}$_3$$CCH_3$] (0.14 g, 90 %), m.p. 230 - 240 °C (decomposed without melting), [Found: C, 53.32; H, 5.24; N,

4.56%; $C_{71}H_{84}N_6O_3Pt_3$ (+ C_6H_6 + 0.3 x C_3H_6O) requires C, 53.46; H, 5.29; N, 4.80%, M 1654.74]; UV-vis λ_{max}/nm (CH_2Cl_2) 310 (ε/dm^3 mol^{-1} cm^{-1} 2141), 454 (456); IR ν_{max}/cm^{-1} 3033w, 2894m, 2861m, 2784m, 1611s, 1576w, 1554w, 1501s, 1476m, 1419m, 1289w, 1244s, 1180s, 1119w, 1028m, 1010w, 886w, 828s, 762w (KBr); ^{1}H NMR ($CDCl_3$) δ (ppm): 9.06 - 9.02 [6 H, m, (6,6')], 7.79 [6 H, s, (3, 3')], 7.30 [6 H, m, (5, 5')], 6.97 [6 H, d, ^{3}J(HH) 9 Hz, (12, 12')], 6.76 [6 H, d, ^{3}J(HH) 9 Hz, (13,13')], 3.97 [6 H, t, ^{3}J(HH) 6 Hz, (10)], 2.72 [6 H, t, ^{3}J(HH) 7.2 Hz, (7)], 2.36 [9 H, s, (ring-CH_3)], 2.08 [3 H, s, (16)], 1.89 [12 H, m, (8 + 9)], 1.05 [18 H, s, ^{2}J(PtH) 86 Hz, (Pt-CH_3)]; [Peaks due to benzene and acetone were observed at 7.35 (s) and 2.16 (s) respectively]; ^{13}C NMR ($CDCl_3$) δ (ppm): 156.85 (11), 156.35, 156.16 (2, 2'), 152.03, 147.97 (4, 4'), 146.65, 146.52 (6, 6'), 141.84 (14), 129.61 (12, 12'), 127.47, 126.67 (5, 5'), 122.97, 122.15 (3, 3'), 113.57 (13, 13'), 67.24 (10), 50.59 (15), 35.46 (7), 30.78 (16), 28.77 (9), 26.42 (8), 21.80 (ring-CH_3), -17.41 [J(PtC) 805 Hz, (Pt-CH_3)]; (Peak due to benzene was observed at 128.31, For numbering the protons and carbons, please refer to the numbering scheme for the ligand); ES-MS (solvents CH_3CN-$CHCl_3$-NH_3H_2O, source temperature 30°C, cone voltages 90V): *m/z* 1908.12 ([M+NH_3+2$CHCl_3$]$^+$, 12%), 1670.23 ([M+NH_3]$^+$, 34%), 1445.33 ([M-Pt-CH_3]$^+$, 22%), all with expected isotope patterns; in addition, peak at 682.82 (100%), and other unassigned peaks at lower mass region were observed.

Preparation of the first genaration Pt(II) alkyl complex {[$PtMe_2$(Me-bipy)-$(CH_2)_4$-O]$_2C_6H_3$-CH_2O-C_6H_4}$_3CCH_3$

This was prepared from the first generation dendrimer {[(Me-bipy)-$(CH_2)_4$-O]$_2C_6H_3$-CH_2O-C_6H_4}$_3CCH_3$ (0.096g, 0.048 mmol) in acetone (20 ml) and [$Pt_2Me_4(SMe_2)_2$] (0.10 g, 0.17 mmol) in benzene (6 ml) and a reaction time of 9 hours, using the procedure described previously for the preparation of the binuclear Pt(II) alkyl complex [Me_2Pt{(Me-bipy)-$(CH_2)_5$-(Me-bipy)}$PtMe_2$]. ^{1}H NMR analysis of the sample showed that the reaction was not complete. Thus the product was further reacted with [$Pt_2Me_4(SMe_2)_2$] (0.46 g, 0.78 mmol) in acetone (10 ml) at room temperature for additional 16 hours under nitrogen. The resulting

solid product was washed three times with diethyl ether and then with acetone twice. After drying under high vacuum, the product obtained was an orange-red solid $\{[PtMe_2(Me\text{-}bipy)\text{-}(CH_2)_4\text{-}O]_2C_6H_3\text{-}CH_2O\text{-}C_6H_4\}_3CCH_3$ (0.16 g, 98%), m.p. 230 - 240 °C (decomposed without melting), [Found: C, 50.16; H, 5.12; N, 4.77%; $C_{143}H_{168}N_{12}O_9Pt_6$ requires C, 50.97; H, 5.03; N, 4.99%; M 3369.49]; UV-vis λ_{max}/nm (CH_2Cl_2): 306 (ε/dm^3 mol^{-1} cm^{-1} 6792), 454 (1189); IR ν_{max}/cm^{-1}: 3065w, 2899m, 2786m, 1610s, 1554m, 1501m, 1480m, 1449m, 1420m, 1375m, 1295m, 1244m, 1179m, 1160s, 1062m, 1029m, 891w, 830s, 764w (KBr); ^{1}H NMR ($CDCl_3$) δ (ppm): 9.00 [12 H, m, (6,6')], 7.77 [12 H, m, (3, 3')], 7.26 [12 H, m, (5, 5')], 6.94 [6 H, m, (17, 17')], 6.84 [6 H, m, (18,18')], 6.54 [6 H, d, ^{4}J(HH) 2 Hz, (12,12')], 6.35 [3 H, t, ^{4}J(HH) 2 Hz, (14)], 4.92 [6 H, s, (15)], 3.97 [12 H, t, ^{3}J(HH) 6 Hz, (10)], 2.71 [12 H, t, ^{3}J(HH) 6.8 Hz, (7)], 2.34 [18 H, s, (ring-CH_3)], 2.06 [3 H, s, (21)], 1.85 [24 H, m, (8 + 9)], 1.04 [36 H, s, ^{2}J(PtH) 86 Hz, (Pt-CH_3)]. (For numbering the protons, please refer to the numbering scheme for the ligand). This sample was found to contain the solvent acetone but due to its poor solublity, the amounts of acetone were not verified.

References

1. R.B. King, M.Z. Iqbal and A.D. King, Jr., J. Organomet. Chem., 1979, **171**, 53.
2. R.B. King, in *Organometallic Synthesis*, vol. 1, Eds. J.J. Eisch and R.B. King, Academic Press: New York, 1965, p147.
3. J-A.M. Andersen and J.R. Moss, J. Organomet. Chem., 1995, **494**, 105.
4. R.B. King, in *Organometallic Synthesis*, vol. 1, Eds. J.J. Eisch and R.B. King, Academic Press: New York, 1965, p151.
5. A. Emeran, M. A. Gafoor, J.K.I. Goslett, Y-H. Liao, L. Pimble and J.R. Moss, J. Organomet. Chem., 1991, **405**, 237.
6. J-A.M. Andersen and J.R. Moss, Organometallics, 1994, **13**, 5013.
7. D.K. Huggins and H.D. Kaesz, J. Am. Chem. Soc., 1964, **86**, 2734.
8. G. Bor and G. Sbrignadello, J. Chem. Soc. Dalton Trans., 1974, 440.
9. R.C. Weast and M. J.A. Astle, *CRC Handbook of Chemistry and Physics*, 61st ed., CRC Press Inc: Boca Raton, FL, 1981.
10. a):N. B. Colthup, *Introduction to Infrared and Raman Spectroscopy*, Academic Press: New York, 1990.
    b): C.J. Pouchert, *The Aldrich Library of Infrared Spectra*, 3rd. ed., Aldrich Chemical Company Inc., 1981.
11. C.J. Pouchert, *The Aldrich Library of NMR Spectra*, 2nd. ed., Aldrich Chemical Company Inc., 1983.
12. E. Breitmaier and W. Voelter, *Carbon-13 NMR spectroscopy*, 3rd ed., VCH, Weinheim, 1987.
13. a): N. A. Beach and H. B. Gray, J. Am. Chem. Soc., 1968, **90**, 5713.
    b): P.M. Treichel in *Comprehensive Organometallic Chemistry*, Eds. G. Wilkinson, F.G.A. Stone and E.W. Abel, Pergamon, 1982, vol 4, p30.
14. D.F. Shriver and K.H. Whitmire in *Comprehensive Organometallic Chemistry*, Eds. G. Wilkinson, F.G.A. Stone and E.W. Abel, Pergamon: New York, 1982, vol 4, p 247.

15. S.J. Dossett, A.F. Hill, J.C. Jeffery, F. Marken, P. Sherwood and F.G.A. Stone, J. Chem. Soc. Dalton Trans., 1988, 2453.

16. E.O. Fischer, T.L. Lindner, G. Huttner, P. Friedrich, F. R. Kreiβl and J.O Besenhard, Chem. Ber., 1977, **110**, 3397.

17. U. Nagel, Chem. Ber,.1982, **115**, 1998.

18. G.B. Kauffman and L.A. Teter, Inorg. Synth., 1963, **7**, 245.

19. T. Yoshida and S. Otsuka, Inorg. Synth., 1979, **19**, 101.

20. a): G.M. Whitesides, J.F. Gaasch and E.R. Stedronsky, J. Am. Chem. Soc., 1972, **94**, 5258.
b): G.M. Whitesides and J.F. Gaasch, J. Organomet. Chem., 1971, **33**, 24.

21. For a recent procedure for the preparation of $[Pt(CO_3)(PPh_3)_2]$, see, M.A. Andrews, G.L. Gould, W.T. Klooster, K.S. Koenig and E.J. Voss, Inorg. Chem., 1996, **35**, 5478.

22. V.V. Grushin, I.S. Akhrem and M.E. Vol'pin, J. Organomet. Chem., 1989, **371**, 403.

23. a): R.K. Merwin and D.M. Roddick, J. Organomet. Chem., 1995, **487**, 69.
b): G. Vasapollo, L. Toniolo, G. Cavinato, F. Bigoli, M. Lanfranchi and M.A. Pellinghelli, J. Organomet. Chem, 1994, **481**, 173.
c): K. Werner and W. Beck, Chem. Ber.,1972, **105**, 3947.

24. D.M. Blake and L.M. Leung, Inorg. Chem., 1972, **11**, 2879.

25. P.L. Bellon, M. Manassero, F. Porta and M. Sansoni, J. Organomet. Chem., 1974, **80**, 139.

26. P. Chini and G. Longoni, J. Chem. Soc. (A), 1970, 1542.

27. A.L. Tan, P.M.N. Low, Z-Y. Zhou, W. Zheng, B-M. Wu, T.C.W. Mak and T.S.A. Hor, J. Chem. Soc. Dalton Trans., 1996, 2207.

28. A. Dobson, S.D. Robinson and M.F. Uttley, Inorg. Synth., 1977, **17**, 124.

29. R.S. Paonessa, A.L. Prignano and W.C. Trogler, Organometallics, 1985, **4**, 647.

30. E.G. Cox, H. Saenger and W. Wardlaw, J. Chem. Soc., 1934, 182.

31. J.D. Scott and R.J. Puddephatt, Organometallics, 1983, **2**, 1643.

32. N. Chaudhury and R.J. Puddephatt, J. Organomet. Chem., 1975, **84**, 105.

33. P.K. Monaghan and R.J. Puddephatt, Organometallics, 1984, **3**, 444.

34. E. Uhlig and M. Maaser, Z. Anorg. Allg. Chem., 1966, **344**, 205.

35. H.C. Clark and L.E. Manzer, J. Organomet. Chem., 1973, **59**, 411.

36. R. B. King and M. B. Bisnette, J. Organomet. Chem., 1967, **7**, 311.

37. L. G. Scott, M. Sc. Thesis, university of Cape Town, 1984.

38. N. A. Bailey, P. L. Chell, C. P. Manuel, A. Mukhopadhyay, D. Rogers, H. E. Tabbron and M. J. Winter, J. Chem. Soc. Dalton Trans., 1983, 2397.

39. Y. Zhou and J. A. Gladysz, Organometallics, 1993, **12**, 1073.

40. C. G. Pitt, H. H. Seltzman, Y. Sayed, C. E. Twine, Jr. and D. L. Williams, J. Org. Chem., 1979, **44**, 677.

41. B. Giese, J. Hartung, C. Kesselheim, H. J. Lindner and I. Svoboda, Chem. Ber., 1993, **126**, 1193.

42. J. H. Merrifield, G-Y. Lin, W. A. Kiel and J. A. Gladysz, J. Am. Chem. Soc., 1983, **105**, 5811.

43. J-A. M. Andersen and J.R. Moss, J. Organomet. Chem., 1995, **494**, 105.

44. J.R. Moss, J. Organomet. Chem., 1982, **231**, 229.

45. H.B. Friedrich, P.A. Makhesha, J.R. Moss and B.K. Williamson, J. Organomet. Chem., 1990, **384**, 325.

46. H.B. Friedrich, K.P. Finch, M.A. Gafoor and J.R. Moss, Inorg. Chim. Acta, 1993, **206**, 225.

47. R.H. Schmehl, R.A. Auerbach, W.F. Wacholtz, C.M. Elliott, R.A. Freitag and J.W. Merkert, Inorg. Chem., 1986, **25**, 2440.

48. M. Furue, T. Yoshidzumi, S. Kinoshita, T. Kushida, S. Nozakura and M. Kamachi, Bull. Chem. Soc. Jpn., 1991, **64**, 1632.

49. see Chapter 4 of this thesis.